

## Dankwoord

*Regrets, I've had a few,  
But then again, too few to mention,  
I did, what I had to do:  
I did it my way!*

Aan het einde van een periode in je leven, is het toch altijd leuk om even je tijd te nemen, nog even terug te blikken op kleine successen en grote mislukkingen, om vast te stellen dat het mooi geweest is, alvorens met een tevreden gevoel een nieuwe start te nemen. Een van die kleine dingen die ik in de voorbije jaren heb opgestoken, is dat vele 'lezers' van een werk als dit niet verder raken dan deze pagina. Daarom houd ik er ook aan om van dit stukje een mooie afsluiter van een fantastische periode te maken. Want wie had lang geleden ooit verwacht dat ik vandaag dit stukje zou schrijven? Ik niet in het minst: ik was immers niet meteen de allergrootste uitbinker als het over studieresultaten ging, misschien ook niet altijd even geconcentreerd, of zeker niet altijd even gedetailleerd, dus doctoreren was voor mij niet meteen een optie die er lang op voorhand zat aan te komen. Daarom, en dat durf ik toch wel toegeven, ben ik best een beetje trots, blij, gelukkig en zelfs vereerd dat ik vandaag dit laatste stukje tekst mag schrijven. Nog eenmaal krijg ik hier de kans om mijn verhaal te doen, en ja, je weet hoe dat gaat bij mij, ik neem er mijn tijd voor...

'Als we nu eens aan Jeroen vragen of hij niet geïnteresseerd is om te doctoreren.' Die vraag is op een zekere dag opgedoken in het hoofd van (toen nog) Bart. Intussen heb ik zo wat alles wat ik hier meegemaakt en gepresteerd heb te danken aan (intussen) Prof. Dr. ir. Bart Van der Bruggen. Hij ontwaarde in mij, als student, bepaalde onderzoekskwaliteiten, hij geloofde volop in mijn capaciteiten en heeft me ook altijd onvoorwaardelijk gesteund, ook toen het allemaal wat minder ging. Hij was de grote bezieler achter dit project, bij hem kon ik altijd terecht, zelfs als zijn deur niet open stond, en ook voor een filosofische discussie (700 km naar Irsee en terug) of een platvloerse mop was hij altijd te vinden. Dit creëerde een heel bijzondere band tussen ons beiden, die gelukkig niet verbroken moet worden als je professionele wegen scheiden. Ik ben dan ook heel blij dat Prof. Dr. ir. Van der Bruggen altijd gewoon Bart is gebleven, en dat ook in de toekomst zal blijven. Bedankt Bart!

Prof. Dr. Carlo Vandecasteele deelde in het geloof van Bart in mij en steunde hem hierin. Hij zorgde voor de financiering van dit project en trachtte mij, vooral in de beginperiode, mee op het goede pad te zetten. Zijn kritische kijk op resultaten en publicaties zal ik niet snel vergeten.

Prof. Dr. ir. Jan Degrève en Prof. Dr. ir. Paula Moldenaers zou ik willen danken voor de inspanningen die zij leverden om de kwaliteit van dit werk te controleren. Alleen het vele leeswerk al, zelfs niet geheel in hun eigen expertisedomein, zal veel van hun tijd gevergd hebben. Ik ben dan ook blij dat zij dit ter harte hebben willen nemen.

Wie mij een beetje kent, weet dat ik niet om een straffe en ongenueanceerde uitspraak verlegen zit. Een van mijn bekende boutades was ongetwijfeld: ‘Collega’s moeten geen vrienden zijn!’ Achter dergelijke uitspraken zat echter meestal een klein hartje, dat veel beter wist: toffe collega’s zijn onbetaalbaar, je ziet ze haast meer dan je partner. De sfeer op onze afdeling was ronduit fantastisch. Wat konden we genieten als ‘de membranen’ een overwinning boekten tegen ‘de vasten afval’. Een van mijn andere favoriete boutades, ‘een dag niet gelachen, is een dag niet geleefd’, kon ik hier gelukkig alle dagen in de praktijk brengen, er werd echt wel geleefd in onze afdeling. Collega’s, vrienden, ik vond het zeer fijn om met jullie samen te werken: Tom (*een waardig verliezer bij het squashen, maar ook nog zo veel meer*), Leen (*mijn compagne de route*), Katleen (*een band gaat nooit stuk*), Geert (*een halve denktank is ook een tank!*), Stefanie (*ik een showman? Oooh!*), Ben (*belachelijk*), Michèle en Christine (*niet alleen voor de ontelbare analyses, ook voor het haast even ontelbaar aantal cola’s dat we zijn gaan halen, of voor het glaasje champagne dat we best smaakten*), Herman (*wandelt zelfs in Linkhout*), Kathleen (*kort, maar krachtig, een nieuwe adem in het oerconservatieve feestcomité*), Daneel, Dimitri en Karola (*vroeger verdwenen, maar zeker niet vergeten*), ik ben blij dat jullie in mijn team zaten!

Binnen het CIT liepen er nog tal van mensen rond die meer dan hun steentje bijdroegen aan mijn werk, soms in hoge nood, als er b.v. weer eens een bestelling extreem prioritair was of die verdomde pomp het wééral had begeven, soms gewoon met een deugddoend babbeltje, je hebt het allemaal nodig om je goed in je vel te voelen op je werk. Bedankt Guido, Marie-Claude, Alena, Beatrice, Bart, Tony, Herman, Marc, René en Jaak.

Een belangrijk deel van dit onderzoek gebeurde in samenwerking met mijn thesisstudenten. Ook zij hebben een belangrijke rol gespeeld voor mij en mogen hier dus zeker niet vergeten worden. Koen, An, Katrien, Anne-Sophie, Arne, jullie leverden prima werk !

Chris, Anita, Roger, Tim en Bart, allemaal van Vito, waren bijzonder geïnteresseerd in mijn studie. De discussies met hen waren een verrijking voor mijn onderzoek. Bovendien zorgden zij, alleen al door keramische membranen ter beschikking te stellen, voor een onmisbare peiler in mijn onderzoek.

Ook Petrus Cuperus (SolSep) was vanaf het prille begin geboeid door dit project. Hij was bovendien bereid zijn membranen ter beschikking te stellen. Het was uitermate leerrijk om een man met zo veel ervaring zo persoonlijk te kunnen benaderen.

In dit onderzoek werden ook twee casestudies uitgevoerd. Dit was enkel mogelijk dankzij de interesse van bepaalde mensen in mijn onderzoek. Daarom ook mijn oprechte dank aan Gert Martens en Philip De Tandt van (toen nog) UCB, en Bruno De Witte van Janssen Pharmaceutica.

Sim, jij leverde allicht het minst boeiende deel van dit werk: het nalezen van een dik boek op het taalgebruik, terwijl je van de inhoud vermoedelijk even weinig begreep als ik van pakweg bloemschikken of kantklossen, je moet het maar (willen) doen. Heel erg bedankt.

Sommige mensen hebben ogenschijnlijk helemaal niets met je doctoraat te maken. Toch vind ik dat ook zij hier een speciale vermelding verdienen. Hugo, bedankt voor de prettige samenwerking in het kader van de MIRA, je nuchtere kijk en heerlijk realisme waren uniek! Toen het er even naar uitzag dat ik misschien wel helemaal nooit mijn onderzoek zou kunnen afmaken, zorgden Patrick en Diane voor een haast surrealistische noodoplossing; dit resulteerde in een van de mooiste avonturen die ik ooit beleefde, en vooral in een prachtige vriendschap!

Om onbezorgd door het leven te kunnen stappen, is het onontbeerlijk om in een stabiele, rustige en ontspannende omgeving te kunnen toeven. Vrienden en familie, of je ze nu alle dagen ziet of maar heel af en toe eens hoort, ze maken dat je dingen waard vindt om ze te doen. En één iemand is nu al vele jaren veel meer dan zo maar een vriendin of een familielid: het leukste aan elke dag vind ik nog altijd om 's avonds thuis te komen, bij mijn Karen. Want zij gelooft in mij... (en ik in haar hoor)! Meisje, bedankt!

Jeroen  
Februari 2006

---

**List of symbols**

$a$	model constant (-)
$A$	membrane surface ( $m^2$ )
$b$	model constant (-)
$B_0$	viscous flow parameter ( $m^2$ )
$c$	concentration ( $kg/m^3$ )
$c$	concentration at the feed side after time $t$ in cell diffusion (mol/l)
$c_0$	initial feed concentration in cell diffusion (mol/l)
$c'$	concentration at the permeate side after time $t$ in cell diffusion (mol/l)
$c'_0$	initial concentration at the permeate side in cell diffusion (mol/l)
$\overline{c}_f$	real concentration at the feed side (mol/l)
$c_{f,i}$	concentration of component $i$ in the feed (mol/l)
$c_p$	heat capacity (J/mol.K)
$c_{p,i}$	concentration of component $i$ in the permeate (mol/l)
$c_{r,i}$	concentration of component $i$ in the retentate (mol/l)
$d_c$	effective diameter of component $c$ (m)
$d_e$	equator (m)
$d_p$	pore diameter (m)
$d_s$	apex diameter (m)
$d_p^{eff}$	effective pore diameter (m)
$D_c^s$	diffusion coefficient of component $c$ in solvent $s$ ( $m^2/s$ )
$D_c^{M,s}$	solute diffusivity of component $c$ through membrane $M$ in solvent $s$ ( $m^2/s$ )
$D_i$	diffusivity of the solvent in the polymer matrix ( $m^2/s$ )
$D_{ij}$	diffusion coefficient between components $i$ and $j$ ( $m^2/s$ )
$D_{ij}^T$	multicomponent thermal diffusion coefficient ( $m/s^2$ )
$f_1$	membrane parameter characteristic for the NF layer (m/s)
$f_2$	membrane parameter characteristic for the UF layer ( $m^{-1}$ )
$F$	feed flow ( $m^3/h$ )
$F$	total external force on the solution (N/mol)
$F$	empirical constant for determination of surface tension (-)
$F_i$	external force on component $i$ (N/mol)
$F_m$	molar feed flow (mol/h)
$g$	gravitational constant ( $m/s^2$ )

---

$H_F$	wall correction parameter (-)
$J$	flux (l/h.m <sup>2</sup> )
$J_C$	component flux (mol/h.m <sup>2</sup> )
$J_D$	diffusive flux (mol/h.m <sup>2</sup> )
$J_f$	feed flux (l/h)
$J_i$	flux of component i (mol/h.m <sup>2</sup> )
$J_p$	permeate flow (l/h)
$J_r$	retentate flow (l/h)
$J_s$	flux of solvent s (l/h.m <sup>2</sup> )
$k$	Boltzmann constant (m <sup>2</sup> .kg/s <sup>2</sup> .K)
$K^*$	capillary constant (mm <sup>2</sup> /s <sup>2</sup> )
$K_i$	partition coefficient between component i and polymer
$L$	permeability (l/h.m <sup>2</sup> .bar)
$L_i$	normalised permeability of solvent i (l/h.m <sup>2</sup> .bar)
$L_m^0$	initial methanol permeability (l/h.m <sup>2</sup> .bar)
$L_i^{\text{exp}}$	experimental permeability of solvent i (l/h.m <sup>2</sup> .bar)
$L_m^i$	methanol permeability after permeation of solvent i (l/h.m <sup>2</sup> .bar)
$m$	regression parameter (-)
$M_s$	molecular weight of component s (g/mol)
$p$	regression parameter (-)
$P$	octanol-water partition coefficient (-)
$P_f$	feed side pressure (bar)
$P_p$	permeate side pressure (bar)
$P_s$	solute permeability (m/s)
$q$	solvent parameter; for alcohols equal to number of C-atoms (-)
$Q$	degree of swelling (ml/g)
$Q$	reboiler duty (W)
$Q_f$	feed flow (l/h)
$Q_p$	permeate flow (l/h)
$r$	pore radius (m)
$r_c$	radius of component c (m)
$\bar{r}$	mean pore size (m)
$R$	rejection (%)
$R$	universal gas constant (J/mol.K)
$s_e^2$	error variance ((l/h.m <sup>2</sup> .bar) <sup>2</sup> )

---

$S$	recovery (%)
$S_F$	steric hindrance parameter (-)
$S_p$	standard deviation of the pore size distribution (m)
$t$	time (s)
$T$	temperature (K)
$u_i$	transport velocity of component i (m/s)
$V_c$	molar volume of component c at the boiling point (m <sup>3</sup> /mol)
$V_{cell}$	volume of diffusion cell (m <sup>3</sup> )
$V_m$	solvent molar volume (m <sup>3</sup> /mol)
$W_{dry}$	weight of a dry membrane sample (g)
$W_{wet}$	weight of a wet membrane sample (g)
$x_i$	mole fraction of component i (-)
$X$	regression parameter (-)
$X_{sm}$	friction factor (-)
$Y$	regression parameter (-)
$\alpha, \beta, \delta$	fitting parameters (-)
$\alpha'_i$	constant (-)
$\beta$	cell constant (m <sup>-2</sup> )
$\varepsilon$	porosity (-)
$\phi$	association parameter of the solvent (-)
$\phi$	sorption value (g/g polymer)
$\phi'$	solvent parameter (s/m <sup>2</sup> )
$\gamma_c$	critical membrane surface tension (mN/m)
$\gamma_i^d$	disperse contribution to surface tension of phase i (mN/m)
$\gamma_i^p$	polar contribution to surface tension of phase i (mN/m)
$\gamma_{lv}$	liquid-vapour interfacial tension (mN/m)
$\gamma_{sl}$	solid-liquid interfacial tension (mN/m)
$\gamma_{sv}$	solid-vapour interfacial tension (mN/m)
$\eta$	dynamic viscosity (Pa.s)
$\eta$	pump efficiency (-)
$\eta$	ratio $d_c$ to $d_p$ (-)
$\phi$	Hagenbach correction factor (s)
$\mu_i$	chemical potential of component i
$\nu$	kinematic viscosity (m <sup>2</sup> /s)

$\nu$	van 't Hoff factor (-)
$\theta_s$	contact angle of solvent s ( $^\circ$ )
$\rho_s$	density of solvent s ( $\text{kg/m}^3$ )
$\sigma$	reflection coefficient (-)
$\tau$	tortuosity (-)
$\psi_o$	surface tension weight factor for organic fraction (-)
$\psi_w$	surface tension weight factor for aqueous fraction (-)
$\Delta c$	concentration difference (mol)
$\Delta E$	difference in electric potential (V)
$\Delta P$	pressure difference (bar)
$\Delta t$	time difference (s)
$\Delta T$	temperature difference ( $^\circ\text{C}$ )
$\Delta V$	difference in volume (l)
$\Delta H^{vap}$	molar heat of vaporisation (J/mol)
$\Delta x$	membrane thickness (m)
$\Delta \gamma$	difference in surface tension (mN/m)
$\Delta \pi$	osmotic pressure (bar)

**List of acronyms**

AOH	alcohol
API	active pharmaceutical ingredient
BATNEEC	best available technique not entailing excessive costs
BFC	bromofluorocarbon
BHP	brake horsepower
BTEX	benzene, toluene, ethyl benzene, xylene
CFC	chlorofluorocarbon
CTE	chronic toxic encephalopathy
DMAc	dimethyl acetamide
DMF	dimethyl formamide
DMSO	dimethyl sulfoxide
EA	ethyl acetate
EPA	Environmental Protection Agency
EtOH	ethanol
EURAL	Europese afvallijst
FID	flame ionisation detector
GC	gas chromatography
HITK	Hermsdorfer Institut für Technische Keramik
HP	Hagen-Poiseuille
HPLC	high pressure liquid chromatography
IDLH	immediate danger to life or health
IPI	intermediate pharmaceutical ingredient
JB	Jonsson and Boesen
KMI	Koninklijk Meteorologisch Instituut
LD <sub>50</sub>	50% lethal dosis
LRTAP	Long-Range Transboundary Air Pollution
MBTE	methyl tert-butyl ether
MC	methylene chloride
MEK	methyl ethyl ketone
MeOH	methanol
MET	Membrane Extraction Technology
MF	microfiltration
MW	molecular weight
MWCO	molecular weight cut-off
NEC	National Emissions Ceilings



NF	nanofiltration
NMVOC	non-methane volatile organic component
OPS	organic psycho syndrome
OVAM	Openbare Afvalstoffenmaatschappij van het Vlaamse Gewest
PA	polyamide
PAH	polyaromatic hydrocarbon
PALS	positron annihilation lifetime spectroscopy
PAN	polyacrylonitrile
PAN	peroxyacetylene nitrate
PDMS	polydimethylsiloxane
PEG	polyethylene glycol
PES	polyethersulphon
PI	polyimide
PTC	phase transfer catalysis
RO	reverse osmosis
SD	solution-diffusion
SEM	scanning electron microscopy
SHP	steric hindrance pore model
TFC	thin film composite
THF	tetrahydrofurane
TMC	transition metal catalysis
UF	ultrafiltration
UNECE	United Nations Economic Commission for Europe
VMM	Vlaamse Milieumaatschappij
VOC	volatile organic component
WGK	Wassergefährdungsklassen



## Table of content

Abstract.....	1
Nederlandstalige samenvatting .....	3
<hr/>	
Chapter 1.....	21
Membrane technology .....	21
<hr/>	
1. Membrane technology .....	22
2. Pressure driven membrane processes and nanofiltration .....	23
3. Principles and definitions.....	25
4. Nanofiltration of organic solvents .....	27
5. Aim of this work.....	29
<hr/>	
Chapter 2.....	33
Methods and materials.....	33
<hr/>	
1. Membrane filtration units.....	34
1.1 Dead-end filtration module .....	34
1.2 Cross-flow filtration installation.....	34
2. Membranes.....	36
2.1 Membrane types .....	36
2.2 Surface characterisation techniques.....	38
3. Solvents.....	40
3.1 Selection of solvents .....	40
3.2 Composition of liquid feed mixtures .....	42
3.3 Kinematic and dynamic solvent viscosity.....	42
3.4 Dielectric constant .....	43
3.5 Liquid surface tension.....	43
4. Solutes.....	44
4.1 Introduction .....	44
4.2 Effective solute diameter.....	46
4.3 Logarithm of the octanol-water partition coefficient.....	47
4.4 Solute concentration: analytical techniques .....	47
<hr/>	
Chapter 3.....	49
The effect of organic solvents on polymeric nanofiltration membranes.....	49
<hr/>	
1. Introduction .....	50
2. Influence of organic solvents on polymeric nanofiltration membranes.....	51
2.1 Introduction .....	51
2.2 Experimental set-up .....	51
2.3 The effect of organic solvents on polymeric nanofiltration membranes .....	52
2.3.1 Results .....	52
2.3.2 Discussion.....	55
2.4 Reorganisation of polymer chains .....	57
3. Swelling and rejection.....	58
3.1 Determination of the membrane swelling.....	58
3.2 Changes in rejection due to membrane swelling.....	59
4. Water permeability and membrane surface hydrophilicity.....	61
4.1 Determination of the membrane surface hydrophilicity .....	61

---

4.2 Changes in water permeability due to differences in hydrophilicity .....	62
5. Conclusion.....	63
<hr/>	
Chapter 4.....	65
Permeability of organic solvents through nanofiltration membranes .....	65
<hr/>	
1. Introduction .....	66
2. Parameters affecting the solvent flux.....	66
2.1 Literature review.....	66
2.2 Experimental set-up .....	68
2.3 Results and discussion .....	69
2.3.1 Comparison of feed and permeate composition .....	69
2.3.2 Hydrophilic membranes .....	71
2.3.3 Hydrophobic membranes.....	73
2.3.4 Semi-hydrophilic membranes.....	74
2.4 Ceramic versus polymeric membranes .....	76
3. Modelling of the solvent flux .....	78
3.1 Introduction .....	78
3.2 Theoretical background.....	79
3.3 A new transport model for solvent permeation .....	81
3.4 Results and discussion .....	82
3.4.1 Required parameters.....	82
3.4.2 Model fitting and statistical analysis.....	84
3.4.3 Evaluation of the transport models .....	86
4. Permeability of pure solvents .....	90
4.1 Permeability of a homologous series of alcohols .....	90
4.2 Permeability of other solvents .....	92
5. Summary and conclusion .....	93
<hr/>	
Chapter 5.....	95
Solute transport in non-aqueous nanofiltration .....	95
<hr/>	
1. Introduction .....	96
2. Parameters affecting solute transport.....	97
2.1 Introduction .....	97
2.2 Experimental set-up .....	97
2.3 Results and discussion .....	98
2.3.1 Experimental data .....	98
2.3.2 Discussion.....	99
2.4 Ceramic versus polymeric membranes .....	103
3. Solute transport in non-aqueous nanofiltration .....	104
3.1 Introduction .....	104
3.2 Solute rejection in organic solvents from different chemical classes .....	105
3.2.1 Experimental set-up .....	105
3.2.2 Results and discussion.....	105
3.3 Transport mechanism for solute permeation in non-aqueous nanofiltration.....	112
3.3.1 Experimental set-up .....	112
3.3.2 Results and discussion.....	113
4. Modelling of solute transport in non-aqueous nanofiltration.....	115
4.1 Introduction .....	115
4.2 Modelling of the reflection curve in non-aqueous media .....	116
4.2.1 Theoretical background .....	116

---

4.2.2 Correction for modelling in different solvents .....	119
4.3 Results and discussion .....	120
4.3.1 Descriptive modelling .....	121
4.3.2 Predictive modelling .....	126
5. Conclusion.....	128
<hr/>	
Chapter 6.....	131
Industrial application of non-aqueous nanofiltration .....	131
<hr/>	
1. Introduction .....	132
2. Organic solvents in industrial environments.....	132
2.1 The use of organic solvents in the contemporary industry .....	132
2.2 Environmental problems related to industrial use of organic solvents.....	134
2.2.1 Introduction .....	134
2.2.2 Solvent containing waste streams .....	134
2.2.3 Air pollution.....	135
2.2.4 Soil pollution .....	136
2.2.5 Water pollution .....	136
2.2.6 Regulations .....	137
3. Applications of non-aqueous nanofiltration.....	137
3.1 Introduction .....	137
3.2 Solvent recovery from lube oil filtrates .....	138
3.3 The vegetable oil industry.....	139
3.4 Homogeneous catalyst separation and re-use.....	139
3.5 Solvent exchange.....	141
4. Case-study: Solvent recovery in the pharmaceutical industry .....	142
4.1 Introduction .....	142
4.2 Results.....	143
4.2.1 Experimental.....	143
4.2.2 Toluene.....	143
4.2.3 Methanol.....	145
4.2.4 Methylene chloride .....	145
4.3 Model calculation .....	145
4.3.1 Design of a membrane installation.....	145
4.3.2 Energy consumption.....	148
5. Summary and conclusion .....	149
 Summary and general conclusions .....	 151
 References.....	 157
 Appendices.....	 171
 List of publications .....	 175
 Curriculum vitae.....	 179



## **Abstract**

This dissertation focuses on the use of polymeric and ceramic nanofiltration membranes as a separation tool in organic solvents.

The performance of both polymeric and ceramic membranes, expressed in terms of the solvent flux and the solute rejection, is solvent dependent. Polymeric membranes are liable to a plasticising effect, which leads to a reorganisation of the membrane material, resulting in a new pore size distribution and a change of the degree of hydrophilicity of the membrane surface. Hydrophobic membranes show a better solvent resistance than hydrophilic membranes.

The solvent flux appears to depend on three parameters: transport of momentum, steric hindrance effects and the affinity between the solvent and the membrane material. A new model for solvent transport is developed, which can be applied on experimental data of both hydrophilic and hydrophobic membranes, and for a broad range of organic solvents and solvent mixtures.

Solute transport in non-aqueous nanofiltration mainly occurs by convection. As ceramic membranes show similar results as polymeric membranes, differences in membrane performance can not be attributed to swelling effects. Transport of dissolved components is also found to be determined by three parameters: the nominal pore size, the degree of solvation of the solute, and the degree of pore wall solvation. A new methodology, incorporating a solvent effect for both the solute and the pore size is presented. Model parameters, characteristic for specific membrane-solvent combinations, are determined and provide excellent results for predictive modelling.

A case-study on solvent recovery from a pharmaceutical production process indicates that non-aqueous nanofiltration is a technically feasible alternative for traditional separation processes. A membrane unit is calculated to consume approximately 200 times less energy than a throughput distillation unit. Economic feasibility must however be further investigated.





## **Nederlandstalige samenvatting**

### **Mechanismen en modellering van nanofiltratie in organisch milieu**

#### **1. Inleiding**

In de voorbije eeuw is de industriële activiteit wereldwijd enorm toegenomen. Deze evolutie heeft tot ongekende mogelijkheden geleid, maar heeft ook steeds meer de beperkingen die hiermee gepaard gaan blootgelegd. Grondstoffen en energie worden aan een schrikwekkend tempo geconsumeerd. Tal van redenen (economisch, veiligheid, milieu, legislatief,...) hebben ertoe geleid dat er steeds meer naar duurzame alternatieven gezocht wordt voor bestaande activiteiten.

Een voorbeeld van een dergelijk alternatief is het gebruik van membraantechnologie voor het uitvoeren van verschillende soorten scheidingen. De werking van membraanprocessen is gebaseerd op het gebruik van een semi-permeabele barrière, die selectief transport van componenten toelaat. De drijvende kracht over een membraan kan variëren afhankelijk van de procesvereisten. Het belangrijkste voordeel van dergelijke processen is dat ze aanzienlijk minder energie verbruiken dan traditionele scheidingsprocessen, zoals distillatie of evaporatie.

Nanofiltratie (NF) is een drukgedreven membraanproces waarbij laagmoleculaire componenten (200 - 1000 Da), opgelost in een vloeibaar medium, selectief verwijderd worden. NF wordt reeds geruime tijd toegepast in diverse milieutoepassingen, zoals de ontharding van drinkwater of de verwijdering van pesticiden uit oppervlaktewater. De techniek werd echter meer recent ook ontdekt als alternatief voor energie-intensieve scheidingstechnieken in de (chemische) procesindustrie. Hierdoor kan immers niet enkel een belangrijke besparing in energieverbruik nagestreefd worden, ook de operationele veiligheid neemt toe t.g.v. de minder kritische procescondities bij membraanprocessen, en milieugerelateerde risico's, zoals diffuse emissies, nemen sterk af. Het gebruik van membraantechnologie in industriële processen stelt echter andere vereisten aan de kwaliteit van de gebruikte membranen. Deze moeten in eerste instantie een hoge graad van stabiliteit vertonen in zure en organische middens, en bovendien moet de realiseerbare performantie economisch te verantwoorden te zijn, m.a.w. hoge solventfluxen en scheidingsgraden zijn een absolute voorwaarde.

Hoewel er met de productie van nieuwe solventresistente membranen, zowel polymeer als keramisch, al een belangrijke stap voorwaarts werd gezet, blijft de beperkte kennis over transportmechanismen een belangrijk nadeel voor de implementatie van deze techniek. NF-membranen situeren zich tussen dense omgekeerde osmose (RO) en poreuze ultrafiltratiemembranen (UF). De mechanismen die zich voordoen bij transport door deze twee laatste typen membranen is goed gekend en gemodelleerd,

gebaseerd op respectievelijk diffusief en convectief transport. De structuur van NF-membranen is echter niet eenduidig gedefinieerd (dens vs. poreus), zodat zowel diffusieve als convectieve bijdragen verwacht kunnen worden. Bovendien zijn bestaande modellen veelal ontwikkeld voor applicaties in waterige middelen. De toepassing van membraantechnologie in organische solventen zorgt voor een complexer geheel van interacties en parameters die het de prestatie van de membraaneenheid bepalen. Deze solventafhankelijk is nog ontoereikend bestudeerd.

De doelstelling van deze thesis is daarom het in kaart brengen van de prestatie van NF-membranen in organische solventen. In een eerste deel wordt het effect van organische solventen op polymere NF-membranen bestudeerd. Er zal nagegaan worden of een langdurige blootstelling van dergelijke membranen aan verschillende solventen de prestatie ervan beïnvloeden. Op deze manier kan de vereiste solventresistentie bestudeerd worden.

In een tweede deel wordt de permeabiliteit van organische solventen door verschillende NF-membranen bestudeerd. Er wordt getracht de belangrijkste parameters m.b.t. solventtransport door NF-membranen te identificeren; dit zijn zowel solventeigenschappen als membraankarakteristieken. De identificatie van deze parameters leidt tot de ontwikkeling van een nieuw transportmodel om de flux van organische solventen door NF-membranen te beschrijven.

In een derde deel wordt het transportgedrag van componenten, opgelost in organische solventen, doorheen diverse NF-membranen onderzocht. Door de membraanprestatie te bepalen voor verschillende membraan-solvent-component-combinaties kunnen ook hiervan de belangrijkste transportparameters bepaald worden. Op basis hiervan wordt een nieuwe methodologie voorgesteld om de retentie van opgeloste componenten in verschillende media te bepalen.

Tot slot wordt in een laatste deel de industriële toepasbaarheid van deze techniek nagegaan. Een overzicht van de verschillende toepassingsdomeinen wordt opgebouwd. Een gevalstudie uit de farmaceutische industrie wordt uitgewerkt met experimentele, technische en economische argumenten.

## **2. Materialen en methoden**

Om de transportmechanismen te bestuderen werden verschillende filtratie-experimenten uitgevoerd. Solventfluxen werden gemeten op een dead-end module (Sterlitech HP4750), retentieproeven op een zelf geconstrueerde cross-flow module. Deze testen werden uitgevoerd met binaire mengsels van water, methanol en/of ethanol, en met zuivere solventen uit verschillende chemische klassen: methanol, ethanol, aceton, ethylacetaat, *n*-hexaan, methyleenchloride en toluen. Referentiecomponenten met verschillende fysische eigenschappen werden geselecteerd op basis van moleculair

gewicht, polariteit, analyseerbaarheid en toxiciteit. Concentratiebepalingen van deze componenten gebeurden met UV/VIS-spectrofotometrie, gaschromatografie of HPLC.

Naast de dynamische filtratie-experimenten, die de volledige performantie (en dus totaal transport) in kaart brengen, werden ook statische celdiffusie-experimenten uitgevoerd. Deze maken het mogelijk om het belang van zuiver diffusief transport te bepalen.

In dit onderzoek werden zowel polymere als keramische membranen gebruikt. Deze werden aangeleverd door verschillende producenten, of commercieel verworven. NF-membranen zijn meestal composietmaterialen. De toplaag van solventresistente polymere NF-membranen bestaat meestal uit PES, PDMS, PA, PI of PAI. De polymere membranen die in dit onderzoek gebruikt werden zijn N30F en NF-PES-010 (Nadir), Desal-5-DK en Desal-5-DL (GE Osmonics), MPF-44 en MPF-50 (Koch), SolSep-169, SolSep01 en SolSep-030505 (SolSep), StarMem-120, StarMem-122 en StarMem-228 (MET). Keramische NF-membranen bestaan uit  $\text{TiO}_2$ ,  $\text{Al}_2\text{O}_3$  of  $\text{ZrO}_2$ ; membranen die in deze studie gebruikt werden zijn HITK-T1 (HITK), FSTi-128 en FSTi-129 (Vito). Er werden zowel hydrofiele als hydrofobe membranen bestudeerd. De MWCO's van al deze membranen, d.i. de moleculaire massa van een referentiecomponent die voor 90% weerhouden wordt, varieert tussen 150 en 1000 Da.

### **3. Effect van organische solventen op polymere NF-membranen**

In diverse disciplines en toepassingen vormt de beperkte resistentie van polymere materialen tegen organische solventen een belangrijk nadeel. De performantie van polymere NF-membranen is ook sterk solventafhankelijk. Dit is ten dele terug te brengen op de productiewijze van deze membranen. Een groot deel hiervan wordt immers aangemaakt via een fase-inversietechniek. Hierbij wordt een polymeeroplossing op een poreuze steunlaag gebracht door de oplossing in een 'niet-solvent' te brengen om een membraan te vormen. Als het membraan vervolgens echter opnieuw in een 'solvent' gebracht wordt, kan dit de samenstelling en de performantie ervan ernstig beïnvloeden, gaande van beperkt performantieverlies tot volledige desintegratie.

Om het effect van organische solventen op polymere NF-membranen te bestuderen, werd de performantie van N30F, NF-PES-010, MPF-44 en MPF-50 gekarakteriseerd aan de hand van een schoonwaterflux en de retentie van een referentiecomponent (maltose, MM 342) in een waterige oplossing. Vervolgens werden de gebruikte membranen gedurende 10 dagen blootgesteld aan 5 solventen (ethanol, aceton, ethylacetaat, methyleenchloride en *n*-hexaan), waarna de oorspronkelijke karakterisatie in waterig milieu herhaald werd. De resultaten van deze experimenten staan weergegeven in Tabel 1.

	Schoonwaterflux (l/u.m <sup>2</sup> )				Maltose-retentie (%)							
	N30F	NF-PES-010	MPF-44	MPF-50	N30F		NF-PES-010		MPF-44		MPF-50	
	(1)	(2)	(1)	(2)	(1)	(2)	(1)	(2)	(1)	(2)	(1)	(2)
A	36.4	-	162.8	-	38	-	22	-	96	27	30	64
B	38.3	32.1	162.7	92.8	39	4	11	23	97	-	30	43
C	33.7	38.0	148.0	34.5	39	5	16	17	80	78	37	44
D	35.0	27.5	144.8	167.8	47	29	17	19	90	78	35	34
E	37.5	-	172.2	-	25	-	24	-	87	82	34	21

Tabel 1: Schoonwaterflux en maltose-retentie voor N30F, NF-PES-010, MPF-44 en MPF-50 voor (1) en na (2) blootstelling aan verschillende organische solventen (A: methyleenchloride; B: *n*-hexaan; C: ethylacetaat; D: ethanol; E: aceton).

Het werd vastgesteld dat 3 van de 4 membranen zichtbare beschadiging vertoonden na blootstelling aan een of meerdere solventen. Bovendien wijzigde de performantie van alle membranen aanzienlijk. De interactiemechanismen tussen organische solventen en polymere membranen zijn verschillend voor hydrofiele en hydrofobe membranen. Hydrofiele membranen (N30F, NF-PES-010, MPF-44) ondergaan een reorganisatie van de polymeerketens, wat leidt tot grotere poriën, en bijgevolg lagere retenties van opgeloste componenten; schoonwaterfluxen blijven ongeveer constant. Hoewel grotere poriën een grotere schoonwaterflux zouden moeten opleveren, kan het constant blijven van deze flux voor en na solventbehandeling eveneens verklaard worden door de reorganisatie van het polymeermateriaal. Deze zorgt immers voor een afname van de hydrofiliciteit van het membraanoppervlak, wat het effect van grotere poriën neutraliseert. Deze afname van hydrofiliciteit van het membraanoppervlak werd bevestigd door contacthoekmetingen en de bepaling van de oppervlakte-energie van het membraan voor en na solventbehandeling. Bij hydrofobe membranen (MPF-50) wordt een omgekeerd effect waargenomen, hoewel minder uitgesproken. Er werd geconcludeerd dat MPF-50 de hoogste graad van solventresistentie vertoonde van de hier bestudeerde membranen. De hypothese van de reorganisatie van het membraan-materiaal werd eveneens ondersteund door SEM-opnames.

#### 4. Permeabiliteit van organische solventen door NF-membranen

Bij toepassingen van membraantechnologie in waterig milieu werd slechts beperkte aandacht besteed aan de eigenschappen van het 'solvent' water, met uitzondering van de afhankelijkheid van de viscositeit. Bij de uitbreiding van de technologie naar niet-waterige toepassingen moet echter de

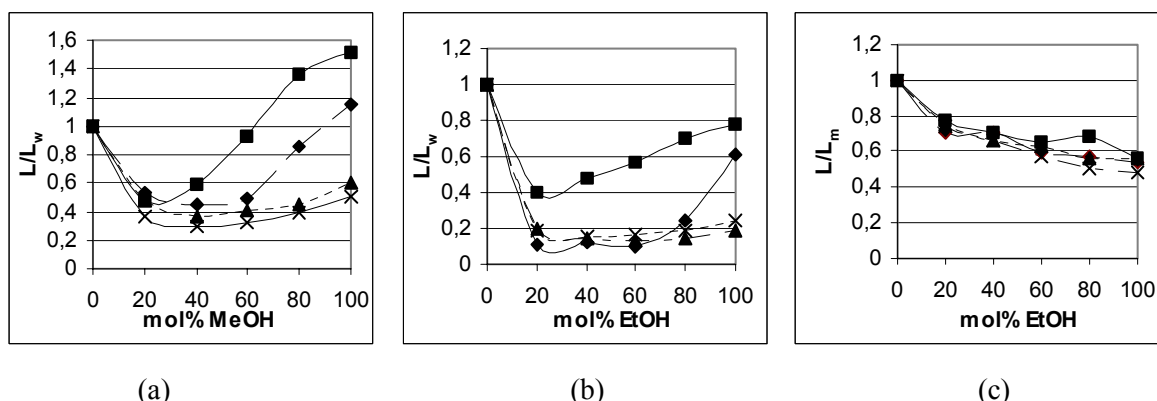
solvent-afhankelijkheid van de procesperformantie in rekening gebracht worden. Hiervoor moeten zowel de transportmechanismen bepaald worden, als de solveiteigenschappen en membraankarakteristieken die hiermee gepaard gaan. Op deze manier kan een transportmodel voor de permeabiliteit van organische solventen doorheen NF-membranen opgesteld worden.

#### *Parameters die de solventpermeabiliteit beïnvloeden*

Om meer inzicht in de parameters die de solventpermeabiliteit beïnvloeden, werd het fluxgedrag van binaire mengsels van water, methanol en/of ethanol bestudeerd. Hierdoor kan ondubbelzinnig geanalyseerd worden welke eigenschappen van het vloeistofmengsel, afhankelijk van de voedingssamenstelling, de permeabiliteit beïnvloeden. De experimenten werden uitgevoerd met 7 polymere membranen en 1 keramisch (MPF-44, MPF-50, Desal-5-DK, Desal-5-DL, NF-PES-010, N30F, SolSep-030505, FSTi-209) in een dead-end module.

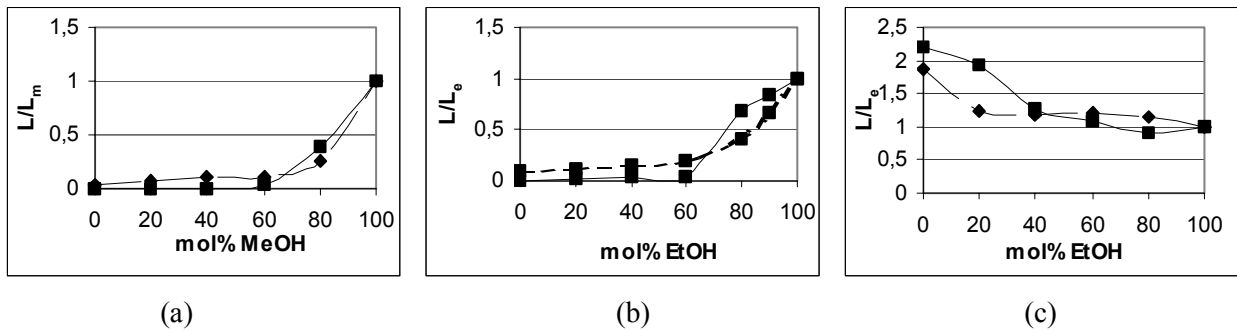
Uit vergelijking van de GC-analyses van voedings- en permeaatstalen bleek dat er geen wijziging ontstond in de samenstelling van het mengsel. Aangezien water, methanol en ethanol verschillende diffusiesnelheden door een zelfde materiaal hebben, wijst dit er op dat solventtransport door deze membranen quasi volledig door convectie of gekoppelde diffusie gebeurt.

De permeabiliteit door NF-membranen hangt af van diverse parameters, niet alleen membraankarakteristieken, zoals de poriegrootte, de porositeit, de tortuositeit, of de membraandikte, maar ook van verschillende solveiteigenschappen. De permeabiliteit doorheen hydrofiele membranen (Figuur 1) vertoonden een hoge correlatie met de inverse viscositeit. Het geobserveerde minimum in permeabiliteit bij water-alcohol-mengsels beantwoordt inderdaad aan een maximum in viscositeit van deze mengsels.



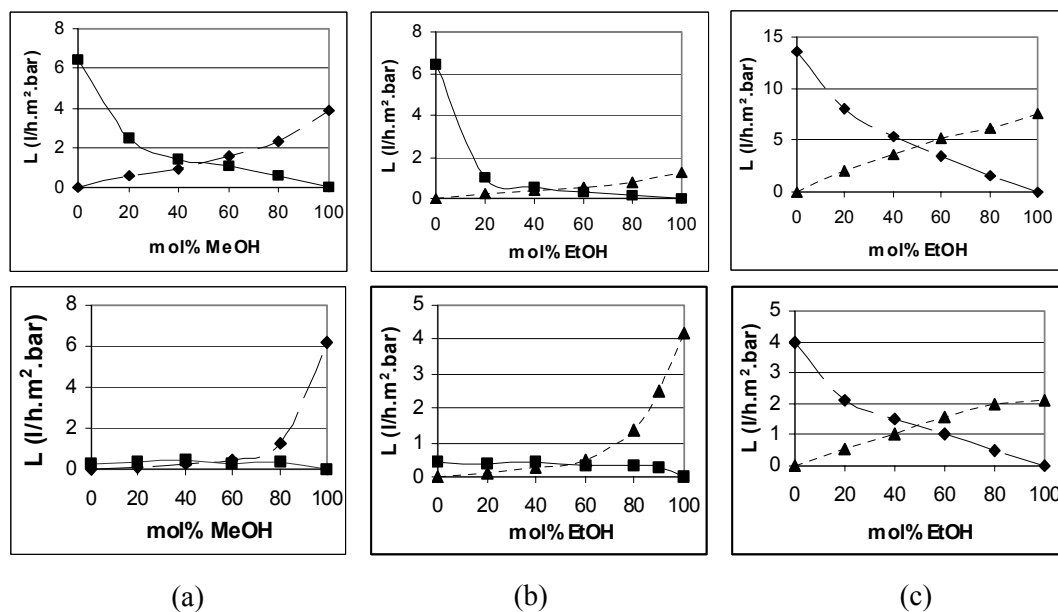
Figuur 1: Genormaliseerde permeabiliteit doorheen hydrofiele membranen voor (a) water-methanol, (b) water-ethanol en (c) methanol-ethanol (◆: MPF-44); (■: NF-PES-010); (▲: Desal-5-DL); (×: Desal-5-DK)

De permeabiliteit doorheen hydrofobe membranen (Figuur 2) vertoont echter geheel ander gedrag. Er werd geen minimum in de permeabiliteitscurves vastgesteld. Dit betekent dat de experimentele data niet beantwoorden aan de wet van Darcy, en er bijgevolg andere parameters dan enkel de solventviscositeit de permeabiliteit beïnvloeden. Zoals verwacht spelen ook polariteitseffecten aan de vloeistof-membraan-interfase een belangrijke rol. Polaire solventen, in het bijzonder water, moeten bij hydrofobe membranen een veel grotere oppervlakteweerstand overwinnen alvorens permeatie mogelijk is.



Figuur 2: Genormaliseerde permeabiliteit doorheen hydrofobe membranen voor (a) water-methanol, (b) water-ethanol en (c) methanol-ethanol (◆: MPF-50); (■: SolSep-030505)

Het belang van polariteitseffecten wordt bevestigd door de bepaling van de partiële fluxen voor de verschillende membraan-solvent-combinaties (Figuur 3). Hieruit bleek dat de permeabiliteit van de relatief meest polaire component uit een binair mengsel doorheen een hydrofiel membraan sterker beïnvloed wordt door de toevoeging van een apolaire component dan omgekeerd. Voor de partiële fluxen doorheen hydrofobe membranen werd het omgekeerde vastgesteld.



Figuur 3: Partiële permeabiliteit voor (a) water-methanol, (b) water-ethanol and (c) methanol-ethanol mixtures (■: water; ◆: methanol; ▲: ethanol) doorheen Desal-5DK (boven) en MPF-50 (onder).

De permeabiliteit van de water-methanol-ethanol-mengsels doorheen het keramisch membraan (FSTi-209) vertoonde gelijkaardig gedrag als de hydrofiel polymere membranen. Fluxen in zuiver solvent zijn echter aanzienlijk lager dan doorheen polymere membranen.

#### *Modellering van de solventflux*

Op basis van de experimentele gegevens en de in de literatuur beschikbare transportmodellen (Hagen-Poiseuille, Jonsson and Boesen, Machado *et al.* en Bhanushali *et al.*) werd geconcludeerd dat een veralgemeend transportmodel voor de beschrijving van solventfluxen doorheen NF-membranen ten minste drie parameters moet bevatten: een maat voor transport van momentum, een maat voor de sterische hinder die solventmoleculen ondervinden bij permeatie, en een maat voor de membraan-solvent-interactie (m.a.w. de polariteitseffecten).

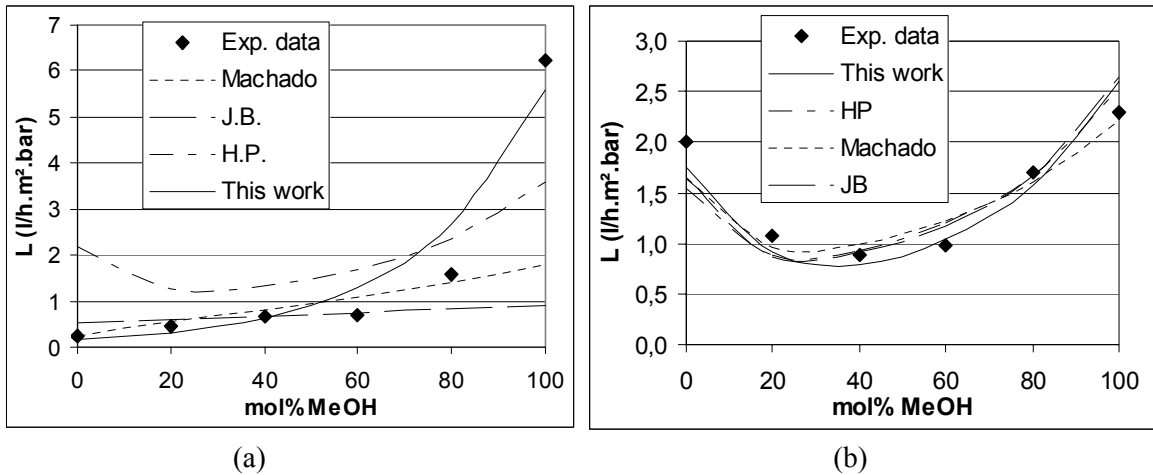
Transport van momentum wordt in verschillende modellen weergegeven door de viscositeit  $\eta$  van het solvent in rekening te brengen. Deze parameter werd ook voor het nieuwe model weerhouden. Sterische hinder is gerelateerd aan de grootte van de solventmoleculen. Op basis van het model van Bhanushali *et al.* werd geopteerd om het molair volume van de solventmolecule  $V_m$  als maat te gebruiken. De membraan-solvent-interacties werden tenslotte voorgesteld door het verschil in oppervlaktespanning tussen het membraanoppervlak en het solvent  $\Delta\gamma$ . Dit is gebaseerd op massaoverdrachtsbeperkingen bij interfase-componenttransport, en werd door Machado *et al.* voorgesteld als maat voor polariteitseffecten bij membraanprocessen. Dit resulteerde in volgend transportmodel:

$$J \propto \frac{V_m}{\eta \cdot \Delta\gamma} \quad (1)$$

De experimentele data voor de filtratietesten met de binaire water-methanol-ethanol-mengsels werden gefit met 4 modellen: Hagen-Poiseuille, Jonsson-Boesen, Machado *et al.* en het nieuwe model dat zelf voorgesteld werd. Niet-beschikbare modelparameters, zoals de tortuositeit of de porositeit van het membraan, werden verwerkt in de fitparameter. Om de fitresultaten voor de verschillende modellen met elkaar te kunnen vergelijken, en bijgevolg de beste fit te bepalen, werden de foutenvarianties berekend.

Het nieuwe model leverde significant betere fitresultaten op voor de beschrijving van de solventpermeabiliteit doorheen hydrofobe NF-membranen (Figuur 4.a). De combinatie van lage permeabiliteit voor waterrijke mengsels en de sterk toenemende permeabiliteit voor alcoholrijke mengsels kon enkel door het nieuwe model benaderd worden. De verschillende modellen leverden vergelijkbare fitresultaten op voor de beschrijving van de flux doorheen hydrofiel membranen (Figuur 4.b). Hoewel het nieuwe model een duidelijke verbetering is in vergelijking met bestaande modellen, moet dit model verder verfijnd worden door aan de verschillende parameters

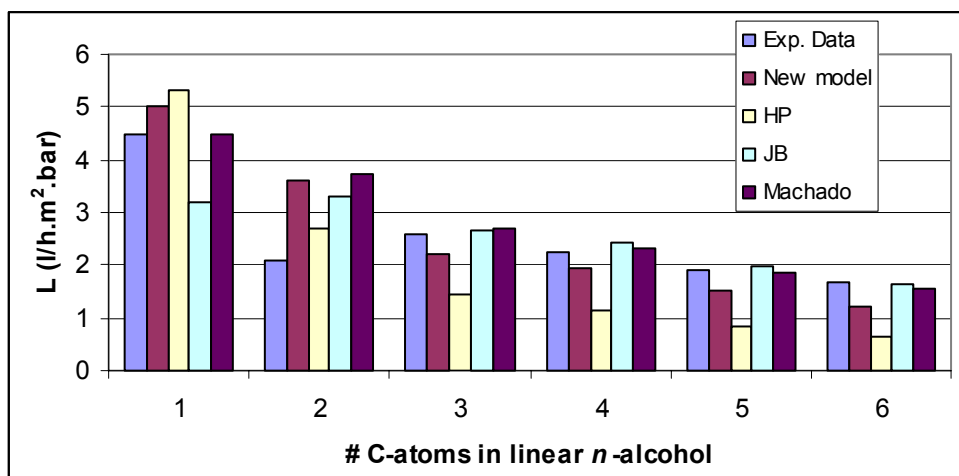
gewichtsfactoren toe te kennen, die rekening houden met verschillende membraankarakteristieken, in het bijzonder de verhouding van de grootte van de solventmoleculen en de poriegrootte.



Figuur 4: Experimentele permeabiliteitsgegevens voor een water-methanol-mengsel doorheen (a) een hydrofoob MPF-50 membraan en (b) een hydrofiel MPF-44 membraan, gefit met de modellen van Hagen-Poiseuille (HP), Jonsson en Boesen (JB), Machado *et al.* en het zelf voorgestelde model.

#### Permeabiliteit van zuivere solventen

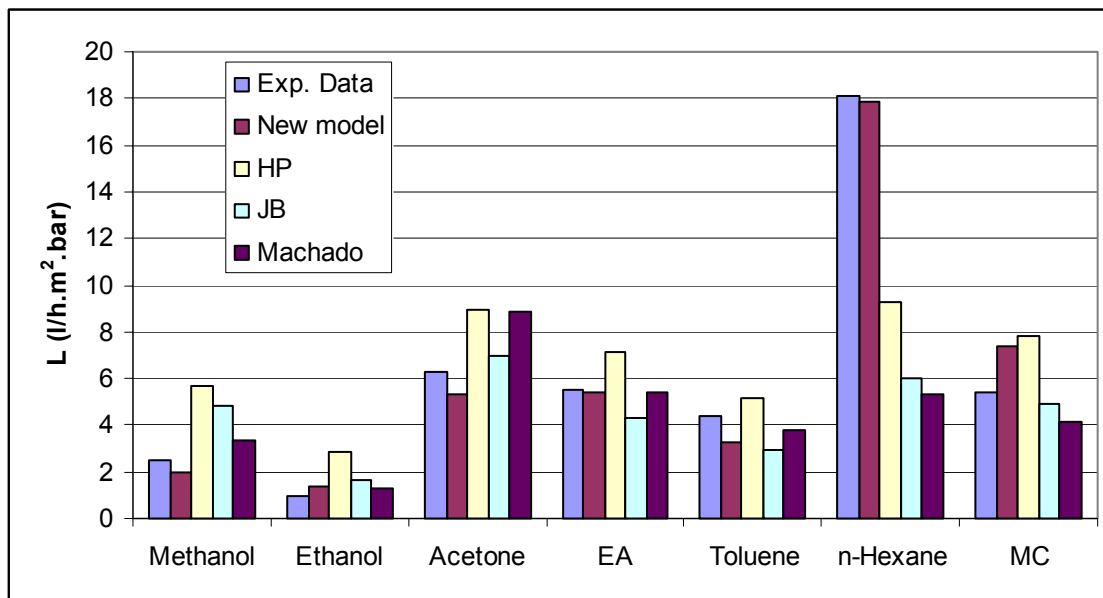
De waarde van het nieuwe model werd ook nagegaan voor het fluxgedrag van zuivere solventen doorheen NF-membranen. In eerste instantie werd de permeabiliteit van een homologe alcoholreeks (methanol – 1-hexanol) doorheen het hydrofobe SolSep-030505 membraan bepaald (Figuur 5). De permeabiliteit van deze alcoholen bleek af te nemen met stijgend aantal koolstofatomen. Het nieuwe model leverde vergelijkbare resultaten op als het model van Machado, dat ontwikkeld werd op basis van experimentele gegevens uit metingen met homologe solventreeksen, en aanzienlijk betere resultaten dan de modellen van Hagen-Poiseuille en van Jonssen-Boesen.



Figuur 5: Modelling van de permeabiliteit van een homologe reeks van primaire alcoholen doorheen een SolSep-030505 membraan, m.b.v. het nieuwe model en de modellen van Hagen-Poiseuille (HP), Jonsson en Boesen (JB) en Machado *et al.*



Vervolgens werden ook de fluxen voor zuivere solventen uit verschillende solventklassen (methanol, ethanol, aceton, ethylacetaat, toluen, *n*-hexaan en methyleenchloride) doorheen een MPF-50 membraan bepaald. Deze resultaten blijken op het eerste gezicht moeilijk te interpreteren, aangezien de relevante transportparameters zeer verschillend kunnen zijn voor deze solventen. De fitresultaten (Figuur 6) tonen echter aan dat het nieuwe model significant betere resultaten oplevert dan de drie andere modellen.



Figuur 6: Modelling van de permeabiliteiten van organische solventen uit verschillende chemische klassen doorheen een MPF-50 membraan, m.b.v. het nieuwe model en de modellen van Hagen-Poiseuille (HP), Jonsson en Boesen (JB) en Machado *et al.* (EA: ethylacetaat; MC: methyleenchloride)

### Besluit

De permeabiliteit van organische solventen doorheen NF-membranen is afhankelijk van de solventviscositeit, de moleculaire grootte van het solvent en het verschil in oppervlaktespanning tussen het membraanoppervlak en de solventmolecule. Er werd een nieuw model ontwikkeld voor de beschrijving van de solventflux doorheen NF-membranen. Dit model kon zowel de flux van solventmengsels, als van een homologe reeks van alcoholen, als van zuivere solventen uit verschillende chemische klassen beschrijven, en kan bijgevolg als een krachtig model met een breed toepassingsbereik beschouwd worden.

## 5. Transport van opgeloste componenten bij NF in organische solventen

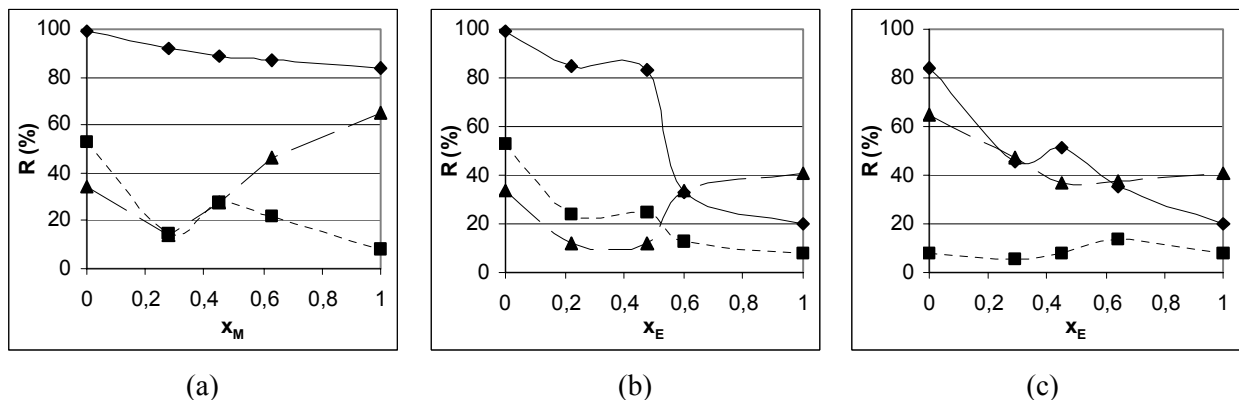
Om een indicatie te geven over de poriegrootte en het scheidingsvermogen van NF-membranen (in waterige oplossing) wordt veelal gebruik gemaakt van de moleculaire gewichtscut-off (MWCO), d.i.

de moleculaire massa van een referentiecomponent die voor 90% weerhouden wordt. Deze parameter kan echter niet toegepast worden als indicatie voor de prestatie van eenzelfde membraan in organische solventen. Membraan-solvent-component-interacties worden dan immers niet in rekening gebracht.

*Parameters die het transport van opgeloste componenten doorheen NF-membranen beïnvloeden*

Om te bestuderen welke parameters (van solvent, membraan en component) bepalend zijn voor het transportgedrag van organische componenten, opgelost in organische solventen, doorheen NF-membranen, werden in eerste instantie een reeks van filtratie-experimenten uitgevoerd met een 0,1 mM raffinose oplossing in een reeks van binaire mengsels van water, methanol en/of ethanol. Volgende NF-membranen werden gebruikt, in een crossflow-module: Desal-5-DK, N30F, MPF-50 en FSTi-209.

Figuur 7 toont de resultaten voor de 3 polymere membranen. In zuiver water is de retentie het hoogst voor Desal-5-DK, dan voor N30F, en het laagst voor MPF-50. Dit beantwoordt aan de gespecificeerde MWCO's, respectievelijk 180, 400 en 700 Da. De poriëgrootte is inderdaad een eerste bepalende transportparameter, en de MWCO wordt vaak als maat hiervoor gebruikt. Voor de hydrofiele membranen (Desal-5-DK en N30F) blijkt het echter dat de suikerretentie in de water-alcohol-mengsels daalt bij toenemende alcoholfractie in de voeding. Dit kan verklaard worden door de interactie tussen de opgeloste componenten en de organische solventen; solvatatie van organische componenten beïnvloedt de effectieve diameter van deze componenten, die bijgevolg solventafhankelijk is. Aangezien solvatatie een minder sterke interactie is dan hydratatie (met watermoleculen) daalt de effectieve diameter van raffinose naarmate er meer alcohol in het mengsel, en daalt hierdoor de retentie. Dit effect werd ook kwantitatief bepaald; de effectieve diameters van raffinose bedragen 1,25, 1,09 en 1,03 nm in respectievelijk water, methanol en ethanol. Bijgevolg zijn de component-solvent-interacties een tweede parameter die het transport beïnvloeden.



Figuur 7: Retentie van raffinose voor Desal-5-DK, N30F en MPF-50, in mengsels van (a) water-methanol, (b) water-ethanol en (c) methanol-ethanol

Nog uit Figuur 7 blijkt echter dat voor het hydrofobe MPF-50 de retentie van raffinose in de water-alcohol-mengsels toeneemt bij grotere alcoholfractie in de voeding, wat op het eerste gezicht in tegenspraak lijkt met het solvatatie-effect dat beschreven werd voor de hydrofiele membranen. De verklaring hiervan wordt echter gevonden in membraan-solvent-interacties. Net zoals de opgeloste componenten wordt ook het membraanmateriaal gesolvateerd door de gebruikte solventen. Hierdoor wordt de poriegrootte solventafhankelijk. Bovendien is de affiniteit van het membraanmateriaal voor verschillende organische solventen sterk afhankelijk van het solvent zelf; hydrofobe membranen interageren bijvoorbeeld niet met watermoleculen, zodat er ook geen hydratatie van de poriwand optreedt. Alcoholen solvateren het hydrofobe materiaal wel en zorgen voor een verkleining van de poriegrootte, en dus voor een stijging van de retentie. Membraan-solvent-interacties zijn bijgevolg de derde factor die het componenttransport beïnvloeden.

De resultaten voor het keramische FSTi-209 membraan waren vergelijkbaar met deze voor het polymere Desal-5-DK membraan. Aangezien de dalende retenties in alcoholrijke mengsels ook bij keramische membranen optreedt, kan gesteld worden dat dit fenomeen niet enkel te wijten is aan zwellingeffecten van de gebruikte NF-membranen. Dit bevestigt dat het transport van opgeloste componenten doorheen NF-membranen in organische solventen afhankelijk is van de nominale poriegrootte (MWCO), de component-solvent-interacties (effectieve componentdiameter) en de membraan-solvent-interacties (effectieve poriediameter).

#### *Transport van opgeloste componenten in NF van organische solventen*

NF-membranen situeren zich op alle vlakken tussen poreuze UF- en dense RO-membranen. Aangezien er in de literatuur nog steeds geen consensus bestaat of transport van opgeloste componenten doorheen NF-membranen gebeurt door convectie dan wel diffusie, werd er vervolgens een experiment opgezet om het relatieve belang van beide transportmechanismen te bepalen. Op basis van statische celdiffusie-experimenten kan het diffusief transport voor een gegeven membraan-solvent-component-combinatie bepaald worden. Door deze resultaten te vergelijken met die van dynamische filtratieproeven (en dus het totaaltransport) kan het belang van diffusief en convectief transport eenduidig bepaald worden.

Deze reeks van experimenten werd uitgevoerd met een hydrofiel en een hydrofoob membraan (Desal-5-DK en MPF-50) in methanol en ethanol. 6 referentiecomponenten werden geselecteerd. Het werd vastgesteld dat de diffusieve bijdrage maximaal 7,5% was. Transport van opgeloste componenten doorheen NF-membranen in organische solventen gebeurt dan ook hoofdzakelijk door convectie.

*Modellering van transport van opgeloste componenten in NF van organische solventen*

In de literatuur zijn verschillende modellen beschikbaar voor de beschrijving van het transport van opgeloste componenten in waterig milieu. Deze modellen kunnen echter niet zonder meer gebruikt worden voor de beschrijving van de membraanperformantie in organische solventen, aangezien er geen solventafhankelijkheid in rekening gebracht wordt. Daarom werd een methodologie ontwikkeld die toelaat om deze modellen te kunnen toepassen voor de beschrijving van het transport van opgeloste componenten bij NF in organische solventen.

Essentieel voor de modellering van het transport van opgeloste componenten doorheen NF-membranen in organische solventen is het in rekening brengen van effectieve component- en poriediameters. De effectieve componentdiameter kan op verschillende manieren berekend worden (b.v. Stokes-Einstein). Aangezien dit echter vaak omslachtige berekeningen omvat, gebaseerd op parameters die onbekend zijn, blijft dit veelal slechts benaderend. Daarom werd geopperd om een empirische methode te hanteren en de effectieve componentdiameter in water te bepalen op basis van de moleculaire massa van de component:

$$d_c = 0,065(MW)^{0,438} \quad (2)$$

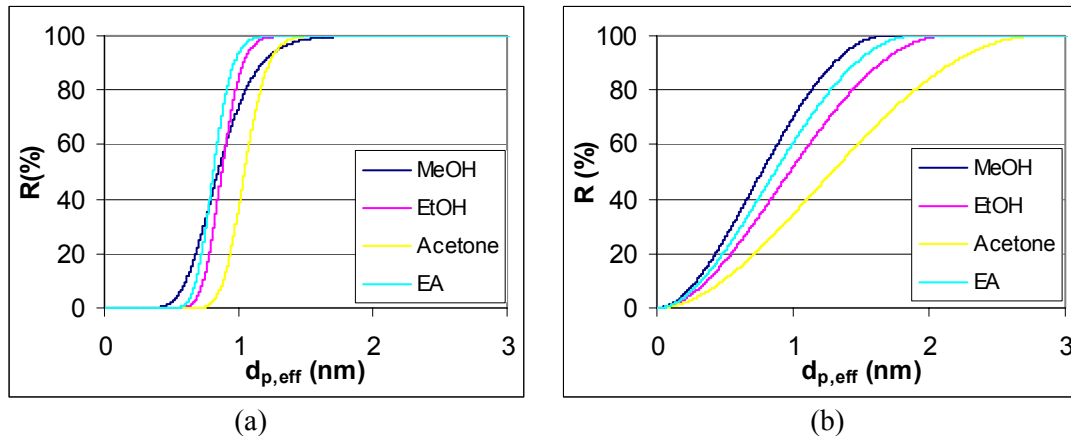
Vervolgens kan de effectieve diameter van de betreffende component in een willekeurig solvent bepaald worden m.b.v. de Wilke-Chang-vergelijking:

$$\frac{d_c^{s_2}}{d_c^{s_1}} = \frac{(\phi_{s_1} M_{s_1})^{1/2}}{(\phi_{s_2} M_{s_2})^{1/2}} \quad (3)$$

Aangezien ook de poriediameter solventafhankelijk is, dient deze ofwel gespecificeerd te zijn door de fabrikant, ofwel moet deze experimenteel bepaald worden (door fitting).

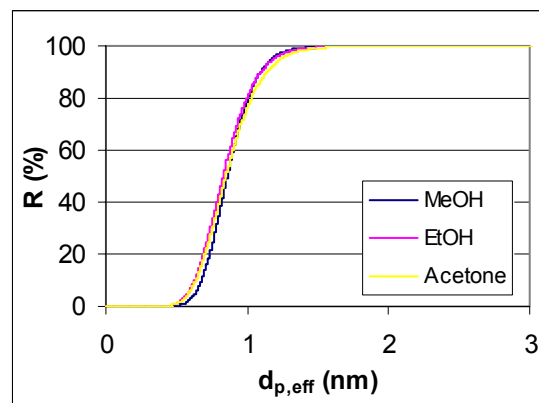
Deze methodologie werd toegepast op 4 beschikbare modellen: SHP-model, Ferry-model, Verniory-model en lognormaal-model. Aangezien de effectieve poriediameters niet gekend zijn, werd in een eerste deel een beschrijvende modellering uitgevoerd, zodat ongekende modelparameters door datafitting bepaald konden worden. Hiervoor werden experimentele gegevens gebruikt van filtratieproeven met 6 referentiecomponenten in methanol, ethanol, aceton, ethylacetaat en *n*-hexaan. Zowel polymere (MPF-44, MPF-50, Desal-5-DK, SolSep-169) als keramische membranen werden gebruikt (FSTi-128, HITK-T1).

Als illustratie toont Figuur 8 de verschillende reflectiecurven (d.i. de retentie als functie van de effectieve componentdiameter) voor het hydrofiele MPF-44, berekend met het lognormaal- en het Ferry-model. Hieruit blijkt dat de reflectiecurven (voor een bepaald model) duidelijk solventafhankelijk zijn. Daar er reeds gewerkt wordt met effectieve componentdiameters, bevestigt dit dat ook de poriegrootte solventafhankelijk is en dat hiervoor in de verschillende modellen een specifieke parameter in rekening gebracht moeten worden.



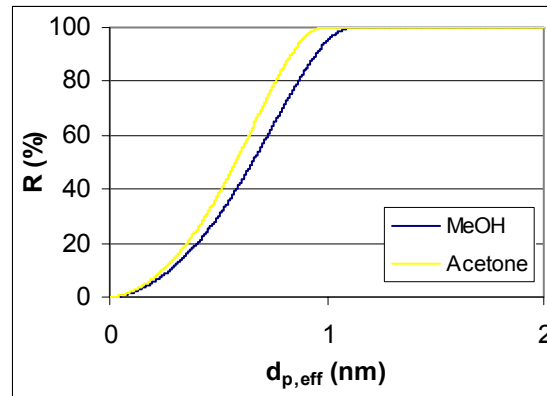
Figuur 8: Effect van het solventtype (methanol, ethanol, aceton, ethylacetaat) op de reflectiecurve voor MPF-44, berekend met (a) het lognormaal-model en (b) het Ferry-model

De modellering van de reflectiecurven voor het hydrofobe MPF-50 membraan vertoont echter een ander resultaat (Figuur 9). Het werd vastgesteld dat de reflectiecurven in de verschillende solventen quasi identiek zijn. De solventafhankelijkheid blijkt dus veel minder sterk te zijn dan voor hydrofiele membranen, wat in overeenstemming is met eerdere experimentele bevindingen (Hfdst. 3); hydrofobe membranen vertonen een betere solventstabiliteit dan hydrofiele membranen.



Figuur 9: Effect van het solventtype (methanol, ethanol, aceton) op de reflectiecurve voor MPF-50, berekend met het lognormaal-model

De modellering van de reflectiecurven voor keramische membranen (Figuur 10) toont nogmaals dat ook voor dergelijke membranen de effectieve poriegrootte solventafhankelijk is, en dat membraan-solvent-interacties daadwerkelijk het transport van opgeloste componenten beïnvloeden onder de vorm van solvatatie-effecten. Transport van opgeloste componenten moet hierdoor niet noodzakelijk aan zwellings-effecten gerelateerd worden.



Figuur 10: Effect van het solventtype (methanol, aceton) op de reflectiecurve voor HITK-T1, berekend met het lognormaal-model

Om deze methodologie te valideren werden de gefitte modelparameters gebruikt voor de predictieve modellering van de retentie van raffinose in zuiver methanol en ethanol, die ook voorafgaand experimenteel bepaald werd (Tabel 2).

	Parameters MPF-50	$R_{MeOH}$	$R_{EtOH}$	Parameters Desal-5-DK	$R_{MeOH}$	$R_{EtOH}$
SHP	$d_p^{MeOH} = 1,42$ $d_p^{EtOH} = 1,41$	54	48	$d_p^{MeOH} = 1,05$ $d_p^{EtOH} = 1,72$	87	33
Ferry	$d_p^{MeOH} = 1,80$ $d_p^{EtOH} = 1,82$	54	48	$d_p^{MeOH} = 1,21$ $d_p^{EtOH} = 2,33$	85	33
Verniory	$d_p^{MeOH} = 1,97$ $d_p^{EtOH} = 2,00$	54	48	$d_p^{MeOH} = 1,29$ $d_p^{EtOH} = 2,56$	85	33
Lognormal	$\bar{d}_p^{MeOH} = 0,86; S_p = 0,19$ $\bar{d}_p^{EtOH} = 0,83; S_p = 0,22$	53	47	$\bar{d}_p^{MeOH} = 0,17; S_p = 1,75$ $\bar{d}_p^{EtOH} = 0,96; S_p = 0,29$	82	28
Exp. data	-	65	41	-	84	20

Tabel 2: Voorspelde retentie van raffinose in methanol en ethanol met MPF-50 en Desal-5-DK, vergeleken met experimentele data

Uit de resultaten in Tabel 2 blijkt dat de retenties van raffinose, voorspeld met de 4 verschillende modellen, vergelijkbare resultaten oplevert voor een gegeven membraan-solvent-combinatie. Het maximale verschil bedraagt 5% (voor Desal-5-DK in methanol). Bij vergelijking van de modelwaarden met de experimentele data, wordt er een hoge correlatie gevonden.

## 6. Industriële toepasbaarheid van NF in organisch milieu

In 2002 waren ruim een half miljoen mensen tewerkgesteld in de Vlaamse industrie, die bijgevolg een belangrijke speler is in de regionale economie. Deze industriële activiteit gaat echter gepaard met een ongewenste belasting op de omgeving. Mede door de toenemende, wereldwijde concurrentie en de steeds strengere wetgeving op diverse domeinen ontstaat de noodzaak om industriële productie steeds efficiënter te laten verlopen. Het gebruik van membraantechnologie kan vanuit deze optiek een belangrijk alternatief worden voor traditionele processen als distillatie en evaporatie. Diverse toepassingen in waterig milieu werden reeds geïmplementeerd; het gebruik van membraantechnologie in organische solventen is echter nog veel minder verspreid.

### *Toepassingen van nanofiltratie in organische solventen*

In de literatuur worden enkele verschillende toepassingen beschreven in verschillende industriële sectoren. De grootste industriële NF-plant voor het behandelen van organische solventen wordt gebruikt in de petrochemische industrie voor het hergebruik van extractiesolvent, gebruikt voor de verwijdering van wassen uit olie. Op de Exxon-Mobil raffinaderij in Beaumont (Texas, USA) wordt op deze manier dagelijks 11500 m<sup>3</sup> solvent behandeld.

Ook in de voedingsindustrie worden organische solventen zeer vaak als extractiemiddel gebruikt voor voedingsoliën, meer bepaald hexaan en aceton. In de VS alleen wordt jaarlijks meer dan 2 miljoen ton extractiesolvent verbruikt. NF kan hier een belangrijk alternatief zijn, aangezien in de voedingsindustrie vaak met thermolabiele componenten gewerkt wordt.

In de chemische industrie worden diverse toepassingen gevonden. De meest gerapporteerde is de herwinning van katalysatoren bij chemische synthesestappen. Deze katalysatoren zijn kritisch in de procesvoering, maar vormen meestal een zeer hoge kost. Herwinning van deze katalysator is bijzonder moeilijk met traditionele procestechnieken. Het gebruik van solventresistente NF-membranen kan echter een oplossing bieden.

Ook voor processen waarbij solventuitwisseling plaats vindt, biedt het gebruik van membraantechnologie een belangrijk alternatief voor bestaande uitkookprocedures, in het bijzonder voor nauwkokende en azeotrope mengsels, en voor solventuitwisselingen waarbij het kookpunt van het tweede solvent aanzienlijk lager ligt dan het eerste solvent.

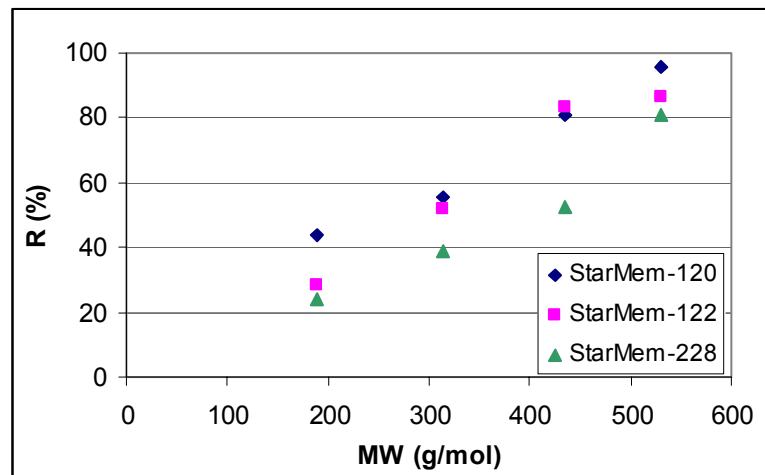
Belangrijke toepassingen kunnen ook gevonden worden in de farmaceutische sector. Hierover werd een gevalstudie uitgevoerd.

### *Gevalsstudie: solventhergebruik in de farmaceutische industrie*

De farmaceutische sector neemt met 29 bedrijven een belangrijke plaats in in de Vlaamse industrie. Vier van deze bedrijven hebben ook een productie-afdeling voor actieve farmaceutische ingrediënten (API's) in Vlaanderen. Hierbij worden zeer grote volumes organische solventen verbruikt, in hoofdzaak als reactiemedium en als grondstof. In dit onderzoek werd een gevalstudie uitgevoerd in

samenwerking met Janssen Pharmaceutica (Geel, België), waarin de mogelijkheid van solvent-recyclage door middel van NF onderzocht werd.

In een eerste deelonderzoek werd nagegaan of NF-membranen bruikbaar zijn voor de verwijdering van API's uit toluen. Hiervoor werden filtratie-experimenten uitgevoerd met 4 API's (10 ppm in toluen), waarvan de moleculaire massa's varieerden van 189 tot 531. Figuur 11 toont de experimenteel bepaalde retenties voor de 3 bestudeerde membranen (StarMem-120, StarMem-122, StarMem-228). Het blijkt dat voor de 2 grootste API's (MM 435 en 531) retenties van meer dan 80% kunnen gerealiseerd worden. Met betrekking tot hun specifieke productieprocessen, bestond er vanuit Janssen Pharmaceutica echter hoofdzakelijk interesse in de combinatie van toluen met de kleinste API (MM 189), waarbij slechts 43% retentie gerealiseerd werd. Specifiek onderzoek moet aantonen of dit volstaat om bestaande processen verder te optimaliseren.



Figuur 11: API-retentie in toluen

In een tweede deelonderzoek werd de verwijdering van een API (MM 721) uit methanol bestudeerd. Hiervoor werden het StarMem-120 en StarMem-228 membraan gebruikt, welke een retentie van respectievelijk 91% en 93% opleverden. Aangezien dit economisch te verantwoorden waarden zijn, werd het potentieel voor deze scheiding verder onderzocht.

De bestudeerde stroom wordt tot op heden behandeld in een distillatieproces, met een debiet van 417 l/u. Als een opbrengst van 80% gewenst is, beantwoordt dit aan een permeaatdebiet van 334 l/u. Hiervoor is een membraanoppervlakte van 4,05 m<sup>2</sup> nodig (StarMem-120). Membrane Extraction Technology levert spiraalgewonden modules van verschillende dimensies; 1 module van 4" x 40" (à 3700 Euro) volstaat om het gespecificeerde debiet te behandelen. Ten gevolge van de hoge opbrengst daalt echter de geobserveerde retentie tot 77%. In een 2-stapsproces kan de retentie tot 93% gebracht worden, met slechts een beperkt verlies aan opbrengst (76% i.p.v. 80%).



Om het volledige methanoldebiet te behandelen in een traditionele distillatie is een vermogen van 162 MWh vereist. Een membraanopstelling vergt slechts 795 kWh om hetzelfde debiet te behandelen, m.a.w. ruim 200 keer minder.

Het blijkt inderdaad dat membraanprocessen beduidend minder energie-intensief zijn dan klassieke scheidingsprocessen. Een gedetailleerde economische analyse blijft echter noodzakelijk om te implementatie van de technologie in een productie-omgeving te verantwoorden. Hierbij moeten bovendien de optimale procescondities voor het membraanproces bepaald worden.

## **Besluit**

In dit onderzoek werd het gebruik van nanofiltratie als scheidingstechniek in organische solventen bestudeerd. De implementatie van membraantechnologie in niet-waterig milieu vereist de beschikbaarheid van solventresistente materialen. Voor de productie van dergelijke membranen werden polymeren met verhoogde solventresistentie en keramische materialen gebruikt.

Solventtransport doorheen NF-membranen gebeurt hoofdzakelijk door convectie (of gekoppelde diffusie). De flux van organische solventen doorheen NF-membranen is afhankelijk van zowel viskeuze als oppervlakte-effecten. Een transportmodel voor de beschrijving van de solvent-permeabiliteit werd opgesteld; hierin zitten 3 parameters vevat: de viscositeit van het solvent, de grootte van de solventmoleculen en het verschil in oppervlaktespanning tussen het solvent en het membraanmateriaal. Dit model kon de permeabiliteit van zowel water-alcohol-mengsels beschrijven, als de fluxen voor een homologe reeks van alcoholen, als de fluxen voor zuivere solventen uit verschillende chemische klassen.

Het transport van opgeloste componenten doorheen NF-membranen gebeurt eveneens hoofdzakelijk door convectie. De retentie wordt beïnvloed door 3 effecten: de nominale poriegrootte, de effectieve componentdiameter (solvatatie t.g.v. component-solvent-interacties) en de effectieve poriediameter (solvatatie t.g.v. membraan-solvent-interacties). Op basis van bestaande modellen voor de beschrijving van reflectiecurven in waterig milieu werd een methodologie ontwikkeld om ook het transport van opgeloste componenten doorheen NF-membranen in organische solventen te beschrijven. Hiervoor dienen zowel de effectieve component- als de effectieve poriediameter in rekening gebracht te worden. De modellering van de reflectiecurven bevestigde dat de effectieve poriediameter solventafhankelijk is. Na bepaling van onbekende modelparameters kon de methodologie ook gehanteerd worden voor predictieve modellering.

Een gevalstudie toonde aan dat het gebruik van membraantechnologie een belangrijk alternatief kan worden voor traditionele scheidingsprocessen in de farmaceutische industrie. Het energieverbruik voor een membraanopstelling ligt ruim 200 keer lager dan een distillatie die eenzelfde stroom kan behandelen.



# *Chapter 1*

## *Membrane technology*

## 1. Membrane technology

Blood cleaning in human kidneys, making a cup of coffee, using air masks in dusty situations, air filtering in car engines, rinsing vegetables with a colander, ... applications of filters and membranes are found all around in daily life, often even without the user's knowledge.

Membranes are selective barriers that can be used to separate mixtures of liquids or gases, into a concentrated and a diluted stream. They are at the heart of every membrane process and can be considered as a semi-permeable material between two phases. Membranes have the ability to transport one component more readily than others because of differences in physical and/or chemical properties between the membrane and the permeating components (Mulder, 1996). Figure 1.1 shows a schematic generalised representation of membrane separation.

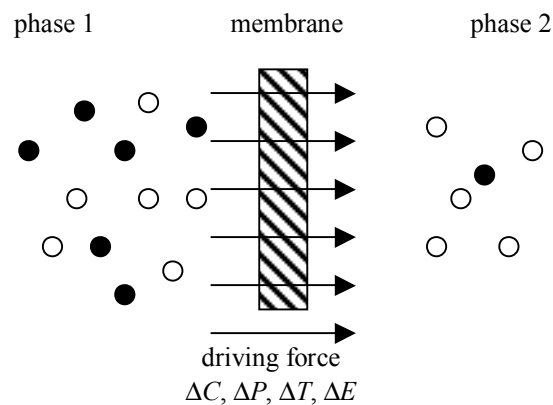


Figure 1.1: Schematic representation of a two-phase system separated by a membrane

The first scientific milestones concerning membrane technology date already from the 18<sup>th</sup> century (Nollet, 1748), but for a long time membrane technology was restricted to laboratory scale experiments, e.g. as a bacteria filter in the 20's and 30's of the previous century (micro- and ultrafiltration) (Zsigmondy and Bachmann, 1918). The membranes available in those days provided insufficient separations for use in large-scale applications. However, in the second half of the 20<sup>th</sup> century, the development of asymmetric polymeric membranes by Loeb and Sourirajan created a breakthrough for the opportunities of membrane technology as an industrial separation tool (Loeb and Sourirajan, 1962). These membranes consist of a very thin top layer supported by, possibly different, porous sublayers, allowing the actual separation to take place in the thin top layer (or skin), whereas the other layer(s) are only used as support. Since the permeation rate is inversely proportional to the thickness of the actual barrier layer, this structure leads to higher permeation rates than symmetric membranes of the same thickness. Since the development of these membranes, membrane technology has grown steadily with different new industrial applications, e.g. the treatment of drinking water (Watson and Hornburg, 1989), process water (van 't Hul *et al.*, 1997) and wastewater (Belfort *et al.*,

1973), dehydration of organic solvents (Tusel and Brüsckhe, 1985) and solvent recovery in lube oil refinery (White and Nitsch, 2000).

Today, a large number of membrane processes exist. These processes have some important advantages compared to the traditional separation processes, such as continuous working mode, reduced energy consumption, easy up-scaling and flexible construction due to modular design (Mulder, 1996). Furthermore, no additional chemicals are required during membrane processes and combination with other separation techniques can lead to improved separations. The main disadvantages are loss of performance due to membrane fouling and additional costs from membrane cleaning and replacement. The different types can be classified based on the driving force for the separation. Possible driving forces are pressure difference, temperature difference, concentration difference and a difference in electric potential across the permselective membrane. Table 1.1 summarises the different types of membrane processes and their respective driving force (Mulder, 1996).

Pressure difference	Concentration difference	Temperature difference	Electric potential difference
Microfiltration	Pervaporation	Thermo-osmosis	Electrodialysis
Ultrafiltration	Gas separation	Membrane distillation	Electro-osmosis
Nanofiltration	Dialysis		
Reverse osmosis	Liquid membranes		

Table 1.1: Overview of membrane processes and their driving force

## 2. Pressure driven membrane processes and nanofiltration

Pressure driven membrane processes are used to remove different types of solutes from a liquid feed stream. Transport of the solvent occurs from the feed side to the permeate side because a pressure is applied over the membrane. Solutes are retained by the membrane; the fraction of the solvent that remains at the feed side of the membrane contains an increased concentration of the solute. This fraction is usually a waste stream, except when the concentrated fraction is the desired product.

Generally, four types of pressure driven membrane processes are distinguished (Mulder, 1996): microfiltration (MF), ultrafiltration (UF), nanofiltration (NF) and reverse osmosis (RO). Although these separation techniques are related to each other, each of them has specific characteristics. The differences are mainly situated at the level of pore sizes, transport mechanisms and applied pressure. The main features of the four processes are summarised in Table 1.2. The pore sizes, which correspond to the size of the molecules retained by the membrane, are illustrated in Figure 1.2.

Nanofiltration is one of the most recently introduced terms in membrane technology. Eriksson (1988) was the first author to use the word ‘nanofiltration’ explicitly. Nanofiltration membranes found their origin in modified reverse osmosis membranes having high water fluxes. Whereas reverse osmosis membranes are dense materials, without a distinct pore structure and where diffusion is thus the main transport mechanism, nanofiltration operates at the interface of porous and non-porous membranes, and sometimes the term ‘loose RO’ is used instead of nanofiltration. Nanofiltration therefore requires much lower working pressures than reverse osmosis, leading to significant energy savings. Rejections may be somewhat lower, but the removal of multivalent ions and relatively small organic molecules (> 200 g/mol) is still nearly complete. On the low-pressure side of nanofiltration, ultrafiltration is situated. Although nanofiltration membranes with ‘large’ pores are similar to ultrafiltration membranes with ‘small’ pores, ultrafiltration is basically a different process. In ultrafiltration, distinct pores are present and these membranes work as sieves. For nanofiltration, the transport system has characteristics of both sieving and diffusion. Most nanofiltration membranes also have a surface charge, so that electric interactions also add to the transport and rejection behaviour.

The most important drawback of nanofiltration membranes is the problem to control the reproducibility of the membrane pore size and the pore size distribution. Moreover, nanofiltration membranes are liable to fouling, possibly resulting in important flux decline.

	Applied pressure (bar)	Flux range (l/h.m <sup>2</sup> .bar)	Transport mechanism	Application range
Microfiltration	0.1-2	> 50	Sieving	Removal of particles
Ultrafiltration	1-5	10-50	Sieving	Removal of macromolecules
Nanofiltration	5-15	1.4-12	Sieving Diffusion Charge effects	Removal of multivalent ions and relatively small organic molecules
Reverse osmosis	10-100	0.05-1.4	Diffusion	Removal of ions and (small) organic molecules

Table 1.2: Overview of pressure driven membrane processes

Nanofiltration membranes are used in a wide range of applications from several types of industries: water softening (Bodzek *et al.*, 2002), removal of pesticides and other organic micropollutants (Berg *et al.*, 1997; Van der Bruggen *et al.*, 1998), concentration of whey and other protein containing streams (Atra *et al.*, 2005), purification of pharmaceutical broths (Capelle *et al.*, 2002), treatment of waste water from the textile industry (Van der Bruggen *et al.*, 2001; Koyuncu *et al.*, 2004), water reuse in the brewery sector (Braeken *et al.*, 2004), removal of heavy metals (Abu Qdais and Moussa, 2004), solvent recovery in soybean oil extraction (Raman *et al.*, 1996),...

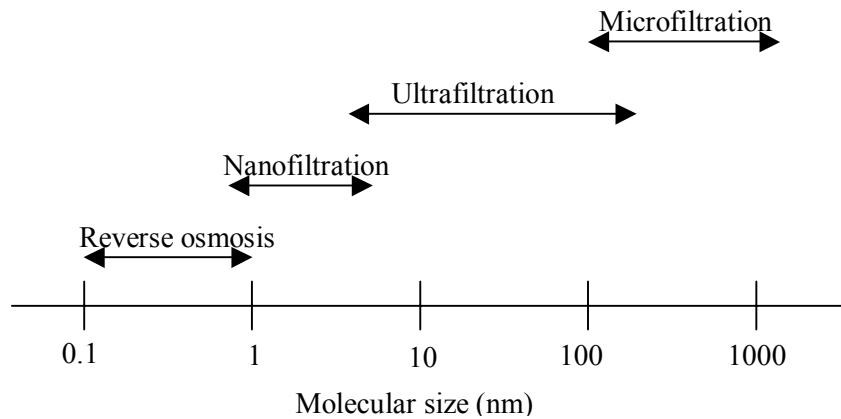


Figure 1.2: Pore sizes in pressure driven membrane processes

### 3. Principles and definitions

Membrane processes can be classified on the base of the system design as well. Because of the large number of applications and module configurations, the design of membrane filtration systems can differ significantly (Mulder, 1996; Koros *et al.*, 1996).

The simplest design is the dead-end operation. Here all the feed is forced through the membrane, which implies that the concentration of rejected components in the feed increases and consequently the quality of the permeate decreases with time. For industrial applications, a cross-flow mode is preferred because of the lower fouling tendency relative to dead-end systems. In the cross-flow operation, the feed flows parallel to the membrane surface with the inlet feed stream entering the membrane module at a certain composition. Cross-flow filtration requires more energy, due to the pumping, but remains interesting in case of nanofiltration and reverse osmosis, where the energy surplus is small compared to the energy required for the separation. The feed stream is separated into two: a permeate and a retentate stream. Figure 1.3 provides a schematic drawing of the two module operations.

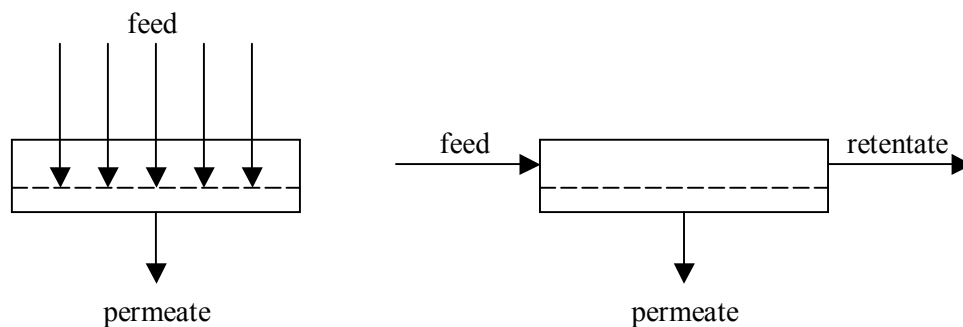


Figure 1.3: Schematic drawing of dead-end and cross-flow filtration

Membrane processes are indeed characterised by the fact that the feed stream is divided into two streams, namely into the retentate (or concentrate) stream and the permeate stream (Figure 1.4). Either the permeate or the retentate stream can be the desired product. If the aim is concentration, the retentate is the product stream; in the case of purification, both the permeate and the retentate can yield the desired product, depending on the impurities to be removed.

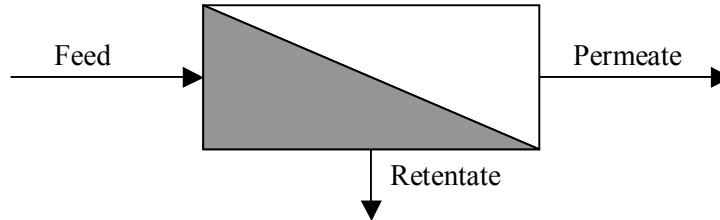


Figure 1.4: Schematic representation of a membrane process

The performance of a membrane process is essentially determined by three parameters: the solvent permeability through the membrane, the solute rejection and the recovery (Mulder, 1996; Koros *et al.*, 1996).

The solvent flux  $J$  is the volume of the solvent permeating through the membrane ( $V$ ) per unit of time and area. In case of a linear relationship between the solvent flux and the transmembrane pressure, the solvent permeability  $L$  is defined as the ratio of the solvent flux and the pressure difference applied. At elevated pressures, the linear relationship between flux and pressure is no longer valid.

$$L = \frac{J}{\Delta P} = \frac{\Delta V}{A \cdot \Delta t \cdot \Delta P} \quad (1.1)$$

The rejection  $R$  of a given component  $i$  is defined as:

$$R = \left( 1 - \frac{c_{p,i}}{c_{f,i}} \right) \cdot 100\% \quad (1.2)$$

Where  $c_{p,i}$  is the permeate concentration and  $c_{f,i}$  is the feed concentration of component  $i$ .  $R$  is a dimensionless parameter and its value normally varies between 0 % (free transport of solvent and solute through the membrane) and 100 % (complete rejection of the solute). In particular cases, negative rejections have been reported, e.g. due to charge effects with multicomponent salt solutions or for solutes with a high degree of affinity for the membrane surface.

The recovery (or the yield)  $S$  is defined as the ratio of the permeate stream ( $Q_p$ ) and the feed stream  $Q_f$ :

$$S = \frac{Q_p}{Q_f} \cdot 100\% \quad (1.3)$$



This is mainly a parameter used for the design of industrial applications rather than a membrane characteristic. The recovery can be varied by the module design and typical values for industrial plants are near 80 %.

#### **4. Nanofiltration of organic solvents**

Solvents are substances or mixtures of substances that are used to dissolve, to dilute, to emulsify or to suspend other substances, enabling a treatment or a removal. In a narrower sense, the term solvent is only used for an organic solvent. Some of the more important properties of a solvent are the polarity, the volatility, the stability, the toxicity, the flammability and the colour (Durrans and Davies, 1971).

Based on their volatility, organic solvents are typically divided into three classes: non-volatile components, semi-volatile components and volatile components (VOC) (Loncke *et al.*, 1996). The latter are all solvents with a vapour pressure higher than 0.1 kPa at normal conditions (Block *et al.*, 2004). In general, these are small molecules, characterised by a high vapour pressure and a large Henry-constant. VOCs are by far the largest class of organic solvents and are commonly used in industrial processes.

Organic solvents are also often classified based on their chemical structure. Different functional groups are distinguished for organic solvents: hydrocarbons, halogenated hydrocarbons, alcohols, esters, ketones, ethers, amines, amides, aldehydes, phenols,... (Bräutigam and Kruse, 1992; Reichardt, 2003)

Initially, research on nanofiltration was only focused on applications with aqueous feed streams, such as, e.g. the softening of drinking water and the removal of pesticides from surface water. Several large-scale nanofiltration plants have been realised, e.g. in Florida (USA), in Méry-sur-Oise (France) and in Safron Waldon (England). However, more recently, the potential of nanofiltration membranes as a separation tool in non-aqueous media has been discovered (Raman *et al.*, 1996; Schmidt *et al.*, 1999; Zwijnenberg *et al.*, 1999). The first generation of nanofiltration membranes, which were polymeric loose RO-membranes, did not allow application in organic solvents. This was due to the lack of chemical resistance of the membrane polymers against these solvents, leading to important losses in performance (Reddy *et al.*, 1996; Whu *et al.*, 2000; Nwaha, 2000).

The increased interest in nanofiltration of organic solvents, from both researchers and membrane consumers, was the direct consequence of the improved quality of a new generation of nanofiltration membranes (Cuperus and Ebert, 2002). On the one hand, membrane manufacturers succeeded in producing thin film composite (TFC) membranes, consisting of specialty polymers, being highly resistant against a large number of organic solvents. TFC membranes are membranes having a thin

dense top layer (tens of nanometers) deposited on an asymmetric support (Figure 1.5). The asymmetric support is a membrane, in its turn consisting of a thin top layer (thickness 0.1-1  $\mu\text{m}$ ) supported by a porous sublayer (thickness 50-500  $\mu\text{m}$ ) (Mulder, 1996). TFC-membranes combine the high selectivity of a dense membrane with the high permeation rate of a very thin (but mechanically less stable) membrane. The different layers mostly consist of different polymeric materials and each layer is optimised independently, so that optimal performance is obtained with respect to selectivity, permeation rate, and chemical, thermal and mechanical stability. Typical polymers used for non-aqueous nanofiltration are polydimethylsiloxane (PDMS), polyethersulphon (PES), polyamide (PA), polyimide (PI), polyacrylonitrile (PAN),... (Cuperus and Ebert, 2002)

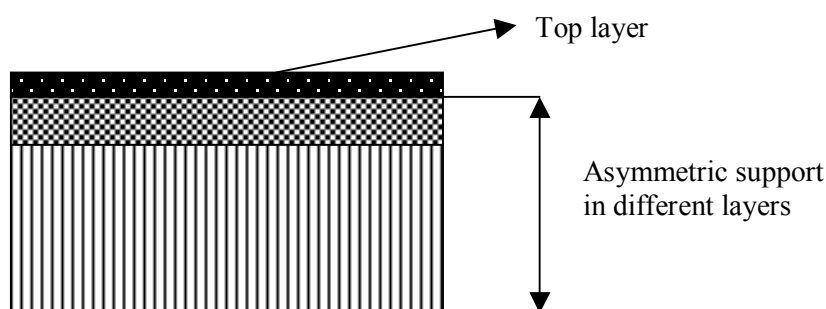


Figure 1.5: Schematic representation of a thin film composite membrane

On the other hand, the investigation of ceramic materials made significant progress (Tsuru *et al.*, 2000; Van Gestel *et al.*, 2002). When compared to polymeric materials, ceramics have a high degree of chemical, thermal and mechanical stability. Therefore, for a long time ceramic membranes appeared to be a promising technique for applications in non-aqueous media. Yet, the production process of ceramic membranes was poorly controllable and membranes showed a low degree of reproducibility. Moreover, the typical pore sizes obtained with traditional production techniques were situated only in the range of micro- and ultrafiltration. These were the two major drawbacks, together with the high material cost of ceramics, for fruitful use of ceramic membranes in large-scale applications. Current research could overcome these drawbacks and nowadays reproducible ceramic nanofiltration membranes are commercially available. Most common materials for ceramic NF-membranes are  $\text{Al}_2\text{O}_3$ ,  $\text{TiO}_2$  and  $\text{ZrO}_2$ .

The availability of solvent stable nanofiltration membranes was gratefully discovered by potential users in industry. Increasing competition asks for process intensification, optimal production processes and minimal waste of natural resources and energy (Cuperus and Ebert, 2002). Compared to traditional separation techniques in non-aqueous media, such as distillation and evaporation, membrane processes consume a significantly smaller amount of energy, thus potentially leading to important cost savings (Mulder, 1996). Furthermore, in contrast to distillation processes, which mostly

run at elevated working temperatures, membrane units can operate at moderate temperatures, which may have several advantages: thermolabile components are no longer submitted to the risk of deterioration, liquid streams require smaller set-ups than similar vapour streams, the amount of diffuse losses of volatile organic components (VOCs) can be reduced, and the general risks involved with organic solvents, e.g. the risk for explosions, decrease as well. The implementation of membrane processes as a separation tool in organic solvents therefore has not only economical benefits; also important advantages concerning safety and environmental related problems must be pointed to.

In different industrial branches, especially nanofiltration membranes have a very promising future. Non-aqueous nanofiltration is investigated in different fields in the pharmaceutical, in the food and in the (petro)chemical industry. Some applications are: the recovery of solvent in lube oil dewaxing processes (Gould *et al.*, 2001), the reuse of extraction solvent in food industry (Raman *et al.*, 1996; Ebert and Cuperus, 1999), the recovery of homogeneous catalyst in chemical synthesis (Nair *et al.*, 2001), decolourisation of waste streams (Desai *et al.*, 2002), purification of pharmaceutically active ingredients (Whu *et al.*, 2000),...

## **5. Aim of this work**

The aim of this work is to gain insight in the transport mechanisms occurring in nanofiltration of organic solvents. This information can be used to evaluate existing transport models, or establish new models that describe nanofiltration of organic components. This would allow characterising a membrane in terms of a set of well-defined parameters from which the filtration properties can then be derived.

Since nanofiltration membranes are situated at the interface of porous and non-porous materials, the discussion about whether transport occurs by convection or diffusion is still on-going. Furthermore, expanding the use of this technology from aqueous applications to a large number of solvents, complicates the process significantly. In previous work, the influence of the solvent (water) could often be ignored. In this work, however, the performance of the membranes has to be evaluated in terms of all solvent-solute-membrane interactions.

More specifically, the research should cover three fields: membrane stability in organic solvents, parameters that influence the solvent flux through the membrane, and parameters that influence the rejection of organic molecules by nanofiltration membranes. Both for the solvent flux as for the determination of solute rejections, existing models will be evaluated, and new models will be developed based on the insight in the transport mechanisms.

Chapter 2 presents the methods and materials that have been used in this work.

Different research papers reported the loss in performance of polymeric nanofiltration membranes in organic solvents, due to solvent-membrane interactions (Raman *et al.*, 1996; Subramanian *et al.*, 1998; Musale and Kumar, 2000; Bridge *et al.*, 2002). The effect can vary from little swelling to complete dissolution or disintegration, which is mostly related to the phase inversion techniques used for membrane manufacturing. Over the last years, membranes with improved solvent resistance came on the market, resulting in significantly better performances of these membranes in organic solvents. As a high degree of membrane stability is required for application, the stability of polymeric membranes in organic solvents is discussed in Chapter 3.

As mentioned before, the performance of a membrane unit is mostly characterised by the solvent permeability and the solute rejection. Chapter 4 deals with the first parameter. It is known that the permeability of organic solvents through nanofiltration membranes is affected by a number of solvent properties. More parameters should be taken into account for the description of the solvent flux than has been done before for the modelling of the water flux. Several authors suggested solvent and membrane properties that affect the solvent flux: the viscosity, the dielectric constant, the molecular size, the surface tension and the diffusion coefficient have been reported as relevant solvent properties (Reddy *et al.*, 1996; Machado *et al.*, 1999; Bhanushali *et al.*, 2001), important membrane characteristics are the pore size, the porosity, the tortuosity, the membrane thickness, and the surface tension of the membrane (Mulder, 1996; Machado *et al.*, 2000; Hestekin *et al.*, 1999).

Different models for the description of the solvent permeability have been presented (Jonsson and Boesen, 1975; Mulder, 1996; Machado *et al.*, 2000; Bhanushali *et al.*, 2001), but none of these could cover the whole range of membranes and solvents used in non-aqueous nanofiltration. New experimental data will be used to develop a new transport model for the description of the solvent flux through nanofiltration membranes, based on the models available in the literature.

The second parameter characterising the membrane performance, namely the solute rejection, will be studied in detail in Chapter 5. A parameter often used as an indication for the rejections that can be realised with a given membrane in aqueous solution is the Molecular Weight Cut-Off (MWCO), which is the molecular weight of a reference component that is rejected for 90% (Mulder, 1996). However, in non-aqueous nanofiltration a larger number of membrane-solvent-solute interactions are observed. It was reported that solute rejections are mostly lower in organic solvents than in aqueous solution. The MWCO, characterised in aqueous solution, is therefore not of use in other solvents. This was confirmed by experimental data on solute rejection in organic solvents (Whu *et al.*, 2000; Yang *et al.*, 2001; White, 2002).

As nanofiltration membranes are situated between porous ultrafiltration and dense reverse osmosis membranes, it is still not clear whether solute transport occurs by convection or diffusion. As a

consequence, no suitable models for the description of the solute transport are available in the literature. Different attempts have been presented (Gibbins *et al.*, 2002; White, 2002), but not all membrane-solvent-solute interactions observed in experiments could be incorporated. Therefore, the balance between convective and diffusive transport must be analysed, and existing transport models for solute transport in aqueous solution (Ferry, 1936; Verniory *et al.*, 1973; Nakao and Kimura, 1982; Van der Bruggen, 2000) will be modified to enable the application in organic solvents.

Finally, different applications have been reported in the literature. Several authors reported on the use of solvent resistant nanofiltration as a tool for solvent recovery from lube oil filtrates (Bhore *et al.*, 1999; White and Nitsch, 2000). Raman *et al.* (1996) studied the application of membrane technology in the vegetable oil industry. A large number of research papers are dedicated to using nanofiltration membranes in chemical synthesis, in terms of homogeneous catalyst separation and re-use (Nair *et al.*, 2001; Luthra *et al.*, 2001; Scarpello *et al.*, 2002; Aerts *et al.*, 2004). Livingston *et al.* (2003) reported the use of solvent resistant nanofiltration membranes as an alternative technique for solvent exchange. The industrial application of solvent resistant nanofiltration will be discussed in Chapter 6, in which the theoretical findings from the previous chapters will also be further developed in a case study. The applicability of non-aqueous nanofiltration will be considered in industrial streams: solvent recovery from waste streams from pharmaceutical production processes will be investigated.



# *Chapter 2*

## *Methods and materials*

## 1. Membrane filtration units

### 1.1 Dead-end filtration module

Batch filtration experiments were carried out with a Sterlitech HP4750 Stirred Cell (Figure 2.1).



Figure 2.1: Sterlitech HP4750 Stirred Cell

The dead-end filtration module is manufactured from stainless steel and can be used for pressures up to 69 bar. A circular membrane disk with a diameter of 49 mm is placed at the bottom of the filtration module, the active top layer towards the feed solution. The membrane is sealed between a teflon O-ring and a stainless steel porous support. In this way, the membrane surface has an active area of 0.00146 m<sup>2</sup>. The feed solution can be magnetically stirred with a (teflon coated) stirrer bar. The rotation of the stirrer can be varied from 0 to 1200 rpm. Pressure at the feed side is supplied by an inert gas (N<sub>2</sub>). Fluxes are determined by measuring the time difference  $\Delta t$ , required to collect a certain volume of permeate  $V_p$  (or mass  $m_p$ ). The flux can then be calculated from Eq. 2.1:

$$J\left(\frac{l}{h.m^2}\right) = \frac{V_p(ml) \cdot 3600\left(\frac{s}{h}\right)}{1000\left(\frac{ml}{l}\right) \cdot \Delta t(s) \cdot A(m^2)} \quad (2.1)$$

where  $A$  (m<sup>2</sup>) is the effective membrane area.

### 1.2 Cross-flow filtration installation

For the filtration experiments in continuous mode, a solvent compatible laboratory scale filtration apparatus was built (Figure 2.2). It is important that all materials used are solvent resistant, in order to



guarantee continuous operation and to avoid diffuse losses of organic vapours. For safety reasons, the apparatus is positioned under an exhaust hood. Piping is made from stainless steel and all sealings are from teflon or kalrez. Also the pump, flow and pressure controls have to be compatible with a large range of organic solvents. Furthermore, the use of organic solvents includes the risk of a discharge of static electricity; the piping is therefore earthed at several places. A schematic diagram of the equipment is shown in Figure 2.3.



Figure 2.2: Cross-flow filtration unit

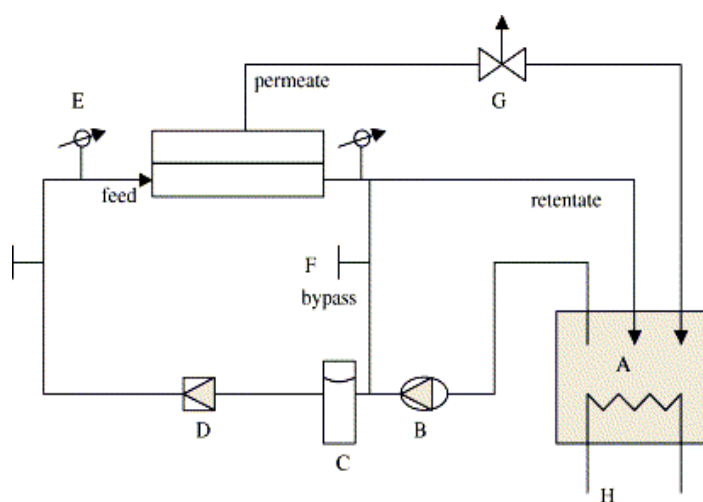


Figure 2.3: Cross-flow nanofiltration equipment (A = feed tank; B = pump; C = pulsation dampener; D = flow meter; E = pressure meter; F = bypass valve; G = permeate sampling; H = cooling coil)

From a feed container (4 litre volume) the liquid feed solution is supplied to the membrane cell by a plunger pump (Heukelom LN-40), having a capacity of 420 l/h and a maximal working pressure of 30 bar. The pump is manually controlled. Before the feed reaches the membrane module, it passes a pulsation dampener (Flowguard FG-30-215-FPM-SS-A-3/4" BSP) to create a continuous and constant feed flow, independent on the pump pulses. The filtration system is completed with a flow control (Kobold DF-K) and a pressure control over the membrane unit (Kobold SCH-DCM-63). Circular flat sheet membranes are used with a diameter of 25 mm and an active surface of 0.000405 m<sup>2</sup>. The design of the module (for flat sheet membranes) with the flow pattern is shown in Figure 2.4. Ceramic membranes are tested with a tubular module, also shown in Figure 2.4. The length of these ceramic membranes was 100 mm (including sealings) and the inner diameter was 5 mm. The active surface of the ceramic membranes was 0.0014 m<sup>2</sup>.

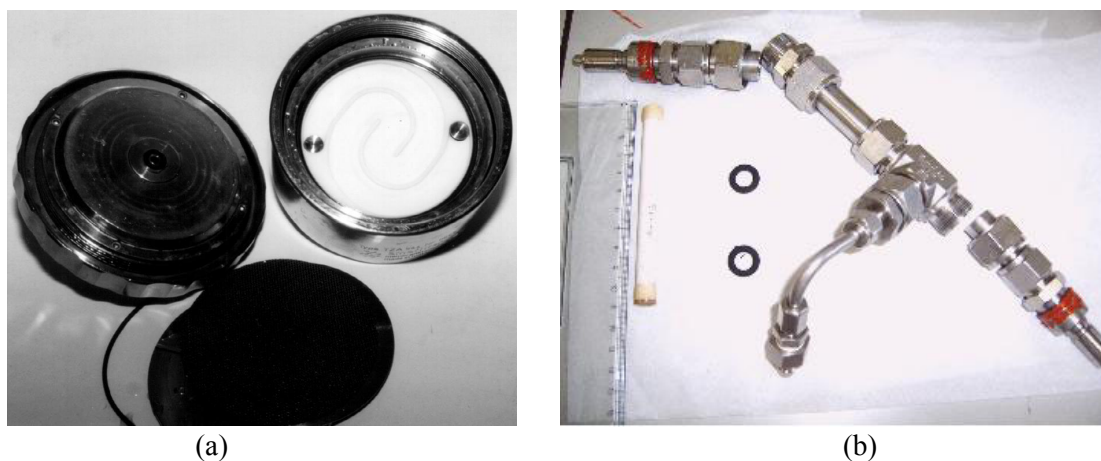


Figure 2.4: The nanofiltration module for (a) flat sheet membranes, with the design of the filtration path, and (b) tubular ceramic membranes

## 2. Membranes

### 2.1 Membrane types

In this work several solvent resistant NF-membranes from different manufacturers have been studied. All the solvent resistant polymeric membranes available on the market have been used in this work. Ceramic membranes were prototypes manufactured by research institutes. Table 2.1 provides a review of the membranes used, along with the most important characteristics, as provided by the manufacturers. The MWCO or Molecular Weight Cut-Off is defined as the molecular weight of a reference solute corresponding to a 90 % rejection for a given membrane and a given solvent, and is a parameter that is often used in membrane technology for the indication of the separation quality of the

membrane. It is expected that other membrane properties, such as the pore size, the pore size distribution and the degree of hydrophilicity, are more important with respect to the performance, but none of this information is provided by the manufacturers. Figure 2.5 shows the molecular structures of the different top layer materials.

Membrane	Manufacturer	Material	MWCO (Da)	T <sub>max</sub> (°C)	L (l/h.m <sup>2</sup> .bar)	R (%)	Used since
N30F	Nadir <sup>a</sup>	PES	400	95	1.0-1.8 <sup>h</sup>	70-90 <sup>l</sup>	2000
NF-PES-010	Nadir <sup>a</sup>	PES	1000	95	5-10 <sup>h</sup>	30-50 <sup>l</sup>	2000
MPF-44	Koch <sup>b</sup>	PDMS	250	40	1.3 <sup>h</sup>	98 <sup>m</sup>	2000
MPF-50	Koch <sup>b</sup>	PDMS	700	40	1.0 <sup>i</sup>	-°	2000
Desal-5-DK	Osmonics <sup>c</sup>	PA	150-300	90	5.4 <sup>h</sup>	98 <sup>n</sup>	2002
Desal-5-DL	Osmonics <sup>c</sup>	PA	150-300	90	9.0 <sup>h</sup>	96 <sup>n</sup>	2002
SolSep-030505	SolSep <sup>d</sup>	-*	-°	90	1.0 <sup>j</sup>	>90 <sup>p</sup>	2002
SolSep-169	SolSep <sup>d</sup>	-*	-°	150	10 <sup>j</sup>	95 <sup>p</sup>	2002
SolSep-01	SolSep <sup>d</sup>	-*	-°	150	10 <sup>j</sup>	97 <sup>q</sup>	2002
HITK-1T	HITK <sup>e</sup>	TiO <sub>2</sub>	220	-°	5 <sup>h</sup>	-°	2003
FSTI-128	VITO <sup>f</sup>	TiO <sub>2</sub>	420	-°	21 <sup>h</sup>	-°	2003
FSTI-209	VITO <sup>f</sup>	TiO <sub>2</sub>	430	-°	22 <sup>h</sup>	-°	2004
StarMem-120	MET <sup>g</sup>	PI	200	60	1.0 <sup>k</sup>	-°	2005
StarMem-122	MET <sup>g</sup>	PI	220	60	1.0 <sup>k</sup>	-°	2005
StarMem228	MET <sup>g</sup>	PI	280	60	0.26 <sup>k</sup>	-°	2005

Table 2.1: Solvent resistant nanofiltration membranes used in this study and membrane characteristics as specified by the manufacturers (<sup>a</sup> Nadir Filtration GmbH, Wiesbaden, Germany; <sup>b</sup> Koch Membrane Systems, Wilmington, MA, USA; <sup>c</sup> GE Osmonics, Vista, CA, USA; <sup>d</sup> SolSep BV, Apeldoorn, The Netherlands; <sup>e</sup> Hermsdorfer Institut für Technische Keramik, Hermsdorf/Thüringen, Germany; <sup>f</sup> Vlaamse Instelling voor Technologisch Onderzoek, Mol, Belgium; <sup>g</sup> Membrane Extraction Technology, London, UK; <sup>h</sup> pure water permeability; <sup>i</sup> methanol permeability; <sup>j</sup> ethanol permeability; <sup>k</sup> toluene permeability; <sup>l</sup> 4 % lactose (MW 342); <sup>m</sup> 5 % sucrose (MW 342); <sup>n</sup> MgSO<sub>4</sub>; <sup>p</sup> MW~500 in ethanol; <sup>q</sup> MW~1000 in acetone; -\* covered by secrecy and non-analysis agreement; -° not specified)

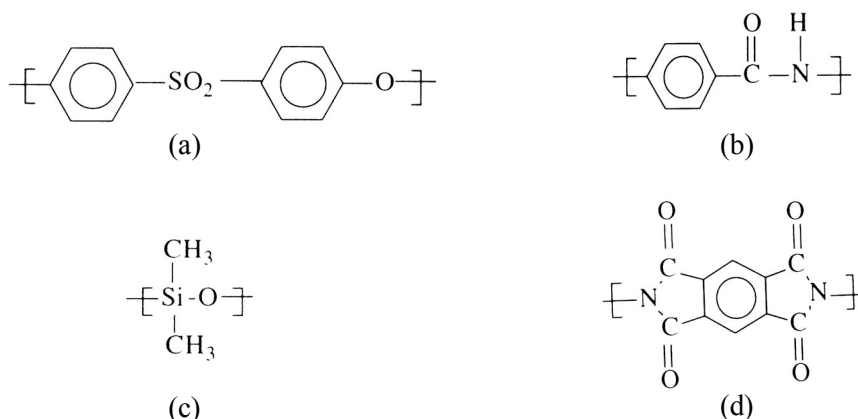


Figure 2.5: Chemical structure of the membrane top layers: (a) polyethersulfone, (b) polyamide, (c) polydimethylsiloxane and (d) polyimide

## 2.2 Surface characterisation techniques

### 2.2.1 Contact angle measurement

When a liquid drop is applied on a solid substrate, the drop will take a specific shape, characteristic of the interactions in a 3-phase system (Figure 2.6).

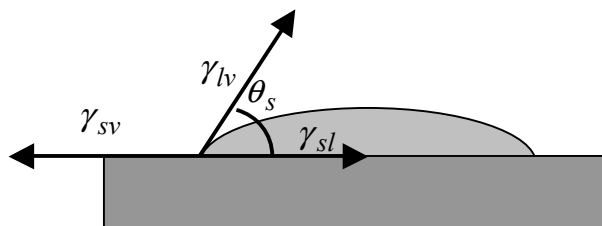


Figure 2.6: Contact angle formation on a solid surface according to Young's equation

The drop shape will strive towards equilibrium, based on Young's equation (Young, 1805):

$$\gamma_{sv} = \gamma_{sl} + \gamma_{lv} \cos \theta \quad (2.2)$$

where  $\gamma$  is the interfacial tension and the subscripts represent the phases of interest ( $s$ : solid, i.e. the membrane surface;  $l$ : liquid solvent;  $v$ : vapour phase, mostly air), and  $\theta$  the characteristic contact angle.

Contact angles with a standard solvent, mostly water, are used as a measure for the degree of hydrophilicity/hydrophobicity. The value of the contact angle theoretically ranges from 0° to 180°. The higher the affinity between the solvent drop and the membrane surface, the smaller the contact angle, resulting in a higher degree of surface wetting. In case of water as solvent, hydrophilic surfaces show a small value for the contact angle, whereas hydrophobic surfaces show a large contact angle. Contact angle measurements are carried out with a Krüss DSA10 set-up. For sessile drop fitting, the

Young-Laplace fitting, theoretically being the most exact method for calculating contact angles, is used.

### 2.2.2 Membrane surface tension

If the contact angles of (at least) two different liquids are known, the surface tension of the solid surface can be determined as well (Roudman and DiGiano, 2000). The surface tension of a solid is a material intrinsic property, which is a useful measure for the degree of hydrophilicity/hydrophobicity. A high surface tension corresponds to a hydrophilic surface, whereas low values for the surface tension are characteristic of hydrophobic materials.

The calculation of the substrate surface tension is made with the Owens, Wendt, Rabel and Kaelble method (Owens and Wendt, 1969). According to this theory, the surface tension of each phase can be split up into a polar and a disperse fraction. The sum of both contributions is equal to the total surface tension:

$$\gamma_i = \gamma_i^p + \gamma_i^d \quad (2.3)$$

Furthermore, an estimation for the interfacial tension between two phases 1 and 2 can be made with the geometric mean equation:

$$\gamma_{12} \approx \gamma_{1v} + \gamma_{2v} - 2\sqrt{\gamma_{1v}^d \gamma_{2v}^d} - 2\sqrt{\gamma_{1v}^p \gamma_{2v}^p} \quad (2.4)$$

Combined with the Young equation, the mathematical system can be solved with a linear regression method, if the contact angle for 2 liquids is known. The linear regression results into:

$$\frac{(1 + \cos \theta) \gamma_{lv}}{2\sqrt{\gamma_{lv}^d}} = \sqrt{\gamma_{sv}^p} \sqrt{\frac{\gamma_{lv}^p}{\gamma_{lv}^d}} + \sqrt{\gamma_{sv}^d} \quad (2.5)$$

The principle is shown schematically in Figure 2.7.

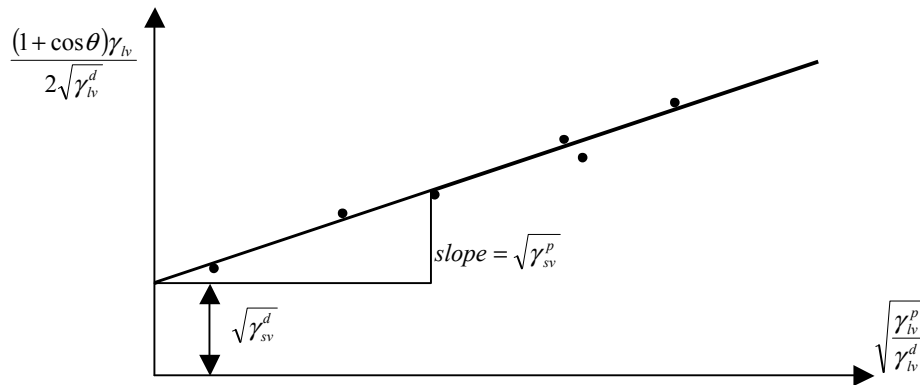


Figure 2.7: Determination of the disperse and polar fraction of the surface tension of a solid substrate, according to Owens, Wendt, Rabel and Kaelble

For the calculations of the surface tension of a membrane, the contact angles of de-ionised water and di-iodomethane were determined experimentally.

### 2.2.3 Scanning Electron Microscopy

The surfacial microstructure of solid materials, e.g. membrane disks, can be studied by several microscopic techniques. In this work, Scanning Electron Microscopy (SEM) was applied on some membrane samples. A Philips SEM XL30 FEG was used, operating at different electric potentials. The substrate in SEM is scanned stepwise with a very thin electron beam (smaller than 10 nm). Due to scattered electrons or emitted X-rays, a resolution of 100 nm is obtained. In case of using secondary electrons, the resolution can be below 10 nm.

The apparatus requires samples in a dry state. Therefore, membranes were placed in an exsiccator for 15 hours. The samples were stuck on a conductive carbon support. Afterwards, a conductive carbon coating was applied with a carbonwire coater, nebulizing a carbon wire due to a high electric potential.

## 3. Solvents

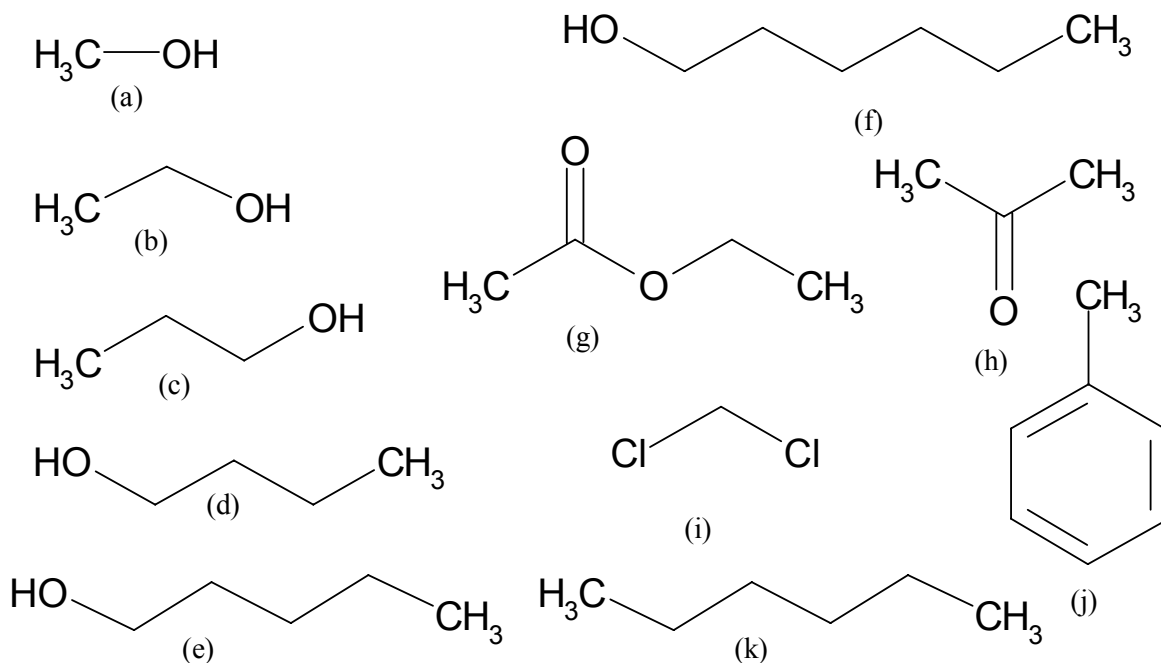
### 3.1 Selection of solvents

The aim of this research is to expand the technology for the use of organic solvents. The number of different organic solvents is very large and therefore a selection had to be made.

Organic solvents are often classified in families according to their functional groups: alcohols, ketones, esters, ethers, linear, cyclic and aromatic hydrocarbons, halogenated hydrocarbons,... Solvents were selected from these different chemical families. In addition a series of homologous solvents with the same functional groups can be studied. This would provide information that is relatively more interesting for quantitative analysis within these series of solvents, whereas the first selection can be preferred for qualitative comparison between the performance in a wide range of organic solvents. Table 2.2 summarises the different solvents used in this work with the most important solvent properties (Weast, 1970; Daubert and Danner, 1989; Kirk and Othmer, 1984; McClellan, 1989). The selection of solvents is well-considered as the main solvent classes are included; moreover, a representative list of solvents used in realistic and industrial applications is composed. The structures of the solvents are shown in Figure 2.8. Unless indicated otherwise, the solvents used in experimental set-ups were technical grade. Water was of distilled quality.

Solvent	Formula	MW	Density	Viscosity	Surface tension	Water solubility	Boiling point	Dielectric constant	Dipole moment
	-	g/mol	g/ml	mPa.s	mN/m	g/l	°C	-	D
Water	H <sub>2</sub> O	18.0	0.998	1.00	72.8	-	100	78.2	3.11
Methanol	CH <sub>3</sub> OH	32.0	0.791	0.54	22.6	∞	65	32.6	2.92
Ethanol	C <sub>2</sub> H <sub>5</sub> OH	46.1	0.789	1.08	23.3	∞	78	24.3	3.01
1-Propanol	C <sub>3</sub> H <sub>7</sub> OH	60.1	0.804	2.04	23.8	∞	97	20.6	3.03
1-Butanol	C <sub>4</sub> H <sub>9</sub> OH	74.1	0.810	2.57	24.6	111	117	17.1	3.07
1-Pentanol	C <sub>5</sub> H <sub>11</sub> OH	88.2	0.814	3.52	25.6	27	137	13.9	2.98
1-Hexanol	C <sub>6</sub> H <sub>13</sub> OH	102.2	0.814	4.59	26.6	6	158	13.3	2.95
Acetone	C <sub>3</sub> H <sub>6</sub> O	58.1	0.790	0.34	23.3	∞	56	20.7	3.09
Ethyl acetate	C <sub>4</sub> H <sub>8</sub> O <sub>2</sub>	88.1	0.900	0.43	23.8	81	77	6.0	1.68
n-Hexane	C <sub>6</sub> H <sub>14</sub>	86.2	0.659	0.33	17.9	0	69	1.9	0.09
Toluene	C <sub>6</sub> H <sub>5</sub> CH <sub>3</sub>	92.1	0.867	0.59	27.9	0.5	110	2.4	0.32
Methylene chloride	CH <sub>2</sub> Cl <sub>2</sub>	84.9	1.326	0.39	17.9	20	40	8.9	1.82

Table 2.2: Solvent properties

Figure 2.8: Structures of the different solvents used in the experiments: methanol (a), ethanol (b), 1-propanol (c), 1-butanol (d), 1-pentanol (e), 1-hexanol (f), ethyl acetate (g), acetone (h), methylene chloride (i), toluene (j) and *n*-hexane (k)

The different risks involved in these solvents are represented by the international R-phrases: R11-20-23/25-40-48, corresponding to highly flammable, harmful by inhalation, toxic by inhalation, in contact with skin or if swallowed, limited evidence of carcinogenic effect and danger of serious damage to health by prolonged exposure (Willink, 1993). Therefore, the required safety precautions have been taken during the experiments.

Although many data are available in literature, the most important solvent properties were also determined experimentally in this work. This was necessary in order to obtain data determined in the same conditions, i.e. at constant pressure and temperature. Moreover, a series of experiments was carried out with binary mixtures of water, methanol and/or ethanol. Data on mixture properties are only sparsely available in literature.

### 3.2 Composition of liquid feed mixtures

The composition of mixtures of organic solvents can be determined by using gas chromatography (GC). In gas chromatography, the sample is vaporised and injected onto the head of a chromatographic column. Elution is brought about by the flow of an inert gaseous mobile phase. The components are separated based on a difference in boiling point. Also the affinity between the components and the packing material affects the separation.

The analysis of alcohol solutions is carried out with a Shimadzu GC-14A, equipped with an 80/120 Mesh Carboxpack B/3% SP-1500 column. N<sub>2</sub> is used as a carrier gas. The column temperature is programmed at 140 °C, which is well above the boiling point of the components to be determined. The sample volume is 1 µl. The internal standard method was applied for the quantitative analysis of the samples. Iso-propanol is used as an internal standard for the binary mixtures of water, methanol and/or ethanol. The samples are analysed with a Flam Ionisation Detector (FID).

### 3.3 Kinematic and dynamic solvent viscosity

The kinematic viscosity of liquid samples was determined with a KPG-Ubbelohde Viskosimeter. A capillary 0a was used for the required range of viscosities. The system is placed in a thermostatic water bath, at 25 °C. Due to gravitation, the liquid flows in the capillary and the time difference between two levels is measured. The kinematic viscosity  $\nu$  can then be determined as:

$$\nu = K^* (\Delta t - \varphi) \quad (2.6)$$

with  $K^*$  a constant, intrinsic for the capillary used, and  $\varphi$  is the Hagenbach correction factor. The  $K^*$ -value for capillary 0a is 0.004971 mm<sup>2</sup>/s<sup>2</sup>.



The dynamic viscosity  $\eta$  is calculated as the product of the kinematic viscosity and the liquid density, determined experimentally with a pycnometer.

### 3.4 Dielectric constant

The static dielectric constant of liquid samples was determined experimentally with a HP 4284A Precision LCR-meter. The space between two concentric cylinders is filled with the fluid of which the dielectric constant is to be determined. The apparatus measures at a constant temperature (i.c. 25 °C) the capacitance and the conductivity of the system over a broad frequency domain, ranging from 20 Hz to 1 MHz. The software packet uses these data to calculate the dielectric constant.

### 3.5 Liquid surface tension

The surface tension of a liquid sample was also determined with a Krüss DSA10 set-up, but unlike surface tension measurements for membrane surfaces, a pendant drop technique has to be used (Figure 2.9).

$$\gamma_l = F(d_s/d_e)d_e^2 g |\rho_1 - \rho_2|$$

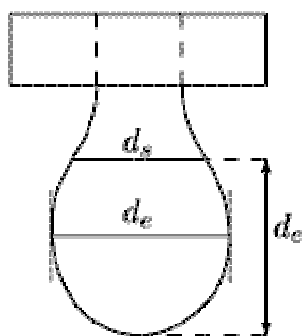


Figure 2.9: Pendant drop technique for the determination of the liquid surface tension

If a drop of liquid is hanging from a syringe needle, it takes a characteristic shape and size from which the surface tension can be determined. A requirement is that the drop is in hydromechanical equilibrium, i.e. the force of gravity acting on the drop corresponds to the Laplace pressure, which is given by the curvature of the drop contour at this point (Hansen and Rodsrud, 1991). The method is only applicable on drops that show a maximum diameter, i.e. an equator. This equator represents the first selected plane ( $d_e$ ). The second selected plane is constructed by subtracting  $d_e$  from the apex of the drop and measuring the diameter of the corresponding horizontal plane ( $d_s$ ). From the ratio of these diameters the interfacial tension can be calculated.  $F(d_s/d_e)$  is a set of empirical constants,  $g$  the gravitational constant. The density difference also enters the equation.

A continuous flow streams out at 6.32  $\mu\text{l}/\text{min}$  of the syringe and a calculation is made every 0.1 s, until the drop falls down from the needle.

## 4. Solutes

### 4.1 Introduction

Throughout the experiments, a number of solutes are used. Components were selected based on different criteria: a molecular weight between 200 and 1000 (NF-range), non-toxic and non-harmful, soluble in a desired range of solvents, and analysable at low concentrations. For the study of solute transport through nanofiltration membranes, synthetic solutions were prepared with the components summarised in Table 2.3. The molecular structures are shown in Figure 2.9.

Component	Formula	MW (g/mol)	$V_c$ ( $\text{m}^3/\text{kmol}$ )	Log P (-)
Eusolex	$\text{C}_{14}\text{H}_{12}\text{O}_3$	228.25	0.251	3.52
2,2-methylenebis-(6-tert-butyl-4-methyl-phenol)	$\text{C}_{23}\text{H}_{32}\text{O}_2$	340.51	0.453	7.97
Maltose	$\text{C}_{12}\text{H}_{22}\text{O}_{11}$	342.32	0.358	-5.41
Raffinose	$\text{C}_{18}\text{H}_{32}\text{O}_{16}$	504.52	0.530	-6.76
Victoria Blue	$\text{C}_{33}\text{H}_{32}\text{ClN}_3$	506.09	0.593	3.28
DL- $\alpha$ -tocopherol hydrogen succinate	$\text{C}_{33}\text{H}_{54}\text{O}_5$	530.79	0.707	12.00
Bromothymol Blue	$\text{C}_{27}\text{H}_{28}\text{Br}_2\text{O}_5\text{S}$	624.40	0.575	8.99
Erythrosin B	$\text{C}_{20}\text{H}_{64}\text{I}_4\text{Na}_2\text{O}_5$	879.92	0.439	-0.05

Table 2.3: Components used in nanofiltration experiments of synthetic solutions

Experiments were carried out at low concentrations, so that for the filtration experiments the effect of osmotic pressure could be ignored. Osmotic pressure is the phenomenon occurring when dissolved components cannot permeate the (nanofiltration) membrane: a concentration gradient between the feed and the permeate side arises and the system strives towards a renewed chemical and mechanical equilibrium; as a result, the solvent will permeate through the membrane in the opposite direction, so that equilibrium is reached by dilution of the feed side (Mulder, 1996). For correctness, the osmotic pressure has to be subtracted of the applied transmembrane pressure. A rough calculation of the osmotic pressure is provided by the Van't Hoff equation:

$$\Delta\pi = \nu \cdot c_f \cdot R \cdot T \quad (2.7)$$

with  $\Delta\pi$  the osmotic pressure,  $c_f$  the feed concentration,  $R$  the universal gas constant and  $T$  the absolute temperature. As indicated by Eq. 2.7, the osmotic pressure of diluted solutions is negligible compared to the applied transmembrane pressure.

The experiments with real industrial solvent streams contain other solutes. This will be discussed more in detail in Chapter 6.

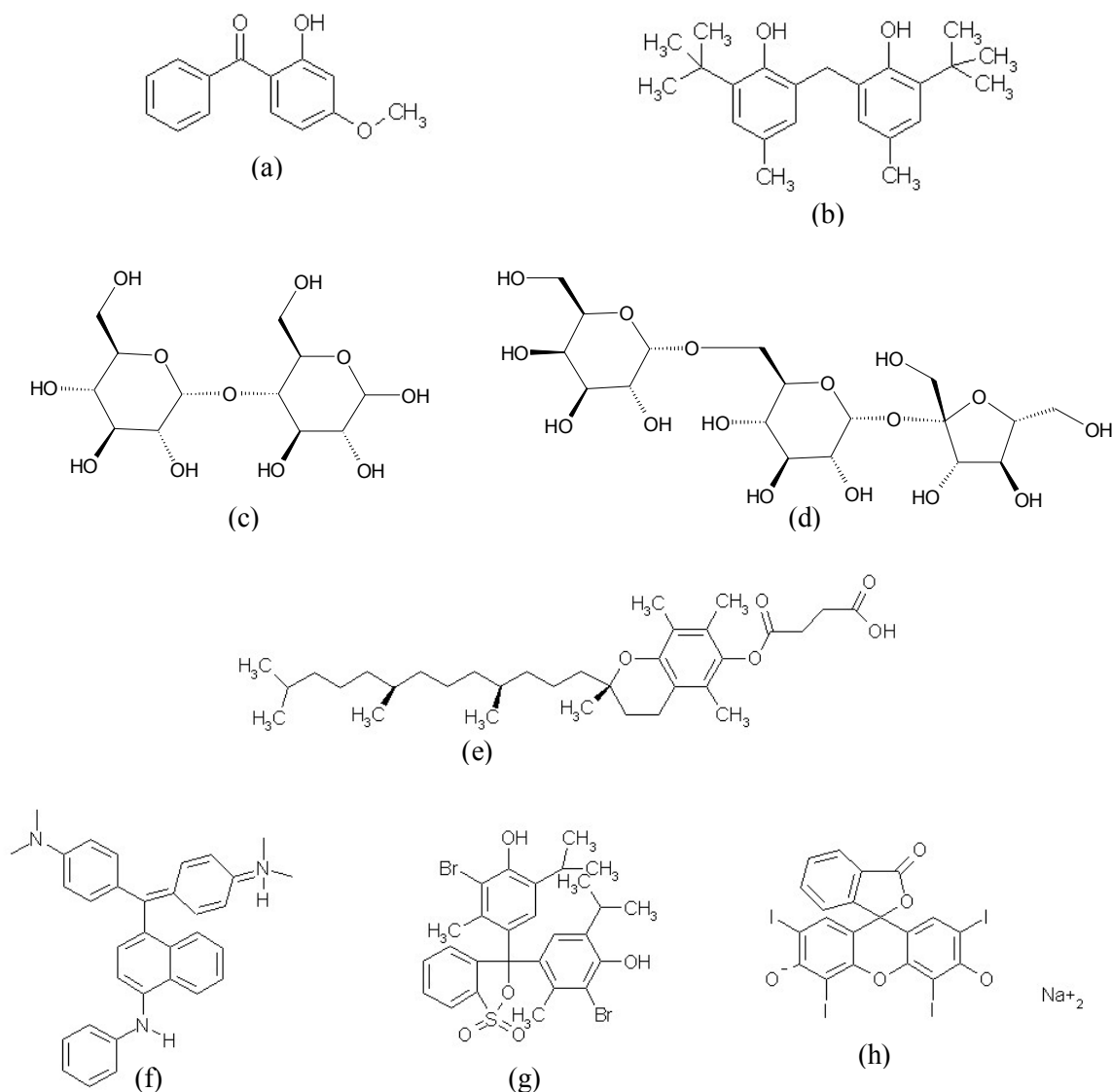


Figure 2.9: Solutes used in synthetic feed solutions: (a) eusolex, (b) 2,2-methylenebis-(6-tert-butyl-4-methyl-phenol), (c) maltose, (d) raffinose, (e) Victoria Blue, (f) DL- $\alpha$ -tocopherol hydrogen succinate, (g) Bromothymol Blue and (h) Erythrosine B

## 4.2 Effective solute diameter

Molecular size is an important parameter for the modelling of the rejection of organic molecules. Most studies focus on molecular weight to obtain information about rejection of uncharged molecules by nanofiltration. The MWCO is often taken as a measure for the rejection properties of the membrane, although it does not provide any information on the rejection for molecules with a molecular weight below the MWCO.

However, due to the small pore width in nanofiltration membranes, from a physical point of view, it is more appropriate to use a unity of length or volume instead of the molecular weight. Therefore, the Stokes diameter is calculated as size parameter. The Stokes diameter is defined by the Stokes-Einstein equation as (Mulder, 1996):

$$d_c = \frac{kT}{3\pi\eta D_{cs}} \quad (2.8)$$

with  $k$  the Boltzmann constant and  $D_{cs}$  the diffusion coefficient of component  $c$  in solvent  $s$ .

Experimental data for diffusion coefficients are only sparsely available. Therefore, the diffusion coefficients were determined with the Wilke-Chang equation (Wilke and Chang, 1955):

$$D_{cs} = 7.4 \cdot 10^{-8} (\phi M_s)^{1/2} \frac{T}{\eta_s V_c^{0.6}} \quad (2.9)$$

with  $V_c$  the solute molar volume at the boiling point and  $M_s$  the molecular weight of the solvent.  $\phi$  is an association parameter of the solvent, where  $\phi$  is 2.6 for water, 1.9 for methanol, 1.5 for ethanol, 1.0 for benzene, ether, heptane and other unassociated solvents.

The solute molar volume at the boiling point  $V_c$  was obtained using a group contribution method, presented by Geankoplis (1978). As an example, Table 2.4 provides the calculation of the molar volume for eusolex. Other values are included in Table 2.3.

Material	Amount	Atomic volume (cm <sup>3</sup> /mol)	Total
C	14	14.8	207.2
H	12	3.7	44.4
O (double bound as carbonyl)	1	7.4	7.4
O (in methyl ether)	1	9.9	9.9
O (in alcohol)	1	12.0	12.0
Ring, 6-membered	2	-15.0	-30.0
Total			250.9

Table 2.4: Calculation of the molar volume at the boiling point for eusolex (C<sub>14</sub>H<sub>12</sub>O<sub>3</sub>)

### 4.3 Logarithm of the octanol-water partition coefficient

Different solute properties are correlated to their degree of polarity or hydrophobicity, e.g. the permanent dipole moment, the polarisability, the dielectric constant, the water solubility, the Small number and the modified Small number or the Taft parameter (Van der Bruggen *et al.*, 2002). However, in this work, the logarithm of the octanol-water partition coefficient was selected as a measure for the components polarity, as both empirical and theoretical data are available in the literature, and models are developed for the calculation of this parameter. In contrast to most of the other parameters, the log P is thus available for all components.

The octanol-water partition coefficient  $P$  is a physical property used extensively to describe the hydrophobic properties of a component. It is the ratio between the concentration of a component in the octanol-phase ( $c_o$ ) and the concentration in the aqueous phase ( $c_w$ ) of a 2-phase system at equilibrium. Since measured values range from  $10^{-4}$  to  $10^{+8}$ , the logarithm of the octanol-water partition coefficient is commonly used as a measure for the hydrophobicity of a component. The different values of log P were calculated on the base of a group contribution method (Syracuse Research Corporation, 2003) and correspond well to experimentally measured values of log P available in literature (Lide, 2000). As an example, Table 2.5 represents the calculation of log P for 2,2-methylenebis-(6-tert-butyl-4-methyl-phenol); other values are included in Table 2.3.

Fragment description	Amount	Coefficient	Value
-CH <sub>3</sub> (aliphatic carbon)	8	0.5473	4.3784
-CH <sub>2</sub> - (aliphatic carbon)	1	0.4911	0.4911
C (aromatic carbon)	12	0.2940	3.5280
-OH (hydroxy, aromatic attach)	2	-0.4802	-0.9604
C (-tert carbon; 3 or more carbon attach)	2	0.2676	0.5352
-CH <sub>2</sub> - (aliphatic), 2 phenyl attach correction	1	-0.2326	-0.2326
Equation constant			0.2290
Log P			7.9687

Table 2.5: Calculation of the logarithm of the octanol-water partition coefficient for 2,2-methylenebis-(6-tert-butyl-4-methyl-phenol) (C<sub>23</sub>H<sub>32</sub>O<sub>2</sub>)

### 4.4 Solute concentration: analytical techniques

#### 4.4.1 UV/VIS-spectrophotometry

The concentration of several components was determined spectrophotometrically with a Shimadzu UV-1601 double beam set-up. Dyes can be analysed by measuring the absorption of visible light, other organic components, containing conjugated double bonds, can be analysed by measuring the absorption of UV-light. Calibration curves are based on Lambert-Beer's law, assuming a proportionality between the solute concentration and the amount of absorbed light.

In the presence of sulphuric acid, mono- and oligosaccharides, or their derivatives react to form furfural derivatives. The addition of phenol provides then a rapid procedure for quantitative colourimetric determination of the sugar concentrations, since a condensation reaction occurs, resulting in an orange-yellow coloured product. The absorbance maximum is situated at nearly 485 nm (Dubois *et al.*, 1956). Equal quantities (1 ml) of a sample and a 5 w% phenol solution are brought into a test tube. 5 ml of concentrated sulphuric acid (98 %) is added. Temperature is kept constant at 30 °C by using a thermostatically controlled water bath. The absorption is measured precisely after 30 minutes.

#### 4.4.2 Gas Chromatography

GC-analysis can also be used for the determination of solute concentration in liquid samples, as long as the solute can be vaporised. 2,2-methylenebis-(6-tert-butyl-4-methyl-phenol) and DL- $\alpha$ -tocopherol-hydrogen-succinate were determined by gas chromatography instead of by UV/VIS-spectrophotometry in order to obtain a higher sensitivity.

For the GC-analyses of single solute solutions, a Perkin Elmer Autosystem GC with built-in autosampler was used. A sample volume of 1  $\mu$ l was, via a splitter, injected on top of a Elite Series PE-1 column N610-3196 (length of 5 m; inner diameter 0.120 mm; film thickness 0.20  $\mu$ m). The analysis was temperature controlled, starting at 90 °C for 1 minute before increasing at maximal heating rate to obtain a temperature platform at 280 °C for 20 minutes. A FID is used as a detector. The same procedure could be used for the two solutes.

#### 4.4.3 High Performance Liquid Chromatography

High Performance Liquid Chromatography (HPLC) is a chromatographic technique using, unlike GC, a liquid as mobile phase. Components are distributed between the stationary phase in the column and the mobile phase depending on their affinity for each.

The analyses were carried out with a Waters TM 600S Controller, equipped with a Waters TM 626 pump and a Waters 486 MS Tunable Absorbance Detector. All components could be analysed with a Prevail C18 column, 5  $\mu$ m, 4.6 x 150 mm (pore size of 1.10 nm; surface area of 350 m<sup>2</sup>/g). As mobile phase, a mixture of 75 % acetonitrile and 25 % methanol was used, with a flow varying between 1 and 1.5 ml/min, and a constant temperature of 30 °C.

# *Chapter 3*

*The effect of organic  
solvents on polymeric  
nanofiltration membranes*

## 1. Introduction

In contrast to the use in aqueous media, the first applications studied in non-aqueous media were not very successful. Membranes showed important loss in performance, due to chemical instability of the polymeric materials in organic solvents. Different problems occurred: zero-flux due to membrane collapse (Raman *et al.*, 1996), ‘infinite’ flux due to membrane swelling (Raman *et al.*, 1996), membrane deterioration (Bridge *et al.*, 2002), poor separation quality (Subramanian *et al.*, 1998),...

The observed problems were thus all correlated to the compatibility of polymers and organic solvents. This is a well-known problem, also in application fields other than membrane technology. The insufficient performance of the first polymer nanofiltration membranes in organic solvents must be understood from the chemistry and the manufacturing process of these membranes. Polymeric membranes are mostly produced with a phase inversion technique (Mulder, 1996). Hereby, a polymer is transformed in a controlled manner from a liquid to a solid state. Although different procedures exist, most commercially available membranes are prepared by immersion precipitation: a polymer solution (polymer plus solvent) is cast on a suitable support and immersed in a coagulation bath containing a non-solvent. Precipitation occurs because of the exchange of solvent and non-solvent. The membrane structure ultimately obtained results from a combination of mass transfer and phase separation. Figure 3.1 illustrates the principle of this process.

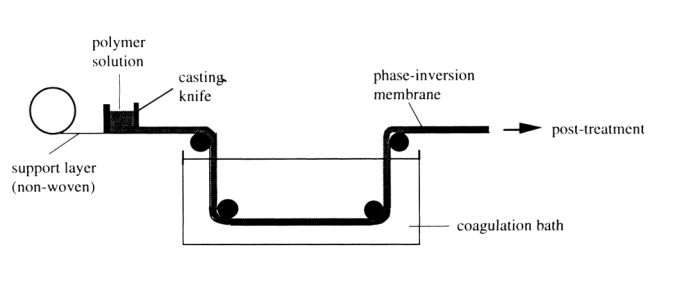


Figure 3.1: Phase inversion by immersion precipitation

Problems with polymeric nanofiltration membranes can be brought back to this production process. When the filtration experiments are carried out in an organic solvent that is also a solvent for the polymer matrix, the membrane structure might dissolve again. Musale and Kumar (2000) distinguish five degrees of resulting interactions after contact of polymeric membranes with organic solvents: (a) no chemical effect; (b) little swelling, being compatible for short-time use; (c) extensive swelling and slow dissolution of the membrane; (d) complete dissolution or disintegration of the membrane; or (e) relaxation of polymer chains due to plasticisation in organic solvents, resulting in swelling with subsequent pore size reduction.

Recently, nanofiltration membranes of improved solvent stability appeared on the market, leading to an important evolution in the potential of and the research on non-aqueous nanofiltration. Although



the newer membranes are so-called solvent resistant, it is necessary to investigate if there still are relevant interactions between the membranes and the solvents used. Therefore, the chemical stability of different membranes will be analysed in this chapter.

## **2. Influence of organic solvents on polymeric nanofiltration membranes**

### **2.1 Introduction**

Usually, the influence of organic solvents is studied by measuring the solvent flux and the rejection of molecules in organic solvents. In a first stadium of this work, however, the membrane performance was tested in terms of the pure water permeability and the solute rejection. After the characterisation, a membrane treatment was applied. Finally, the initial membrane characterisation was repeated to evaluate the effects of organic solvents on the performance of polymeric nanofiltration membranes. Changes in the performance, either in the permeability or in the solute rejection, are indeed indicative for the influence of organic solvents on these membranes. The impact of solvents on the membrane structures is also investigated with different material analyses, in order to support the experimental findings and theoretical hypotheses.

The reason for this approach is that rejections and permeabilities with nanofiltration membranes are better known in aqueous solution, so that this can be taken as a reference for the membrane performance.

Comparisons are not made within a series of homologous solvents (e.g., alcohols, acetates, ketones,...), but between solvents with considerably different properties (molecular size, polarity, dielectric constant, functional group, ...). This allows studying the influence of different parameters on the performance of nanofiltration membranes, in order to gain insight in the interaction mechanisms between membrane and solvent.

### **2.2 Experimental set-up**

The water flux and maltose rejection (using distilled water containing 100 mg/l maltose) was measured for five new sheets of 4 membrane types. After a thorough selection based on information of the manufacturers and data from literature, four solvent stable membranes were selected. The membranes used are N30F, NF-PES-010, MPF-44 and MPF-50. Experiments were carried out on the cross-flow filtration set-up and the following operating conditions, typically for nanofiltration, were applied: a transmembrane pressure of 20 bar, a constant temperature of 20 °C and a cross-flow velocity of 2 m/s. The permeate fraction and the retentate fraction were recycled continuously to the feed tank, so that no concentration effects occurred. Samples were taken after a stabilisation period of

15 minutes. The flux was then further measured as a function of time during 1 hour (for the hydrophilic membranes, i.e. N30F, NF-PES-010 and MPF-44) to 4 hours (for the hydrophobic membrane, i.e. MPF-50), time needed to gather the samples. The maltose concentration in the permeate and retentate fraction was then determined spectrophotometrically with the sulfuric acid-phenol method, and the rejection was calculated with Eq. 1.2.

After the filtration experiments, each sheet of the four membrane types was exposed during 10 days to different organic solvents. Solvents were chosen in order to cover a wide range of different chemical structures: a halogenated hydrocarbon (methylene chloride), an aliphatic hydrocarbon (*n*-hexane), an ester (ethyl acetate), an alcohol (ethanol), and a ketone (acetone). All solvents were analytical grade. The exposure was done by immersing the membrane sheets in Petri dishes, filled with the respective solvents, and refilled daily so that the membranes never became dry due to solvent evaporation. An exposure time of 10 days was selected because no visual damage could be observed after this period in preliminary experiments with each of the solvents.

All experiments were repeated twice with the same membranes, i.e., measurement of initial pure water fluxes and maltose rejections and final measurements of pure water fluxes and maltose rejections after solvent exposure.

## 2.3 The effect of organic solvents on polymeric nanofiltration membranes

### 2.3.1 Results

Initial water fluxes and water fluxes after exposure to one of the solvents are presented in Table 3.1. The initial fluxes (1) for a given membrane with each of the solvents are expected to be constant, since the membrane has not yet been in contact with the solvent at this point. However, variations up to 10% were found for each of the membranes (standard deviations were 1.9, 11.4, 1.5, and 1.2 l/m<sup>2</sup>.h for N30F, NF-PES-010, MPF-44, and MPF-50, respectively). These variations may be caused by differences in pore size distribution between samples of one membrane type. Because only small surface areas are used, the experiments are susceptible to such differences between membrane samples. Other factors such as membrane setting conditions are thought to play a minor role; all fluxes measured remained constant in time during 1-4 h.

For MPF-50, a small water flux was found, although a zero flux was expected because of the hydrophobicity of the membrane.

	N30F		NF-PES-010		MPF-44		MPF-50	
	(1)	(2)	(1)	(2)	(1)	(2)	(1)	(2)
Methylene chloride	36.4	-	162.8	-	33.5	31.0	5.1	6.1
<i>n</i> -Hexane	38.3	32.1	162.7	92.8	32.7	-	4.3	10.3
Ethyl acetate	33.7	38.0	148.0	34.5	34.4	33.7	5.0	39.6
Ethanol	35.0	27.5	144.8	167.8	36.1	40.0	6.5	22.6
Acetone	37.5	-	172.2	-	36.1	34.6	7.3	11.8

Table 3.1: Water fluxes ( $l/m^2.h$ ) obtained with N30F, NF-PES-010, MPF-44 and MPF-50, before (1) and after (2) exposure to different organic solvents

As could be expected on the base of the classification presented by Musale and Kumar (2000), some of the membranes were visually damaged after exposure, to the extent that nanofiltration experiments were impossible because the integrity of the mechanical structure of the membrane was affected. This was found for N30F and NF-PES-010 after exposure to methylene chloride and acetone, and for MPF-44 after exposure to hexane, which proves that they are compatible with these solvents (in contradiction to the manufacturer's information). The MPF-50 was the only membrane for which no mechanical damage was observed for any of the solvents. As an illustration, Figure 3.2 shows a new N30F membrane and a membrane that was exposed to methylene chloride.

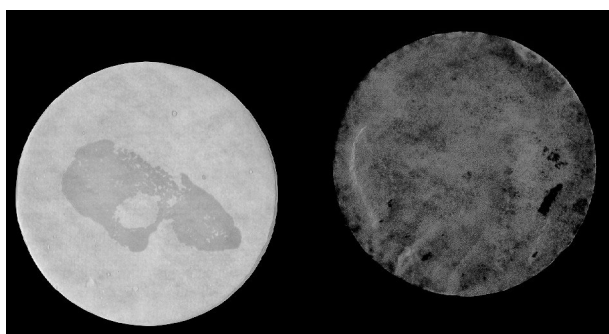


Figure 3.2: New N30F membrane (left) and N30F membrane exposed to methylene chloride (right)

From Table 3.1, it can be seen that the water fluxes for N30F and MPF-44 are approximately constant before and after exposure to the organic solvents. MPF-50 shows a general increase of the water flux. For ethyl acetate, the water flux increases with a factor 8, so that the final water flux is in the same range as for the hydrophilic N30F and MPF-44 membranes. Somewhat different results were obtained for NF-PES-010. For two of the three solvents that were incompatible with this membrane, the water flux decreased drastically. The third solvent, ethanol, resulted in a slight increase of the water flux.

The results for the fluxes before and after solvent exposure were confirmed in all cases by repeating the experiments. The variation between the experiments with different samples of the same membrane-solvent combination was below 5% with N30F, NF-PES-010, and MPF-44. Somewhat larger differences were found with MPF-50: the differences before exposure to solvents were 8.0, 2.0, 3.7, 2.8, and 2.0% for methylene chloride, *n*-hexane, ethyl acetate, ethanol, and acetone, respectively, and 2.6, 5.7, 2.8, 1.5, and 7.0% after exposure. These larger differences can be explained by the more difficult measurement of the water flux for the hydrophobic MPF-50 membrane, and possibly by non-uniformity in membrane structure.

The maltose rejections before and after exposure to the organic solvents are presented in Table 2.2. Again, the rejections before exposure to the organic solvents should be the same, but significant differences that cannot be explained by analytical errors were found (standard deviations were 8.1, 5.2, 7.1, and 3.1% for N30F, NF-PES-010, MPF-44, and MPF-50, respectively). Thus, these differences must be attributed to differences in pore size distributions within one membrane type.

	N30F		NF-PES-010		MPF-44		MPF-50	
	(1)	(2)	(1)	(2)	(1)	(2)	(1)	(2)
Methylene chloride	38	-	22	-	96	27	30	64
<i>n</i> -Hexane	39	4	11	23	97	-	30	43
Ethyl acetate	39	5	16	17	80	78	37	44
Ethanol	47	29	17	19	90	78	35	34
Acetone	25	-	24	-	87	82	34	21

Table 3.2: Maltose rejection obtained with N30F, NF-PES-010, MPF-44 and MPF-50, before (1) and after (2) exposure to different organic solvents

The initial rejections are in all cases lower than the values indicated by the manufacturers, with whom these are available. The difference is especially remarkable for N30F (70–90% indicated value; 25–47% experimental) and for NF-PES-010 (30–50% indicated value; 11–24% experimental), but lower rejections were also found for MPF 44 (98% indicated value; 80–97% experimental). All of the membranes except MPF-44 have a rather open porous structure, and NF-PES-010 in particular might be characterised as a tight ultrafiltration membrane. Differences between the manufacturer's specifications and experimental rejections were also reported by Whu *et al.* (2000).

The hydrophilic membranes N30F and MPF-44 showed a general decrease of the maltose rejection after exposure to the solvents. For N30F, this effect was dramatic: for two out of the three solvents that were incompatible with the membrane (*n*-hexane and ethyl acetate), the maltose rejection was reduced to below 5%. For ethanol, a decrease of 39% was obtained. MPF-44 showed a somewhat comparable

effect: the maltose rejection was lower after exposure for all incompatible solvents (although for ethyl acetate the effect is not significant). The effect was smaller than for N30F (except for methylene chloride), which might be due to a difference in membrane material. The results for NF-PES-10 are different: in the cases where the membrane was not damaged, the maltose rejection was equal or higher than before exposure to the solvents. A repetition of the experiment confirmed the maltose rejections for the three hydrophilic membranes to be within 5%.

For the hydrophobic MPF-50 membrane, no general decrease in maltose rejection was found; rejections after exposure to organic solvents seem to be even higher than before (except for acetone, for which rejection is lower; for ethanol, the rejection is comparable). However, the differences that were found by repeating the experiment were considerably higher than for the hydrophilic membranes. All differences were in the range between 5 and 15%.

### 2.3.2 Discussion

Solvent-stable membranes may be defined as membranes that are not damaged or changed by any organic solvent in any way, which includes that their performance (fluxes and rejections) should remain constant. The results show that this is not the case for any of the membranes used, although a gradation between the four membranes can be seen. Membranes that are not visually damaged by the solvents can be denoted as “semi” stable in the specific solvent. A semi solvent-stable membrane keeps its mechanical strength, but its performance has changed due to the impact of organic solvents.

For an interpretation of these results, a distinction should be made between hydrophilic membranes (N30F, NF-PES-010, and MPF-44) and the hydrophobic MPF-50 membrane. The latter membrane shows a general increase of the water flux due to exposure to an organic solvent. The initial fluxes are very small due to the hydrophobic character of the membrane top layer; after exposure to organic solvents, the top layer apparently becomes more hydrophilic. This can be explained by a reorganisation of the polymer chains in the membrane top layer, as suggested by Roudman and DiGiano (2000) and by Bridge *et al.* (2002), and in agreement with phenomena in polymer chemistry (Flory, 1953). Hydrophilic groups tend to form small “clusters” so that the membrane becomes locally hydrophilic. This should have only a minor effect on the pore size, because the fraction of hydrophilic groups is supposed to be very small. Nevertheless, the effect is sufficiently pronounced to lead to a flux increase.

The effect of chain reorganisation is more dramatic for the hydrophilic membranes because the fraction of hydrophilic groups is obviously larger. The clusters become larger so that in this case, chain reorganisation might affect the pore sizes as well. The corresponding effect of clustering on the pores would indeed result in less, but larger pores. Thus, the influence on the total surface taken by the pores at the membrane surface is small. The hydrophilic character is also supposed to remain unchanged, due to the larger initial fraction of hydrophilic groups; reorganisation would not affect the overall hydrophilicity. As a result, the water flux should be approximately the same before and after

exposure to the different solvents, with small effects in either direction. This was found indeed for N30F and MPF-44, for which the difference between both water fluxes was less than 10% (MPF-44) or 20% (N30F). Moreover, deviations were found in both directions, i.e. increase of the flux as well as decrease.

The surprising results for NF-PES-10 with *n*-hexane and ethyl acetate are possibly related to the large initial pore sizes of the membrane, which makes flux increase due to clustering difficult.

No correlation between solvent properties and the effect on the water flux was found. This is not surprising, because the nanofiltration experiments themselves are carried out in an aqueous phase, not in a solvent phase. An additional problem is that the changes in water flux are a result of interactions between the solvent and the membrane material, and the latter is largely unknown.

Rejection of maltose is mainly a result of size exclusion, and depends on pore size and pore size distribution in the membrane top layer (Van der Bruggen *et al.*, 1999). Thus a change in rejection properties due to the exposure to an organic solvent should be related to a change in pore size or pore size distribution.

Clustering of hydrophobic and hydrophilic groups obviously increases the pore size of the N30F membrane, so that maltose rejections were accordingly lower after exposure to an organic solvent. The effect is smaller for MPF-44, because the solvent apparently had less impact on the membrane. Methylene chloride is an exception: this solvent is obviously more aggressive to the membrane material than the other solvents used, given the relatively large influence on maltose rejection. The more solvent proof the membrane, the less mobile the polymeric chains in the top layer, and thus, the less the membrane performance is affected by organic solvents. In this view, N30F should be characterised as semi-solvent stable, allowing chain mobility and clustering of hydrophobic/hydrophilic groups. More aggressive solvents such as methylene chloride have a stronger effect, resulting in a complete dissolution or decomposition of the membrane.

The slight increase in maltose rejection for NF-PES-010 is related to the larger pore size in comparison to the other membranes. By comparing Tables 2.1 and 2.2, it can be deduced that the decrease of the water flux was due to an obstruction of the pores in the top layer. Because this is only possible when the polymeric chains are mobile, NF-PES-010 should also be characterised as a semi-solvent stable membrane.

For MPF-50, the shift towards a more hydrophilic nature of the membrane caused higher water fluxes. The pores in the top layer may remain approximately unchanged if the fraction of hydrophilic components is small; if the chain reorganisations are more significant, the same effects as obtained with the hydrophilic membranes may occur. If the pore sizes would remain constant, then the same amount of maltose molecules is retained, but the amount of water permeating through the membrane increases, so that the concentration of maltose in the permeate decreases (the rejection of maltose increases). If the effects of pore size increase are more significant, a decrease of rejections should be

found. Thus, the maltose rejections may increase or decrease. However, no definite conclusions can be drawn from the results on this point, given the relatively large uncertainties on the maltose rejections that were found (large differences between the two experimental measurements).

Interactions between organic solvents and a membrane may take place instantly or gradually; it is assumed that a steady state is approximately obtained after 10 days. This is acceptable, because the membranes were described by the manufacturers as solvent stable, i.e. in a steady state relatively quickly after immersion in the organic solvents. The rate at which the interactions between solvents and membranes take place was not studied, but might also play a role in the loss of membrane performance.

## 2.4 Reorganisation of polymer chains

The hydrophilic membranes showed lower rejections after solvent treatment, indicating an increase of the pore size. On the other hand, the same membranes showed a decrease of the pure water flux after solvent exposure, which is not expected when pore size increases. Based on the experimental findings, it was hypothesised that organic solvents may cause a reorganisation of the structure of polymeric nanofiltration membranes. Since this is a phenomenon at microscopic scale, the membranes were investigated with Scanning Electron Microscopy.

The SEM images for the different membranes before and after exposure to the organic solvents confirm that there were changes in the morphology of the top layer. Figure 3.3 shows the MPF-44 membrane before and after exposure to methylene chloride. The dark spots, with a diameter of several  $\mu\text{m}$ , are not the pores (which are expected to have a diameter of around 1 nm), but rather micro “valleys” at the membrane surface. After having been immersed in methylene chloride, these valleys are scarcer and the distance between the valleys is larger. This is only possible when the polymeric chains are mobile during the immersion in the solvent, and it can be expected that these changes also affect the (nanoscale) pores.

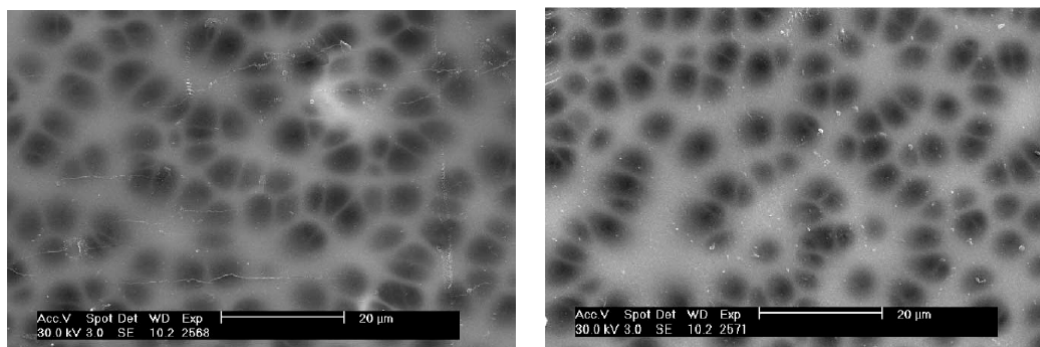


Figure 3.3: Scanning Electron Microscopy image of the MPF-44 membrane before (left) and after (right) exposure to methylene chloride

The same conclusions can be drawn for the hydrophobic MPF-50 membrane. Figure 3.4 shows the surface structure of MPF-50 before and after immersion in ethyl acetate. Valleys in the top layer are larger and scarcer after exposure to the solvent. Comparable results were obtained for other solvents.

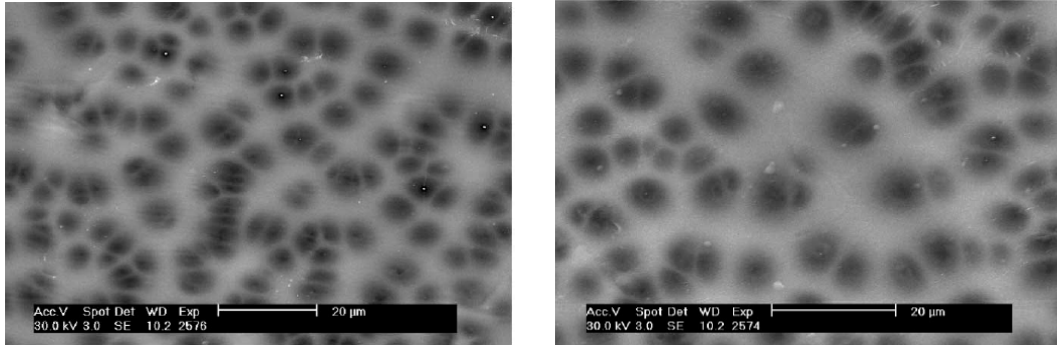


Figure 3.4: Scanning electron microscopy images of the MPF-50 membrane before (left) and after (bottom) exposure to ethyl acetate

### 3. Swelling and rejection

#### 3.1 Determination of the membrane swelling

Since the conclusions from the filtration experiments and the SEM images are still speculative, further experiments were carried out to support the hypothesis of a reorganisation of the polymer structure. The additional experiments were carried out with the hydrophilic membranes, as the effect of reorganisation was the largest for these membranes.

In a first series of experiments, the degree of swelling of the polymeric top layer of the membranes was determined in the different solvents. Swelling is a measure for the volume of liquid absorbed by the membrane and is defined as:

$$Q = \frac{1}{\rho_s} \frac{W_{wet} - W_{dry}}{W_{dry}} \quad (3.1)$$

with  $Q$  the degree of swelling,  $\rho_s$  the liquid density,  $W_{wet}$  the weight of a wet membrane sample and  $W_{dry}$  the weight of a dry membrane sample. According to the procedure of Ho and Sirkar (1992), swelling was measured by immersion of the membrane samples in the different organic solvents for 48 h. After wiping dry, the samples were weighed and then dried in a vacuum oven at 0.85 bar and 75°C during 24 h, until constant mass of the dry membrane.

However, the measurement of swelling for commercial membranes is complicated by the multilayer structure. As the swelling of the porous backing has only little influence on the membrane



performance, it was peeled off after immersion in liquid nitrogen. The remaining samples, consisting of the two top layers that determine the membrane performance, were exposed to solvent.

### 3.2 Changes in rejection due to membrane swelling

The degree of *swelling* for the different membrane-solvent combinations is presented in Table 3.3. The ratio of the permeating fraction of maltose ( $1 - \text{Rejection}$ ) after solvent treatment and before solvent treatment is included in this Table. For a given membrane, the swelling degree is the highest in *n*-hexane. In all cases, the degree of swelling is higher in water than in the other organic solvents. This phenomenon was also reported by Oikawa *et al.* (1991) for reverse osmosis membranes and by Shukla and Cheryan (2002) for ultrafiltration membranes. Furthermore, swelling for ethanol is also more important than for the other organic solvents. When comparing the performance of new and solvent treated membranes, one has to keep in mind that the impact of organic solvents on polymeric nanofiltration membranes is partly irreversible.

	MPF-44		N30F		NF-PES-010	
	Q	$\frac{1-R_2}{1-R_1}$	Q	$\frac{1-R_2}{1-R_1}$	Q	$\frac{1-R_2}{1-R_1}$
Water	2.68	1.0	1.86	1.0	1.33	1.0
Ethanol	2.19	2.4	1.52	1.3	0.84	1.0
<i>n</i> -Hexane	-	-	1.97	1.6	1.97	0.9
Ethyl acetate	0.84	1.0	0.35	1.6	0.35	1.0
Acetone	0.45	1.4	-	-	-	-
Methylene chloride	0.28	18.3	-	-	-	-

Table 3.3: Degree of swelling (in ml/g) of the hydrophilic membrane top layers in different solvents and the ratio of permeating fraction of maltose after ( $1-R_2$ ) and before ( $1-R_1$ ) solvent treatment

Table 3.3 shows that, in general, the hydrophilic membranes MPF-44 and N30F have a lower maltose *rejection* in water after solvent treatment than before (ratio > 1). For MPF-44 maltose rejection is high and remains high after solvent exposure, except for methylene chloride. N30F is a membrane with a MWCO of 400, but initial maltose rejection in water was rather low. After solvent exposure the rejections were even lower. For NF-PES-010 rejections were low both before and after solvent exposure and thus barely influenced by solvent treatment, as can be seen in Table 3.3 (ratio near 1).

When explaining the influence of swelling on component rejection, it was argued (Ebert, 2002) that for dense membranes polymeric chains move further apart during swelling, thus increasing the free volume; the membrane becomes more open. This would result in lower rejections. On the other hand, when a porous membrane swells, the pores become narrower. The membrane becomes ‘less open’, which results in higher rejections. This principle is illustrated in Figure 3.5.

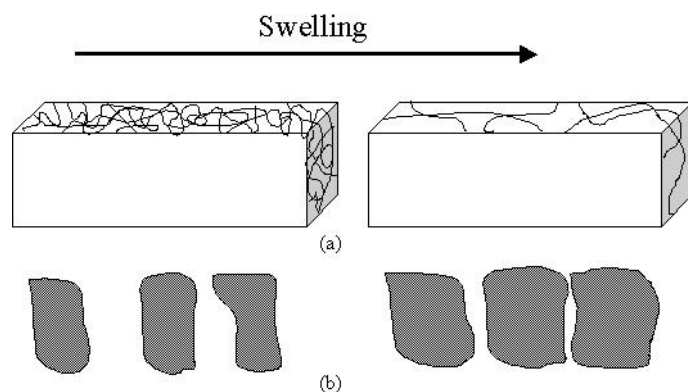


Figure 3.5: The influence of swelling on a dense (a) and a porous (b) membrane

The changes in sugar rejections of the three hydrophilic membranes can be explained with the data from the swelling measurements, as these changes are in agreement with the earlier arguments about the influence of swelling on porous membranes. This is obviously the case for MPF-44. Membranes swell less in organic solvents than in water and rejections for solvent treated membranes are lower. It must be remarked that that this membrane has a specified MWCO of 250, which is below the molecular weight of maltose. The influence of ethanol, acetone and *n*-hexane on the MPF-44 membrane is too small to enable permeation of a large fraction of the maltose molecules, which corresponds to a lower degree of swelling. MPF-44 showed the lowest degree of swelling in methylene chloride (0.28 ml/g), which means that the pore diameter was most influenced in this medium. Rejection of maltose heavily dropped after exposure of the membrane to this solvent. The same explanation can be used for N30F membranes treated with ethanol and ethyl acetate. It is not clear why the reduced rejection for *n*-hexane treated membranes is not confirmed by swelling experiments. NF-PES-010 has a MWCO of 1000, which is relatively high for nanofiltration, so it must certainly be considered as a porous material. Yet, rejection of maltose in water is already low before solvent treatment of the membrane and does not change significantly.

It is thus clear that the swelling experiments confirm the hypothesis on changes in solute rejection, resulting from the exposure to organic solvents. In general, the decrease of rejection due to reduced swelling is most important for membranes with a small pore size (N30F and MPF-44), close to the molecular size of the solute and less for NF-PES-010.

## 4. Water permeability and membrane surface hydrophilicity

### 4.1 Determination of the membrane surface hydrophilicity

The observations of the filtration experiments indicated a double effect. Beside the effect on the pore structure, also a change in the degree of hydrophilicity of the membrane surfaces was assumed. To obtain experimental evidence, the surface tension of both new and solvent-treated membranes was also determined. Solvent-treated membranes were exposed to the different solvents for 10 days as well. Before contact angle measurement, remaining solvent was removed by soaking the samples in water for 2 h. Contact angles of water and formamide were measured in order to calculate the surface tension. Table 3.4 summarises the results of the contact angle measurements, Table 3.5 gives the calculated surface tensions.

		N30F	NF-PES-010	MPF-44
New	$\theta_w$	$75.5 \pm 3.9$	$79.9 \pm 2.7$	$34.8 \pm 3.5$
	$\theta_f$	$72.2 \pm 2.4$	$64.7 \pm 4.0$	$29.7 \pm 2.8$
Ethanol	$\theta_w$	$90.6 \pm 3.0$	$67.3 \pm 3.7$	$30.3 \pm 2.6$
	$\theta_f$	$74.4 \pm 5.3$	$62.5 \pm 3.6$	$28.7 \pm 1.3$
<i>n</i> -Hexane	$\theta_w$	$99.1 \pm 4.7$	$89.8 \pm 3.2$	-
	$\theta_f$	$87.5 \pm 1.3$	$72.5 \pm 3.6$	-
Ethyl acetate	$\theta_w$	$71.3 \pm 5.9$	$85.9 \pm 3.7$	$46.5 \pm 4.7$
	$\theta_f$	$67.4 \pm 3.6$	$73.9 \pm 2.5$	$44.2 \pm 3.8$
Acetone	$\theta_w$	-	-	$41.9 \pm 2.2$
	$\theta_f$	-	-	$32.3 \pm 5.9$
Methylene chloride	$\theta_w$	-	-	$36.5 \pm 3.3$
	$\theta_f$	-	-	$30.8 \pm 2.8$

Table 3.4: Contact angles (with standard deviation) of water ( $\theta_w$ ) and formamide ( $\theta_f$ ) on new and solvent-treated membranes.

As contact angles are low and (total) surface tension is high, it is clear that MPF-44 consists of a very hydrophilic material. N30F and NF-PES-010 have higher contact angles. Surface tensions of the solvent treated membranes are different from those of the new membranes. These differences are solvent dependent and can be either positive or negative. Total surface tension is lower for the N30F membranes treated with ethanol and *n*-hexane than for new membranes, and slightly higher for the

ethyl acetate treated membrane. NF-PES-010 membranes show decreased surface tension for the *n*-hexane and the ethyl acetate treated samples and increased surface tension for the ethanol treated sample. The MPF-44 membranes show a slight decrease in all cases except for treatment with ethanol, but surface tension remains relatively high.

		N30F	NF-PES-010	MPF-44
New	$\gamma^d$	8.45	20.64	16.96
	$\gamma^p$	20.82	9.05	43.44
	$\gamma$	29.87	29.68	60.40
Ethanol	$\gamma^d$	19.34	12.05	15.34
	$\gamma^p$	4.36	22.95	48.16
	$\gamma$	23.97	35.00	63.51
<i>n</i> -Hexane	$\gamma^d$	11.76	21.16	-
	$\gamma^p$	4.17	4.37	-
	$\gamma$	15.92	25.53	-
Ethyl acetate	$\gamma^d$	10.49	15.51	13.58
	$\gamma^p$	21.25	8.27	38.40
	$\gamma$	31.74	23.78	51.98
Acetone	$\gamma^d$	-	-	19.46
	$\gamma^p$	-	-	36.04
	$\gamma$	-	-	55.50
Methylene chloride	$\gamma^d$	-	-	17.20
	$\gamma^p$	-	-	42.01
	$\gamma$	-	-	59.21

Table 3.5: Surface tension (in mN/m) of new and solvent treated membranes ( $\gamma^d$ : dispersive component;  $\gamma^p$ : polar component;  $\gamma$ : total surface tension; -: not solvent compatible)

#### 4.2 Changes in water permeability due to differences in hydrophilicity

The nanofiltration experiments indicated a change of the pure water flux for hydrophilic membranes exposed to organic solvents. It was hypothesised that the changes in pure water flux after solvent treatment were caused by the reorganisation of the membrane material. Beside a shift of the pore size distribution, a change of the surface hydrophilicity was also assumed.

The calculated surface tensions can be used to explain the previously observed differences in pure water flux between new and solvent treated membranes. Although swelling gives a good explanation for the changes in maltose rejection, it does not completely describe the solvent-membrane interactions that take place. The swelling of the membrane structure may influence the pure water flux. After solvent exposure, pores are larger in case of a porous membrane showing a lower degree of swelling (corresponding to a higher flux, due to larger pores) and dense membranes become even denser after solvent exposure (corresponding to a lower flux, due to decreased free volume and decreased diffusivity). Experimental flux results do not confirm this hypothesis. Another membrane property, namely the surface hydrophilicity, may be even more important than the swelling behaviour of the membrane.

This is fully confirmed by the contact angle measurement and the surface tension calculation. For N30F the differences in surface tension between new and solvent treated membranes completely correspond to the changes of the pure water flux. Surface tension is significantly lower for ethanol and *n*-hexane treated membranes. For these membranes an important flux decrease was reported. The results of the surface tension of NF-PES-010 are also in agreement with the values for the water flux (increased hydrophilicity for ethanol treated membranes, reduced hydrophilicity for ethyl acetate and *n*-hexane treated membranes). For MPF-44 constant fluxes can be explained by a combination of slightly decreased hydrophilicity (lower flux) and increase of average pore size due to less swelling in organic solvents (higher flux).

## **5. Conclusion**

Three out of four solvent stable membranes studied in this research showed visible defects after 10-day exposure to one or more organic solvents, and the characteristics of all four membranes changed notably after exposure to the solvents. This implies that the membranes should be denoted as semi solvent stable instead of solvent stable.

The interaction mechanisms between solvent and membrane are different for hydrophilic and hydrophobic membranes. Hydrophilic membranes are thought to undergo a reorganisation of the polymeric chains, resulting in larger pores and correspondingly lower rejections of dissolved components; water fluxes remain approximately unchanged. For hydrophobic membranes, the influence on the local character of the pores is thought to be more important: the pores become locally more hydrophilic, so that the water flux increases. Rejections may be smaller or equal when the chain reorganisation is limited. Scanning electron microscopy images confirmed these mechanisms. Additional evidence was found in the determination of membrane swelling and the calculation of the surface tension of new and solvent treated membranes.

The performance of a nanofiltration membrane in an organic solvent instead of water is expected to be more complicated. Although membranes are specified as solvent resistant, important solvent-membrane interactions affect the performance of the membrane. Experimental determination of the membrane performance in organic solvents should further clarify the mechanisms of interactions between membranes and organic solvents. However, understanding the impact of organic solvents on the performance of a membrane in aqueous solution will help to provide insight in the mechanisms involved during transport of organic solvents through the membrane.

# *Chapter 4*

## *Permeability of organic solvents through nanofiltration membranes*

## 1. Introduction

For a long time, the use of membrane technology was limited to separations in aqueous media. Since water was the only ‘solvent’ used, relatively little attention was paid to the properties of the solvent and its way of affecting the permeability. It is well known that the transmembrane pressure and the temperature influence the pure water flux. Water is a highly polar liquid and repulsion forces should be minimised. Therefore, membrane top layers are preferentially manufactured from relatively hydrophilic materials, as these are favourable for higher water fluxes. However, further research on the influence of water as a solvent on the membrane performance was relatively limited.

In contrast, the broad spectrum of organic solvents makes it indispensable to investigate in detail the influence of solvent properties on the permeability through nanofiltration membranes. It can be assumed that a number of solvent parameters each affect the membrane process in a different way. Whereas water at a constant temperature has constant values for, e.g. the viscosity, different organic solvents have different viscosities at the same temperature; although the solvents used in this work are low viscosity solvents, the differences have a significant effect on the solvent permeability. It is furthermore clear that not only the viscosity may differ between organic solvents, also the effective size of the solvent molecules varies, just like the solvent polarity.

A final argument for the investigation of the influence of solvent properties on the permeability is found in the lack of a suitable transport model for the description and/or prediction of organic solvent fluxes through nanofiltration membranes. Transport models exist for the permeation of water through these membranes, but these existing models appear to be inadequate for a suitable description of the performance in non-aqueous nanofiltration, since an insufficient number of solvent parameters, affecting the solvent flux, are included in the different models.

## 2. Parameters affecting the solvent flux

### 2.1 Literature review

Organic solvents can be classified by a number of properties: functional groups, molecular structure, volatility, density, viscosity, polarity, refractive index, ... With respect to solvent permeation through nanofiltration membranes, it is definitely not useful to check the effect of all available solvent parameters. Rather, a limited set of solvent parameters should be found with which an accurate description and/or prediction of the solvent permeability can be made.

Over the last years, several research groups investigated the effect of different solvent properties. Similarly, as for aqueous feed streams, a linear relationship is generally observed between the applied transmembrane pressure and the solvent flux. Guizard *et al.* (2002) reported, however, possible



deviations from Darcy's law, due to an additional contribution of the surface energy (the disjoining pressure) for the permeation of non-polar solvents through ceramic membranes.

Machado *et al.* (1999) showed a significant increase of the solvent permeability with increasing temperature. This can be attributed to a decrease in the solvent viscosity, which is typically correlated to temperature by an Arrhenius-relationship. Tsuru *et al.* (2000) measured the permeability for different alcohols at different temperatures to investigate the indirect effect of temperature by changes in viscosity. In addition, it was clear that, when comparing different solvents, parameters other than only the solvent viscosity played a role with respect to the permeability.

As pioneers in non-aqueous nanofiltration, Machado *et al.* (1999) provided an excellent review on possible solvent properties affecting the solvent permeability. Significant variations in the flux, due to differences in physical properties, were reported. As indicated, the solvent *viscosity* is one of the major parameters that influence the flux. The viscosity depends both on the type of solvent and on the temperature. The effect of temperature on the other solvent parameters is significantly smaller. Furthermore, solvent fluxes through hydrophobic membranes appeared to depend largely on the *polarity* of the solvents. Higher fluxes through hydrophobic membranes are evident in the case of non-polar solvent, while lower fluxes are indicated in the case of polar solvents. Similar results were reported by Bhanushali *et al.* (2001) and by Hestekin *et al.* (1999) for hydrophilic membranes. Except for solvents having a low dielectric constant, such as linear hydrocarbons, the effect of the dielectric constant appeared relatively small.

Machado *et al.* (1999) did not observe a clear correlation between the flux and the solvent *molar volume*, although a flux decrease was found within homologous series of linear alcohols with increasing molecular volume. It was, however, not clear whether this decrease must be attributed to the molecular size, the relative hydrophobicity or the hydrogen bonding capacity. In contrast, Bhanushali *et al.* (2001) suggested a linear relationship with the molar volume, as an indirect measure for the solvent diffusivity in the membrane matrix. Reddy *et al.* (1996) reported a minor effect of the molecular structure on the solvent permeability: branched alcohols showed lower fluxes than analogous linear alcohols.

Finally, Machado *et al.* (1999) found important indications that, apart from viscous forces, *surface properties* can have an effect on the solvent permeability as well. In analogy to transport of solvent molecules from one medium to another, a surface resistance is assumed to be proportional to the difference in surface tension between the liquid solvent and the membrane top layer. Later on, also Bhanushali *et al.* (2001) used the membrane surface tension to describe repulsion and attraction forces at the membrane-solvent interface, in combination with a sorption value of the solvent on the membrane material. Vankelecom *et al.* (2004) suggested that membrane swelling might be used as a measure for the membrane-solvent interactions. Recently, Robinson *et al.* (2004) suggested the use of the Hildebrand solubility parameters of the solvent and the membrane to describe these interfacial interactions.

Beside solvent properties, also the membrane characteristics influence the solvent permeability. All the same, it can indeed be expected that these effects are relatively similar as for aqueous solutions. Characteristics such as the pore diameter, the porosity or the free volume of the membrane, the tortuosity and the membrane thickness influence the over-all resistance against solvent permeation. Water being the only solvent, only minor attention was paid to the precise effect of surface phenomena. It has been shown that for organic solvent nanofiltration, these effects play a dominant role.

Further on, Shukla and Cheryan (2002) reported that the membrane pretreatment could severely affect the membrane performance. It is hence important to use a suitable and standardised procedure for membrane conditioning, in order to avoid inconsistent flux data.

## **2.2 Experimental set-up**

In order to obtain more insight in the set of parameters affecting the solvent permeability, it was decided not to study a number of different organic solvents, but to investigate the flux behaviour of binary solvent mixtures. In this way, the liquid properties of the solvent mixtures and their dependence on the feed composition clearly indicate whether they affect the solvent permeability or not.

For different reasons water-methanol, water-ethanol, and methanol-ethanol mixtures were selected for the experiments:

- the solvents must be miscible over the entire range of feed compositions;
- water and ethanol had only a minor (non-disruptive) effect on the membrane structure;
- differences in pure solvent properties are larger between water and organic solvents than among organic solvents, so that possible effects should become more obvious;
- parallels between water-methanol and water-ethanol series should confirm hypothetical findings;
- results from the methanol-ethanol series should be consistent with the results from the aqueous alcohol mixtures;
- methanol and ethanol are solvents that have a high level of significance for industrial applications.

This series of permeability experiments was carried out with 7 polymeric membranes: MPF-44, MPF-50, N30F, NF-PES-010, Desal-5-DK, Desal-5-DL and SolSep-030505. The surface tension was determined using the contact angle method previously described and the results are shown in Table 3.1. The results will be compared to those obtained with a ceramic membrane (FSTi-209).

Membrane	$\theta_w$ (°)	$\theta_d$ (°)	$\gamma$ (mN/m)
MPF-44	34.2	42.3	68.1
NF-PES-010	47.4	38.0	59.8
Desal-5-DL	49.4	34.1	59.7
Desal-5-DK	50.1	38.8	58.0
N30F	58.6	42.3	52.1
MPF-50	111.6	86.4	11.3
SolSep-030505	110.6	97.4	14.9

Table 4.1 Contact angles with water ( $\theta_w$ ) and di-iodomethane ( $\theta_d$ ), and surface tension  $\gamma$  for the different membranes

Solvent fluxes through polymeric membranes were determined at room temperature in dead-end mode with a Sterlitech HP4750 Stirred Cell. A transmembrane pressure of 6 bar was applied for the Desal-5-DL and Desal-5-DK membranes, and of 10 bar for the other membranes. The set-up was stirred at the maximum rate of 1200 rpm. Permeabilities were determined both by measuring the time required to obtain a representative permeate volume and by weighing the mass of the permeate volume over a prefixed period of time. No significant differences were observed between the two methods. Binary mixtures of water-methanol, water-ethanol and methanol-ethanol were used (0, 20, 40, 60, 80 and 100 mole%). Fluxes through one membrane sample were measured after 10, 20, 30, 40 and 50 minutes. The composition of the different mixtures was determined by gas chromatography. The mixture viscosity and dielectric constant, as a measure for the mixture polarity, were also determined, with a KPG-Ubbelohde-Viskosimeter and with a HP 4284A Precision LCR meter, respectively.

The same membrane sheet was used for a complete series of feed compositions (e.g. water-methanol), and each series was repeated with three different samples of the same membrane sheet. In this way, the obtained permeability is the average of 15 experimental values. The experimental errors were up to 5%. Membranes were pretreated by soaking them for over 20 hours in the liquid a measurement series is started with, i.e. water for the water-methanol and water-ethanol series, and methanol for the methanol-ethanol series.

## 2.3 Results and discussion

### 2.3.1 Comparison of feed and permeate composition

GC-analyses of feed and permeate samples showed that no significant differences in composition occur. This indicates that liquid transport occurs (almost) completely by convection or by coupled diffusion. Since water, methanol and ethanol have different diffusion rates through a given material, a

significant contribution of uncoupled diffusive transport would lead to changes in composition between feed and permeate, which was clearly not the case here. This also confirms that, for the membranes used in this study, liquid mixtures can be considered as a bulk liquid.

Figure 4.1 shows the viscosity of the different mixtures as a function of the composition. For water-methanol and water-ethanol mixtures maximal viscosity occurs at around 75 mole% water. These maxima are explained by the self-association of alcohols into a series of n-mers in polar solvents, by means of hydrogen bonds, resulting into important excess viscosities (Yilmaz, 2002). Methanol-ethanol mixtures have an almost linearly varying viscosity curve. Figure 4.2 shows the dielectric constant of the different mixtures. Water is highly polar compared to methanol and ethanol. Water-alcohol mixtures show a steep decrease in polarity when relatively little alcohol is added. Methanol-ethanol mixtures have a more or less linear decrease of the dielectric constant with increasing ethanol concentration.

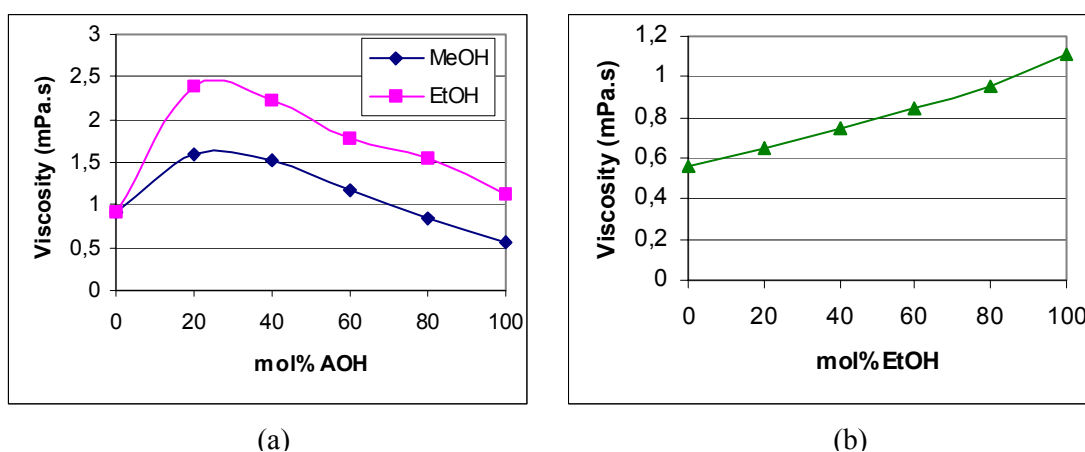


Figure 4.1: Viscosity of binary mixtures of (a) water-methanol and water-ethanol, and (b) methanol-ethanol

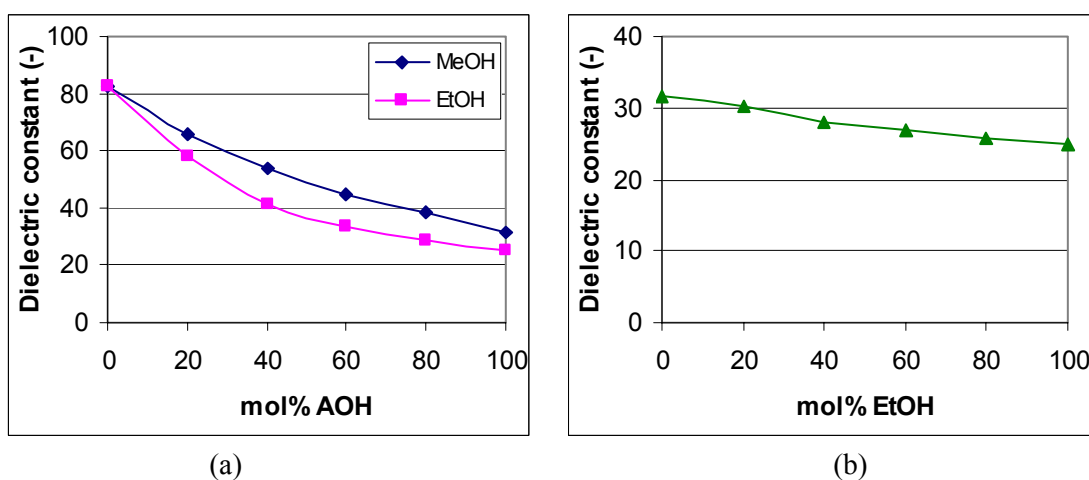


Figure 4.2: Dielectric constant of binary mixtures of (a) water-methanol and water-ethanol, and (b) methanol-ethanol

## 2.3.2 Hydrophilic membranes

MPF-44, NF-PES-010, Desal-5-DL and Desal-5-DK are considered as completely hydrophilic membranes. Figure 4.3 shows the normalised permeability of the water-methanol, water-ethanol and methanol-ethanol-mixtures as a function of the feed composition for these membranes.

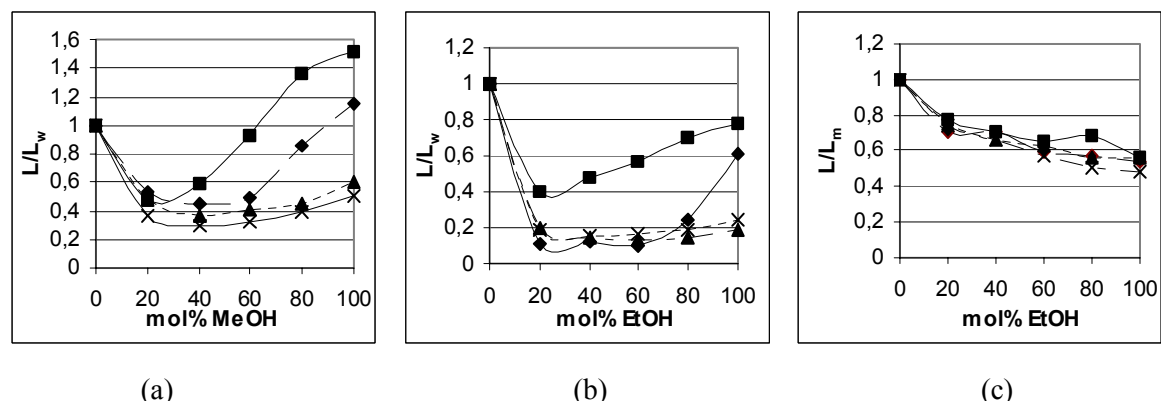


Figure 4.3: Normalised permeability of hydrophilic membranes for (a) water-methanol, (b) water-ethanol and (c) methanol-ethanol (absolute values in l/h.m<sup>2</sup>.bar, for water, methanol and ethanol respectively are: 2.0, 2.3 and 1.2 (◆: MPF-44); 12.3, 18.7 and 14.0 (■: NF-PES-010); 6.5, 3.9 and 1.2 (▲: Desal-5-DL); 5.9, 3.0 and 1.5 (×: Desal-5-DK))

As mentioned above, transport mainly occurs by convection, and thus transport of momentum, which implies that solvent viscosity strongly affects the total permeate flux. According to Darcy's law, convective transport is inversely proportional to the solvent viscosity. Since the viscosity of the water-alcohol mixtures shows a maximum as a function of the composition, a corresponding minimum of permeability can be expected. MPF-44 and NF-PES-010 show such minima for the water-methanol and the water-ethanol mixtures. Shukla and Cheryan (2002) observed similar behaviour for ultrafiltration membranes. For MPF-44 and NF-PES-010 a linear correlation between the permeability and the reciprocal viscosity was observed. Correlation coefficients, for respectively water-methanol, water-ethanol and methanol-ethanol, are 0.82, 0.94 and 0.87 for MPF-44 and 0.86, 0.96 and 0.88 for NF-PES-010. Although viscosity seems to be the dominant transport parameter for these two membranes, other factors also influence the permeability. For instance, the pure water permeability for MPF-44 is comparable to the pure methanol permeability, although the viscosity of water is almost twice as high as the one for methanol. Based only on viscosity, a lower pure water permeability is thus expected. Membranes that are more hydrophilic show higher affinity for water, causing a relative increase of the pure water flux. This effect is more pronounced with decreasing pore size: smaller pores will lead to higher resistance against convection and the relative importance of polarity effects and surface interactions will increase. This is confirmed by the permeability curves of the NF-PES-010 membrane. As indicated by the MWCO (1000), this membrane has the largest pore size and the

permeabilities of the pure liquid decreases in the order methanol, water, ethanol, corresponding to the respective viscosities. MPF-44 has smaller pores (MWCO 250), so that the relative importance of polarity increases: the ratio of the methanol flux and the water flux comes closer to the ratio of the methanol viscosity and the water viscosity with increasing pore size.

These observations are also confirmed when the permeability of Desal-5-DL and Desal-5-DK is analysed. The two types of Desal-5-membranes show very similar flux behaviour. A minimum is still observed for the water-alcohol mixtures, but it is less pronounced. Compared to the pure methanol and pure ethanol permeability, the permeability of pure water is much higher for both membranes than can be expected only based on a difference in viscosity. This is also confirmed by the lower correlation coefficients between the permeability and the reciprocal viscosity ( $R^2$  0.12, 0.60, 0.89 for Desal-5-DL and 0.10, 0.66, 0.94 for Desal-5-DK), when compared to NF-PES-010. Polarity differences and surface phenomena are even more important than for MPF-44. This is obviously confirmed by the flux behaviour. Due to the high degree of hydrophilicity of the membrane surface, a high affinity with water, and therefore high pure water permeabilities, can be observed. The addition of relatively little alcohol decreases the mixture polarity, leading to higher resistance at the membrane-solvent interface. As previously mentioned, this resistance is relatively more important with decreasing pore size. The Desal-5 membranes have the smallest pore size, leading to an increased resistance against convective pore flow.

Finally, the partial permeability of the two components in each of the three binary mixtures was calculated. The partial permeability of a component is calculated as the total permeate flux multiplied by the molar fraction of the component in the permeate sample. Partial permeabilities of the four hydrophilic membranes were very similar for the same component. Figure 4.4 shows the partial permeabilities for Desal-5-DK.

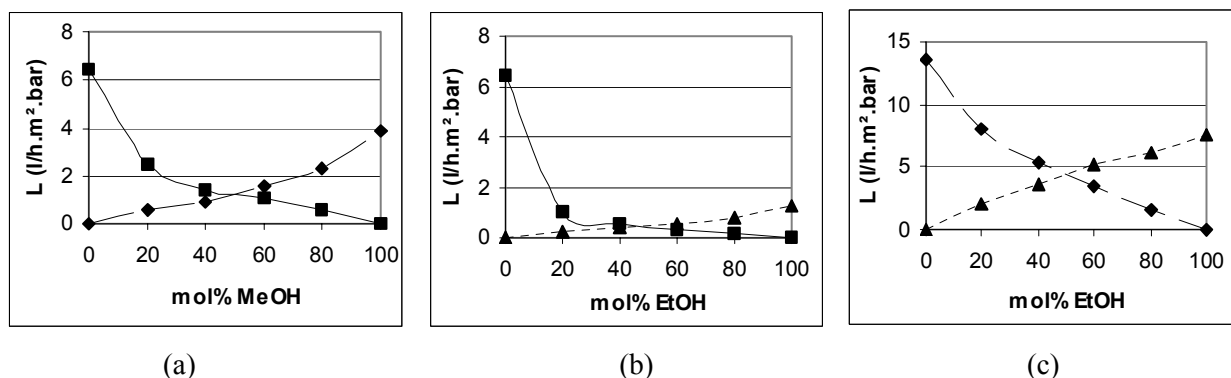


Figure 4.4: Partial permeabilities for (a) water-methanol, (b) water-ethanol and (c) methanol-ethanol mixtures (Desal-5-DK). (■: water; ◆: methanol; ▲: ethanol)

The slope of the partial water permeability curve is much steeper than that of the partial methanol permeability curve. It appears that the addition of methanol more strongly affects the partial water permeability than the addition of water affects the methanol permeability. For the water-ethanol mixture the difference is even larger. The mutual influence is the weakest for the methanol-ethanol mixtures, as the slopes of both curves have a smooth trend. Methanol permeability is more affected by the addition of ethanol than vice versa. The following conclusion can be drawn: when hydrophilic membranes are used, the relatively most apolar component of a binary mixture has a stronger influence on the partial permeability of the relatively most polar component; this influence becomes stronger with increasing polarity difference between the pure components. This can be explained based on the polarity of the mixtures. As previously mentioned, convection is the main transport mechanism and mixture properties can be evaluated as bulk properties. Considering Figure 3.2, the addition of a small amount of alcohol to pure water strongly influences the polarity, whereas the addition of a small amount of water to pure alcohol causes a much smaller change in polarity. The changes are also larger for water-ethanol than for water-methanol mixtures (i.e. with increasing polarity difference between the pure liquid components). As water has the highest affinity for hydrophilic membranes, the addition of alcohol has a stronger effect on the water permeability. Methanol and ethanol have lower affinity for hydrophilic membranes and alcohol permeabilities are therefore less influenced by the addition of water.

### 2.3.3 Hydrophobic membranes

MPF-50 and SolSep-030505 are hydrophobic membranes. Figure 4.5 shows the normalised permeability of the water-methanol, water-ethanol and methanol-ethanol mixtures as a function of the feed composition for these membranes.

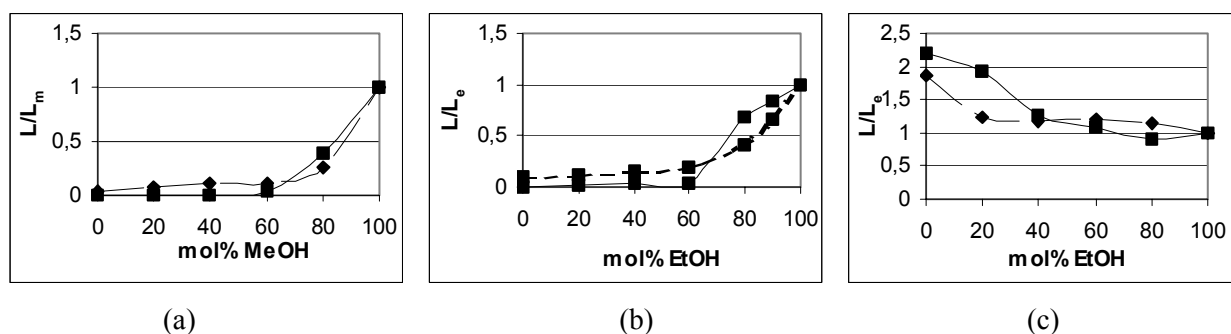


Figure 4.5: Normalised permeability of hydrophobic membranes for (a) water-methanol, (b) water-ethanol and (c) methanol-ethanol (absolute values in  $l/h.m^2.bar$ , for water, methanol and ethanol respectively are: 0.3, 6.2 and 4.2 (◆: MPF-50); 0, 1.8 and 1.2 (■: SolSep-030505))

As expected, almost no flux is observed for mixtures with a high water fraction. For mixtures containing less than 40 mole% of water, a linear increase of the permeability is observed with

increasing alcohol concentration. No minimum occurs for the water-alcohol mixtures. Solvent viscosity is clearly no longer the dominating transport parameter. In contrast hand repulsion between water and the hydrophobic membrane material becomes more important with increasing water amount, indicating that solvent polarity becomes a dominant transport parameter.

Figure 4.6 shows the partial permeabilities of the MPF-50 membrane. For the SolSep-030505 membrane similar curves were obtained. It is clear that partial permeabilities show behaviour different from that for hydrophilic membranes.

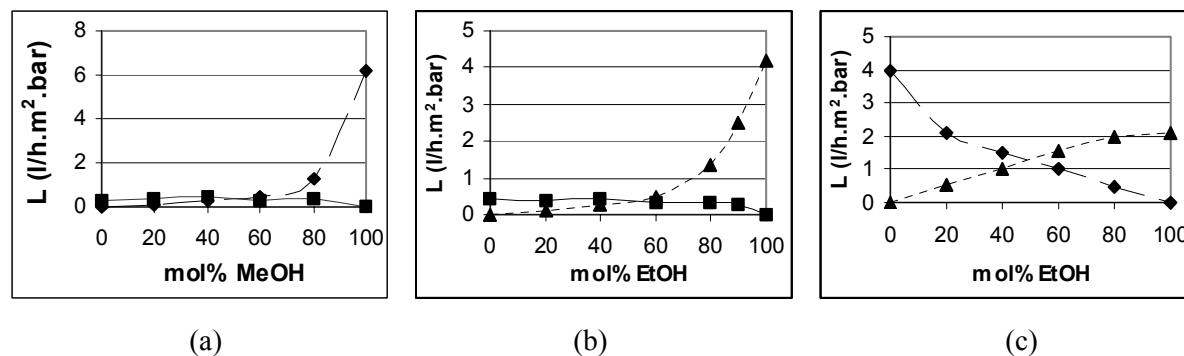


Figure 4.6: Partial permeabilities for (a) water-methanol, (b) water-ethanol and (c) methanol-ethanol mixtures (MPF-50). (■: water; ◆: methanol; ▲: ethanol)

The influence of water on the partial permeability of the two alcohols is large; methanol permeability is more affected than ethanol permeability. The water permeability is barely influenced by alcohol addition. Methanol and ethanol influence each other's permeability to a small extent. Methanol is more polar than ethanol, so that water-methanol mixtures will be more polar than water-ethanol mixtures with the same composition. As previously mentioned, repulsions between the hydrophobic membrane surface and the liquid solvent become more important with increasing solvent polarity. Therefore water-methanol mixtures will experience stronger repulsions than water-ethanol mixtures and methanol permeability will be more strongly affected by water than ethanol permeability.

#### 2.3.4 Semi-hydrophilic membranes

Experimental permeabilities of N30F (Figure 4.7) are at first sight very similar to the behaviour observed for the hydrophilic membranes (Figure 4.3). The permeability of the water-alcohol mixtures shows a minimum. This confirms the importance of the viscosity of the mixture. Contact angle measurement and surface tension calculation of the membrane surface indicated a lower degree of hydrophilicity for this membrane than for the hydrophilic membranes discussed before. This lower value explains the deviating permeability of pure water through N30F. The correlation between permeability and reciprocal viscosity improves significantly when the value for pure water is omitted: from 0.92 to 0.96 for water-methanol mixtures and from 0.78 to 0.97 for water-ethanol mixtures.



Interactions between the membrane surface and polar water molecules are less strong than with hydrophilic membranes and thus permeability is lower (as observed for hydrophobic membranes) and both viscosity and polarity determine the permeability. As the influence of polarity is obviously present, but less dominant than for hydrophobic membranes, N30F can be considered as a semi-hydrophilic membrane, as indicated by the surface tension calculation (Table 4.1).

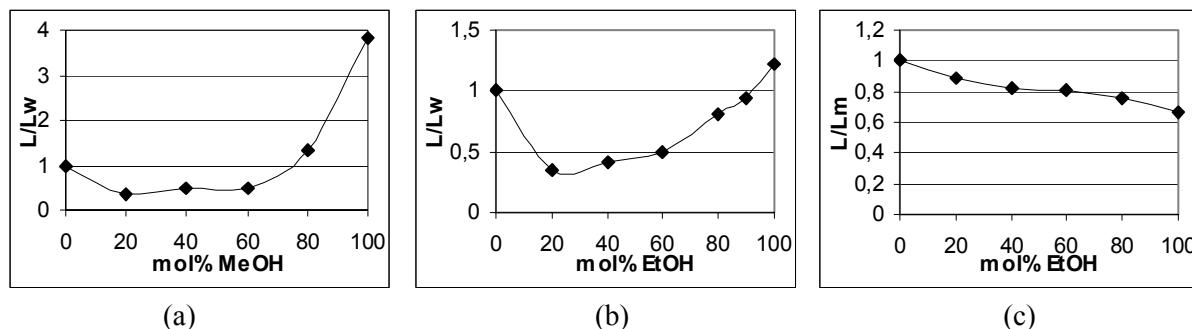


Figure 4.7: Normalised permeability of N30F for (a) water-methanol, (b) water-ethanol and (c) methanol-ethanol (absolute values in  $l/h.m^2.bar$ , for water, methanol and ethanol respectively are: 2.4, 9.3 and 2.5)

The intermediate degree of hydrophilicity of this membrane is also confirmed by the partial permeabilities, presented in Figure 4.8. Both trends typical for hydrophilic and hydrophobic membranes can be observed. On the one hand partial permeabilities of the water-ethanol mixture correspond to the expected behaviour of hydrophilic membranes: ethanol has a larger influence on the water permeability than vice versa. On the other hand water-methanol mixtures show different behaviour: methanol has a large influence on the water permeability (hydrophilic membrane), but water affects the methanol permeability as well (hydrophobic membrane).

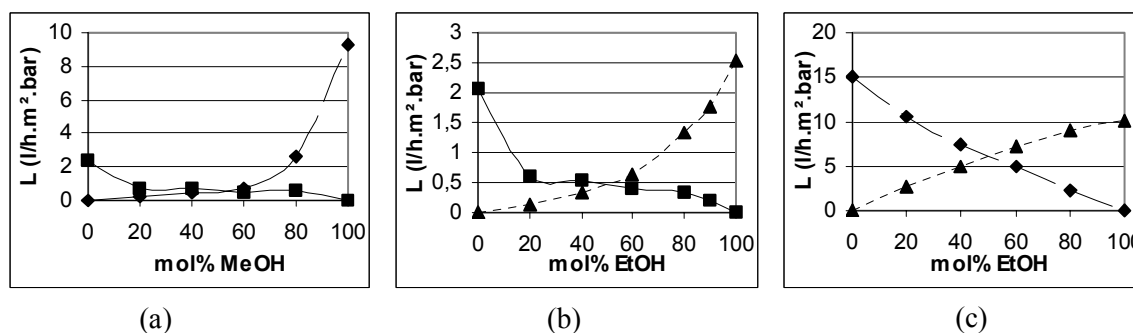


Figure 4.8: Partial permeabilities for (a) water-methanol, (b) water-ethanol and (c) methanol-ethanol mixtures (N30F). (■: water; ◆: methanol; ▲: ethanol)

## 2.4 Ceramic versus polymeric membranes

The experimental results discussed so far clearly indicate that solvent transport through polymeric nanofiltration membranes is influenced both by viscosity and polarity effects. Nevertheless, the objection can be raised that fluxes are strongly affected by swelling effects, i.e. the instability of the polymer material in organic solvents, and that the conclusions based on these experiments might be a misrepresentation. Therefore, similar experiments were carried out with a ceramic nanofiltration membrane: FSTi-209. Ceramic membranes are not susceptible to swelling effects and thus possible changes in solvent permeability with changing feed composition cannot be attributed to this phenomenon. Experiments with ceramic membranes were carried out on the cross-flow filtration set-up, but other operating conditions were similar as for the polymeric membranes, i.e. 10 bar TMP and 20 °C. A feed flow of 2 l/min was used.

FSTi-209 consists of a TiO<sub>2</sub> top layer and is thus very hydrophilic. The surface tension of the membrane could not be determined as FSTi-209 is a tubular ceramic membrane, so that no flat surface is available, as required for the determination of the surface tension with contact angle measurements. The results obtained with this membrane should however, in the first place, be compared with the results of the hydrophilic polymeric membranes.

Figure 4.9 shows the normalised permeabilities through the FSTi-209 membrane for the different mixtures. In all cases, a monotonic decrease of the permeability was observed (more or less similarly as for Desal-5-DK and Desal-5-DL), which clearly indicates that Darcy's law is not met and that the viscosity can not be the sole transport parameter. Since the top layers of ceramic nanofiltration membranes consist of very hydrophilic materials, i. c. of FSTi-209 TiO<sub>2</sub>, it is indeed expected that less polar solvents are liable to repulsive interactions at the membrane-solvent interface. The polarity of the water-methanol, water-ethanol and methanol-ethanol mixtures decrease with increasing fraction of the latter component of each mixture. The reduced polarity results in lower fluxes. As the permeability curves present a monotonic decrease, it appears that for ceramic membranes, the polarity effects strongly dominate the other transport parameters, in particular the solvent viscosity. Although ceramic membranes generally have larger pores than polymeric membranes (Mulder, 1996), and thus convective flow might be expected, deviations from Darcy's law with ceramic membranes (silica-zirconia) were also reported by Tsuru *et al.* (2000) for a series of measurements with methanol, ethanol and 1-propanol at different temperature. Furthermore, Garcia *et al.* (2005) found reduced permeability for n-hexane through zirconia-alumina ultrafiltration membranes. Van Gestel *et al.* (2003) reported the possibility to modify the surface of hydrophilic ceramic nanofiltration membranes ( $\gamma$ -Al<sub>2</sub>O<sub>3</sub>/anatase-TiO<sub>2</sub>) by a silane coupling treatment, in order to obtain nanofiltration membranes applicable in non-polar solvents such as n-hexane, whereas normally zero-fluxes are observed for

these solvents through a ceramic membrane. This confirms the importance of polarity effects acting during the nanofiltration process.

The partial permeabilities of the different mixtures are presented in Figure 4.10 and confirm entirely the findings of the polymeric membranes. Since the ceramic membrane is highly hydrophilic, it appears indeed that the partial permeability of the most polar component of a binary mixture (i.e. water for the water-alcohol mixtures and methanol for the methanol-ethanol mixture) is strongly affected by the less polar component, whereas conversely the most polar component has only a minor effect on the partial permeability of the second component. Due to the high degree of hydrophilicity of the ceramic membrane, this effect is even more pronounced: whereas for the polymeric membranes only small effects were observed for the partial permeabilities of the methanol-ethanol mixture, a strongly non-linear decrease of the partial methanol-permeability through the ceramic membrane is observed, which is indeed in accordance with the previous findings, and reconfirms the importance of polarity effects in nanofiltration.

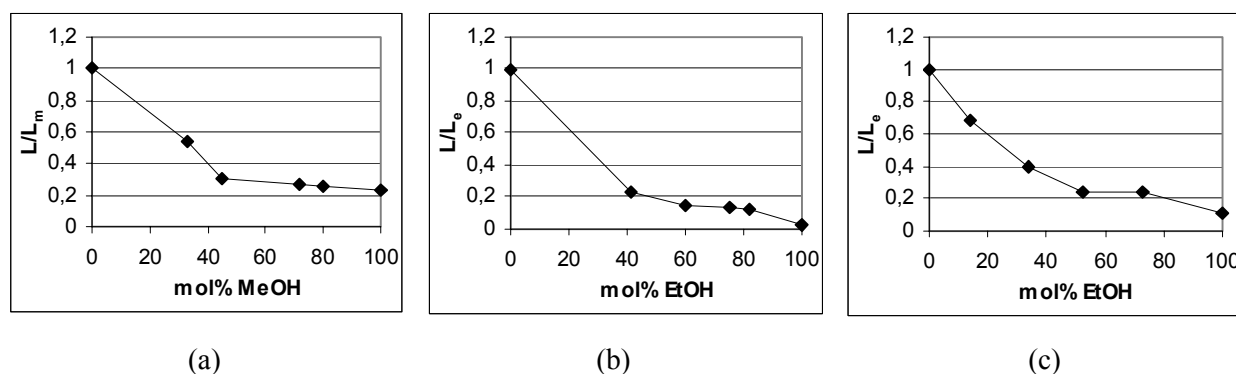


Figure 4.9: Normalised permeability of FSTi-209 for (a) water-methanol, (b) water-ethanol and (c) methanol-ethanol (absolute values in  $\text{l/h.m}^2\text{.bar}$ , for respectively water, methanol and ethanol are: 1.59, 0.37 and 0.04)

Due to its high degree of mechanical and chemical stability, FSTi-209 is not liable to swelling effects and the observed phenomena can therefore not be attributed to swelling. The same conclusions could be drawn for the ceramic membrane as for the polymeric ones, namely that the solvent viscosity is not the only parameter influencing the transport through nanofiltration membranes. Other aspects, such as the solvent polarity and the solvent-membrane interactions, play a major role in solvent permeation as well. It can thus be concluded from the experimental data that the effects observed for polymeric nanofiltration membranes also occur for the ceramic membrane and that the results for the polymeric membranes are not the consequence of membrane instability and swelling effects.

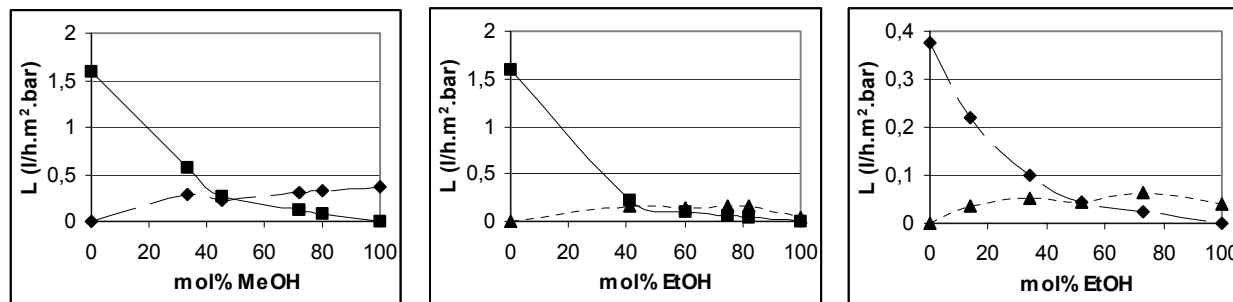


Figure 4.10: Partial permeabilities for (a) water-methanol, (b) water-ethanol and (c) methanol-ethanol mixtures (FSTi-209). (■: water; ◆: methanol; ▲: ethanol)

When the absolute values of the fluxes for the ceramic membrane are compared with those for the hydrophilic polymeric membranes, it can be seen that the permeability is lower through the ceramic membrane, which can mainly be explained by the low degree of affinity between the hydrophilic  $\text{TiO}_2$  top layer and the less polar solvents. The lower permeability can also partly be attributed to the thickness of the membrane top layer. The permeability is indeed inversely proportional to the membrane thickness and polymeric TFC-membranes have a very thin top layer, which is significantly smaller than those of ceramic membranes (Mulder, 1996). The thicker top layers of ceramic nanofiltration membranes are due to the manufacturing process and are therefore inherent in the process.

It can be seen from the results that the differences between hydrophilic polymeric membranes (e.g. Desal-5-DK) and ceramic membranes (FSTi-209) are smaller than the differences between hydrophilic and hydrophobic polymeric (e.g. MPF-50) membranes. It can thus be concluded that ‘hydrophobic’ ceramic membranes might provide a suitable solution for separation in non-aqueous nanofiltration, as these will combine the advantages of increased solvent resistance of the membrane material, and of high permeabilities in non-polar solvents.

### 3. Modelling of the solvent flux

#### 3.1 Introduction

It can be concluded from the experimental data presented above that solvent transport through nanofiltration membranes occurs mainly in a convective way. As expected from Darcy’s law, the solvent viscosity appeared as a dominant transport parameter. However, polarity differences and surface interactions influence the permeability as well. It is thus clear that a generalised transport model for solvent transport through nanofiltration membranes should be based on convective transport models that incorporate a measure for the affinity between the solvent and the membrane.

Over the years, different models were developed. However, current transport models for non-aqueous nanofiltration are limited to specific experimental data and lack generalisation. Further research and improvement of the transport models therefore remain necessary. Based on the experimental findings, and on the transport models available in literature, a new semi-empirical model will be developed.

### 3.2 Theoretical background

Different models have been developed for the description of a solvent flux through a membrane. It is not the objective here to give an exhaustive review of flux models; main classes of models with different dependence of solvent and membrane properties will be discussed.

The Hagen-Poiseuille model (Eq. 4.1) is commonly used for aqueous systems permeating through porous media, such as microfiltration and ultrafiltration membranes:

$$J = \frac{\epsilon r^2}{8\eta\tau} \frac{\Delta P}{\Delta x} \quad (4.1)$$

This equation was established, nearly at the same time but independently from each other, by Hagen (1839) and by Poiseuille (1841). The equation, which is commonly named after both researchers, was developed on the base of the flow of blood, and is used to determine the viscosity of fluids in a capillary viscosimeter (Bird *et al.*, 2002a).

The only solvent property that is taken into account here to describe the permeability is the viscosity  $\eta$ . The influence of the membrane on the solvent flux is represented by its pore size  $r$ , porosity  $\epsilon$ , tortuosity  $\tau$ , and membrane thickness  $\Delta x$ . The inverse correlation with solvent viscosity, according to Darcy's law for convective transport, appears in every flux model. It is however clear that a model in which the viscosity is the only solvent parameter is not appropriate for the description of organic solvent fluxes. Indeed, for hydrophilic membranes the water flux is higher than the *n*-hexane flux through the same membrane, although the viscosity of the latter solvent is almost three times lower than that of water. One needs more than only the solvent viscosity as a solvent parameter for the description of the permeate flux.

Jonsson and Boesen (1975) modified the Hagen-Poiseuille model to obtain a combined viscous flow and frictional model for the description of transport of solutes through reverse osmosis membranes:

$$J = \frac{\epsilon r^2}{8\eta} \left[ \frac{1}{1 + \frac{r^2 X_{sm} C}{8\eta M}} \right] \frac{\Delta P}{\tau \Delta x} \quad (4.2)$$

This model is based on a balance of applied and frictional forces acting on a solute in a uniform membrane pore; the molecular weight  $M$  of the solute is introduced as a novel parameter. Machado

(1998) further adapted this model for the description of the pure solvent flux: by replacing the mass balance of the solute by that of the pure solvent, the same equation is obtained, in which  $M$  represents the molecular weight of the solvent and  $X_{sm}$  a friction factor between the solvent and the pore wall. Compared to the model of Hagen-Poiseuille an additional factor is introduced in which the molecular weight of the solvent molecule is used as a measure of the molecular size. Machado *et al.* (1999) showed indeed that within homologous series of solvents, the flux decreases with increasing molecular size. It is clear that the molecular size of a solvent influences the flux, whether the solvent mechanism is convection (increased steric hindrance with increasing molecular size) or diffusion (reduced diffusivity with increasing molecular size). Although this model introduces a measure for the molecular size, the model is not appropriate for the description of all organic solvent fluxes. The friction must be determined experimentally for each solvent-membrane combination. Moreover, friction between the solvent molecules and membrane material might not be the right parameter to describe the reduction of fluxes. For instance, the molecular weight of ethanol is more than twice that of water, and the viscosity of ethanol is also a little higher than for water; although higher friction should occur for ethanol than for water molecules, higher ethanol fluxes are observed through hydrophobic membranes.

Machado *et al.* (2000) developed a resistance-in-series model for the permeation of pure solvents and solvent mixtures:

$$J = \frac{\Delta P}{\phi'[(\gamma_c - \gamma_l) + f_1\eta] + f_2\eta} \quad (4.3)$$

where  $f_1$  and  $f_2$  are solvent independent parameters characterising the nanofiltration and ultrafiltration sublayers,  $\phi'$  a solvent parameter,  $\gamma_c$  the critical surface tension of the membrane material and  $\gamma_l$  the surface tension of the solvent. This model is also based on the dependency of the flux on two parameters, namely the solvent viscosity and the difference in surface tension between the solid membrane material and the liquid solvent. The introduction of the latter parameter was very innovative and makes this model highly valuable. The model was in good correlation with the experimental data. However, this model is not covering the whole area of membranes and solvents, as shown by Yang *et al.* (2001). The model is developed for hydrophobic membranes, and seems inadequate for the description of fluxes through hydrophilic membranes. Moreover, for each solvent-membrane combination an empirical parameter  $\phi'$  must be determined as a measure for the interaction between a solvent and the membrane material.

The three models discussed so far are based on convective transport of the solvent. Solvent transport by diffusion has also been studied and modelled. These models are based on the solution-diffusion

(SD) model. With respect to flux modelling of organic solvents, a valuable diffusion based model was presented by Bhanushali *et al.* (2001):

$$J \propto \left( \frac{V_m}{\eta} \right) \left( \frac{1}{\phi^n \gamma_m} \right) \quad (4.4)$$

This model combines different approaches of existing models by introducing at the same time the solvent viscosity, the molar volume  $V_m$  (as a measure for the molecular size), the surface tension of the solid membrane material and a sorption value  $\phi$  (as a measure for membrane-solvent interactions). In this way, Bhanushali *et al.* (2001) were the first to suggest an influence of at least three parameters: the viscosity, the molecular size and the affinity between the solvent and the membrane material (in order to deal with differences in polarity). The model showed high correlation with experimental data. Other important SD-based transport models were presented by White (2002), providing a predictive model for feed solutions with a high concentration of aromatics, by Scarpello *et al.* (2002) and by Gibbins *et al.* (2002).

### 3.3 A new transport model for solvent permeation

Although the models discussed above show shortcomings, it must be concluded that they form a very valuable basis for the development of a generalised transport model for the description of permeation of different solvents and solvent mixtures. It is likely that such a model should incorporate at least three parameters, namely the solvent viscosity, a molecular size parameter and a measure for the affinity between the solvent and the membrane material.

Since the model of Bhanushali *et al.* (2001) is one of the most recent models for solvent transport, the new model presented in this work is partly based on the former model. However, some assumptions made by Bhanushali *et al.* (2001) must be questioned. On the one side the inverse correlation with the sorption value (Eq. 4.4) can be discussed. A high value for this parameter corresponds with a high degree of affinity between the solvent and the membrane, and for such solvent-membrane combinations, higher solvent fluxes can be expected. By putting the sorption value in the denominator, the opposite is suggested: with increasing affinity lower fluxes are predicted.

On the other hand the dependence of the membrane surface tension must be pointed out. The Bhanushali model predicts higher fluxes with decreasing hydrophilicity of the membrane surface (i.e. decreasing surface tension). This of course is only valid for non-polar solvents. The more polar a solvent will be, the lower fluxes are expected with hydrophobic membranes, which can not be described by this model.

The development of a new model for solvent transport is based on a combination of the qualitative elements from existing models. The model is assumed to integrate three parameters: one for the transport of *momentum*, one for the contribution of *steric hindrance* effects, and one for the description of the *membrane-solvent interaction*.

The first two parameters are adopted from Bhanushali *et al.* (2001), namely the solvent viscosity and the molar volume of the solvent. The solvent viscosity is incorporated as a measure of the resistance against pore flow (transport of momentum). This parameter appears in all transport models for transport through porous membranes. The porous nature of the membrane was confirmed when the compositions of feed and permeate samples were compared. Also Vankelecom *et al.* (2004) reported the porous nature of PDMS-membranes. The molar volume of the solvent is used as a measure for the molecular size and the steric hindrance effects. It is indeed obvious that the resistance against permeation increases with increasing solvent size: the influence of the membrane material (pore wall) is stronger when the ratio of the solvent molecule diameter and the pore diameter is increasing.

It is now suggested to replace the interaction parameter as presented by Bhanushali *et al.* (2001), which is a combination of a sorption value and the membrane surface tension, by a single and more suitable parameter to describe the affinity. The experimental data showed significant membrane-solvent interactions and the observed contribution of the resistance against permeation was described by Machado *et al.* (2000) as the difference in surface tension between the solvent and the membrane (Eq. 4.3).

In the new transport model, the combined interaction parameter of Bhanushali *et al.* (2001) is therefore replaced by this difference in surface tension, leading to the following equation:

$$J \propto \frac{V_m}{\eta \cdot \Delta\gamma} \quad (4.5)$$

### 3.4 Results and discussion

#### 3.4.1 Required parameters

To evaluate the accuracy of the different models used to describe the experimental permeability data for the binary mixtures of water-methanol-ethanol, different solvent and membrane parameters are required for the calculations: viscosity, molecular weight, molar volume and surface tension of the solvent, surface tension of the membrane, and the sorption value  $\phi$ . The viscosities of the different mixtures were already shown in Figure 4.1, as well as the surface tension of the membranes in Table 4.1. For the sorption value  $\phi$ , no theoretical or literature values are available. As composite, multi-layered membranes were used, the sorption values could neither be determined experimentally. Therefore, the Bhanushali-model could not be evaluated for its accuracy. However, the model was already discussed in qualitative terms and shortcomings are well recognised. For the models of Hagen-Poiseuille, Jonsson and Boesen, Machado *et al.* and the newly developed model, all required



parameters are available, either experimentally or theoretically. The flux modelling was not applied to the results of the ceramic membrane, as the membrane surface tension was not available and could not be determined experimentally for tubular membranes.

The molecular weight of a mixture of solvents was calculated with a linear mixing rule, which is standard, due to the law of conservation of mass in non-reacting mixtures.

$$M_m = \sum_i x_i M_i \quad (4.6)$$

The molar volume was calculated as the ratio of the molecular weight and the mixture mass density. In contrast to the molecular weight, the liquid density is not conservative, and was therefore determined experimentally using a pycnometer.

Finally, the liquid surface tension was calculated with the mixing rule of Tamura *et al.* (1955) for aqueous solutions:

$$\gamma_m^{1/4} = \psi_w \gamma_w^{1/4} + \psi_o \gamma_o^{1/4} \quad (4.7)$$

with  $\psi_w$  being defined by the relation:

$$\log_{10} \frac{(\psi_w)^q}{(1-\psi_w)} = \log_{10} \left[ \frac{(x_w V_w)^q}{x_o V_o} (x_w V_w + x_o V_o)^{1-q} \right] + 44.1 \frac{q}{T} \left[ \frac{\gamma_o V_o^{2/3}}{q} - \gamma_w V_w^{2/3} \right] \quad (4.8)$$

For the methanol-ethanol series, the method of Winterfeld *et al.* (1978) is applicable. The difference between the surface tension of pure methanol and pure ethanol is however relatively small. Figure 4.11 shows the surface tension of water-alcohol mixtures as a function of the feed composition for water-methanol and water-ethanol mixtures. The liquid surface tension was also experimentally measured as described in Chapter 2. No significant deviations from the theoretical curve were observed.

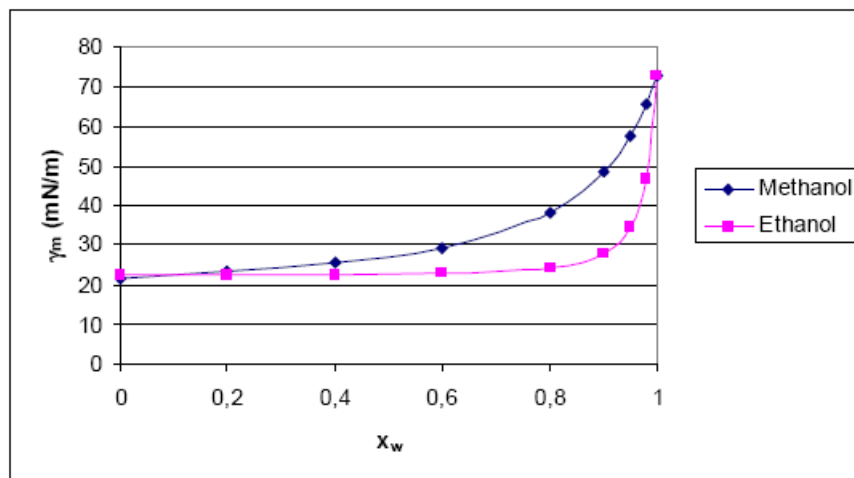


Figure 4.11: Surface tension of water-alcohol mixtures as a function of mixture composition

### 3.4.2 Model fitting and statistical analysis

Not all model parameters are known or can be determined experimentally (e.g.,  $\varepsilon$ ,  $\tau$ ,...). Therefore, model fitting requires some mathematical manipulations. First, unknown model constants  $a$  and  $b$  are introduced. The models of Hagen-Poiseuille, Jonsson and Boesen, Machado *et al.* and the newly presented model were reformulated in a mathematical form enabling linear regression of different groups of parameters  $X$  and  $Y$ , including the model variables (Appendix A):

$$Y = mX + p \quad (4.9)$$

Table 4.2 shows the different transport models with the respective mathematical forms for linear regression, model constants and fit parameters. The regression parameters  $m$  and  $p$ , which are both functions of original model constants  $a$  and  $b$ , are found as the slope and the intercept from the linear regression.

The  $m$ - and  $p$ -values can be used to calculate the unknown model constants  $a$  and/or  $b$ . The resulting  $a$ - and/or  $b$ -values are in turn used in the original equations as specific model parameters for a given membrane-solvent mixture combination. Finally, the solvent and the membrane properties ( $\eta$ ,  $M$ ,  $\gamma$ ,  $V_m$ ,  $\Delta\gamma$ ) are inserted in the equations in order to calculate model values for the solvent flux. The model values can be compared statistically with the experimental flux data.

All data sets consist of 6 data couples (experimental and model values at 0, 20, 40, 60, 80 and 100 mole% of one component). Descriptive statistical analysis consists of calculations of the fit error  $e$  and the error variance  $s_e^2$  (Bickel and Doksum, 1977). The model providing the lowest fit error variance corresponds to the best fit of the experimental data. Further statistical analysis in terms of statistical significance was not carried out; data sets containing at least 20 data couples are required for mathematical validation, which is not the case here. Statistical formulas are summarised in Appendix B.

Transport model	Equation	a	b	Linear regression $Y=mX+p$	X	Y
<b>Hagen-Poiseuille</b>	$J = \frac{a}{\eta} \Delta P$	$\frac{\epsilon r^2}{8\tau \Delta x}$	-	$L = \frac{a}{\eta}$	$\frac{1}{\eta}$	L
<b>Jonsson-Boesen</b>	$J = \frac{a}{\eta} \frac{1}{1 + \frac{b}{\eta M}} \Delta P$	$\frac{\epsilon r^2}{8\tau \Delta x}$	$\frac{r^2 f_{sm} C_s}{8}$	$\frac{M}{L} = \frac{\eta M}{a} + \frac{b}{a}$	$\eta M$	$\frac{M}{L}$
<b>Machado et al.</b>	$J = \frac{\Delta P}{a \Delta \gamma + b \eta}$	$\phi'$	$f_1 \phi' + f_2$	$\frac{1}{\eta L} = a \frac{\Delta \gamma}{\eta} + b$	$\frac{\Delta \gamma}{\eta}$	$\frac{1}{\eta L}$
<b>This work</b>	$J = a \frac{V_m}{\eta} \frac{\Delta P}{\Delta \gamma}$	$f(\epsilon, r, \tau, \dots)$	-	$L = a \frac{V_m}{\eta} \frac{\Delta \gamma}{\Delta \gamma}$	$\frac{V_m}{\eta} \frac{\Delta \gamma}{\Delta \gamma}$	L

Table 4.2: Equations used for linear regression: models are reformulated into the mathematical form  $Y = mX + p$

## 3.4.3 Evaluation of the transport models

The results of the model fitting are summarised in Table 4.3, which presents the error variance of the different membrane-model combinations analysed. The results can again be separated into two classes: hydrophobic and hydrophilic membranes.

Water-Methanol	HP	JB	Machado	This work
Hydrophobic: MPF-50	2.22	4.79	3.29	0.32
SolSep	0.25	1.14	5.01	0.03
Hydrophilic: MPF-44	0.06	0.06	0.04	0.04
Desal-5-DK	2.17	2.29	0.97	1.85
Desal-5-DL	2.36	2.52	0.55	2.06
NF-PES-010	3.02	3.72	3.59	8.73
N30F	2.62	5.05	0.60	2.06

(a)

Water-Ethanol	HP	JB	Machado	This work
Hydrophobic: MPF-50	1.54	1.45	1.36	0.22
SolSep	0.20	0.28	0.76	0.05
Hydrophilic: MPF-44	0.15	39.57	0.28	0.14
Desal-5-DK	2.30	0.36	1.85	2.39
Desal-5-DL	1.60	0.15	1.72	2.13
NF-PES-010	1.59	1.81	1.71	6.69
N30F	0.10	0.11	0.06	0.07

(b)

Methanol-Ethanol	HP	JB	Machado	This work
Hydrophobic: MPF-50	0.09	0.13	0.10	0.12
SolSep	0.47	0.17	0.01	0.09
Hydrophilic: MPF-44	0.02	0.03	0.02	0.06
Desal-5-DK	0.40	0.56	0.36	2.33
Desal-5-DL	0.50	0.92	0.54	1.76
NF-PES-010	2.31	2.32	1.74	3.51
N30F	1.67	0.13	0.09	0.15

(c)

Table 4.3: Fit error variance for the different membrane-model combinations for (a) water-methanol, (b) water-ethanol, (c) methanol-ethanol (HP: Hagen-Poiseuille; JB: Jonsson and Boesen)

The hydrophobic membranes (MPF-50 and SolSep-030505) provided very typical permeability curves, with a low permeability for mixtures with a high fraction of water, and a steep permeability increase for mixtures with high alcohol fractions. As can be seen in Table 4.3, MPF-50 and SolSep-030505 generally have a much smaller error variance for the new model than for the literature models. Figure 4.12 shows, as an example, the experimental permeability data for a water-methanol mixture through MPF-50, with the different model fits. It is clear that the new model offers a significantly improved description of the flux behaviour. Other data sets gave similar results. For the methanol-ethanol mixtures, the error variance of the new model is comparable with this for the Machado model, but better than for the Hagen-Poiseuille and the Jonsson and Boesen model.

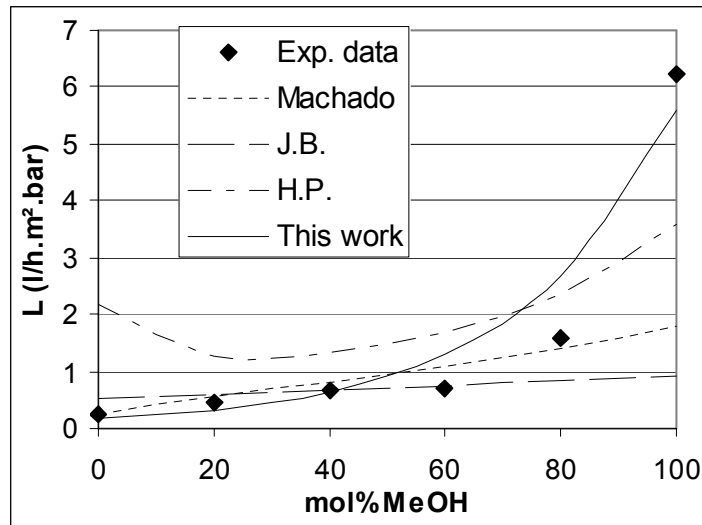


Figure 4.12: Experimental permeability data for a water-methanol mixture through a hydrophobic MPF-50 membrane, as fitted by the models given by Hagen-Poiseuille (HP), Jonsson and Boesen (JB), Machado *et al.* and this work

The results for the different hydrophilic membranes (MPF-44, Desal-5-DK, Desal-5-DL and N30F) are similar. Figure 4.13 shows, as an example, the experimental permeability data with the different model fits for MPF-44 with a water-methanol mixture.

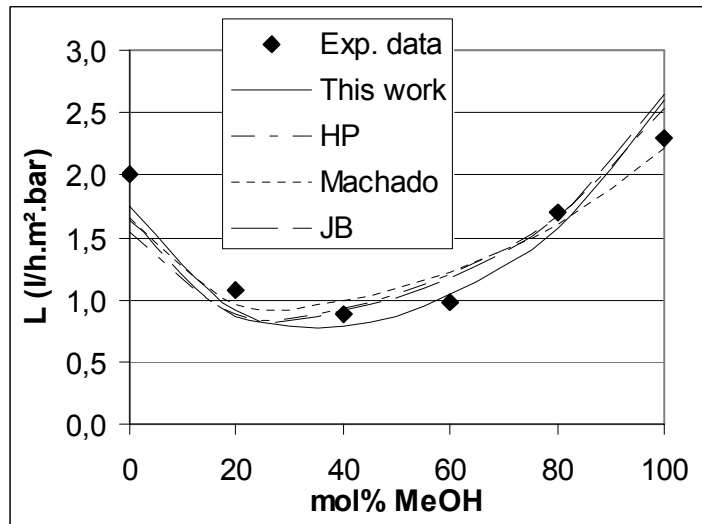


Figure 4.13: Experimental permeability data for a water-methanol mixture through a hydrophilic MPF-44 membrane, as fitted by the models given by Hagen-Poiseuille (HP), Jonsson and Boesen (JB), Machado *et al.* and this work

For the sake of completeness, Figure 4.14 illustrates the experimental data and different model fits for all membranes (except for Desal-5-DL, which has similar results as Desal-5-DK) with the water-ethanol mixtures.

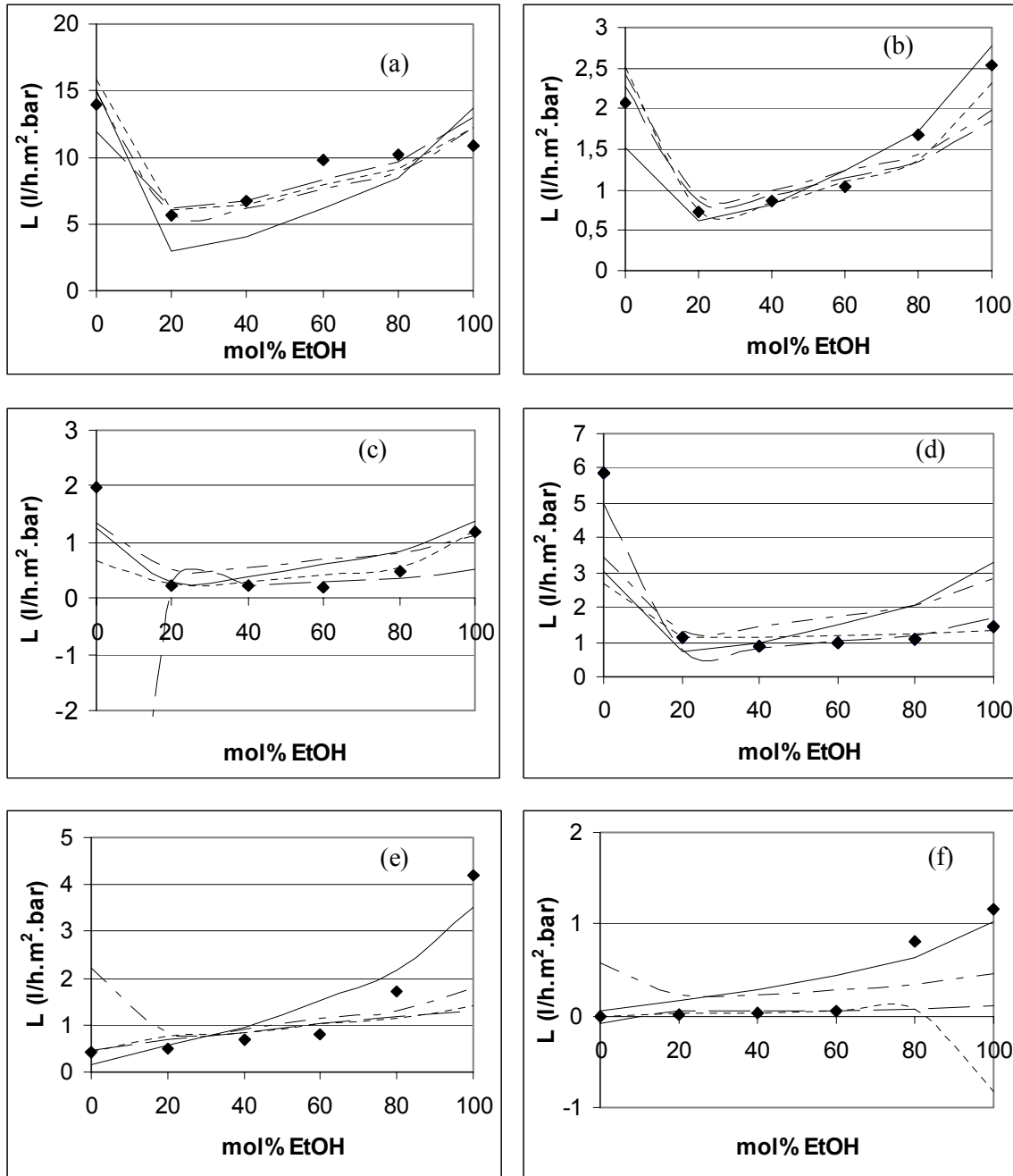


Figure 4.14: Experimental data and model fits with water-ethanol mixtures for (a) NF-PES-010, (b) N30F, (c) MPF-44, (d) Desal-5-DK, (e) MPF-50 and (f) SolSep-030505

The descriptive quality of the model of Machado *et al.* (2000) is above the average for hydrophilic membranes, the model of Jonsson and Boesen (1975) is mainly below the average. The new model seems to provide similar results when compared to the Hagen-Poiseuille and the Jonsson and Boesen

model. However, differences in error variance are relatively small for the hydrophilic membranes. This can be attributed to working with polar solvents: the solvents used have a relatively high degree of affinity for the hydrophilic membrane surfaces, resulting in smaller repulsion forces. Consequently, the influence of membrane-solvent interactions is reduced. Theoretical data showed a good correlation with experimental data (thus relatively smaller error variances) for MPF-44 and for N30F, which are the most typical nanofiltration membranes used. Larger error variances are observed for NF-PES-010 and for Desal-5-DK and Desal-5-DL. This can be attributed to the membrane characteristics. The former membrane is nearly an UF-membrane, having relatively large pores. The experimental data showed that, for this kind of membrane, the relative importance of viscous flow might dominate the polarity effects. In contrast, Desal-5-DK and Desal-5-DL are nearly RO-membranes, having a relatively dense structure and small pore size. Solvent transport through these membranes is more susceptible to polarity effects and the relative importance of viscous flow is reduced.

It appears thus that correction factors may be required for less typical nanofiltration membranes. Literature models can be considered as 3-parameter models ascribing different weight factors to the different contributions; even if only one or two parameters are taken into account, at least one parameter has a weight factor of zero. It appears that for the less typical nanofiltration membranes, these different ‘weight factors’ lead to a better fit than the new model. Therefore, the model was further expanded with weight parameters  $\alpha$ ,  $\beta$  and  $\delta$  for the three transport parameters:

$$J = a \frac{V_m^\alpha}{\eta^\beta (\Delta\gamma)^\delta} \quad (4.10)$$

Although a slight improvement was observed for the fitting, this was not significant and thus unnecessarily complicating the available results. Further attempts to improve the model involved the use of dimensional analysis (Elmaleh *et al.*, 1998; Bird, 2002b), but no fruitful result was obtained either. It can be conjectured that an ultimate transport model might probably consist of a more complex mathematical structure than presented in the new model. Nevertheless, when comparing the overall fitting results, both for hydrophilic and hydrophobic membranes, and for the three mixtures studied, the new model shows a significant improvement over the literature models, providing, as the only model, a powerful tool to describe the experimental data within the correct order of magnitude for all combinations. Taking into account that at least one value should be known, typically the pure water flux provided by the membrane manufacturer, the model can also be used for the prediction of the flux behaviour for an extended range of feed compositions.

## 4. Permeability of pure solvents

Although methanol and ethanol are solvents that are often used in industrial applications, it is necessary to develop a suitable model, applicable to a large variety of organic solvents. Therefore, the experiments were complemented by two additional series of measurements: the membrane permeability is also determined experimentally for a series of homologous solvents and for a series of organic solvents from different chemical classes. A suitable model should not only be useful to describe the data discussed in the previous section, but will also have to deal with the experimental data from the non-aqueous nanofiltration experiments.

### 4.1 Permeability of a homologous series of alcohols

In the first place, the permeability for 6 primary alcohols through the SolSep-030505 membrane was determined with the Sterlitech dead-end module. This membrane was selected since it is specified for applicability in alcohols. The permeabilities were measured through the same membrane disk, in order of different solvents with increasing number of carbon atoms in the molecular chain, thus starting with methanol and ending with 1-hexanol. The permeability of a solvent was measured by weighing the permeate sample over a constant period of time, and this after 1, 2, 3, 4 and 5 hours. It was observed that the permeability relatively quickly reaches a constant value and the permeability was therefore calculated as the average of the 5 measurements.

	L (l/h.m <sup>2</sup> .bar)
Methanol	4.5
Ethanol	2.1
1-Propanol	2.6
1-Butanol	2.2
1-Pentanol	1.9
1-Hexanol	1.7

Table 4.4: Permeability of a homologous series of primary alcohols through SolSep-030505

The results, summarised in Table 4.4, show a decrease in solvent permeability with increasing number of carbon atoms. This was expected for several reasons. Within homologous series of solvents, the viscosity increases for larger solvents, leading to an increased resistance against viscous flow. Furthermore, larger molecules are exposed to increased steric hindrance effects, resulting in reduced



permeabilities. Finally, the solvent surface tension increases for larger molecules, and due to the very high degree of hydrophobicity of SolSep-030505, the difference in surface tension, and thus the resistance against solvent permeation, increases for larger alcohols. Similar findings were reported by Machado *et al.* (1999) for a MPF-50 membrane, not only for alcohols, but also for ketones, alkyl acetates and linear hydrocarbons. An anomaly, which was not further investigated, was observed for the ethanol permeability,

The experimental data were modelled similarly as the data for the binary mixtures of water, methanol and/or ethanol and the results are shown in Figure 4.15. The four models used can all describe the observed decrease in solvent permeability. However, it appears from the statistical analysis that large deviations exist between the descriptive qualities of the different models used for this series of flux data. The error variance is 1.08, 0.36, 0.01 and 0.17 respectively for the models of Hagen-Poiseuille, Jonsson and Boesen, Machado *et al.* and the newly developed model. The experimental data are clearly best described by the model of Machado *et al.*, but this is not surprising at all. Indeed, it was developed based on experimental flux data for a homologous series of organic solvents, measured with hydrophobic membranes and it was thus expected that this model might provide a better fit compared to the new model for this series of permeability data. However, the error variance of the new model is still in the same order of magnitude as the error variances of this model obtained with the binary mixtures, which indicates that the new model is quite robust and that it can deal with the different types of solvents very well. Furthermore, when the results are compared with those from the Hagen-Poiseuille and the Jonsson and Boesen models, it is obvious that the latter two models lead to significantly poorer modelling results.

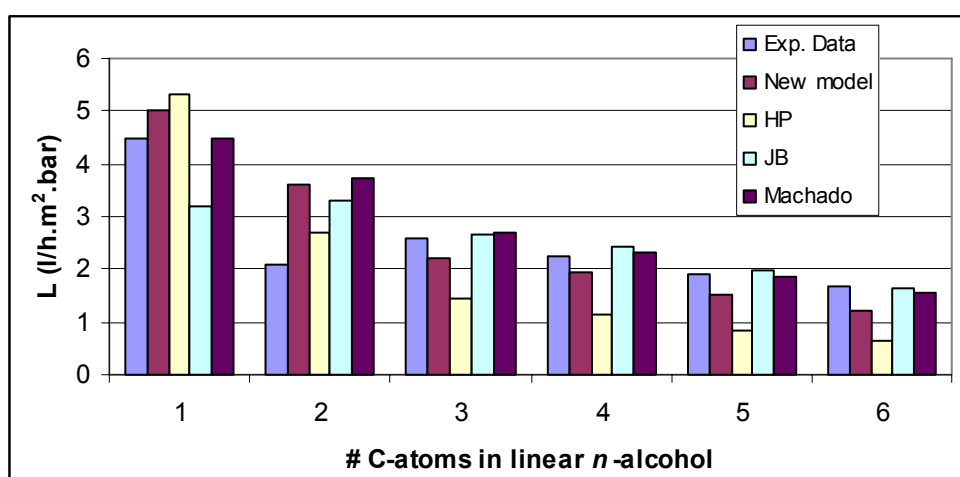


Figure 4.15: Modelling of the permeability of a homologous series of primary alcohols through a SolSep-030505 membrane, using the new model, and the models of Hagen-Poiseuille (HP), Jonsson and Boesen (JB) and Machado *et al.*

## 4.2 Permeability of other solvents

Finally, the study of the solvent flux was extended to a broad range of organic solvents. The permeability of a series of solvents was determined for a MPF-50 membrane, using the Sterlitech dead-end filtration module, at an operating pressure of 10 bar and the permeability was determined after 1, 2 and 3 h. A stationary regime was observed over this time period. The MPF-50 membrane was selected, as preliminary experiments (see Chapter 3) indicated that this membrane was solvent resistant for a wide range of organic solvents. The permeability was determined subsequently for methanol, ethanol, acetone, ethyl acetate, toluene, *n*-hexane and methylene chloride. The permeability of the different solvents was determined in a one-run experiment, thus all fluxes were measured with the same membrane disk. In order to take possible ‘membrane history’, due to membrane-solvent interactions, into account, the experimental permeabilities were normalised with the methanol permeability, which is a standard procedure in research on membrane technology. Therefore, the initial methanol permeability  $L_m^0$  was determined first, followed by the ethanol permeability, and before the measurement of the permeability  $L_i^{\text{exp}}$  of each other solvent  $i$ , the methanol permeability  $L_m^i$  is determined again. The effective solvent permeability  $L_i$  of solvent  $i$  is then calculated as:

$$L_i = L_i^{\text{exp}} \frac{L_m^i}{L_m^0} \quad (4.11)$$

	L (l/h.m <sup>2</sup> .bar)
Methanol	2.5
Ethanol	1.0
Acetone	6.2
Ethyl acetate	5.5
Toluene	4.3
<i>n</i> -Hexane	18.2
Methylene chloride	5.4

Table 4.5: Permeability of organic solvents from different chemical classes through MPF-50

The permeability data, summarised in Table 4.5, are difficult to interpret as such, since a number of parameters affect the solvent permeability. Taking into account that both the solvent viscosity and the surface tension influence the solvent flux, it is logical that *n*-hexane, having the lowest viscosity and surface tension (and thus the smallest difference in surface tension with the hydrophobic membrane) of the solvents used, shows a significantly higher permeability than the other solvents. In contrast,

ethanol showed the lowest permeability, as it is the most viscous and in addition a relatively polar solvent. The permeabilities of the other solvents vary and are therefore a useful and representative data set for the evaluation of the different transport models.

Figure 4.16 shows the experimental data and the results of the different model fits. It can be seen that the newly developed model describes all experimental data satisfactorily. It is moreover the only model to provide a close approximation for the value of the *n*-hexane permeability. The other models can not deal with the entire range of organic solvents. This is confirmed by the statistical analysis of the model fits. The error variances were found to be 15.6, 22.9, 24.9 and 0.9 respectively for the models of Hagen-Poiseuille, Jonsson and Boesen, Machado *et al.* and the new model. This clearly confirms that the 3-parameter model presented before offers a significant improvement in the modelling of the experimental permeability data for non-aqueous nanofiltration.

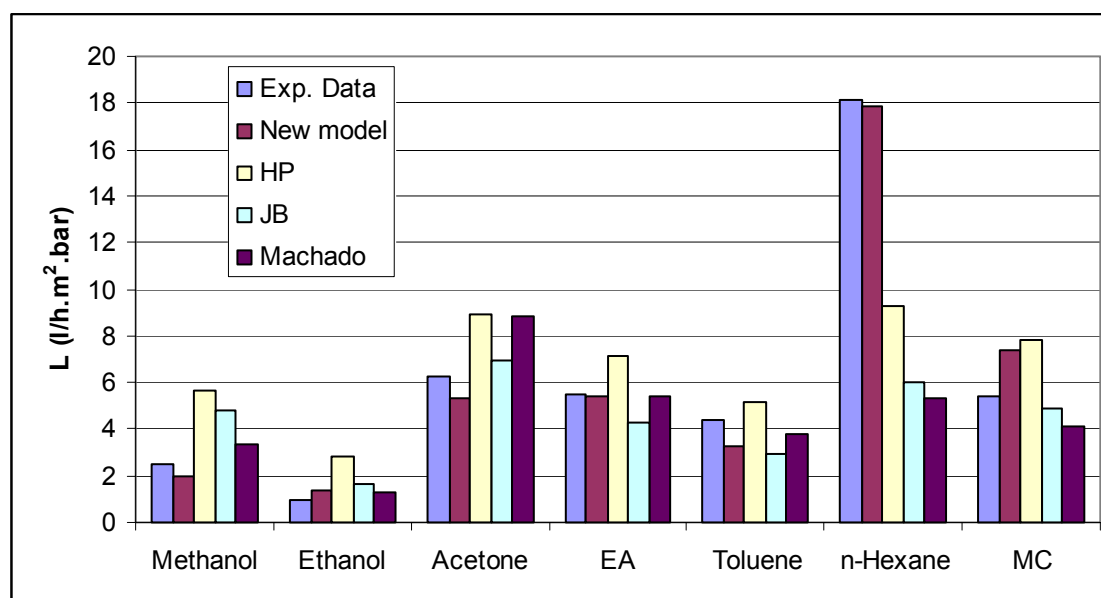


Figure 4.16: Modelling of the permeability of organic solvents from different chemical classes through a MPF-50 membrane, using the new model, and the models of Hagen-Poiseuille (HP), Jonsson and Boesen (JB) and Machado *et al.* (EA: ethyl acetate; MC: methylene chloride)

## 5. Summary and conclusion

It was concluded from filtration experiments with binary mixtures of water, methanol and/or ethanol that solvent transport through nanofiltration occurs mainly by convection, or by coupled diffusion.

Therefore, liquid mixtures could be considered as bulk material and liquid properties of given feed and permeate samples remained constant.

The pore size, the porosity, the tortuosity and the thickness of the membrane are typical transport parameters in filtration processes. But more than these material constants, other properties affect the solvent permeability.

It was found that the experimental data did not meet Darcy's law and that the viscosity cannot be the sole solvent parameter with respect to solvent permeability. The observed fluxes through hydrophobic nanofiltration membranes clearly indicated the strong influence of polarity effects at the membrane-solvent interface. The polarity effects were also confirmed by the calculation of the partial permeabilities of the different components in the binary mixtures. It was observed that the permeability of the most polar component through hydrophilic membranes is more affected by the addition of a less polar component than vice versa. In contrast, for hydrophobic membranes the opposite was observed, namely that the permeability of the least polar component was most affected by the presence of the other component. The comparison between polymeric and ceramic membranes showed no important differences, eliminating the objection of swelling effects.

A new transport model for the permeation of organic solvents was developed. It was found that at least three parameters should be included in a suitable transport model, namely a measure for the transport of momentum, a measure for steric hindrance effects, and a measure for the polarity effects between the membrane and the solvent. Based on the experimental data for the binary mixtures, and on transport models available in literature, the solvent viscosity, the solvent molar volume and the difference in surface tension were selected as representative transport parameters. Compared to literature models, the newly developed model provided a significantly improved model fit for the permeability data through hydrophobic nanofiltration membranes; the error variance was reduced by about one order of magnitude. For the hydrophilic membranes, the different models evaluated showed similar results.

The model was validated for a broad range of solvents with additional filtration experiments. The model was also useful to describe the permeation data for a homologous series of six primary alcohols. For the description of the permeability data of organic solvents from different chemical classes (methanol, ethanol, acetone, ethyl acetate, toluene, *n*-hexane and methylene chloride), the new model provided a notable improvement when compared to the literature models. Whereas existing models show important problems when dealing with all solvents and the number of varying solvent properties, the permeability values calculated with the new model showed a very high correlation over the entire range of solvents used.

It can thus be concluded that the permeability of organic solvents through nanofiltration membranes is influenced by the solvent viscosity, the molecular size of the solvent and the difference in surface tension between the membrane and the solvent, and that the model presented offers a powerful tool to describe and predict the permeability of a large number of organic solvents.

# *Chapter 5*

## *Solute transport in non-aqueous nanofiltration*

## 1. Introduction

It was mentioned before that the performance of a membrane process is characterised by the solvent permeability, the solute rejection and the recovery. It is thus necessary to obtain, besides the understanding of transport mechanisms during solvent permeation, a clear insight in the transport behaviour of dissolved components. Whereas in aqueous media, no particular attention was paid to interactions between the solute and the water molecules, non-aqueous nanofiltration requires a complete insight in all possible membrane-solvent-solute interactions, and this considerably complicates the problem to be analysed.

Traditionally, the Molecular Weight Cut-Off (MWCO) of a membrane is used as an indication of the separation performed by the given membrane. The MWCO is defined as the molecular weight of a reference component that is 90% rejected and is usually determined experimentally by measuring the reflection curve (i.e. the rejection as a function of the molecular weight of the solutes) for an aqueous solution of a mixture of polyethylene glycols (PEG). Figure 5.1 shows such a reflection curve and indicates how the MWCO can be deduced. It is desirable for a high performance membrane that the slope in the reflection curve is very steep, since this provides a very precise separation at a well-defined solute size.

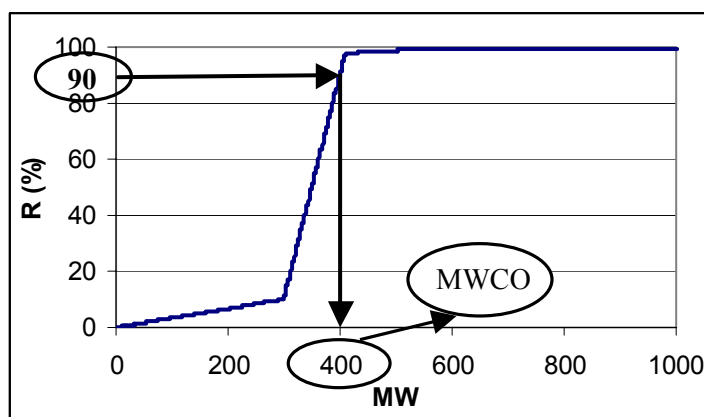


Figure 5.1: Reflection curve and definition of Molecular Weight Cut-Off

However, membrane processes in organic solutions comprise a variety of different solvents, solvent mixtures and solutes. Since membrane-solvent interactions are shown to play a determining role in non-aqueous nanofiltration (see previous chapter), knowledge about the separation performance of one solvent system cannot be transferred right away to another. This implies that cut-off values obtained in aqueous solutions do not allow to predict the membrane performance in organic solutions. This is confirmed by the relatively sparsely available data in literature on solute rejection in organic solvents. Whu *et al.* (2000) and Yang *et al.* (2001) found lower rejections with MPF-60 for Vitamin B12, brilliant blue R and safranin O in methanol than could be expected based on the specified MWCO.

White (2002) suggested that polymer-solvent interactions and the pore structure of the membranes have a strong influence on the separation, which was also found in the work of Koops *et al.* (2001).

Nanofiltration membranes are situated at the interface between dense and porous materials, and the discussion is still on-going whether solute transport occurs by convection or diffusion. The principal transport mechanism has important repercussions on the parameters, both of the solvent, the solute and the membrane, that affect the solute permeation rate, and on the modelling of these phenomena.

## 2. Parameters affecting solute transport

### 2.1 Introduction

The expansion of nanofiltration technology towards non-aqueous media results in a significantly increased number of parameters and interactions affecting the solute transport. It was mentioned before that only few data on solute transport are available in literature. Moreover, most studies available in the literature are focused on specific applications in the food, the pharmaceutical and the chemical industry, e.g. deacidifying vegetable oils (Raman *et al.*, 1996; Zwijnenberg *et al.*, 1999), the separation of tocopherol succinates from deodoriser distillate (Lin *et al.*, 2004), homogeneous catalyst separation (Nair *et al.*, 2002), solvent recovery in lube oil dewaxing (White and Nitsch, 2000), membrane extraction of bioactive components of green tea (Nwuha, 2000) or the separation of linear hydrocarbons and carboxylic acids from ethanol and hexane solutions (Koops *et al.*, 2001).

Bhanushali *et al.* (2002) presented a more systematic approach for the study of solute transport in non-aqueous nanofiltration. It was concluded from the experimental data that solute-solvent coupling plays a determining role in the solute transport rate, and thus both convective and diffusive contributions should be considered with respect to solute transport. In contrast, White (2002) claimed that solute transport through nanofiltration membranes occurs solely by diffusion and that therefore only a solution-diffusion approach should be retained.

As there is still no consensus on the exact mechanism for solute transport in non-aqueous nanofiltration, it is important to identify the solvent and solute properties and the membrane characteristics that influence the permeability of dissolved components in organic solutions. The balance between convective and diffusive transport has to be investigated in detail and the relative importance of the different membrane-solvent-solute interactions should be analysed.

### 2.2 Experimental set-up

For the same reasons as for the study of the solvent permeability through nanofiltration membranes, it was decided to base the parameter analysis for solute transport on experimental data on filtration

experiments with binary liquid mixtures of water, methanol and/or ethanol, containing a single reference solute. The study of such mixtures allows to evaluate the solute rejection as a function of the feed composition and the transitional transport behaviour can be examined qualitatively.

The filtration experiments were carried out on the cross-flow membrane set-up, with three different types of nanofiltration membranes: Desal-5-DK, N30F and MPF-50. Membrane samples were pretreated by soaking them overnight in the solvent mixture used in the subsequent experiment. A different membrane disk was used for every experiment. A transmembrane pressure of 15 bar was applied and the temperature was maintained at 25 °C. The feed flow was set constant at 2 l/min, corresponding to a cross-flow velocity of 3.8 m/s. Reynolds numbers in pure water, methanol and ethanol are respectively  $12 \cdot 10^3$ ,  $15 \cdot 10^3$ ,  $8 \cdot 10^3$  and turbulence is therefore guaranteed. Synthetic solutions of 100 mg raffinose per liter of solvent mixture (0, 25, 50, 75 and 100 mol%) were used as feed streams for the filtration experiments. It was shown before that no shift in liquid composition occurs. In order to determine the solute rejection for one filtration experiment, the raffinose concentrations in the feed and the permeate stream were determined after 20, 40 and 60 minutes, using the phenol-sulphuric acid method. The concentrations remained constant over this period of time; the rejection was calculated from the average of these three measurements.

## 2.3 Results and discussion

### 2.3.1 Experimental data

Table 5.1 and Figure 5.2 show the raffinose rejections for the three membranes in binary mixtures water-methanol, water-ethanol and methanol-ethanol. For Desal-5-DK a smooth decrease of the rejection in water-methanol mixtures (between 99 and 84%) was observed. The water-ethanol mixtures showed a smooth decrease for mixtures containing less than ca. 50 mol% ethanol, but between ca. 50 and 60 mol% ethanol a strong decrease in rejection over a small feed composition range was observed. Finally for methanol-ethanol mixtures a general decrease between 84 and 20% was observed.

For N30F rejections were low for all tested mixtures. A rejection of 53% was measured in pure water. This is lower than can be expected based on the MWCO specifications. For all other measurements with N30F, rejections were below 28%. Rejections in pure methanol and ethanol are only 8%. The rejections for aqueous mixtures generally decreased with increasing alcohol content. For all methanol-ethanol mixtures, rejections were low (below 14%). No clear tendency was found in this case; given the experimental uncertainties in measuring low rejections, these values can be considered constant.

MPF-50 membranes showed a completely different rejection behaviour. For the water-alcohol mixtures a minimum in the curves showing the rejection behaviour was observed. Raffinose rejection in pure water is 34%, decreases to a level of 10 – 15% at 25 mol% of alcohol and finally increases to 65% for methanol and 41% for ethanol. For the methanol-water mixtures, the rejection curve is



smoothly increasing beyond the minimum. The minimum for the water-ethanol mixture is broader (25 – 50%) and the rejection curve increases steeply at about 50 mol% of ethanol to reach a more or less constant value. For methanol-ethanol mixtures, a smooth decrease in rejection is observed (65 – 41%).

Water-Methanol				
$x_w$	$x_m$	Desal-5-DK	N30F	MPF-50
1.0	0.0	99	53	34
0.72	0.28	92	15	14
0.55	0.45	89	28	28
0.37	0.63	87	22	46
0.0	1.0	84	8	65
Water-Ethanol				
$x_w$	$x_e$	Desal-5-DK	N30F	MPF-50
1.0	0.0	99	53	34
0.78	0.22	85	24	12
0.52	0.48	83	25	12
0.40	0.60	33	13	34
0.0	1.0	20	8	41
Methanol-Ethanol				
$x_m$	$x_e$	Desal-5-DK	N30F	MPF-50
1.0	0.0	84	8	65
0.71	0.29	46	6	47
0.55	0.45	51	8	37
0.36	0.64	35	14	38
0.0	1.0	20	8	41

Table 5.1: Rejection (in%) of raffinose (100 mg/l) in binary mixtures of water, methanol and ethanol for Desal-5-DK, N30F and MPF-50

### 2.3.2 Discussion

The high rejection of raffinose in pure water by Desal-5-DK can be explained by the dense nature of this membrane. The MWCO of the membrane is well below the MW of raffinose (180 vs. 504), so that almost complete rejection is expected. It is clear that the membrane pore size is a first parameter that determines the solute rejection.

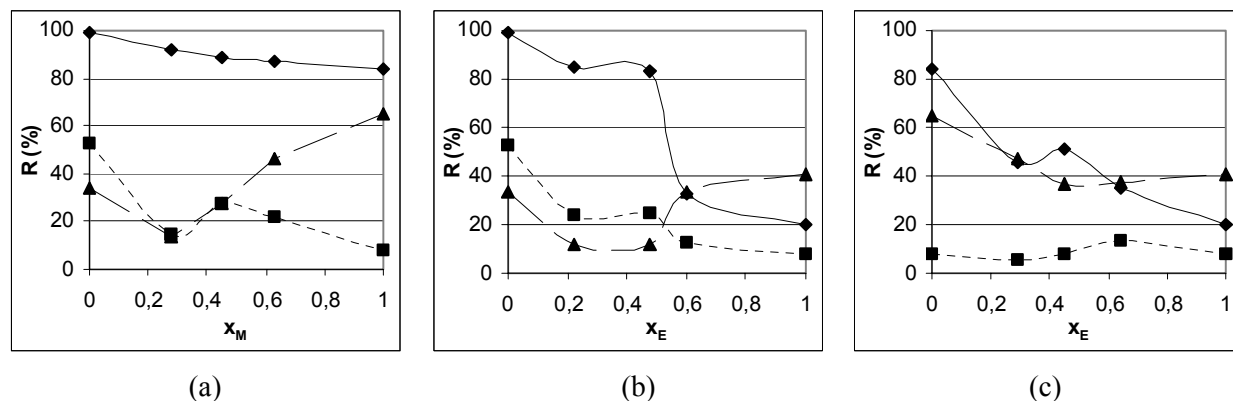


Figure 5.2: Rejection of raffinose for Desal-5-DK (◆), N30F (■) and MPF-50 (▲), in (a) water-methanol, (b) water-ethanol and (c) methanol-ethanol mixtures

Considering the rejections in the mixtures, it must be remarked that the rejection generally decreases with increasing alcohol concentration. This can be explained by the fact that the effective size of a molecule is larger in water, due to hydration. When the water concentration is reduced, it can be postulated that hydration by water molecules is replaced by solvation by alcohol molecules. Regardless of the fact whether convection or diffusion is the most important process for solute transport, hydration/solvation of the solute molecule hinders the permeation of a component, as the effective solute diameter increases. With increasing alcohol fraction, raffinose is rather solvated instead of hydrated. Solvation is less effective than hydration, since different intermolecular forces are involved: whereas strong interaction forces between permanent dipoles (hydrogen bonds) or between an induced and a permanent dipole occur for hydration, solvation is based on weaker interaction forces between induced dipoles (and thus based on the polarisability), also known as London dispersion forces (Silberg and Gold, 1996). These are typically one order of magnitude smaller than hydration forces (Kotz and Purcell, 1991). Because of the phenomenon of solvation, the effective solute size, and thus the solute rejection, decreases with increasing alcohol fraction. Moreover, the effect is expected to be more pronounced in ethanol than in methanol, as ethanol is less polar than methanol; solvation by ethanol is less effective than by methanol. This is confirmed by the calculation of the effective solute diameters in the pure liquids. When using the group contribution method of Geankoplis (1978), the molar volume at the boiling point for raffinose was found to be  $530.3 \text{ m}^3/\text{mol}$ . Based on the Wilke-Chang equation (1955), the diffusivity of raffinose in water, methanol and ethanol is  $3.55 \cdot 10^{-10}$ ,  $7.25 \cdot 10^{-10}$  and  $3.86 \cdot 10^{-10} \text{ m}^2/\text{s}$  respectively. These diffusivities were used to determine the effective solute diameter for raffinose with the Stokes-Einstein equation (Mulder, 1996): 1.25 nm, 1.09 nm and 1.03 nm in water, methanol and ethanol respectively. These diameters are comparable to literature values. Stokes-Einstein diameters could not be calculated for the mixtures, as the parameter  $\phi$  in the Wilke-Chang equation, which is an association parameter for the solvent, is only available for the pure liquids (2.6 for water, 1.9 for methanol and 1.5 for ethanol). As the hydrogen bonding capacity

decreases with increasing polarity of the solvent, it is however acceptable to assume that the parameter  $\phi$  decreases monotonically with increasing alcohol fraction. This leads to a monotonic decrease of the Stokes-Einstein diameter of raffinose with increasing methanol or ethanol fraction in the different feed mixtures.

The relatively high rejection in pure methanol (> 80%) shows that the solvation effect of this solvent is large enough to cause steric hindrance for molecules with a diameter of 1.09 nm. The steric hindrance is a combined effect of the effective solute size and the small pore size of the membrane. In water-ethanol mixtures, hydration can compensate for the presence of ethanol up to 50 mol% ethanol. At high ethanol level, solvation becomes too weak and raffinose transport is facilitated. The decrease for the methanol-ethanol mixture indicates that methanol cannot compensate for the presence of ethanol in the same way as water can.

For N30F the rejection in pure water is only 53%, which is below the specifications of the membrane (MWCO 400). The membrane obviously has pores larger than indicated by the manufacturer. As N30F has larger pores than Desal-5-DK, solvation of raffinose by methanol is not strong enough to give relatively high solute rejection. Therefore, rejections are low for all methanol-ethanol mixtures.

It must be emphasised that, when the rejections of different membranes are compared, only the membrane itself is different for these experiments; the feed mixtures and the transmembrane pressure were the same. Therefore, differences in rejection between the different types of membranes can only be the result of different membrane characteristics and different membrane-solvent-solute interactions. As the feed mixtures are the same, no difference in hydration/solvation of the raffinose molecule can occur (for mixtures of the same composition).

The curves for MPF-50 are different when compared to those for Desal-5-DK and for N30F. This can only be explained by different membrane characteristics, as solvent-solute interactions are identical. Beside the different MWCO, the most important difference is that MPF-50 is a hydrophobic membrane. The affinity decreases in the order ethanol, methanol, water.

The rejection of raffinose in pure solvents decreases for MPF-50 in the order methanol – ethanol – water. This is in contradiction with previously reported work by Yang *et al.* (2001), who reported that rejections in water are always higher than in organic solvents. Considering the results for Desal-5-DK and N30F, the statement of Yang *et al.* (2001) appears correct for hydrophilic membranes, but it is no longer valid for hydrophobic membranes.

Firstly, MPF-50 has very large pores (MWCO 700) so that convection is the dominant transport mechanism. Since the raffinose molecule is smaller than the specified MWCO, its rejection should be rather low. However, the increasing rejection with increasing alcohol fraction cannot be explained only by hydration/solvation of the solute, as the raffinose diameter decreases in methanol and ethanol.

The increasing rejection can be explained by interactions with the membrane material: analogously to the hydration/solvation of the solute, the membrane polymer is also hydrated or solvated. As MPF-50 consists of a highly hydrophobic material, the interaction with water molecules is minimal so that hydration is almost non-existing. Still, solvation occurs, and is more efficient for methanol than for ethanol. Solvation is determined by two factors: the relative affinity of the solvent for the membrane and the molecular size and structure of the solvent. Although the affinity with the membrane is larger for ethanol than for methanol, solvation by methanol is more efficient due to its smaller size. This might be the most important conclusion for the MPF-50 membrane. Consequently, due to solvation of the pore wall, the effective pore size is thought to decrease in the order methanol - ethanol - water, which is the same order as observed for the rejections in the pure solvents. The principles of pore wall solvation and a solvent dependent effective pore diameter are illustrated in Figure 5.3.

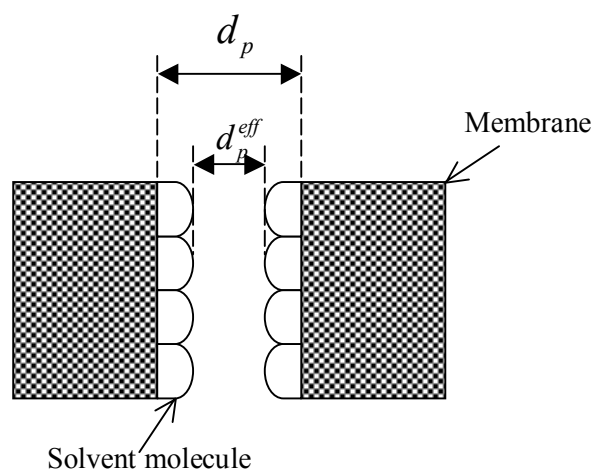


Figure 5.3: Principle of pore wall solvation: due to the presence of solvent molecules, the pore diameter  $d_p$  is reduced to an effective pore diameter  $d_p^{eff}$

Moreover, the minimum in the rejection curve for the water-methanol mixtures is less wide than for water-ethanol: due to its high affinity for the membrane polymer, methanol can replace the water molecules more efficiently than ethanol. Therefore, not only the rejection in pure methanol is higher than in pure ethanol, but rejection is higher in every water-methanol mixture than in the water-ethanol mixture of the same composition. For the same reason, a smooth decrease in the rejection curve for methanol-ethanol mixtures is observed.

Finally, the hydration/solvation of the solute still remains important for transport. The rejection in pure water is higher than for a mixture containing 25% of alcohol. Since hydration of the membrane is non-existing for MPF-50, the higher rejection in pure water must be explained by the hydration of the solute (and thus by the increased effective solute size).

It must be added that the effect of hydration/solvation of the pore wall also occurs for Desal-5-DK and N30F. These membranes are hydrophilic and thus hydration of the membrane polymer is more important than solvation. Therefore, the effective pore size is the smallest in water, it increases in methanol and is the largest in ethanol. This phenomenon reinforces even the previously described effect of hydration/solvation of the solute.

The quantitative analysis can therefore be expanded to both solute size and pore diameters. Gibbins *et al.* (2002) calculated pore diameters for Desal-5-DL (comparable to Desal-5-DK) and for MPF-50 (respectively 1.10-1.12 nm and 1.12-1.16 nm). The data show the importance of the solvation of the membrane material. Although the specified MWCO's for Desal-5-DL and MPF-50 are respectively 180-300 and 700 (in water), the difference in pore diameter in methanol is much smaller. Considering the pore diameters of the Desal membrane, it appears that raffinose, dissolved in water or methanol, is larger than the pore size (1.25 and 1.09 nm versus 1.10 – 1.12 nm) and thus high rejections can be expected. In ethanol, raffinose is smaller (1.07 nm) than the pore size and thus the rejection drops. For MPF-50, the size of raffinose in methanol is comparable to the calculated pore diameter in methanol and thus rejection is relatively high. In ethanol, raffinose is smaller and the pore diameter is larger, leading to lower rejections. For N30F no data are available for the pore diameters.

## 2.4 Ceramic versus polymeric membranes

Literature data on solute rejection in non-aqueous nanofiltration with nanofiltration are extremely sparse to date. Tsuru *et al.* (2001) reported that the rejection of low molecular weight ethylene glycols was lower in ethanol than in methanol, which is in agreement with the experimental results mentioned above. Yet, to counter again the possible objection that decreased solute rejection must be attributed to swelling effects, also this series of experiments is repeated with a ceramic, and thus non-swelling, nanofiltration membrane. As for the study of the solvent permeability, the FSTi-209 membrane is used. The filtration conditions were the same as for the experiments with the polymeric nanofiltration membranes.

Figure 5.4 shows the solute rejection for the water-methanol and the water-ethanol mixtures. It is observed that the rejection is almost constant for the water-methanol mixture (93 – 89%). In contrast, a clear decrease in solute rejection is observed for the water-ethanol mixture (93 – 63%). A smooth decrease in solute rejection was observed for the methanol-ethanol mixture. These decreases cannot be explained by swelling of the ceramic membrane material. Instead, the previous findings from the experimental data for the polymeric membranes are confirmed: the decrease in solute rejection is largely due to solute-solvent and solvent-membrane interactions. It was calculated that the effective diameter of the solute diminishes for methanol and even more for ethanol; a similar effect resulting in

a solvent dependent effective pore diameter was assumed. Although this last phenomenon may be presumed for membrane swelling, it must be considered in a broader approach: since the same effects are observed for ceramic and for polymeric membranes, swelling can be excluded as the most important phenomenon with respect to solute permeation, and the term pore wall solvation may be more appropriate.

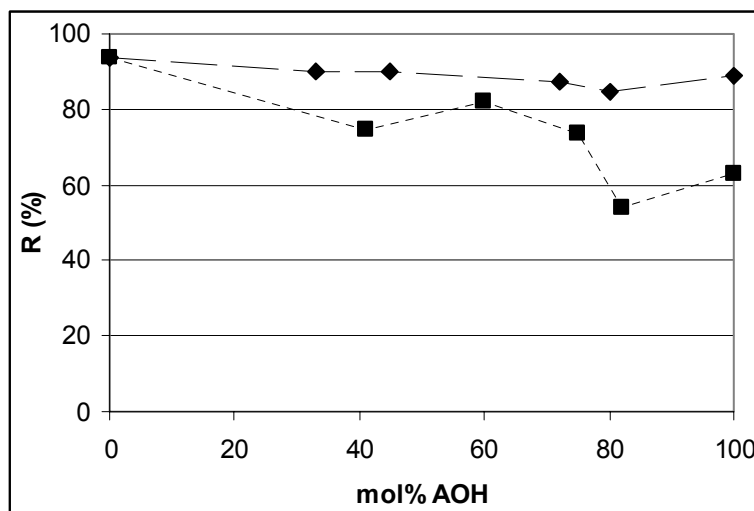


Figure 5.4: Rejection of raffinose (100 mg/l) in binary mixtures of water-methanol (◆) and water-ethanol (■) with the ceramic FSTi-209 membrane

Since it appears that there are no important differences in the solute transport behaviour for polymeric and ceramic membranes, it can be concluded that solute transport through nanofiltration membranes is indeed affected by three parameters: the nominal pore diameter, typically specified by the MWCO, the affinity between the solvent and the solute, resulting in a solvent dependent effective diameter of the solute, and the affinity between the solvent and the membrane, leading to a solvent dependent effective pore diameter.

### 3. Solute transport in non-aqueous nanofiltration

#### 3.1 Introduction

The experiments on solute transport in binary mixtures of water, methanol and/or ethanol clearly indicated that the rejection is not only influenced by pure solvent, solute and membrane properties, but also by different interactions between these three elements.

Nevertheless, the study on raffinose rejection provided no indication on the exact transport mechanisms during non-aqueous nanofiltration. Moreover, as only one solute has been used, possible

effects of solute properties on the permeability might have been ignored. And also, it appears that the solute rejection decreases with decreasing solvent polarity. For these reasons, transport of dissolved components in non-aqueous nanofiltration is investigated in further detail. The balance between convective and diffusive transport will be made and the membrane performance, in terms of solute rejection, will be evaluated for a broader range of organic solvents and solutes.

### 3.2 Solute rejection in organic solvents from different chemical classes

#### 3.2.1 Experimental set-up

Filtration experiments were carried out using the cross-flow membrane set-up. Several membranes with varying properties (polymeric vs. ceramic, hydrophilic vs. hydrophobic, MWCO 180-700) were used: MPF-44, Desal-5-DK, MPF-50, SolSep-169, SolSep-01, HITK-T1 and FSTi-128.

Pure methanol, ethanol, acetone, ethyl acetate and *n*-hexane were used to prepare synthetic feed solutions of 0.1 mM of six reference components: eusolex, 2,2-methylenebis-(6-tert-butyl-4-methylphenol), victoria blue, DL- $\alpha$ -tocopherol hydrogen succinate, bromothymol blue and Erythrosine B. For different reasons, the rejection was not determined for all membrane-solvent-component combinations: limited solubility of components in certain solvents (e.g. dye components in non-polar solvents), poor membrane stability in non-aqueous media (e.g. Desal-5-DK in acetone and ethyl acetate) or restricted significance for scientific or industrial applicability.

A transmembrane pressure of 10 bar was applied. The feed flow was set constant at 2 l/min, corresponding to a cross-flow velocity of 3.8 m/s. Temperature was maintained at 25 °C. Reynolds numbers in methanol, ethanol, acetone, ethyl acetate and *n*-hexane are  $15 \cdot 10^3$ ,  $8 \cdot 10^3$ ,  $25 \cdot 10^3$ ,  $22 \cdot 10^3$  and  $21 \cdot 10^3$  respectively, so that turbulent flow is guaranteed in all cases. Since diluted feed concentrations were used, concentration polarisation could be neglected. The osmotic pressure was 4.5 mbar for all solutions, and was also neglected. Feed and permeate concentrations were determined with UV-VIS-spectrophotometry, GC-analysis or HPLC-analysis, after different periods of time. It was checked that the membrane process was in a steady state regime, so that the permeate concentration did not change with time and the rejection remained constant. The rejection was then calculated as the average of three consecutive measurements.

#### 3.2.2 Results and discussion

The results of the filtration experiments are shown in Tables 5.2-5.8. Since diluted feed solutions were used, no significant differences in solvent flux were observed for the individual experiments, and flux values were almost equal to the pure solvent fluxes. As expected, it can be seen that the solute rejection strongly depends on the membrane characteristics and the solvent properties. Although at first sight no general trends are observable for all experimental data, interesting conclusions can be drawn anyway.

When comparing the solute rejections of all components used, it is found that the ceramic membranes (HITK-T1 and FSTi-128) showed significantly higher rejections. HITK-T1 provides relatively high rejections for all solvent-component combinations (except for eusolex in methanol). As might be expected, no measurable *n*-hexane flux was observed for the ceramic membranes.

All solute rejections measured in *n*-hexane are low. For the polymeric membranes, the performance is also relatively poor in ethyl acetate, except for Erythrosine B with MPF-44. The rejection of this component is high for all membranes in methanol, ethanol and acetone. Furthermore, it is obvious that the solute rejection is not unconditionally increasing with increasing molecular weight, e.g. in all solvents and with all membranes victoria blue provides considerably higher rejections than DL- $\alpha$ -tocopherol hydrogen succinate, although the molecular weight of the latter component is slightly higher than that of the former component, and e.g. eusolex, being the smallest component used in this study did not necessarily show the lowest rejections. At last, it is observed that the solute rejection in most of the experiments is higher in methanol than in ethanol (except for the SolSep membranes), which was also the case for the rejection of raffinose in the experiments with the binary mixtures of water, methanol and ethanol. However, there is no constant correlation between the solute rejections in different solvents for a given membrane: for example, although the rejection in methanol is generally higher for Desal-5-DK than for MPF-50, the opposite is observed for the rejections in ethanol.

MPF-44	Methanol	Ethanol	Acetone	Ethyl acetate
Eusolex	52	7	25	34
2,2-methylenebis-(6-tert-butyl-4-methyl-phenol)	30	3	15	15
Victoria Blue	72	68	27	39
DL- $\alpha$ -tocopherol hydrogen succinate	41	4	21	3
Bromothymol Blue	61	-°	9	-°
Erythrosine B	93	92	84	87

Table 5.2: Rejection of six reference components with MPF-44 in methanol, ethanol, acetone and ethyl acetate; MPF-44 was previously observed not to be stable in *n*-hexane (-°: not determined)



Desal-5-DK	Methanol	Ethanol	<i>n</i> -Hexane
Eusolex	75	16	0
2,2-methylenebis-(6-tert-butyl-4-methyl-phenol)	94	13	0
Victoria Blue	75	63	-°
DL- $\alpha$ -tocopherol hydrogen succinate	62	10	5
Bromothymol Blue	82	10	-°
Erythrosine B	99	79	-°

Table 5.3: Rejection of six reference components with Desal-5-DK in methanol, ethanol and *n*-hexane; Desal-5-DK was observed to dissolve in acetone and in ethyl acetate (-°: insoluble in *n*-hexane)

MPF-50	Methanol	Ethanol	Acetone	<i>n</i> -Hexane
Eusolex	4	0	6	0
2,2-methylenebis-(6-tert-butyl-4-methyl-phenol)	28	18	31	2
Victoria Blue	67	89	73	-°
DL- $\alpha$ -tocopherol hydrogen succinate	21	18	48	11
Bromothymol Blue	87	54	70	-°
Erythrosine B	97	92	93	-°

Table 5.4: Rejection of six reference components with MPF-50 in methanol, ethanol, acetone and *n*-hexane (-°: insoluble in *n*-hexane)

SolSep-169	Methanol	Ethanol	Acetone	Ethyl acetate	<i>n</i> -Hexane
Eusolex	5	22	19	16	0
2,2-methylenebis-(6-tert-butyl-4-methyl-phenol)	5	5	15	26	7
Victoria Blue	63	63	39	65	-°
DL- $\alpha$ -tocopherol hydrogen succinate	2	0	27	30	4
Bromothymol Blue	66	37	57	38	-°
Erythrosine B	72	86	91	24	-°

Table 5.5: Rejection of six reference components with SolSep-169 in methanol, ethanol, acetone, ethyl acetate and *n*-hexane (-°: insoluble in *n*-hexane)

SolSep-01	Methanol	Ethanol	Acetone	Ethyl acetate	<i>n</i> -Hexane
Eusolex	2	5	13	7	0
2,2-methylenebis-(6-tert-butyl-4-methyl-phenol)	5	3	24	5	4
Victoria Blue	11	30	19	19	-°
DL- $\alpha$ -tocopherol hydrogen succinate	0	0	22	13	8
Bromothymol Blue	34	5	28	2	-°
Erythrosine B	58	86	86	29	-°

Table 5.6: Rejection of six reference components with SolSep-01 in methanol, ethanol, acetone, ethyl acetate and *n*-hexane (-°: insoluble in *n*-hexane)

HITK-T1	Methanol	Acetone	Ethyl acetate
Eusolex	30	94	-°
2,2-methylenebis-(6-tert-butyl-4-methyl-phenol)	85	96	-°
Victoria Blue	99	84	92
DL- $\alpha$ -tocopherol hydrogen succinate	76	76	-°
Bromothymol Blue	63	95	-°
Erythrosine B	94	97	94

Table 5.7: Rejection of six reference components with HITK-T1 in methanol, acetone and ethyl acetate (-°: not measured due to irreparable membrane damage)

FSTi-128	Acetone	Ethyl acetate
Eusolex	15	30
2,2-methylenebis-(6-tert-butyl-4-methyl-phenol)	52	73
Victoria Blue	80	85
DL- $\alpha$ -tocopherol hydrogen succinate	-°	22
Bromothymol Blue	95	42
Erythrosine B	91	90

Table 5.8: Rejection of six reference components with FSTi-128 in acetone and ethyl acetate (-°: not determined)

Regardless of the fact whether solute transport is dominated by convection or diffusion it can be assumed that the solute rejection is strongly influenced by the molecular size of the solute: in case of viscous flow, larger components are exposed to increased steric hindrance effects, whereas in case of

solute diffusion, components have decreasing diffusion coefficients with increasing molecular size. Therefore, the effective solute diameters were calculated, using the Stokes-Einstein equation (Eq. 2.8), and are summarised in Table 5.9.

It can be seen that all solute diameters are the largest in acetone. Diameters are significantly smaller in ethanol than in methanol, and a significant decrease of the effective solute diameters was found in ethyl acetate and in *n*-hexane. This confirms again that due to a different degree of affinity between an organic component and an organic solvent, different solvent-solute interactions occur, resulting in a varying degree of component solvation in each solvent. These interactions strongly influence the membrane performance (in terms of solute separation), as the molecular size of the solute is one of the main parameters affecting solute transport.

	Methanol	Ethanol	Acetone	Ethyl acetate	<i>n</i> -hexane
Eusolex	0.70	0.66	0.71	0.58	0.59
2,2-methylenebis-(6-tert-butyl-4-methyl-phenol)	1.00	0.93	1.02	0.82	0.84
Victoria Blue	1.17	1.10	1.20	0.97	(0.98) <sup>a</sup>
DL- $\alpha$ -tocopherol hydrogen succinate	1.30	1.22	1.33	1.08	1.09
Bromothymol Blue	1.14	1.08	1.18	0.95	(0.97) <sup>a</sup>
Erythrosine B <sup>*</sup>	0.98	0.92	1.00	0.81	(0.82) <sup>a</sup>

Table 5.9: Stokes-Einstein diameters of the six reference solutes in methanol, ethanol, acetone, ethyl acetate and *n*-hexane (\*: invalid approximations, only to be used for comparison of these values in different solvents, as Na is not included in the group contribution theory for the calculation of the molar volume at the boiling point; <sup>a</sup> theoretical value, as solutes are insoluble in *n*-hexane)

Again, it is clear that the rejection is strongly influenced by the effective molecular size, as rejections were relatively high for all membranes used. In contrast, lower rejections were observed in ethyl acetate and *n*-hexane, which corresponds to the smaller molecular sizes in these solvents.

However, it was observed that molecular weight or size, and related solvation effects, could not be the only solute parameters affecting the rejection. Figure 5.5 shows the rejection as a function of the molecular weight and the logarithm of the water-octanol partition coefficient for MPF-50 with the methanol feed solutions. The results were similar for the other membrane-solvent combinations.

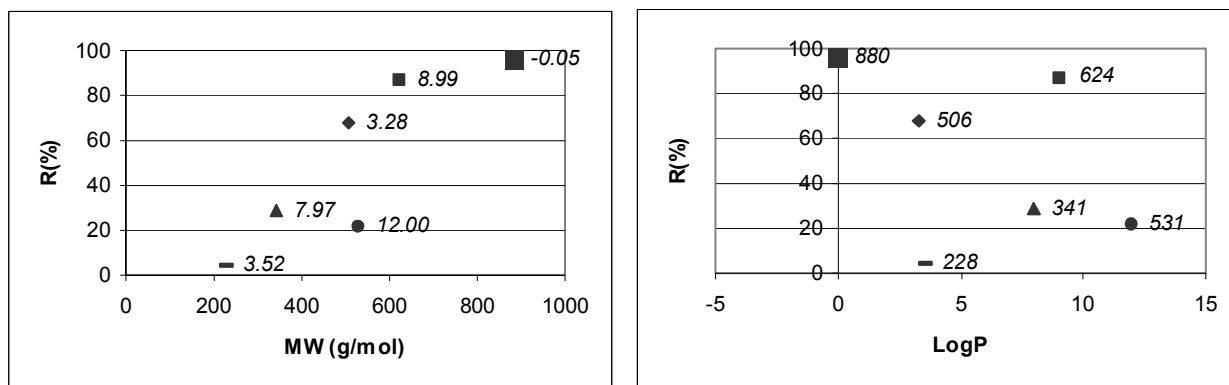


Figure 5.5: Rejection of Eusolex (■), 2,2-methylenebis-(6-tert-butyl-4-methyl-phenol) (▲), Victoria Blue (◆), DL- $\alpha$ -tocopherol hydrogen succinate (●), Bromothymol Blue (▣) and Erythrosine B (■) in methanol with MPF-50 as a function of (a) the molecular weight of a component (logP in label) and (b) the logP of a component (MW in label)

As previously discussed, Machado *et al.* (2000) suggested that, in spite of the viscous nature of the solvent flux, a pure solvent is subject to a so-called surface resistance during permeation. This resistance incorporates a polarity difference between the solvent and the membrane surface and is assumed to be in series with the resistance against viscous flow. The solute rejection experiments indicate that a similar effect occurs for solute transport through nanofiltration membranes; different effects contribute to the overall resistance of the membrane against solute permeation. Beside steric hindrance effects, it appears that also a surface resistance is part of the total resistance. The surface resistance is created by differences in polarity between the solute and the membrane material.

Braeken *et al.* (2005) proved that in aqueous solutions the solute rejection of different organic solutes with a similar molecular weight decreased with decreasing solute polarity (logP). The effect is confirmed by the results from these experiments, carried out in non-aqueous media. Although victoria blue has a smaller effective diameter, the rejection of this component is significantly higher than for DL- $\alpha$ -tocopherol hydrogen succinate. This can be explained by the relatively high polarity of the former component (and thus the reduced affinity for the polymeric membrane material). It can therefore be concluded that molecular size and polarity of the solute both determine solute transport.

Furthermore, it is well known that electrolytes can dissociate considerably in methanol. In this way, charge effects might be introduced as an additional solute-membrane interaction. In contrast to the other solutes used, victoria blue, bromothymol blue and erythrosine B can partly dissociate. These are indeed the solutes that have higher rejections than components with a similar molecular weight or polarity and thus dissociation attributes to the increased solute rejection. However, solute dissociation decreases strongly in ethanol (and in other non-polar solvents), and since the differences in solute rejections discussed above occur both in methanol and in ethanol, they cannot only be attributed to

charge effects either. Solute-membrane interactions are therefore a combination of both polarity and charge effects.

Finally, it was observed that the solute rejection in methanol is higher for Desal-5-DK than for MPF-50, whereas rejections in ethanol are higher for the latter membrane. Nevertheless, the solvent-solute interactions (effective diameters) and the solute-membrane interactions (polarity effects) remain unchanged. Therefore, these data again confirm that the solute rejection is also affected by the membrane-solvent interactions, as previously concluded from the filtration experiments with raffinose solutions in binary mixtures of water, methanol and/or ethanol. Similarly as for the solute solvation, the membrane material is also solvated. In this way, the effective pore diameter is indeed dependent on the solvent type. The principles of pore wall solvation and solvent dependent effective pore size, which were theoretically stated by Matsuura and Sourirajan (1981), and by Machado *et al.* (2000), are unambiguously confirmed by this series of experiments.

Table 5.10 provides the contact angles of water, methanol and ethanol on MPF-50 and on Desal-5-DK. Contact angles decrease in the order water-methanol-ethanol. Compared with the results for MPF-50, the decrease in contact angle is relatively small for Desal-5-DK. This can be explained by the hydrophobic nature of MPF-50 : due to the low surface tension of the membrane, water molecules are strongly repulsed from the surface, whereas the affinity for methanol and ethanol is much higher. Desal-5-DK is much more hydrophilic than MPF-50 and therefore the differences in attractive forces between the solvents and the membranes are much smaller. The contact angle for ethanol, which is the smallest, indicates the largest affinity of the membranes for this solvent. However, as stated above, due to steric hindrance, larger solvent molecules experience more difficulties in solvating the membrane pores. This is confirmed by the Stokes-Einstein equation: the effective diameter of a solvated component (e.g. the membrane polymer) is inversely proportional to the diffusion coefficient  $D_c^s$ , which is for its part proportional to the square root of the molecular weight of the solvent: thus, the lower the molecular weight of the solvent, the lower the diffusion coefficient and the larger the effective diameter.

	Desal-5-DK	MPF-50
Water	50.1	111.6
Methanol	38.4	53.8
Ethanol	34.5	38.2

Table 5.10: Contact angles (in °) with water, methanol and ethanol for Desal-5-DK and MPF-50

The affinity effect is thus less influenced for Desal-5-DK and solvation is stronger affected by steric effects: the degree of pore wall solvation decreases with increasing solvent size and thus the effective pore diameter increases. Therefore rejections are much lower in ethanol than in methanol. For MPF-50 the affinity varies much more for water, methanol and ethanol. For this membrane, the combined effect of affinity and solvent size determines the degree of solvation. Despite the larger size of ethanol molecules, solvation is less influenced for MPF-50, due to the significantly larger affinity for ethanol than for methanol. However, since methanol is a smaller solvent molecule than ethanol, the lower membrane affinity for methanol is compensated. In this way, the effective pore size is much less affected for MPF-50 than for Desal-5-DK, and the decrease in solute rejection is significantly smaller for MPF-50.

As a conclusion, it can be stated that the solute transport through a nanofiltration membrane is affected by three factors:

- solvent-solute interactions, determining the effective solute diameter;
- membrane-solute interactions, creating an in-series resistance based on polarity differences and charge effects;
- solvent-membrane interactions, determining the effective pore diameter.

This is in full agreement with the previous findings based on the filtration experiments with binary raffinose solutions in water, methanol and/or ethanol.

### 3.3 Transport mechanism for solute permeation in non-aqueous nanofiltration

#### 3.3.1 Experimental set-up

It has been pointed out before that the discussion on the precise transport mechanism for solute permeation in (non-aqueous) nanofiltration is still on-going. Therefore, experiments were carried out to gain insight into the relative importance of convective and diffusive solute transport.

In order to determine the diffusive solute flux in nanofiltration processes, static cell diffusion experiments were carried out to measure the solute diffusivity  $D_c^{M,s}$  of component  $c$  through membrane  $M$  in solvent  $s$ . Diffusion cells, shown in Figure 5.6, were made from stainless steel and consisted of two compartments of 0.243 l, separated by a membrane sheet, with a surface of 22.3 cm<sup>2</sup>. The active top layer of the membrane was directed towards the compartment containing feed solutions (0.1 mM), the other compartment was filled with the pure solvent. Both compartments were stirred at 1200 rpm with a teflon coated magnetic stirrer bar. The solute concentration of both compartments was measured as a function of time. At least 10 data points were measured for each experiment. Based on concentration profiles of time and Fick's diffusion law, the solute diffusivity (multiplied by the cell constant  $\beta$ ) can be determined from the following equation:

$$\ln\left(\frac{c_0 - c'_0}{c - c'}\right) = \beta \cdot D_c^{M,s} \cdot t \quad (5.1)$$

This series of experiments was carried out for all components in methanol and ethanol with both a hydrophilic (Desal-5-DK) and a hydrophobic (MPF-50) nanofiltration membrane.

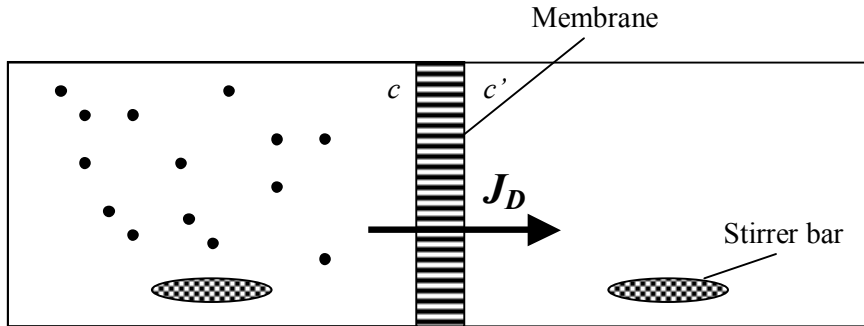


Figure 5.6: Cell diffusion experiments to determine the diffusive flux  $J_D$  occurring due to a concentration gradient ( $\Delta c/\Delta x$ ) across a semi-permeable membrane

### 3.3.2 Results and discussion

In diffusion cells, solute diffusion occurs due to the concentration gradient across the membrane; the system strives towards a new equilibrium. Figure 5.7 shows a typical concentration profile as a function of time (0.1 mM Eusolex in methanol with MPF-50; profiles were similar for all other systems). Table 5.11 provides the solute diffusivities through the two membranes (multiplied by the cell constant  $\beta$ ). Correlation coefficients between the logarithmic factor and time (Eq. 5.1) varied from 0.91 to 0.99. As can be expected, based on the specified molecular weight cut-off values of the membranes used, the diffusivities are lower through Desal-5-DK than through MPF-50, both with methanol and ethanol as solvent. Generally, the diffusivity is higher for smaller or non-polar solutes. Therefore, the diffusivity of Erythrosine B, which is the largest and the most polar solute used in the experiments, is low for all solvent-membrane combinations.

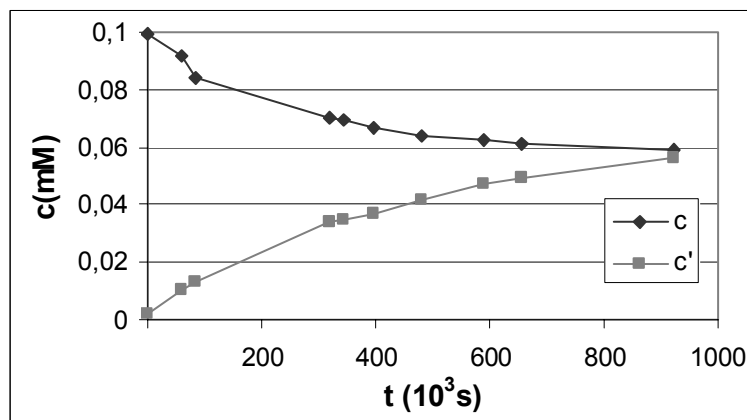


Figure 5.7: Concentration profile from cell diffusion experiments with 0.1 mM Eusolex in methanol and an MPF-50 membrane

	$\beta \cdot D_c^{DK, MeOH}$ ( $\cdot 10^{-8}$ 1/s)	$\beta \cdot D_c^{DK, EtOH}$ ( $\cdot 10^{-8}$ 1/s)	$\beta \cdot D_c^{MPF, MeOH}$ ( $\cdot 10^{-8}$ 1/s)	$\beta \cdot D_c^{MPF, EtOH}$ ( $\cdot 10^{-8}$ 1/s)
Eusolex	126	36	313	286
2,2-methylenebis-(6-tert-butyl-4-methyl-phenol)	27	17	94	215
Victoria Blue	11	5	7	94
DL- $\alpha$ -tocopherol hydrogen succinate	29	10	103	131
Bromothymol Blue	59	13	201	294
Erythrosine B	8	10	14	13

Table 5.11: Solute diffusivities (multiplied by cell constant), derived from cell diffusion experiments

As nanofiltration membranes are situated at the interface of porous ultrafiltration and dense reverse osmosis membranes, it can be assumed that solute transport occurs both by convection and diffusion. Therefore, a balance was calculated from a comparison between static cell diffusion experiments and the dynamic filtration discussed above. The diffusive flux  $J_D$  can be calculated with Eq. 5.2, also based on Fick's law:

$$J_D = \beta \cdot D_c^{M,s} \cdot \frac{V_{cell}}{2A} \cdot (c - c') \quad (5.2)$$

The total solute flux  $J_C$  can be calculated from the filtration experiments as the product of the solvent flux and the solute concentration in the permeate stream:

$$J_C = J_s \cdot c_p \quad (5.3)$$

The contribution of diffusion to the total solute transport can finally be expressed as the ratio of the diffusive flux  $J_D$  and the total flux  $J_C$ . The average methanol flux in the experiments was 132 l/h.m<sup>2</sup> for Desal-5-DK and 39 l/h.m<sup>2</sup> for MPF-50; the average ethanol flux was 64 l/h.m<sup>2</sup> and 21 l/h.m<sup>2</sup> respectively.

The relative contributions of diffusion to the total solute transport for the different membrane-solvent-component combinations used in this series of experiments are summarised in Table 5.12. The contribution of diffusion for Desal-5-DK never exceeds 1% and thus can be neglected. For MPF-50 the maximal diffusive contribution is only 7.7%. It can therefore be stated that for the membranes studied solute transport is, similarly as the transport of organic solvents, mainly dominated by convection (viscous flow).



	Desal-5-DK		MPF-50	
	MeOH	EtOH	MeOH	EtOH
Eusolex	0.76	0.13	1.61	2.63
2,2-methylenebis-(6-tert-butyl-4-methyl-phenol)	0.66	0.06	0.65	2.40
Victoria Blue	0.07	0.04	0.11	7.66
DL- $\alpha$ -tocopherol hydrogen succinate	0.11	0.03	0.65	1.47
Bromothymol Blue	0.47	0.04	7.71	5.82
Erythrosine B	0.91	0.15	2.10	1.57

Table 5.12: Contribution of diffusion to solute transport in filtration experiments (in%)

## 4. Modelling of solute transport in non-aqueous nanofiltration

### 4.1 Introduction

The implementation of membrane processes on industrial scale requires the development of a good descriptive and predictive method that provides useful information from accessible physical property data. Such a model should be physically realistic and be based on a minimum number of assumptions. But at a fundamental level, nanofiltration is a very complex process. The events leading to rejection at nanofiltration membranes are taking place on a length of scale of the order of one nanometre. This is a scale at which assumptions made for macroscopic descriptions are not valid anymore (Bowen and Welfoot, 2002). Ab initio calculations of such phenomena would be immensely complex. Therefore, it is an important challenge to develop models that convey a fundamental understanding and simple quantification of the governing phenomena in a way that has the potential for industrial applications. It is an advantage if such a method does not involve mathematics that is tedious, complicated or difficult to follow (Bowen and Mukhtar, 1996).

The modelling of solute rejection has been extensively investigated in aqueous media. Different approaches exist, resulting in a number of transport models. Descriptions of uncharged solute rejection in nanofiltration have generally been based on continuum hydrodynamic models (Bowen and Welfoot, 2002). In such models, porous membranes are represented as a bundle of straight cylindrical pores and solute transport is corrected for hindered convection and diffusion due to solute-membrane interactions (Deen, 1987). Initial descriptions of ion transport in nanofiltration were based on phenomenological equations defined through irreversible thermodynamics. Two commonly accepted transport models for the description of solute transport in aqueous solution are the Spiegler-Kedem model (1966) and the solution-diffusion model (Lonsdale *et al.*, 1965; Wijmans and Baker, 1995;

Paul, 2004). The former model incorporates both viscous and diffusive flow, whereas the latter can only be used for transport through dense membranes by solute diffusion.

In contrast to nanofiltration in aqueous solution, the modelling of solute transport in non-aqueous nanofiltration has only been sparsely investigated. White (2002) presented an SD-based model for the permeation of several reference solutes, dissolved in toluene, through dense membranes. Bhanushali *et al.* (2002) succeeded to describe experimental data with the Spiegler-Kedem model. Matsuura and Sourirajan (1981) developed a model for convective transport of dissolved components, incorporating a solvent dependent pore diameter. Gibbins *et al.* (2002) calculated the pore radii of MPF-50 and Desal-5-DK based on filtration experiments carried out in methanol, using several models for convective flow through porous membranes. The different attempts for the modelling of non-aqueous solute transport provide, however, models that are limited to specific experimental data. Generalised transport models are based on physicochemical fundamentals resulting in complex mathematical transport models that are difficult to apply on experimental data. Therefore, a more systematic and accessible model for the description and prediction of solute transport in non-aqueous nanofiltration, which is applicable on a wide range of membranes, solvents and solutes, has still to be developed. Based on different models, available in literature, corrections will be introduced for a broad applicability.

## 4.2 Modelling of the reflection curve in non-aqueous media

### 4.2.1 Theoretical background

Several models for the mass transport in membranes have been developed. A review of these transport models has been given by Soltanieh and Gill (1981). A theoretical description was given for the following models: models from irreversible thermodynamics (Kedem-Katchalsky, Spiegler-Kedem,...), frictional model, solution-diffusion model, solution-diffusion imperfection model, preferential-adsorption-capillary flow model, diffusion-viscous flow model, finely porous model. However, all these models are special cases of the statistical-mechanical model, which has been described by Mason and Lonsdale (1990).

According to Mason and Lonsdale (1990), the basic transport equation for the component  $i$  of a multicomponent solution can be written as:

$$\sum_{j=1}^N \frac{c_j}{cD_{ij}} (u_i - u_j) + \frac{u_i}{D_{iM}} = -\frac{1}{RT} (\nabla_T \mu_i - F_i) - \frac{\alpha_i' B_0}{\eta D_{iM}} (\nabla P - cF) - \sum_{j=1}^N \frac{c_j}{cD_{ij}} D_{ij}^T \nabla \ln T \quad (5.4)$$

The left-hand side describes the interdiffusion of component  $i$  with all the other components and diffusion of component  $i$  with the membrane. The three sets of terms on the right-hand side of the

equation respectively describe the driving forces for isothermal diffusion, viscous flow and thermal diffusion .

It is clear that such mathematical model is difficult to work with. For simplicity, assumptions have to be made in order to obtain a suitable and reliable transport model for a relatively easy description of the solute transport in different membrane applications.

Different approaches were followed in literature. For dense membranes, solution-diffusion models are commonly used. This model is derived from the fundamental statement that the flux is proportional to a gradient in solute concentration and it has been the most widely accepted explanation for transport in dialysis, reverse osmosis, gas permeation and pervaporation. White (2002) suggested to apply this model also on experimental data for dense nanofiltration membranes, used in toluene, resulting in the following transport model:

$$J_i = D_i K_i \frac{\left( c_{f,i} - c_{p,i} \exp\left(\frac{-V_i(P_f - P_p)}{RT}\right) \right)}{\Delta x} \quad (5.5)$$

It appeared, however, from the filtration and the cell diffusion experiments that solute transport in non-aqueous nanofiltration is mainly dominated by convection, so that the validity of the White model can be questioned. Transport models based on viscous flow may therefore be more appropriate.

The transport equations of Spiegler and Kedem (1966) are commonly used for the description of the rejection of uncharged molecules in aqueous solution, combining both diffusion and convection:

$$J_s = L(\Delta P - \sigma \Delta \pi) \quad (5.6)$$

$$J_c = P_s \Delta x \frac{dc}{dx} + (1 - \sigma) J_s c \quad (5.7)$$

The rejection of a given molecule can then be calculated as:

$$R = \frac{\sigma(1 - F)}{1 - \sigma F} \quad (5.8)$$

$$\text{with } F = \exp\left(-\frac{1 - \sigma}{P_s} J_s\right) \quad (5.9)$$

The permeability  $P_s$  is a measure of the transport of a molecule by diffusion. The reflection coefficient  $\sigma$  of a given component is the maximal possible rejection for that component. From Eq. 5.8 and 5.9, it can be seen that this corresponds with the rejection at an infinite solvent flux. A model for the reflection coefficient as a function of the molecular diameter of the solute (reflection curve) can then be used to estimate the maximal rejection that can be obtained with a given membrane.

Different models for the description of a reflection curve have been developed and are used for the description and prediction of the performance of porous membranes in aqueous media. These models all have in common that they assume that the separation of different permeants is achieved by size exclusion.

The Steric Hindrance Pore (SHP) model (Nakao and Kimura, 1982) calculates the reflection coefficient from the pore size of the membrane and the diameter of the solute. It should be noted that the fact that an effective pore size can be calculated does not necessarily indicate that geometrically well defined pores exist. The uniform pore size should therefore not be interpreted as a real value for the diameters of the pores, but as the pore size of an imaginary membrane having uniform pores, for which the rejection of uncharged molecules is equal to this with the real membrane.

During transport, dissolved components encounter a certain steric hindrance and interactions with the pore wall. A molecule smaller than the diameter of the membrane is partially retained through these effects. A solute with the same size as the pore diameter is completely rejected. The reflection coefficient is then calculated as:

$$\sigma = 1 - H_F S_F \quad (5.10)$$

$$\text{with } H_F = 1 + \frac{16}{9} \eta^2 \quad (5.11)$$

$$S_F = (1 - \eta)^2 (2 - (1 - \eta)^2) \quad (5.12)$$

$$\eta = \frac{d_c}{d_p} \quad (5.13)$$

$H_F$  is a 'wall-correction parameter' that represents the effect of the pore wall;  $S_F$  is a parameter that represents steric hindrance during the transport through the pores. The diameters of a molecule and of a pore are symbolised by respectively  $d_c$  and  $d_p$ .

Ferry (1936) presented a theoretical model for the description of the reflection curve for ultrafiltration membranes. The pores are considered to be cylindrical with a uniform diameter and a parabolic velocity dependence in the pore is assumed. It describes the rejection of a spherical molecule through a capillary as:

$$\sigma = 1 - 2(1 - \eta)^2 - (1 - \eta)^4 \quad (5.14)$$

Further on, the Verniory model (1973) is based on the incorporation of frictional drag forces acting in cylindrical membrane pores:

$$\sigma = 1 - g(\eta) S_F \quad (5.15)$$

$$\text{with } g(\eta) = \frac{1 - \frac{2}{3} \eta^2 - 0.2 \eta^5}{1 - 0.76 \eta^5} \quad (5.16)$$

$$S_F = (1-\eta)^2(2-(1-\eta)^2) \quad (5.17)$$

At last, in the lognormal model (Van der Bruggen *et al.*, 2000b) the pore size is accepted not to be constant, in contrast to the other models discussed so far. A lognormal distribution is assumed for the pore size. No steric hindrance in the pores or hydrodynamic lag is taken into account, but it is assumed that a molecule permeates through every pore that is larger than the diameter of the molecule. Moreover, the diffusion contribution to the transport through the membrane is considered to be negligible. Therefore, the reflection curve can be expressed as:

$$\sigma = \int_0^{r_c} \frac{1}{S_p \sqrt{2\pi}} \frac{1}{r} \exp\left(-\frac{(\ln(r) - \ln(\bar{r}))^2}{2S_p^2}\right) dr \quad (5.18)$$

with  $r_c = d_c/2$ . This equation comprises two variables,  $S_p$  and  $\bar{r}$ , where  $S_p$  is the standard deviation of the distribution. This standard deviation is a measure for the distribution of the pore sizes.  $\bar{r}$  is a mean pore size, namely the size of a molecule that is retained for 50%.

Other models for the modelling of the reflection curve are present in the literature, e.g. the method of Haberman and Sayre (1958), the model of Zeman and Wales (1981), the model of Bohlin (1959) or the extended pore model of Li *et al.* (2005), but these are similar to one of the other models and are therefore not further discussed.

#### 4.2.2 Correction for modelling in different solvents

The different models for the reflection curve are all typically developed for applications in aqueous solution. No specific parameters are included to deal with different (non-aqueous) solvents. However, the models may be applied if it is taken into account that the different diameters used should be effective diameters (both for the solutes as for the membrane pores), which are definitely solvent dependent, as discussed before.

The influence of organic solvents on a dissolved component can easily be expressed in terms of effective solute diameters, which are calculated using the Stokes-Einstein equation. However, as the number of possible components is infinite, it is not always realistic, or even possible, to calculate the effective solute diameter with the Stokes-Einstein procedure, e.g. when the molar volume at the boiling point cannot be calculated with a group contribution method (as in the case of Erythrosine B). Therefore, Van der Bruggen (2000) presented an empirical correlation between the molecular weight of a component and its effective diameter in water:

$$d_c = 0.065(MW)^{0.438} \quad (5.19)$$

As this correlation only provides the effective diameter in aqueous solution, a correction should be introduced to obtain the effective diameter in other solvents. When comparing the effective diameters of one component in different solvents, it appears that there is a constant ratio between these diameters. This constant ratio is emanating from the Wilke-Chang equation. The ratio of two effective solute diameters results in the elimination of a large number of parameters included in this fraction, leading to a simple relationship between the two effective diameters (derivation in Appendix C):

$$\frac{d_c^{s_2}}{d_c^{s_1}} = \frac{(\phi_{s_1} M_{s_1})^{1/2}}{(\phi_{s_2} M_{s_2})^{1/2}} \quad (5.20)$$

As the effective diameter is known in aqueous solution, a simple and straight-forward approximation can be made of the effective diameters in other solvents. Table 5.13 shows the ratio of the effective diameters of a component in different solvents relative to this in water. If the (solvent dependent) effective pore diameter is known too, the reflection curve can then easily be determined using either the SHP, Ferry, Verniory or lognormal model.

	$\frac{d_c^s}{d_c^w}$
Water	1.000
Methanol	0.877
Ethanol	0.824
Acetone	0.898
Ethyl acetate	0.729
<i>n</i> -Hexane	0.738

Table 5.13: Ratio of effective solute diameters in different solvents relative to the effective diameter in water

### 4.3 Results and discussion

The procedure that was developed to extend existing models for the description of a reflection curve towards applications in non-aqueous media, has been applied on the experimental data reported in the previous section. The procedure can be used from two different points of view. On the one hand, it can be used for descriptive modelling. As the effective pore diameters are unknown for the membranes used, the best fit has been calculated, providing the unknown model parameters, i.e. the pore diameter for the SHP, Ferry and Verniory model, and the pore diameter and the standard deviation of the pore size distribution for the lognormal model. It is expected from the swelling experiments and the filtration experiments, both discussed before, that the effective pore diameter is clearly solvent

dependent. In this way, the procedure can be used as a membrane characterisation tool. On the other hand, the procedure can be used for predictive modelling. Therefore, all model parameters should be known. As these parameters are not provided by the membrane manufacturers, one should first characterise a membrane using the procedure for descriptive modelling of a restricted set of experimental filtration data. Afterwards, the model parameters can indeed be used for predictive modelling of the solute transport through a membrane.

#### 4.3.1 Descriptive modelling

Table 5.14 summarises effective pore diameters obtained with the different models for the different membrane-solvent combinations. As the lognormal model assumes that the membrane pore size is not uniform but according to a lognormal distribution, it must be pointed that the value obtained with this model is a mean value, which means that this represents the diameter of a molecule that is 50% rejected. The modelling was not applied on the data from the filtration experiments in *n*-hexane, since these datasets were too small and modelling would show little relevance. Although the different models provide relatively varying fitting results, they give a good indication of the performance of a membrane in a specific solvent. The results are realistic for nanofiltration applications and are in correspondence with the sparsely available literature data. Gibbins *et al.* (2002) reported pore diameters in methanol, varying respectively between 1.10 and 1.44 nm for Desal-5-DL (which is comparable to Desal-5-DK) and between 1.12 and 1.54 nm for MPF-50.

For a better comparison between the different models, Table 5.15 shows also the theoretical mean diameters, i.e. the diameter of a solute that is 50% rejected, calculated with the different models, as well as the diameter of a component that is 90% rejected, thus comparable to a hypothetical MWCO based on these series of experimental data. It can be seen that for a given membrane-solvent combination, the different models provide similar results for the mean pore diameter. For the diameters at 90 and 100% rejection, larger deviations are observed between the different models: in general, the Steric Hindrance Pore models gives the lowest estimate of the pore diameter, and the Verniory model gives the highest. As the lognormal model incorporates two model parameters, a general comparison with the other models is not significant, as the reflection curves obtained with this model may show different shapes, depending on the second model parameter (i.e. the standard deviation of the pore size distribution). As an example, Figure 5.8 shows the reflection curves, calculated with the different models, for the SolSep-169 membrane in acetone, and for the FSTi-128 membrane in ethyl acetate.

The modelling provided a good indication of the rejection performance of the membranes used in the different solvents. Regardless of which model is used for the data fitting, the calculated model parameters obviously confirm the hypothesis that the pore diameter of a membrane is influenced by the solvent in which transport occurs. As previously suggested, the membrane pore wall is indeed solvated, leading to an effective pore diameter that is solvent dependent. The influence of the solvent

type on the reflection curve for a given membrane is illustrated in Figure 5.9 for MPF-44 with the lognormal model and the Ferry model. The SHP and the Verniory model provided similar figures. The experimental data from the filtration experiments indicated a loss in performance in different solvents, and the corresponding reflection curves show a clear shift towards lower rejections at a given effective solute diameter.

	Solvent	SHP	Ferry	Verniory	Lognormal
MPF-44	Methanol	1.37	1.68	1.83	0.85
	Ethanol	1.57	2.13	2.35	0.87
	Acetone	2.07	2.80	3.09	1.04
	Ethyl acetate	1.42	1.89	2.08	0.81
MPF-50	Methanol	1.42	1.80	1.97	0.86
	Ethanol	1.41	1.82	2.00	0.83
	Acetone	1.49	1.86	2.03	0.85
Desal-5-DK	Methanol	1.05	1.21	1.29	0.18
	Ethanol	1.72	2.33	2.56	0.96
SolSep-169	Acetone	1.71	2.23	2.45	0.95
	Ethyl acetate	1.60	2.11	2.31	1.41
FSTi-128	Acetone	1.27	1.53	1.66	0.75
	Ethyl acetate	1.16	1.42	1.55	0.62
HITK-T1	Methanol	1.12	1.33	1.44	0.65
	Acetone	0.98	0.91	0.77	0.61

Table 5.14: Model parameters obtained from experimental data fitting, i.e. the (effective) pore diameter for the SHP, Ferry and Verniory model, and the mean pore diameter for the lognormal model



50%	Solvent	SHP	Ferry	Verniory	Lognormal
MPF-44	Methanol	0.81	0.77	0.77	0.85
	Ethanol	0.93	0.98	0.98	0.88
	Acetone	1.22	1.29	1.29	1.04
	Ethyl acetate	0.84	0.87	0.87	0.81
MPF-50	Methanol	0.84	0.83	0.83	0.86
	Ethanol	0.83	0.84	0.84	0.83
	Acetone	0.88	0.85	0.85	0.85
Desal-5-DK	Methanol	0.62	0.55	0.54	0.18
	Ethanol	1.02	1.07	1.07	0.96
SolSep-169	Acetone	1.01	1.02	1.03	0.95
	Ethyl acetate	0.94	0.97	0.97	1.41
FSTi-128	Acetone	0.75	0.70	0.70	0.75
	Ethyl acetate	0.68	0.65	0.65	0.62
HITK-T1	Methanol	0.66	0.61	0.60	0.65
	Acetone	0.58	0.42	0.32	0.61

90%	Solvent	SHP	Ferry	Verniory	Lognormal
MPF-44	Methanol	1.17	1.30	1.34	1.18
	Ethanol	1.34	1.65	1.72	1.04
	Acetone	1.77	2.17	2.26	1.23
	Ethyl acetate	1.21	1.46	1.52	0.97
MPF-50	Methanol	1.21	1.39	1.44	1.09
	Ethanol	1.20	1.41	1.46	1.10
	Acetone	1.27	1.43	1.48	1.14
Desal-5-DK	Methanol	0.89	0.93	0.94	1.69
	Ethanol	1.47	1.80	1.87	1.39
SolSep-169	Acetone	1.46	1.72	1.79	1.19
	Ethyl acetate	1.36	1.63	1.69	10.6
FSTi-128	Acetone	1.08	1.18	1.22	0.96
	Ethyl acetate	0.99	1.10	1.13	1.52
HITK-T1	Methanol	0.95	1.03	1.05	0.99
	Acetone	0.84	0.70	0.57	0.63

Table 5.15: Model values for effective diameters of components that would be rejected for respectively 50% and 90%

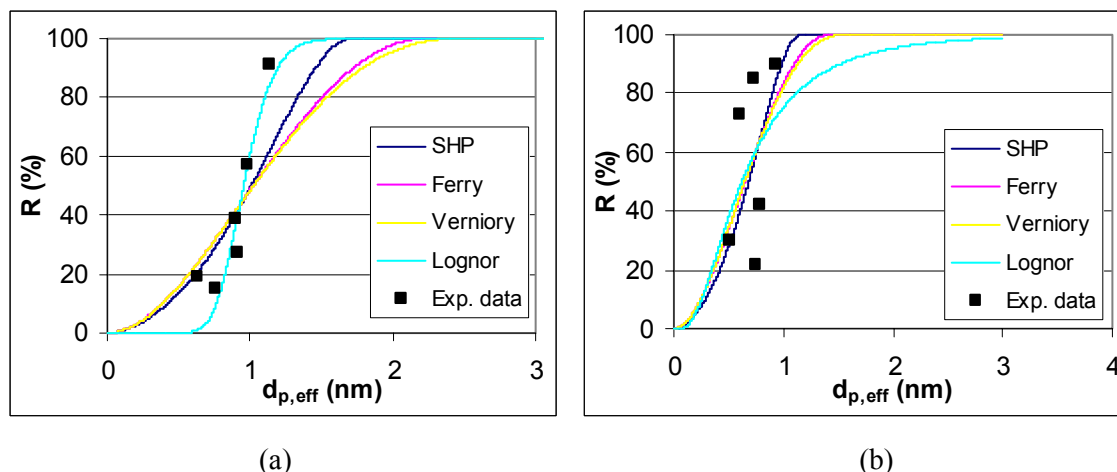


Figure 5.8: Comparison of the reflection curves obtained with the different models (Steric Hindrance Pore Model, Ferry model, Verniory model and Lognormal model) for (a) SolSep-169 in acetone and (b) FSTi-128 in ethyl acetate

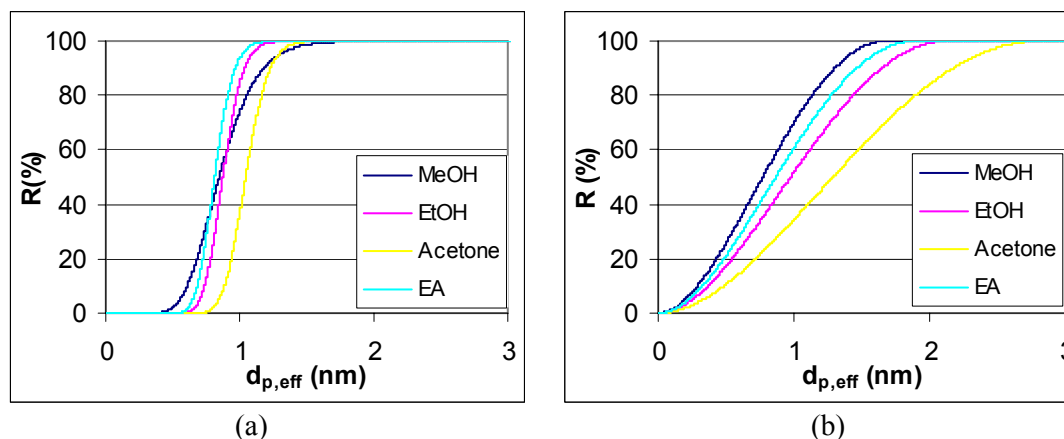


Figure 5.9: Effect of solvent type (methanol, ethanol, acetone, ethyl acetate) on the reflection curve for MPF-44, calculated with (a) the lognormal model and (b) the Ferry model

In contrast to the results for MPF-44, Figure 5.10 shows the reflection curves for the MPF-50 membrane, also calculated with the lognormal model. No clear distinction is observed between the reflection curves in methanol, ethanol or acetone, which indicates that the influence of the solvent type is much smaller for this membrane. Although this might appear somewhat in contradiction with the results for MPF-44, this is strongly confirming the findings from previous experimental data. It was reported (Chapter 3) that MPF-50 could be considered as the membrane that was most stable in organic solvents. Further on, it was, e.g., hypothesised that in methanol the pore diameter of this membrane was smaller than the pore diameter of Desal-5-DK, whereas in ethanol the opposite was suggested. This is now confirmed by the model parameters, summarised in Table 5.14 and 5.15. It can thus again be concluded that hydrophobic nanofiltration membranes are less liable to solvation effects and changes in effective pore diameter, which can also be considered as being solvent resistant.

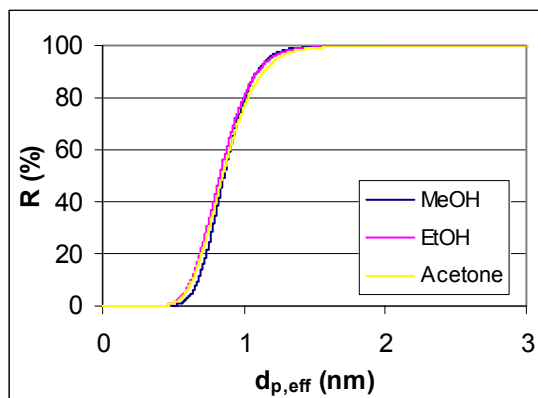


Figure 5.10: Effect of solvent type (methanol, ethanol, acetone) on the reflection curve for MPF-50, calculated with the lognormal model

It is observed that the high degree of solvent stability of MPF-50 appears not only from the comparison of calculated pore diameters with the same model in different solvents. Also the comparison of pore diameters obtained with different models provides interesting information. The variation between all pore diameters obtained is much smaller for MPF-50 than for the other membranes. E.g., the mean pore diameter of MPF-50 varies only between 0.83 and 0.88, a maximal difference of 0.05 nm, which is significantly smaller than observed for the other membranes.

It can also be seen from the results in Table 5.14 and 5.15 that both the HITK-T1 and the FSTi-128 membrane show different pore diameters in each solvent. As an example, Figure 5.11 shows the reflection curves for the HITK-T1 membrane, calculated with the Steric Hindrance Pore model. Again, due to the high mechanical and chemical stability of ceramic materials, the difference in pore diameter cannot be attributed to swelling effects of the membrane material. This confirms that the solvent-membrane interaction must be considered as a solvation effect, which occurs both for polymeric and ceramic membranes, resulting in a solvent dependent effective pore diameter.

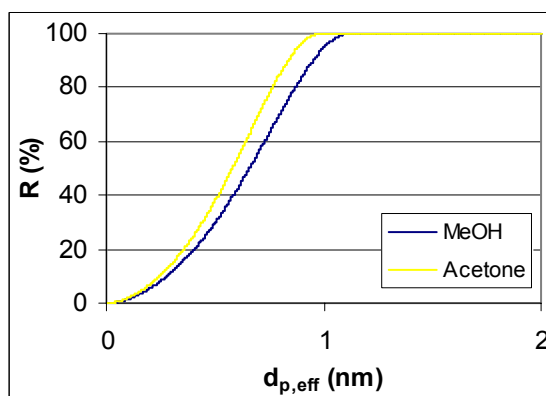


Figure 5.11: Effect of solvent type (methanol, acetone) on the reflection curve for HITK-T1, calculated with the lognormal model

### 4.3.2 Predictive modelling

It might be assumed that the presented models can also be used for predictive modelling of solute transport in non-aqueous nanofiltration. The parameters to be known then, are the effective pore diameter for the Steric Hindrance Pore model, the Ferry model and the Verniory model, and the mean pore diameter and the standard deviation of the pore size distribution for the lognormal model. These parameters can either be specified by the membrane manufacturer, or be determined experimentally. However, this methodology should be validated with other experimental data than these included in the descriptive modelling.

Therefore, the rejection of raffinose (MW 504) in methanol and ethanol is predicted for the Desal-5-DK and MPF-50 membranes. These rejection data have been determined experimentally before (Table 5.1) and can thus be compared to the predicted values for model validation.

For the prediction of the raffinose rejection, the effective solute diameters (in methanol and ethanol) have to be determined. First, the effective diameter in aqueous medium is calculated using the empiric correlation presented by Van der Bruggen (Eq. 5.19), which results in a  $d_c^w$  of 0.99 nm. Then, a correction for the solvent-component interaction has to be introduced. The effect of component solvation is calculated using the constant ratio between the effective diameters in different solvents (Table 5.13). The effective diameters of raffinose in methanol and ethanol are then respectively 0.87 and 0.82 nm. Finally, the effective diameters in methanol and ethanol can be filled in in the original models for the reflection coefficient, together with the model parameters obtained from the descriptive modelling, leading to predicted values for the rejection of raffinose. The results of the predictive modelling are summarised in Table 5.16.

It can be seen in Table 5.16 that the rejections of raffinose, predicted with the four different models, provide very similar results for a given membrane-solvent combination. The maximal variation in predicted rejection is only as high as 5% for the Desal-5-DK, whereas for the MPF-50 membrane only a variation of 1% is observed. This confirms that no specific model can be preferred to the other models.

When the predicted values for the solute rejection are compared to the experimental data, a relatively high degree of correlation is observed. The largest deviation observed is as high as 13%, but in contrast, the prediction in methanol for the same membrane is almost completely perfect for all models used. For MPF-50, a deviation of 12% and 7% is found in respectively methanol and ethanol. Taking into account that the phenol-sulphuric acid method for the determination of the sugar concentration may result in a 5% inaccuracy, the observed deviations between experimental and model data are clearly within reasonable margins.

MPF-50	Model parameters	R <sub>MeOH</sub>	R <sub>EiOH</sub>
SHP	$d_p^{MeOH} = 1.42$ $d_p^{EiOH} = 1.41$	54	48
Ferry	$d_p^{MeOH} = 1.80$ $d_p^{EiOH} = 1.82$	54	48
Verniory	$d_p^{MeOH} = 1.97$ $d_p^{EiOH} = 2.00$	54	48
Lognormal	$\bar{d}_p^{MeOH} = 0.86; S_p = 0.19$ $\bar{d}_p^{EiOH} = 0.83; S_p = 0.22$	53	47
Experimental	-	65	41

Desal-5-DK	Model parameters	R <sub>MeOH</sub>	R <sub>EiOH</sub>
SHP	$d_p^{MeOH} = 1.05$ $d_p^{EiOH} = 1.72$	87	33
Ferry	$d_p^{MeOH} = 1.21$ $d_p^{EiOH} = 2.33$	85	33
Verniory	$d_p^{MeOH} = 1.29$ $d_p^{EiOH} = 2.56$	85	33
Lognormal	$\bar{d}_p^{MeOH} = 0.17; S_p = 1.75$ $\bar{d}_p^{EiOH} = 0.96; S_p = 0.29$	82	28
Experimental	-	84	20

Table 5.16: Predicted rejections of raffinose in methanol and ethanol with MPF-50 and Desal-5-DK compared to experimental data

It was noticed before that the experimentally determined rejection of raffinose in methanol is higher with Desal-5-DK than with MPF-50, whereas in ethanol the opposite was observed. This was explained on the base of membrane-solvent interactions that differ for hydrophilic and hydrophobic membranes. It is striking that the methodology used above effectively can predict these effects. The predicted values in methanol are higher for Desal-5-DK, whereas the values in ethanol are higher for MPF-50.

The results of the predictive modelling show a good correlation with the experimental data. The predicted values are in the desired range, within reasonable variations. The methodology was tested both on a hydrophilic and a hydrophobic membrane, and the changing order of rejections in different solvents could be described. Therefore, it can be concluded that the presented methodology provides a powerful tool to obtain a good estimate of the rejection that can be expected for a given membrane-solvent-solute combination, although no measure for polarity effects between the membrane and the solutes is included so far. The model parameters must however be known in order to apply the predictive modelling.

## **5. Conclusion**

The performance of a membrane process is determined by both the solvent permeability and the solute rejection. In aqueous solution, the separation characteristics traditionally are indicated by the MWCO, i.e. the molecular weight of a component that is 90% rejected. However, in non-aqueous media, the MWCO determined in water is not of much use.

Different solvent-membrane-solute interactions influence the transport of dissolved components. It is observed from experiments with solutions of raffinose in binary mixtures of water, methanol and/or ethanol that the solute rejection is affected by 3 parameters. The nominal pore diameter (which is more or less indicated by the specified MWCO of a membrane) is an inverse measure for the steric hindrance occurring by solute transport through membrane pores. The affinity between the solute and the solvent determines the degree of solvation of the solute, and thus the effective solute diameter. The interactions between the membrane material and the solvent determines the degree of pore wall solvation, and thus the effective pore diameter. It was remarkable that one membrane can have lower rejections than any other in a first solvent, whereas in a second solvent the opposite may occur.

The solute transport in non-aqueous media was further investigated in detail. From the comparison of the solute transport through nanofiltration membranes in dynamic filtration experiments and in static cell diffusion experiments, the relative contributions of convection and diffusion to solute transport

could be determined. The balance between viscous and diffusive transport is mainly directed towards convective transport. Less than 5% of the total solute transport occurs by diffusion. As expected for solute transport by convection, it was confirmed that the effective diameter of the solute plays an important role with respect to solute transport. However, also polarity effects, and to a smaller extent charge effects, between the membrane surface and the solute, resulting in attractive or repulsive forces, may influence the transport of dissolved components through nanofiltration membranes in non-aqueous media.

The filtration experiments in different organic solvents showed that the solute rejection is in general higher for relatively polar solvents. Hydrophilic membranes are more liable to membrane-solvent interactions, leading to changes in the effective pore size, than hydrophobic membranes. This confirms the previous assumption that hydrophobic membranes can be considered as solvent resistant membranes.

A methodology was developed for the modelling of solute transport in non-aqueous media. Literature models were refined to incorporate the influence of solvents other than water. Therefore, solvent dependent effective diameters have to be used, both for the solute as for the membrane pore. The experimental data from filtration experiments showed a good correlation with the model fits, and model parameters could be identified. In this way, descriptive modelling can be used as a tool for membrane characterisation. The developed methodology was tested for predictive modelling and high correlations were found between experimental and predicted solute rejections.

Finally, the effects observed for polymeric membranes also occur for ceramic nanofiltration membranes, which counters the possible objection that a loss of membrane performance must be attributed to swelling effects. Ceramic membranes are mechanically and chemically stable and show no swelling effects. The changes in solute rejection, also observed with ceramic membranes, therefore provide a strong confirmation of the developed assumptions on solute transport in non-aqueous media.





# *Chapter 6*

## *Industrial application of non-aqueous nanofiltration*

## 1. Introduction

The Flemish industry employed in 2002 more than 500,000 people and is therefore a major contributor to the economy of the region (Geens and Van Hooste, 2004). However, industrial activity is accompanied by an unfavourable pressure on the environment. Industrial processes often consume large amounts of energy and may be designed in a more efficient way. Another problem of important concern is the treatment of waste streams caused by the use of organic solvents. Non-aqueous process media are commonly used in different industrial sectors, but these are often resulting in a number of undesired waste streams. These waste streams can be either liquid discharges or controlled and diffuse losses, leading to additional treatment costs and environmental taxes.

Therefore, the industry is always looking for improved production and waste treatment processes. A compromise must be found between technical requirements, financial costs and environmental benefits. Many companies try to implement the Best Available Technology Not Entailing Excessive Costs (BATNEEC), which means that the technology is used to prevent or eliminate, and where that is not practicable, to limit, abate or reduce emissions from the activity (EPA, 2005).

The use of BATNEEC is an important motive for the investigation of new technology platforms, e.g. membrane technology in non-aqueous media. It is thus important to evaluate the potential of such a technology to a maximal extent, in order to conclude whether it can be used as a valuable, powerful alternative for traditional processes. Therefore, the use of organic solvents in the industry will be highlighted, together with the potential benefits of implementing membrane technology as a separation tool. A case-study will be discussed: solvent recovery of liquid waste streams from production processes in the pharmaceutical industry.

## 2. Organic solvents in industrial environments

### 2.1 The use of organic solvents in the contemporary industry

Data on the amount of organic solvents used in the (Flemish) industry are hardly available. In Flanders, no centralised data on solvent use in industry are available (Van Hooste, 2005). In 2000 Theloke *et al.* presented a report on the solvent consumption in the German industry, containing data of 1994. The largest volumes of organic solvents were used in paints and varnishes, for degreasing and chemical cleaning of metal surfaces and electronics and for the production and treatment of chemicals. In total, 2.7 Mton of solvents were used. Although the size of the German industry is much larger than this in Flanders, it is assumed that the two are similarly structured. For Flanders, data on the used volumes of organic solvents are only available for individual sectors from the industry. The most important will be discussed.

A very important industrial activity where organic solvents are used, is the surface treatment of metals. In this case, the solvent polarity is a principle solvent property. Non-polar solvents, like aliphatic, aromatic or halogenated hydrocarbons, have a relatively high dissolving capacity for oils and fats and are therefore often used. Typical examples are dichloromethane or tri- and perchloroethylene. Based on a survey among metal cleaning companies in Flanders, Bogaert *et al.* (2002) reported a use of 818 tons of solvents, of which nearly 27% were chlorinated hydrocarbons. According to the Flemish Environment Agency (VMM), a consumption level of 8 kton would be a more appropriate figure.

Traditionally, the production and industrial use of coatings, paints, varnishes, inks and adhesives are largely based on the use of volatile organic components. However, over the recent years, several applications could be replaced by products on the base of water, or containing only minor fractions of organic solvents. In 2002, 225 kton of paints, inks and adhesives were produced in the Flemish industry, of which 34% was on the base of water (Lodewijcks *et al.*, 2003). The solvents that are most used for these products are ethanol, white spirit (high flash naphtha), ethoxypropyl acetate, methyl ethyl ketone (MEK), xylene and toluene.

The chemical industry also consumes large volumes of organic solvents. A distinction is often made between basic chemical industry and the paracheical industry (Bogaert *et al.*, 2002b). The basic chemical industry produces raw materials for the paracheical industry, and is further separated into refinery, production of basic chemicals, the production of fine chemicals and the production of polymers and plastics in the primary stage. The paracheical industry produces consumer goods. In the basic chemical industry, the largest fraction of solvents is used as a raw material in a chemical reaction during processing. Typical reaction products from the basic chemical industry in Flanders are hydrocarbons, BTEX (benzene, toluene, ethylbenzene, xylene), ethylene oxide, ethylene glycols, vinylchloride, benzyl chloride,...

Bogaert *et al.* (2004) reported that the pharmaceutical industry in Flanders consumed approximately 18.5 kton of organic solvents for the production and the formulation of active pharmaceutical active ingredients. Organic solvents are not only used as reaction media, but also as raw materials or as catalysts. Typical solvents used in the pharmaceutical industry are methanol, ethanol, iso-propanol, toluene and methylene chloride.

In the food industry, relatively large volumes of organic solvents are used, especially for the production of vegetable oils (Van Espen, 2003). These oils are won from different types of beans and seeds, e.g. soybean, with an extraction process. As the most typical extraction solvent, *n*-hexane is commonly used. Miscella are distilled to separate the vegetable oil from the solvent, which can in turn partly be recycled. Further refinery may sometimes be required.

## 2.2 Environmental problems related to industrial use of organic solvents

### 2.2.1 Introduction

The use of organic solvents, either as raw materials, as reaction media or as catalysts, includes an important number of risks and possibly hazardous situations. Organic solvents have a different degree of toxicity for humans. A recurrent problem caused by VOCs is the so-called painter disease (CTE: Chronic Toxic Encephalopathy; or OPS: Organic Psycho Syndrome), the harmful effect of organic solvents on the central nervous system, resulting in tiredness, irritability, reduced ability to concentrate, or even dementia (Justaert and Cambré, 2000). Other potential health problems are skin disorders (eczema), cancers, multiple sclerosis, heart, kidney and liver complaints,... The relative importance of possible effects of organic solvents on humans depends on the concentration and the time of exposure. High doses on a short term may lead to acute damage, whereas lower doses over longer periods of time can result in chronic effects. Typical parameters to characterize the solvent toxicity are the LD<sub>50</sub> (50% lethal dose) (Loncke *et al.*, 1996), the IDLH (Immediate Danger to Life or Health) (Marcus, 1998) or the WGK (Wassergefährdungsklassen) (Loncke *et al.*, 1996). Over the last decades more attention is paid to the substitution of dangerous solvents by safer alternatives, e.g. the use of toluene or xylene instead of the carcinogenic benzene.

However, not only people that are working with organic solvents are exposed to negative effects. Also the environment is negatively influenced. Beside the creation of liquid waste streams, containing large fractions of organic solvents and requiring severe treatment, indirect effects on the environment, due to diffuse or controlled emissions and discharges, may be even more hazardous. The increase of historical pollutions of air, soil and water resulted in the need for strict regulations in order to protect the environment and the next generations.

### 2.2.2 Solvent containing waste streams

Diffuse losses of organic solvents must be prevented to a maximal extent. As several industrial processes cannot reuse or recycle organic solvents from the product streams, large volumes of liquid waste streams containing organic solvents arise. According to the European EURL Waste List, these waste streams have to be reported to special treatment organisations, e.g. OVAM in Flanders. In 1996, 34 kton of industrial waste containing organic solvents were reported. The largest contributors were the petrochemical industry, the paint, varnish and ink industry, the car assembly industry, the chemical and the pharmaceutical industry (Van Braeckel and Claeys, 1999). In 2003, the waste volume of organic solvents increased to 140 kton (of which 108 kton non-halogenated solvents, 29.5 kton halogenated solvents, 2 kton CFCs and BFCs, and 0.5 kton other solvents) (De Groof, 2005).

The treatment of these solvents occurs in different ways: conditioning, recycling, disposal (on a class I landfill) or incineration (Van Braeckel and Claeys, 1999). Over the recent years, the recycling of

solvents is strongly encouraged. In the EU, 60% of all chlorinated solvents are recycled. In Flanders, approximately 7 kton of solvents is recycled, which is only half of the estimated potential. The reuse of organic solvents requires a removal of the contaminants; distillation is commonly applied to regain solvents such as white spirit, toluene, trichloroethane or perchloroethane. Nowadays, 90% of the distilled waste streams, are treated off-site. For the incineration of organic solvents, the process controlling must be very precise, as otherwise carcinogenic pollutants, e.g., polyaromatic hydrocarbons (PAHs) and dioxins, may be emitted. Traditional industrial incinerators are used for the treatment of chlorinated hydrocarbons (in low concentration). For high concentrations (> 2%) thermal oxidation is required, for which only Indaver (Antwerpen) is licensed. Other solvents are often co-incinerated in a cement kiln, although this installation is not designed for such applications.

It is however clear that traditional treatment technology, either distillation or incineration, are energy intensive, and thus relatively expensive, and exerting a relatively high pressure on the environment (emission of greenhouse gases). The implementation of membrane technology might therefore be a strong alternative.

### 2.2.3 Air pollution

A major concern with the use of organic solvents, is the difficult control of diffuse losses. Many organic solvents are volatile components, which can cause serious pollution of the air. The most important VOC is methane, which is of course not a solvent in normal conditions. The concentration of methane in the air is hundreds of times higher than this of other VOCs, but its reactivity is significantly lower. Therefore, a distinction is made between methane and the non-methane volatile organic components (NMVOC). Most organic solvents used in the industry belong to the latter class (Block and Van Hooste, 2004).

The Flemish industry emitted more than 50 kton of NMVOC to the air in 2003, which is nearly 40% of the total emission in Flanders (Geens and Van Hooste, 2004). The largest contributors were indeed the chemical, the metal and the paper industry. Measurements clearly indicate higher concentrations of NMVOC in industrialised areas. In 2003, a concentration of approximately  $3.5 \mu\text{g}/\text{m}^3$  was measured for toluene and of  $1.3 \mu\text{g}/\text{m}^3$  for benzene (Block and Van Hooste, 2004). As many NMVOCs are hazardous components, different problems due to high concentrations are distinguished: increased risk on cancer, irritating odours,... However, even more problematic are the indirect effects of NMVOC-emissions, namely the photochemical air pollution, the development of the ozone hole and the contribution to the greenhouse effect.

The photochemical air pollution is the undesired presence of oxidating components such as ozone ( $\text{O}_3$ ), peroxyacetylene nitrate (PAN), hydrogen peroxide ( $\text{H}_2\text{O}_2$ ) or nitrogen dioxide ( $\text{NO}_2$ ) (Dumont *et al.*, 2004). These components are produced from a chemical reaction between NMVOCs and  $\text{NO}_x$ , catalysed by UV-radiation (Loncke *et al.*, 1996). It is shown that ozone damages physiological and

biological functions of plants, and thus also the habitat and food patterns of animals are indirectly affected. Furthermore, it is proved that ozone and NO<sub>2</sub> cause acute and chronic damage to the human lung function (Heirman, 2004).

In contrast to photochemical ozone, the presence of natural ozone in the stratosphere is indispensable for life on earth, as it serves to absorb many harmful solar UV-rays. Over the last decades, stratospheric ozone over Antarctica and over the Arctic has however been depleted at certain times of the year. This is mainly due to the release of manmade halogenated components that belong to the larger class of NMVOC, typically chlorofluorocarbons (CFC) (Van Braeckel and Claeys, 1999).

The greenhouse effect is the phenomenon that results in global warming. Incoming solar radiation is largely absorbed by the earth surface, resulting in a warming of the earth and the emission of an outward flow of infrared radiation. This IR-radiation is in turn be absorbed by the so-called greenhouse gases, such as water, carbon dioxide and methane, leading to an increase of the average temperature on earth from -18 to 15 °C. Several emitted NMVOCs can however also absorb this IR-radiation and contribute to the global warming. The unwanted increase of the average temperature on earth may have important consequences on the environment (Van Braeckel and Claeys, 1999).

#### 2.2.4 Soil pollution

Due to diffuse or accidental losses, organic solvents can contaminate the soil in the surroundings of industrial plants, or along the traffic routes. Also the leaching of solvent containing landfills may result in soil pollution by organic solvents. The latter can only occur due to the selection of an inaccurate storage method or to incorrect manipulations of the waste streams.

The effect on the environment depends on the properties of both the solvent (i.e. the water solubility, hydrophobicity, lipophilicity and molecular structure) and the contaminated soil (i.e. the mineral and organic composition) (Stemple *et al.*, 2003). Solvents that have a high solubility in water may leach relatively easy and can possibly reach the ground water level. Hydrophobic or lipophilic solvents will show a longer residence time in the soil. If the solvents are moreover inert, or at least not biodegradable, this may result in quasi-permanent soil pollution. The most wide-spread soil pollution consists of contamination by BTEX, PAHs and chlorinated solvents. In 2003, nearly 15,000 soils in Flanders were contaminated with these solvents (and by heavy metals), corresponding to an area of 361 km<sup>2</sup>. Expensive soil treatments are required for at least 11,000 soils (Ceenaeme *et al.*, 2004).

#### 2.2.5 Water pollution

Due to incorrect manipulations of organic solvent waste, waste water and accidental losses from storage and transport, organic solvents can contaminate the water in the environment. Organic solvents cause severe damage to aqueous life and natural ecosystems. Soil pollution by organic solvents may

result in a contamination of the ground water, resulting in problems with potable water (UNEP/IEO, 1989).

### *2.2.6 Regulations*

As the problems for the environment became more urgent, environmental legislation became, at different levels, much more rigorous. Different governments were obliged to develop a strict policy on environmental problems, and cross-border consultation was inevitable.

In 1979, the UNECE (United Nations Economic Commission for Europe) implemented the Long-Range Transboundary Air Pollution (LRTAP) agreement, the first international agreement on environmental topics. It was focused on a reduction of the emission of different pollutants, among which also VOC.

In 1990, the directive on National Emissions Ceilings (NEC) was presented by the European Council as a common policy against the acidification and the eutrophication of the air. The directive was approved in 2001 (2001/81/EC) and provides maximal emissions for 2010 in the different member states. With respect to VOC-emissions, Belgium engaged for a maximal emission of 139 kton VOC, a reduction of 58.1% when compared to 1990. Flanders must provide a reduction of 70.9 kton (-50%). The government did not yet assign a relative weight factor to the different contributors. It is thus not yet clear which reductions are required from the industry. Several industrial subsectors started however with the formulation of a reduction program, based on technically and economically feasible aspects.

Meanwhile, already 8 protocols are written, of which the most recent is the Göteborg-protocol in 1999 (Heirman, 2004). Based on this protocol, the more specific EU directive on solvents (99/13/EC) came into force. This directive is focused on a reduction of emissions caused by the use of organic solvents in specific activities, such as printing, surface cleaning, car assembly, production of drugs,... It sets emission limit values (expressed in terms of the maximum solvent concentration in waste gases) and fugitive emission values (expressed as a percentage of the solvent input). The directive was amended in 2004 (2004/42/EC).

## **3. Applications of non-aqueous nanofiltration**

### **3.1 Introduction**

The increased safety and environmental legislation, in combination with the striving towards maximal economical benefits, had important repercussions on the world-wide industry. As the common use of organic solvents often results in expensive precautions and measures, there is a large potential for new technologies, such as membrane technology. Some of the most important advantages of a suitable

membrane process are the reduced consumption of energy (combined with a reduced emission of greenhouse gases), the recovery of possible waste streams as production media (and thus reduced volumes of waste streams), the operation mode at ambient temperatures (and thus a decrease of diffuse emissions and increased safety), the small footprint required,...

As mentioned before, nanofiltration of organic solvents is still in the early stages of introduction. However, several applications in different subsectors of the industry have been evaluated in literature and a short review will be presented.

### 3.2 Solvent recovery from lube oil filtrates

The largest industrial nanofiltration plant for organic solvent processing is installed in the petrochemical industry (Bhore *et al.*, 1999). Wax is a monoester of fatty acids that severely modifies the properties of lube oil and must therefore be removed (Hart *et al.*, 1995). The traditional process of dewaxing involved the cooling of a hydrocarbon mixture in a solvent or solvent mixture (MEK, acetone) to temperatures typically ranging from  $-5$  to  $-18$  °C. In this chilling section, waxy components coagulated and were precipitated or filtered; the solvent in the filtrate was removed by evaporation and reused in the process (Cuperus and Ebert, 2002).

In a new approach, a membrane unit replaces or supports the distillation step. White and Nitsch (2000) incorporated nanofiltration membranes in the conventional process, so that 25% of the solvent was removed by filtration prior to further purification (Figure 6.1). A great benefit of this process is that filtered solvent does not need to be heated. Hence, an initial plant with 300 m<sup>2</sup> of membrane could handle 25% of the feed of 160 m<sup>3</sup>, resulting in 20% reduction in size and capacity for the recovery section, 25% reduction in heat and 10% in refrigeration requirements. Nowadays, an industrial plant for an ultimate feed rate of 11,500 m<sup>3</sup>/day is running at the Exxon-Mobil refinery in Beaumont, Texas (USA). The throughput in 2001 was 5,800 m<sup>3</sup>/day, consistent with existing demand. The average base oil production increased by over 25% and the improved dewaxed oil yields by 3-5%. The net uplift for additional lube and wax margin, attributed only to the use of membranes, was estimated at \$ 6.1 million/year. The reduction in fuel oil consumption was calculated to 5,800 m<sup>3</sup>/year, corresponding to a reduction of greenhouse gas emissions of about 20,000 tons/year. Cooling water requirements are reduced by approximately 250 Mm<sup>3</sup>/year. The diffuse loss of dewaxing solvents, which are VOCs, into the environment could be decreased by 50-200 tons/year.



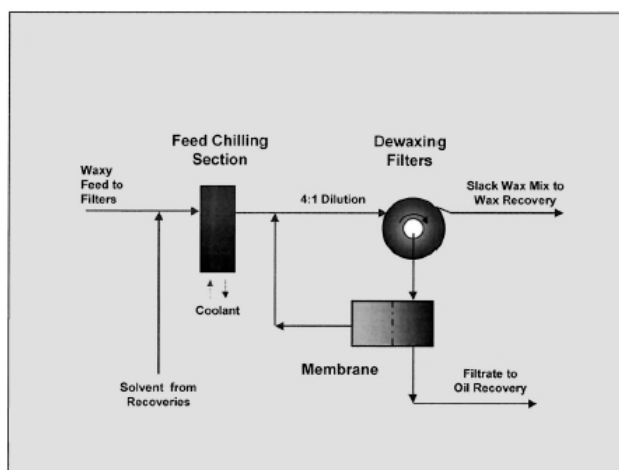


Figure 6.1: Membrane separation of cold solvents from lube oil filtrate

### 3.3 The vegetable oil industry

The vegetable oil industry is a rather special branch of the food industry as it widely uses organic solvents in processing. It is estimated that more than 2 million tons of extraction solvent is used in the USA alone. Starting from seed from plants as soybean or sunflower, oil is won by solvent extraction, eventually in combination with mechanical extraction. Hexane is by far the most common extraction solvent. Currently, evaporation is used to recover these solvents and reuse them in the process, which requires a considerable amount of energy, approximately 530 kJ/kg oil. In addition, the elevated temperatures hold a risk on thermal damage and explosive vapours may create safety problems (Raman *et al.*, 1996). These limitations can be partially overcome by membrane technology.

Oil-micelle mixtures are formed during hexane extraction and consist of triglycerides (oils), phospholipids and solvent. Due to their polarity, phospholipids form very loose conglomerates that can be filtered off by membranes. The process results in a filtrate with clear oil and hexane and a phospholipid fraction that can be worked up more easily. Although hexane has to be removed by stripping, potential savings are found in the reduction of chemicals and improved quality of oil. Raman *et al.* (1996) reported that a mixture containing 20% of oil could be concentrated to 45% with a commercial nanofiltration membrane, resulting in a 50% reduction of the energy consumption for the evaporation unit. Stafie *et al.* (2003) reported oil rejections of over 90% with a PDMS nanofiltration membrane.

### 3.4 Homogeneous catalyst separation and re-use

In organic synthesis of complex molecules, homogeneous catalysis has become increasingly important. Examples of such catalysts are the Heck and the Co-Jacobsen catalysts (Nair *et al.*, 2001;

Aerts *et al.*, 2004). Transition metal catalysis (TMC) is used for the synthesis of enantiomerically pure components. Phase transfer catalysis (PTC) is applied to reactions involving a water soluble electrophilic reagent. Two immiscible phases are contacted and a phase transfer catalyst is used to transfer a reactant from one of these phases into the other, so that the reaction can occur (Figure 6.2) (Luthra *et al.*, 2002). Typically, post-reaction, the catalyst remains in the organic phase. Applications are found in pharmaceuticals, agricultural chemicals and fine chemicals. The advantages include increased productivity and quality, improved environmental performance, avoidance of need to use polar aprotic solvents (DMSO, DMF, DMAc), enhanced safety and reduction of other manufacturing costs.

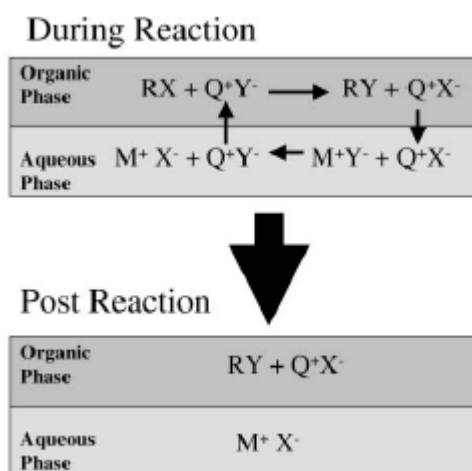


Figure 6.2: Phase transfer catalysis principle (RX: reactant; Q: phase transfer catalyst; Y: nucleophilic anion; M: counter cation in aqueous phase)

However, beside the relatively high cost, one of the major technical drawbacks for the use of TMC and PTC in industrial applications is the need to separate the product and the phase transfer catalyst. The most commonly used methods are extraction by water washing and distillation, but problems with toxic waste streams and degradation may then occur. A mild separation technique could facilitate the use of homogeneous catalysis in larger industrial organic synthesis processes. A straightforward approach to accomplish this, involves the use of membrane filtration (Luthra *et al.*, 2001). Different research groups investigated the potential of non-aqueous membrane technology for the separations in TMC and PTC, and it has become clear that for industrially relevant catalysts, the membranes and the catalysts should be adopted to each other. Scarpello *et al.* (2002) reported catalyst rejections of more than 95%, coupled with good solvent fluxes, which makes this technology very promising. Nair *et al.* (2002) reported rejections up to 97% in MBTE and THF. It must be pointed that for this application, the membrane unit is not used as ‘debottlenecking tool’, but as full part of a hybrid production process, as can be seen in Figure 6.3.

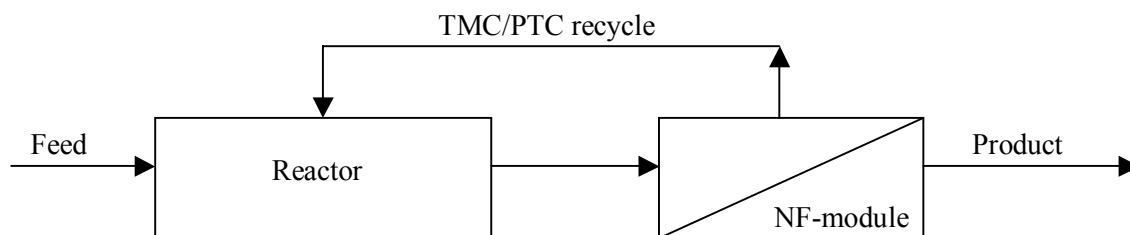


Figure 6.3: Scheme of a hybrid process in synthesis with homogeneous catalysis

### 3.5 Solvent exchange

A large number of fine chemicals or pharmaceutically active ingredients are synthesized with complex reaction paths. It often occurs that different steps require different solvents as reaction medium. In such case, a solvent exchange must take place. A traditional procedure to transport relatively large, non-volatile components to another solvent is a ‘put and take distillation’, in which the original solvent is stepwise boiled out and replaced by similar volumes of the second solvent. The technique is only effective if the first solvent has a much lower boiling temperature than the second solvent, e.g. the replacement of methanol by toluene. Azeotropic mixtures may cause additional problems.

Nanofiltration can become a strong alternative for traditional solvent exchange methods, without the drawbacks of elevated temperatures or azeotropic mixtures (Livingston *et al.*, 2003). The principle requires a membrane that shows high permeation rates for the (first) solvent, whereas the component should be rejected. The feed stream is then filtered until nearly 10-30% of the volume is retained (and thus severely concentrated). Afterwards, the second solvent is added to the retentate and the filtration process can restart. In a stepwise procedure, a concentration of less than 1% of the original solvent can be reached. No external heating is required and the permeate of the first membrane step can directly be reused in the production process.

This procedure was tested for the exchange of toluene by methanol, with tetraoctylammonium bromide (TOABr) as a reference solute. After 5 filtration steps, only 0.3% of toluene was found in the methanol fraction. The solute rejection in all steps was 100%.

The difference in energy consumption between ‘put and take distillation’ and the membrane set-up is difficult to estimate. Both technologies result in waste streams that require further treatment. Moreover, the required pressure for the membrane set-up is hard to define on the base of pilot-scale experiments. It is however clear that the membrane set-up shows a much lower mass intensity than the distillation. Mass intensity is a commonly used concept in the context of green energy, and is defined as the ratio of the total mass of the reactants and the mass of the reaction products (Curzons *et al.*, 2001). Solvent exchange by distillation typically shows a mass intensity of 5-10 kg/kg, whereas the

use of membrane technology results in a value of 2-3 kg/kg. Both values are valid for a 95% exchange, which is often the required value in industrial applications.

## 4. Case-study: Solvent recovery in the pharmaceutical industry

### 4.1 Introduction

The pharmaceutical industry in Flanders is one of the major players in the region's economy. 29 pharmaceutical companies have a production department in Flanders; 4 companies produce active pharmaceutical ingredients (APIs), whereas 25 deal with the formulation of drugs (Bogaert *et al.*, 2004). API-production consumes much larger volumes of organic solvents than drug formulation. Organic solvents are mainly used as reaction medium, but also as raw material. As a consequence, large, and thus expensive, volumes of waste stream occur in the pharmaceutical industry.

In this work, the potential of nanofiltration as a separation tool in the chemical production process of active pharmaceutical components is evaluated. This part of the work was in cooperation with Janssen Pharmaceutica (Geel, Belgium), which nowadays is a part of the Johnson & Johnson Group, the largest company world-wide in the field of healthcare. Janssen Pharmaceutica has a turnover of approximately 1.9 billion euro and an employment of nearly 4,400 people (Janssen Pharmaceutica, 2005).

Due to strict regulations for pharmaceuticals, organic solvents used for chemical production of APIs must be of very high purity. Therefore, most of the organic solvents cannot be reused and are discharged. Nevertheless, important volumes of waste streams are recovered by distillation. Solvents are distilled to virgin quality, which typically involves the following specifications: 99% chromatographic purity, clear colourless liquids, a water content of less than 0.1%, within predefined density and refractive index range and less than 10 ppm residual pharmaceutical intermediate/end product (De Witte, 2005). The application of nanofiltration provides some interesting opportunities (a further reduction of the API/IPI content, impact on the solvent yield, flux in line with throughput distillation), allowing a faster throughput and an increase of the capacity of distillation, resulting in an increase of the number of solvent streams that can be distilled. Important economic and environmental benefits are feasible.

## 4.2 Results

### 4.2.1 Experimental

From the large number of organic solvents used in the chemical production processes of Janssen Pharmaceutica (e.g. methanol, ethanol, 2-propanol, acetone, acetic acid, methylene chloride, chloroform, toluene, THF,...), three were selected for this case-study: toluene, methanol and methylene chloride. These solvents were of specific interest, as they are responsible for the largest volumes of waste streams.

As no preliminary data on solute rejection in toluene were available, 4 APIs with a different molecular weight were selected for filtration experiments. Filtration experiments in methanol and methylene chloride were carried out with only one API. The components' names and properties were covered by a policy and secrecy agreement. For all experiments, the newly available StarMem-membranes were used, since significantly improved results were reported in literature for these membranes.

All experiments were carried out at room temperature in the dead-end filtration module. A transmembrane pressure of 15 bar was applied. Synthetic feed solutions of 10 ppm API were prepared. Table 6.1 summarises the different solvent-solute combinations used in this case-study, together with the molecular weight of the APIs the analytical technique for the determination of the API-concentration.

Solute	MW (g/mol)	Solvent	Analysis
API-1	189	Toluene	GC
API-2	313	Toluene	UV/VIS-spectrophotometry
API-3	435	Toluene / Methylene chloride	UV/VIS-spectrophotometry
API-4	531	Toluene	UV/VIS-spectrophotometry
API-5	721	Methanol	UV/VIS-spectrophotometry

Table 6.1: Solute-solvent combinations used in the case-study on solvent recovery in the pharmaceutical industry

### 4.2.2 Toluene

StarMem membranes consist of a hydrophobic top layer; the average permeabilities are relatively high for toluene: 1.1, 2.2 and 0.39 l/h.m<sup>2</sup>.bar respectively for StarMem-120, StarMem-122 and StarMem-228. Figure 6.4 presents the rejection of the different APIs in toluene as a function of the molecular weight. In contrast to previous experiments in other non-polar solvents, such as *n*-hexane, solute rejections are significantly higher. A clear correlation is observed between the molecular size of the solute and its rejection. The three different membranes show similar rejection curves, but as can be

expected on the base of the MWCOs, specified by the manufacturer, the rejections of a given component decrease in the following order: StarMem-120, StarMem-122 and StarMem-228.

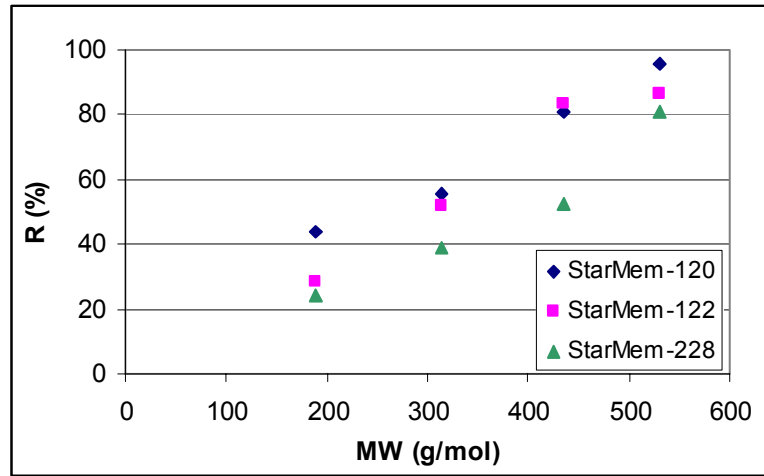


Figure 6.4: API-rejection in toluene

The pore diameters of the 3 membranes in toluene were calculated using different models discussed in Chapter 5. The results are summarised in Table 6.2. Figure 6.5 shows, as an example, the reflection curve, calculated with the lognormal model for the StarMem-122 membrane.

	SHP	Ferry	Verniory	Lognormal
StarMem-120	0.85	1.02	1.10	0.50*
StarMem-122	0.89	1.09	1.89	0.54*
StarMem-228	1.03	1.31	1.44	0.61*

Table 6.2: Effective diameters of the StarMem-membranes in toluene, calculated with the Steric Hindrance Pore model (SHP), the Ferry model, the Verniory model and the lognormal model (\*: mean diameter, corresponding to a 50% rejection).

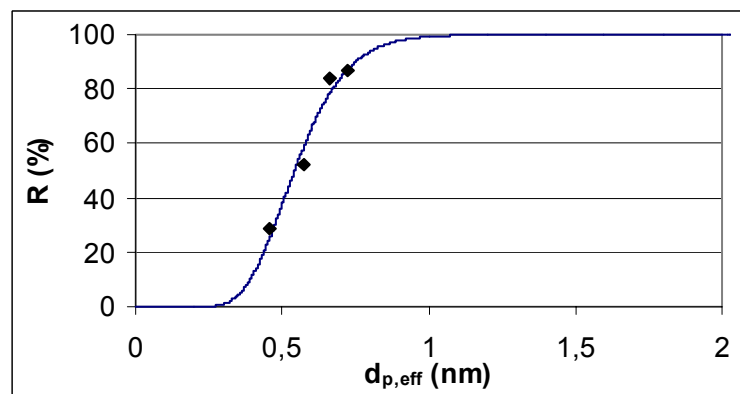


Figure 6.5: Reflection curve for StarMem-122 in toluene, calculated with the lognormal model.

Rejections of more than 80% were observed for solutes with a molecular weight of more than 400, which is reasonable for industrial application. However, specifically for Janssen Pharmaceutica, the combination of toluene and API-1 (MW 189) was of special interest, and only 43% could be obtained (with StarMem-120). Moe (2005) suggested that for the removal of solutes having only twice the size of the solvent, approximately 50% will be the upper limit with membranes currently available on the market. Nevertheless, it appears that the application of nanofiltration membranes may become a powerful separation tool in toluene for solutes larger than 400 g/mol.

#### 4.2.3 Methanol

Filtration experiments in methanol were carried out with API-5 (MW 721). StarMem-120 and StarMem-228 were used as membranes. Table 6.3 summarises the results for these experiments. As high rejections were measured, a significant increase of the retentate concentration was observed during the experiments (doubled). Therefore, as the feed concentration is not constant, the solute rejections presented in Table 6.3 are only approximate.

	L (l/h.m <sup>2</sup> .bar)	R (%)
StarMem-120	5.5	91
StarMem-228	3.6	93

Table 6.3: Toluene permeability and API rejection (MW 721)

Both the flux and the API rejection are high. It appears that nanofiltration has a promising future for this problem. This will be discussed in further detail in Section 4.3.

#### 4.2.4 Methylene chloride

None of the membranes used appeared to be resistant against methylene chloride. The top layer of the StarMem-membranes dissolved from the support layer and low rejections were observed. Therefore, a filtration experiment was carried out with the MPF-50 membrane, but no useful results were obtained either. Therefore, no further attention was paid to the separations in this solvent.

### 4.3 Model calculation

#### 4.3.1 Design of a membrane installation

High rejections were observed for API-5 in methanol (91-93%), which might be useful for industrial upscaling. Therefore, a model calculation was made for this combination. Mass balances were calculated over the system. The different flows are shown with their respective composition for a single-stage design in Figure 6.6.

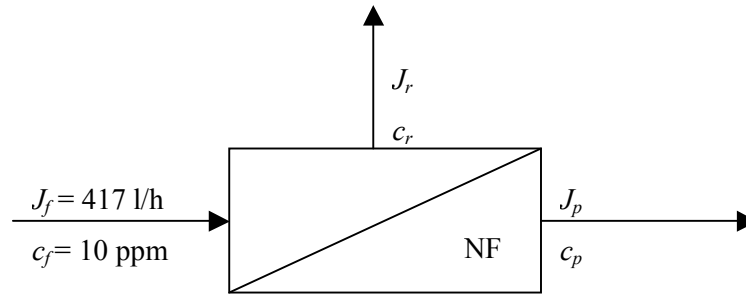


Figure 6.6: Design of a one-stage membrane process

The mass balances are for this system are:

$$J_f = J_p + J_r \quad (6.1)$$

$$\frac{J_p}{J_f} = 0.8 \quad (6.2)$$

$$c_f J_f = c_p J_p + c_r J_r \quad (6.3)$$

$$R = 1 - \frac{c_p}{c_f} = 0.91 \quad (6.4)$$

in which  $J_p$ ,  $J_r$ ,  $c_p$ ,  $c_r$  and  $\overline{c_f}$  are unknown.

The throughput distillation currently in use deals with a feed flow ( $J_f$ ) of 10,000 l a day (De Witte, 2005), corresponding for methanol to a flow of 417 l/h. For industrial applications, typical recoveries are about 80%, i.e. 334 l/h. As can be seen in Table 6.3, the API-5 rejection is similar for StarMem-120 and StarMem-228. As the permeability is significantly higher for StarMem-120, it is opportune to select this membrane for further application and calculations. Assuming a permeability of 5.5 l/h.m<sup>2</sup>.bar, and an applied transmembrane pressure of 15 bar, a permeate flux of 82.5 l/h.m<sup>2</sup> is obtained. As a permeate flux of 334 l/h is required, a membrane surface of 4.05 m<sup>2</sup> is needed.

Membrane Extraction Technology delivers spiral wound modules of different sizes. A module of 4" x 40" provides an active membrane area of 6.0 m<sup>2</sup>, which suffices to deal with the methanol flow of 417 l/h.

It was found in the experiments that StarMem-120 provides a 91% rejection for API-5. However, this cannot be applied straightforward on the initial feed concentration of 10 ppm. As a high recovery is desired, the concentration of API-5 in the retentate is seriously increased when compared to the feed concentration, and the real feed concentration at the membrane surface ( $\overline{c_f}$ ) lies between the initial



feed concentration ( $c_f$ ) and the retentate concentration ( $c_r$ ). A possible assumption is that  $\overline{c_f}$  is the average of the initial feed concentration and the retentate concentration:

$$\overline{c_f} = \frac{c_f + c_r}{2} \quad (6.5)$$

The solution of the mass balances then results in a permeate concentration of 2.3 ppm and a retentate concentration of 40.8 ppm. Thus, the observed rejection would be only as high as 77%.

A more precise solution is obtained by calculating the dependency of the permeate concentration on the recovery in a more accurate way, by dividing the module into an infinite number of small segments, calculating the mass balances over these small segments and integrating the result over the entire membrane module, as presented by Mulder (1996). This method leads to the following equations:

$$c_p = \frac{c_f}{S} [1 - (1-S)^{1-R}] \quad (6.6)$$

$$c_r = \frac{(c_f - c_p S)}{1-S} \quad (6.7)$$

These equations show how the concentrations in the permeate and the retentate are related to the recovery ( $S$ ) and the rejection ( $R$ ). With a feed concentration of 10 ppm, a recovery of 80% and a solute rejection of 91%, the permeate concentration is found to be 1.7 ppm, whereas the retentate concentration will be 43.3 ppm. Thus, the observed rejection is 83%.

When a higher purification is required for solute reuse, a two-stage process can be considered, as shown in Figure 6.7. It was shown before that the concentration that is left in the permeate fraction is approximately a factor 25 lower, whereas the recovery only decreases from 80% to 76.2% (Van der Bruggen, 2000). A permeate flow of 317 l/h with a API-5 concentration of 0.07 ppm is then obtained.

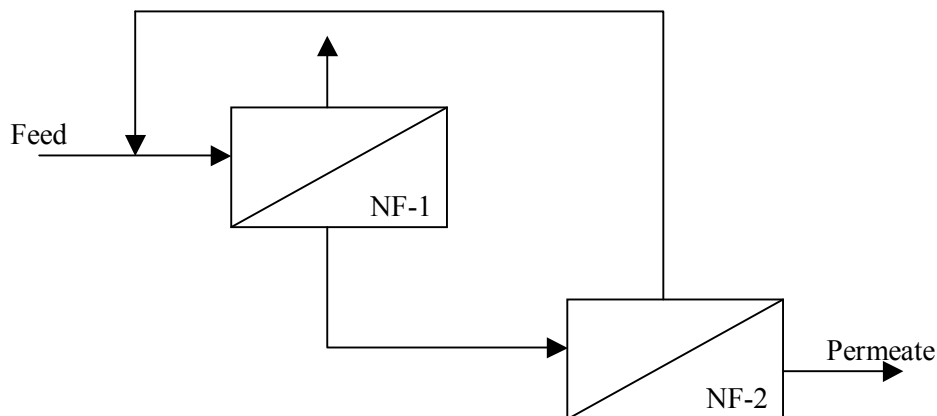


Figure 6.7: Design of a two-stage membrane process

### 4.3.2 Energy consumption

It is known that membrane processes are much less energy consuming than traditional separation processes. It is not the objective of this study to provide an entire cost analysis of a membrane process versus a distillation unit, for the following reasons:

- the distillation column is already available, whereas the membrane module has to be constructed, and thus capital costs should be included;
- the use of a nanofiltration system gives the opportunity to treat other solvent streams in the distillation column;
- due to technical considerations, it is common to use at least two pumps in pressurised systems, a pressure pump and a circulation pump; yet, the circulation pump requires considerably less energy.

Therefore, a simple comparison is made for the energy consumption of the two processes, based on a pressure pump for the nanofiltration system, and a total reboiler for the throughput distillation.

The brake horsepower (BHP) of one pressure pump required to provide a pressure difference  $\Delta P$  for a feed flow  $F$  is given by (Karassik *et al.*, 1986):

$$BHP = \frac{F \cdot \Delta P}{\eta} \quad (6.8)$$

with  $\eta$  the overall pump efficiency.

When a pressure difference of 15 bar is applied on a feed flow of 0.417 m<sup>3</sup>/h, and an overall pump efficiency of 0.3 is assumed (Grundfos, 2005), the BHP is 0.58 kW.

The energy required in a throughput distillation consists of two contributions: heating the fluid to the boiling point, and evaporate the liquid at the boiling point (Seader and Henley, 1998):

$$Q = Q_{boil} + Q_{vap} \quad (6.9)$$

$$Q = F_m \cdot c_p \cdot \Delta T + \Delta H^{vap} \cdot F_m \quad (6.10)$$

with  $F_m$  the molar flow,  $c_p$  the heat capacity at constant pressure,  $\Delta T$  the difference between the temperature of the feed flow and the boiling point and  $\Delta H^{vap}$  the molar heat of vaporisation.

For methanol, a flow of 417 l/h corresponds to a molar flow of 2.856 mol/h. The heat capacity is 81.6 J/mol.K, the boiling temperature 64.7°C and the heat of vaporisation 37.6 kJ/mol. The average temperature in Flanders is 9.8°C (KMI, 2005). This results in a reboiler duty of 120 kW.

At this time, yearly 451 tons of methanol are recovered by distillation, which corresponds to a process time of 1371 h at a feed flow of 417 l/h. The total energy consumption then is 162 MWh, whereas the nanofiltration set-up requires only 795 kWh, which is more than 200 times less. It is indeed clear that a

membrane process is advantageous in terms of energy consumption, and might become a lucrative alternative for a traditional distillation.

However, a complete and careful economic analysis still remains necessary, and the payback period must be calculated. Membrane modules are expensive (3,700 Euro/module) (Nozari, 2005) and the optimal operating pressure must therefore be determined. A higher transmembrane pressure enhances the flux, which allows a reduced membrane surface, but the energy consumption of pumping increases too then. For a complete analysis, also indirect gains must be brought into account, such as the increased number of solvent streams that can be distilled, the safety and environmental aspects

At first sight, it appears that the methanol volume to be treated is too small to account for economic feasibility. However, the membrane installation can also be used for other solvent streams: e.g. API-1 was rejected for 43% in toluene. This can be increased to approximately 80% (or 2 ppm in the permeate) in a two-step filtration process. It depends on further applications whether this meets the specifications or not.

For a comparison: if methanol was completely not recovered, the total cost for the purchase, at the rate of 3 Euro/l (Gerrits, 2005), and the discharge to Indaver, at the rate of 86.5 Euro/ton (Van Baelen, 2005), would be 1.75 million Euro for the volume of 451 tons.

## **5. Summary and conclusion**

With an employment of nearly half a million people, the industry is an important player in the Flemish economy. For economical and environmental reasons, improved performance of industrial processes is desired. During industrial activity, large volumes of organic solvents are consumed (and discharged). The use of organic solvents includes a number of undesired effects, such as increased risks on cancers and mental diseases, contamination of soil and ground water, and important contributions to air pollution, the greenhouse effect, the hole in the ozone layer,...

For processes with such solvents, membrane technology may become an important alternative for traditional separation units, resulting in an increased number of solvent streams that can be reused. Moreover, important energy savings can be realised and smoother operating conditions lead to increased safety and reduced pressure on the environment.

Several membrane processes with organic solvents are already reported in literature: solvent recovery in lube oil dewaxing, in the vegetable oil industry, in heterogeneous synthesis and in chemical processes requiring solvent exchange. Thus, depending on requirements of specific processes and applications, membrane technology may be implemented in almost all sectors working with organic solvents.

In a case-study, it appeared that high rejections of active pharmaceutical ingredients can be realised in methanol (more than 90%). Also in toluene, relatively high rejections were found. The energy required for a full-scale membrane process, with a recovery of 80%, is approximately 200 times lower than the energy consumption of a throughput distillation. As the capital cost of an industrial membrane unit is relatively high, a detailed cost analysis must show whether such a unit is economically feasible.

## Summary and general conclusions

Nanofiltration is a pressure driven membrane process in which small organic components with a molecular weight of 200-1000 are removed from a liquid feed stream. The technique is already successfully implemented in aqueous media, e.g. for drinking water softening or for the removal of dye components from wastewater in the textile industry.

The application of nanofiltration in non-aqueous media is a more recent research topic. Yet, membrane technology can become an important alternative for traditional separation processes, such as distillation. Membrane processes are less energy intensive and can operate at modest conditions.

This study focuses on the potential of nanofiltration membranes as a separation tool in organic solvents. The performance of a membrane process is typically characterised by two parameters: the solvent permeability and the solute rejections. Both parameters are required to be high enough, in order to make the membrane process technically and economically feasible.

Filtration experiments were carried out both with solvents of a same homologous series as with solvents from different chemical classes: water, methanol, ethanol, propanol, butanol, pentanol, hexanol, acetone, ethyl acetate, *n*-hexane, cyclohexane, methylene chloride and toluene. Both polymeric and ceramic membranes were involved in the research. The membranes had a different MWCO (the molecular weight of a component that is retained for 90%).

In the first part of this study, the influence of organic solvents on polymeric nanofiltration membranes was investigated. It is well known from polymer science that the lack of solvent resistance of these materials is one of the major drawbacks in a number of applications.

Nanofiltration membranes are often synthesised with a phase inversion technique. This means that the membrane polymer is solidified by immersing it in a non-solvent, i.e. a solvent in which the polymer is not soluble. However, the exposure of a membrane to a solvent in which the polymer is soluble might have a serious influence on the structure and the performance of this membrane.

It was observed that the membrane performance of different nanofiltration membranes, which was characterised in terms of the pure water flux and the rejection of a reference solute in aqueous solution, was lower than the specifications provided by the manufacturers.

As expected, a long time exposure to a broad range of organic solvents resulted in a strong impact on the membrane performance. Both the pure water flux and the solute rejection, which were measured both before and after the solvent treatment, changed significantly. As both the flux and the rejection decreased for a given membrane, these changes could not only be attributed to an increase of the pore size, or thus swelling effects. It was hypothesised that some organic solvents induce a plasticisation of the membrane material, which leads to a reorganisation of the membrane structure. This reorganisation has a double effect: both the pore size distribution and the degree of hydrophilicity of the membrane

surface changes. These effects were more pronounced for hydrophilic than for hydrophobic membranes.

The reorganisation of polymeric material in the toplayer of the membrane was also suggested by SEM images. Micro valleys that are scarcer and at a larger distance from each other were observed for solvent treated membranes, showing the mobility of the polymeric chains during the immersion in organic solvents. The determination of the degree of swelling of the membranes in different solvents indicated that, at least for porous membranes, the pore size increases. This could be straightforwardly correlated to the decrease in solute rejection. However, the widening of the membrane pores does not necessarily lead to an increase of the pure water flux. It appeared indeed that the exposure to organic solvents modified the degree of hydrophilicity of the membrane surface. This was confirmed by the changes of the surface energy, which is an absolute measure for the degree of hydrophilicity, before and after solvent treatment.

The second part of this research was focused on the permeability of organic solvents through (polymeric and ceramic) nanofiltration membranes. In the study of nanofiltration in aqueous solution, water is the only 'solvent' involved. Therefore, minor attention is paid to the properties of the solvent, except for the reciprocal correlation of the water flux to its viscosity. In this study, nanofiltration is investigated in a broad range of organic solvents. It can be expected that a large number of solvent properties, other than only the viscosity, influence the permeability.

The parameters affecting the solvent permeability, and their relative contribution, were identified by measurement of the permeability for binary mixtures of water, methanol and/or ethanol. The variation of the permeability as a function of a smoothly changing feed composition allowed to analyse the transitional flux behaviour, instead of only the pure solvent fluxes, and to correlate this to the properties of the mixture, also determined as a function of the feed composition.

Hydrophilic membranes showed a minimum in the permeability curve as a function of the feed composition, which was expected as the mixture viscosity of water-alcohol mixtures shows a corresponding maximum. In contrast, hydrophobic membranes showed an increased permeability with increased alcohol fraction in the feed, clearly confirming that the solvent viscosity is not the only parameter affecting the permeability. The determination of the partial permeability showed that for hydrophilic membranes, the least polar component of a binary mixture has a stronger influence on the partial permeability of the most polar component than vice versa. For hydrophobic membranes, the opposite was observed. This effect was larger with increased polarity difference between the two components. It was therefore concluded that both the viscosity and the polarity of the solvent play a major role in the permeability through nanofiltration membranes.

The investigation of polymeric and ceramic membranes provided similar findings. It was therefore concluded that the changes in solvent permeability could not be attributed only to swelling effects, which only occur for polymeric membranes.

Transport models for solvent permeation that are available in literature, are inadequate for the description of the permeability of a broad range of organic solvents through a number of nanofiltration membranes with varying characteristics. Therefore, a new model for solvent permeation was developed, based on a combination of the experimental findings of this work and parameters occurring in literature models. The newly developed model proposes proportionality of the solvent permeability to the molar volume of the solvent and an inverse correlation to the solvent viscosity and the difference in surface energy between the solvent and the membrane surface. In this way, the dependency of three phenomena is included, namely the transport of momentum, steric hindrance effects and the affinity between the solvent and the membrane material.

For hydrophilic membranes, the new model fitted the experimental data as well as the models available in literature, which is ascribed to the dominance of the viscosity as transport parameter for hydrophilic membranes. However, for hydrophobic membranes, polarity effects are at least as important as the viscosity, and only the newly presented model can deal with the different transport parameters at the same time. When compared to the results obtained using the literature models, a significant improvement of the data fitting was observed for the new model.

As the goal of this study was the investigation of nanofiltration in a broad range of organic solvents, the findings were controlled for a large number of pure solvents. For a homologous series of alcohols, it was observed that the permeability decreased with increasing chain length, which can be attributed to a combination of the increased molecular size and the decreased polarity of the solvent. The new model showed good fitting results. When the permeability of solvents from different chemical classes is determined, no clear correlation was distinguished at first sight. However, the varying solvent fluxes could be modelled significantly more precisely, whereas literature models showed important shortcomings in dealing with the whole range of solvents.

In the third part of this study, transport of small organic components, dissolved in different organic solvents, through nanofiltration membranes was investigated. It is clear that solute transport is much more complicated than in aqueous solution. In the literature, only little attention is paid to the potential interactions between water molecules and the organic solute. For solute transport in non-aqueous nanofiltration, all membrane-solvent-component interactions must be brought into account. The molecular weight cut-off (mostly characterised in aqueous medium) appears indeed to be solvent dependent and can no longer straightforwardly be used for the prediction of solute rejection in non-aqueous media.

As nanofiltration membranes are situated at the interface between porous (UF) and dense (RO) membranes, it might be expected that solute transport is affected by both convection and diffusion. However, the relative contribution of the two mechanisms was determined from dynamic filtration experiments and static cell diffusion experiments, and it was found that solute transport is quasi completely dominated by convective flow.

In a first stage, the rejection of a single reference component in binary mixtures of water, methanol and/or ethanol allowed to identify the parameters and the interactions influencing the solute transport. With increased alcohol fraction in the feed stream, hydrophilic membranes showed a decrease in solute rejection, whereas hydrophobic membranes showed an increase. It was concluded that the solute rejection is determined by three parameters: the nominal pore size, the degree of solvation of the solute (resulting in a solvent dependent effective solute diameter), and the affinity between the solvent and the membrane (leading to a solvent dependent effective pore diameter).

In a second stage, the solute rejection of a larger number of reference components was investigated in a broad range of organic solvents. It was confirmed that the rejection is determined by properties and characteristics of the membrane, the solvent and the solute. Although solute rejections are lower in relatively less polar solvents, the effect of the solvent itself is varying dependent on the membrane characteristics. Hydrophobic membranes were observed to be much less liable to solvent influences, and showed, again, a better stability over a broad range of solvents, i.e. a more or less constant effective pore size. With respect to the component properties, it was found that not only the molecular size determines the permeation rate, but also the affinity between the solute and the membrane affects the transport. Again, polymeric and ceramic membranes provided similar results, reconfirming that the observed phenomena were not only due to swelling effects.

As no suitable models for the description of solute transport in organic solvents were available in literature, a new methodology was developed. As transport was found to be dominated by viscous flow, existing transport models for solute transport through porous membranes were selected as the basis for the modelling of solute transport in non-aqueous media. A correction, based on molecular weight and a solvent association parameter, was implemented to incorporate the solvent dependency of the solute. The fitting results confirmed that the pore diameters were indeed solvent dependent, due to solvation of the pore wall. Both polymeric and ceramic membranes showed this effect.

The model parameters obtained from the data fitting (i.e. the effective pore diameters) were used to predict the rejections observed for the reference component in the binary mixtures; excellent results were found, meeting all variations due solvent-membrane interactions.

The potential of non-aqueous nanofiltration in industrial applications was evaluated in the last part of this study. The Flemish industry employs nearly 500,000 people and is a major contributor to the economy of the region. However, beside personal welfare, industrial activity also causes a number of undesired effects on the society and the environment. Specifically, the consumption of large volumes of organic solvents includes increased risks on cancers and mental diseases for man, and leads to environmental problems, such as the existence of photochemical ozone, the hole in the ozone layer or the greenhouse effect.

Due to competitive, environmental and legislative restrictions, industrial companies are urged to implement to a maximal extent the best available technologies. For several reasons, membrane



technology can be a valuable alternative for traditional separation techniques: reduced energy consumption, smaller footprint, less critical operating conditions, increased safety, reduced diffuse losses,... Different (potential) applications are described in literature: solvent recovery in lube oil dewaxing, solvent recovery in the edible oil industry, enhanced productivity in heterogeneous catalysis and solvent exchange in reaction processes consisting of multiple steps. Only the recovery of organic solvents in lube oil dewaxing is already implemented at large scale.

In a case study the potential of non-aqueous nanofiltration was investigated in the pharmaceutical industry. Nowadays, large volumes of organic solvents are distilled. Experiments showed that different process streams, containing rest fractions of active pharmaceutical ingredients, could be highly purified with nanofiltration membranes. Approximately 200 times less energy is required for this separation, compared to a throughput distillation. Capital costs remain however relatively high for membrane installations. It was concluded that membrane technology could become an important separation tool in pharmaceutical applications, either as an alternative or as a support unit for traditional separation techniques.

Although the most important topics in non-aqueous nanofiltration have been pointed in this work, a number of suggestions for further research can be made.

Manufacturers are continuously working on membranes with improved performance in organic solvents. Interesting results are reported with newly developed hydrophobic ceramic membranes. These are ceramic membranes modified by grafting organic chains upon the surface. Promising results are also reported for hybrid membranes, incorporating inorganic materials in polymeric membranes (Gevers *et al.*, 2005; Koros *et al.*, 2005).

As new membranes become denser, the relative importance of diffusive transport may increase. Transport mechanisms must still be investigated, particularly in non-polar solvents. In these solvents, fluxes and solvent rejections were observed to be relatively low and thus the contribution of viscous flow may become smaller. Transport mechanisms are related to the free volume of the membrane material; this can be investigated with new material analysis techniques, such as positron annihilation lifetime spectroscopy (PALS). Useful information can be obtained by the comparison of non-aqueous nanofiltration to other membrane processes, in particular pervaporation.

Further attention must be paid to the precise membrane-solvent-component interactions. It must be clarified which forces act to which extent. Solvation effects should be analysed in detail, partly apart from membrane processes, but as a proper research on material science. As solvation effects influence the pore, a method must be developed to express these interactions in a quantitative way. Due to solvation, also the solute diameter is solvent dependent. In this work, a first approximation was presented with the Stokes diameter. A more correct way should involve the use of a hydrodynamic solute diameter. This would not only incorporate a solvent dependency, also the steric configuration

(linear vs. spherical molecules) can then be taken into account. Yet, the calculation of a hydrodynamic diameter in different solvents, other than water, is a complex and tedious operation.

With respect to modelling, both of solvent flux and solute transport, generalised models, based on physicochemical interactions, rather than semi-empirical models should still be developed. Due to the large number of (complex) interactions, this area still remains relatively unexplored.

For the implementation of nanofiltration in industrial processes, such as solvent recovery in the pharmaceutical industry, a complete economic evaluation should be made. This evaluation includes all aspects of a chemical processing unit, such as capital costs, exploitation costs, taxes, savings (which are not necessary strictly economic, nor objective),... It is however clearly suggested that non-aqueous nanofiltration has a prosperous future in a large number of industrial applications!

## References

Abu Qdais H., Moussa H., 2004. Removal of heavy metals from waste water by membrane processes: a comparative study. *Desalination* 164(2): 105-110.

Aerts S., Weyten H., Buekenhoudt A., Gevers L.E.M., Vankelecom I.F.J., Jacobs P.A., 2004. Recycling of the homogeneous Co-Jacobsen catalyst through solvent-resistant nanofiltration (SRNF). *Chem. Comm.* 6: 710-711.

Atra R., Vatai G., Bekassy-Molnar G., Balint A., 2005. Investigation of ultra- and nanofiltration for utilization of whey protein and lactose. *J. Food Eng.* 67(3): 325-332.

Belfort G., Litmann F.E., Bishop H.K., 1973. Membrane regeneration for wastewater reclamation using reverse osmosis. *Water Research* 7(11): 1547-1559.

Berg P., Hagemeyer G., Gimbel R., 1997. Removal of pesticides and other micropollutants by nanofiltration. *Desalination* 113(2-3): 205-208.

Bhanushali D., Kloos S., Kurth C., Bhattacharyya D., 2001. Performance of solvent-resistant membranes for non-aqueous systems: solvent permeation results and modeling. *J. Membr. Sci.* 189: 1-21.

Bhanushali D., Kloos S., Bhattacharyya D., 2002. Solute transport in solvent-resistant nanofiltration membranes for non-aqueous systems: experimental results and the role of solute-solvent coupling. *J. Membr. Sci.* 208: 343-359.

Bhore N.A., Gould R.M., Jacob S.M., McNally S.D., Smiley P.H., Wildemuth C.R., 1999. *Oil Gas J.*, Nov. 15: 67-74.

Bickel P.J., Doksum K.A., 1977. *Mathematical Statistics: Basic Ideas and Selected Topics*. Chapter 7: Linear Models: Regression and Analysis of Variance. Holden Day, Inc., San Francisco, CA, 248-311.

Bird R.B., Stewart W.E., Lightfoot E.N., 2002a. *Transport Phenomena*. 2<sup>nd</sup> Ed. Chapter 2 Shell momentum balances and velocity distribution in laminar flow. John Wiley & Sons, Inc., New York, 51.

Bird R.B., Stewart W.E., Lightfoot E.N., 2002b. Transport Phenomena. 2<sup>nd</sup> Ed. Chapter 22 Interphase transport in nonisothermal mixtures. John Wiley & Sons, Inc., New York, 671-725.

Block C., Van Hooste H., 2004. Milieu- en natuurrapport Vlaanderen, Achtergronddocument 2004: Verspreiding van vluchtige organische stoffen (VOS). Vlaamse Milieumaatschappij, [www.milieurapport.be/AG](http://www.milieurapport.be/AG).

Bodzek M., Koter S., Wesolowska K., 2002. Applications of membrane techniques in a water softening process. Desalination 145(1-3): 321-327.

Bogaert G., Callens A., Gielen B., Le Roy D., Van Biervliet K., 2002. Evaluatie van het reductiepotentieel voor VOS-emissies naar het compartiment lucht en de problematiek van de implementatie van de Europese Richtlijn 99/13/EG in de sector van de metaalontvetting en de oppervlaktereiniging in Vlaanderen. AMINAL, pp. 441.

Bogaert G., Callens A., Devoldere K., Van Biervliet K., Le Roy D., 2002b. Evaluatie van het reductiepotentieel voor diverse pollutantemissies naar het compartiment lucht in een aantal homogene subsectoren van de chemische industrie in Vlaanderen: Deel I. AMINAL, pp. 458.

Bogaert S., Devoldere K., Van Hyfte A., Van Biervliet K., Le Roy D., 2004. Evaluatie van het reductiepotentieel voor diverse pollutantemissies naar het compartiment lucht in een aantal homogene subsectoren van de chemische industrie in Vlaanderen: Deel III. AMINAL, pp. 410.

Bohlin T., 1959. Trans. Roy. Inst. Technol. (Stockholm), No. 155.

Bowen W.R., Muhktar H., 1996. Characterisation and prediction of separation performance of nanofiltration membranes. J. Membr. Sci. 112: 263-274.

Bowen W.R., Welfoot J.S., 2002. Modelling the performance of nanofiltration membranes. Chapter 6 in Nanofiltration – Principles and Applications, Elsevier Advanced Technology, Oxford, 119-146.

Braeken L., Van der Bruggen B., Vandecasteele C., 2004. Regeneration of brewery waste water using nanofiltration. Water Research 38(13): 3075-3082.

Braeken L., Ramaekers R., Zhang Y., Maes G., Van der Bruggen B., Vandecasteele C., 2005. Influence of hydrophobicity on retention in nanofiltration of aqueous solutions containing organic compounds. J. Membr. Sci. 252: 195-203.

Bräutigam, Kruse, 1992. Ermittlung der Emissionen Organischer Lösemittel in der Bundesrepublik Deutschlands: Grundlagen und Hauptergebnisse. Umweltbundesamt Deutschland.

Bridge M.J., Broadhead K.W., Hlady V., Tresco P.A., 2002. Ethanol treatment alters the ultrastructure and permeability of PAN-PVC hollow fiber cell encapsulation membranes. *J. Membr. Sci.* 195: 51-64.

Capelle N., Moulin P., Charbit F., Gallo R., 2002. Purification of heterocyclic derivatives from concentrated saline solution by nanofiltration. *J. Membr.Sci.* 196(1): 125-141.

Ceenaeme J., Geysen D., Gommeren E., Dedecker D., De Naeyer F., Dries V., Van Dijck W., Van Dyck E., Stalpaert L., 2004. Milieu- en natuurrapport Vlaanderen, MIRA-T 2004. Bodemverontreiniging. Vlaamse Milieumaatschappij, 327-334.

Cuperus P., Ebert K., 2002. Non-aqueous applications of NF. Chapter 21 in *Nanofiltration – Principles and Applications*, Elsevier Advanced Technology, Oxford, 521-536.

Curzons A.D., Constable J.C., Mortimer D.N., Cunningham V.L., 2001. So you think your process is green, how do you know? Using principles of sustainability to determine what is green – a corporate perspective. *Green Chemistry*, 3: 1-6.

Daubert T.E., Danner R.P., 1989. *Physical and thermodynamic properties of pure chemicals: Data compilation*. Hemisphere Publishing Corporation, Pennsylvania.

Deen W.M., 1987. Hindered transport of large molecules in liquid-filled pores. *AIChE J.* 33: 1409-1425.

De Groof M. (OVAM), 2005. Personal communication.

Desai M.C., Mehta M.H., Dave A.N., Mehta J.N., 2002. Degumming of vegetable oil by membrane technology. *Ind. J. Chem. Technol.* 9(6): 529-534.

De Witte B. (Janssen Pharmaceutica), 2005. Personal communication.

Dubois M., Gilles K.A., Hamilton J.K., Rebers P.A., Smith F., 1956. Colorimetric method for determination of sugars and related substances. *Anal. Chem.* 28: 350.

Dumont G., Fierens F., Vandermeiren K., De Geest C., 2004. Milieu- en natuurrapport Vlaanderen. Achtergronddocument 2004, Fotochemische luchtverontreiniging. Vlaamse Milieumaatschappij, pp. 147.

Durrans T.H., Davies E.H., 1971. Solvents. Chapman and Hall Ltd., London, pp. 267.

Ebert K., Cuperus F.P., 1999. Solvent resistant NF membranes in edible oil processing. *Membr. Technol.* 107: 5-8.

Ebert K., 2002. Nanofiltration for non-aqueous applications. Presented at NMG Symposium, 11<sup>th</sup> June 2002, Ede, The Netherlands.

Elmaleh S., Vera L., Villaroel-Lopez R., Abdelmoumni L., Ghaffor N., Delgado S., 1998. Dimensional analysis of steady state flux for microfiltration and ultrafiltration membranes. *J. Membr. Sci.* 139: 37-45.

EPA, 2005. Environmental Protection Agency. BATNEEC – best available technology not entailing excessive costs. <http://www.epa.ie/licenses/batneec.htm>

Eriksson P., 1988. Nanofiltration extends the range of membrane filtration. *Env. Progress* 7(1): 58-62.

Ferry J.D., Ultrafilter membranes and ultrafiltration. *Chem. Rev., Am. Chem. Soc.*, 373-455.

Flory P.J., 1953. Phase equilibria in polymer systems – Swelling of network structures. In *Principles of Polymer Chemistry*, Cornell University Press, Ithaca, New York, 576-577.

Garcia A., Alvarez S., Riera F., Alvarez R., Coca J., 2005. Water and hexane permeate flux through organic and ceramic membranes: Effect of pretreatment on hexane permeate flux. *J. Membr. Sci.* 253: 139-147.

Geankoplis C.J., 1978. *Transport processes and unit operations*, Allyn and Bacon Inc., Massachusetts.

Geens J., Van Hooste H., 2004. Milieu- en natuurrapport Vlaanderen, Achtergronddocument 2004, Industrie. Vlaamse Milieumaatschappij, <http://www.milieurapport.be/AG>

Gerrits D. (CASP), 2005. Personal communication.

Gevers L.E.M., Vankelecom I.F.J., Jacobs P.A., 2005. Zeolite filled polydimethylsiloxane (PDMS) as an improved membrane for solvent-resistant nanofiltration (SRNF). *Chem. Comm.* 19: 2500-2502.

Gibbins E., D'Antonio M., Nair D., White L.S., Freitas dos Santos L.M., Vankelecom I.F.J., Livingston A.G., 2002. Observations on solvent flux and solute rejection across solvent resistant nanofiltration membranes. *Desalination* 147: 307-313.

Gould R.M., White L.S., Wildemuth C.R., 2001. Membrane separation in solvent lube dewaxing. *Env. Progress* 20(1): 12-16.

Grundfos, 2005. Grundfos CR – Innovation Inside – Technical data.

<http://www.grundfos-www.com/cr/technical.htm>.

Guizard C., Ayrat A., Julbe A., 2002. Potentiality of organic solvents filtration with ceramic membranes. A comparison with polymer membranes. *Desalination* 147: 275-280.

Haberman W., Sayre R.M., 1958. Motion of rigid and fluid spheres in stationary and moving liquids inside cylindrical tubes. David Taylor Model Basin Report No. 1143, US Navy Department.

Hagen G., 1839. *Ann. Phys. Chem.*, 46: 423-442.

Hansen F.K., Rodsrud G., 1991. Surface tension by pendant drop: 1. A fast standard instrument using computer image-analysis. *J. Coll. Int. Sci.* 141(1): 1-9.

Hart H., Hart D., Craine L.E., 1995. *Organic chemistry: a short course*. 9<sup>th</sup> Ed. Houghton Mifflin Company, Boston, pp. 572.

Heirman J.P., 2004. NEC-reductieprogramma: Emissiereductieprogramma voor het Vlaamse Gewest voor de pollutanten SO<sub>2</sub>, NO<sub>x</sub>, VOS en NH<sub>3</sub> in het kader van de Richtlijn 2001/81/EG. AMINAL, pp. 136.

Hestekin J.A., Smothers C.N., Bhattacharyya D., Ghorpade A., Hannah R., 1999. Nanofiltration for removal of organics from aqueous and organic solvent streams. Presented at the 4<sup>th</sup> Topical Conference on Separations Science & Technology, Membrane Separation in Food and Pharmaceutical Session, Dallas, November 1999.

Ho W.S.W., Sirkar K.K., 1992. *Membrane Handbook*. Van Nostrand Reinhold, New York, 239-240.

Janssen Pharmaceutica, 2005. Duurzaamheidsverslag 2004.

[http://www.janssenpharmaceutica.be/pdf/Duurzaam\\_verslag\\_04\\_N.pdf](http://www.janssenpharmaceutica.be/pdf/Duurzaam_verslag_04_N.pdf)

Jonsson G., Boesen C.E., 1975. Water and solute transport through cellulose acetate reverse osmosis membranes. *Desalination* 17: 145-165.

Justaert M., Cambré C., 2000. Als een oplossing het probleem is: een brochure over het werken met oplosmiddelen of solventen en het organisch psychosyndroom door solventen (OPS). LCM, Dienst Gezondheidsvoorlichting en –opvoeding, Brussel, pp. 30.

Karassik I.J., Krutzsch W.C., Fraser W.H., Messina J.P., 1986. *Pump Handbook*, 2<sup>nd</sup> Ed., McGraw-Hill Book Company, New York, 3.3-3.4.

Kirk, Othmer, 1984. *Encyclopedia of chemical technology*: 3<sup>rd</sup> Ed., Wiley-Interscience, Volume 1-24.

KMI, 2005. Klimatologisch overzicht van het jaar 2004.

[http://www.kmi.be/nederlands/index.php?menu=Menu1\\_3\\_3](http://www.kmi.be/nederlands/index.php?menu=Menu1_3_3)

Koops G.H., Yamada S., Nakao S.I., 2001. Separation of linear hydrocarbons and carboxylic acids from ethanol and hexane solutions by reverse osmosis. *J. Membr. Sci.* 189: 241-254.

Koros W.J., Ma Y.H., Shimidzu T., 1996. Terminology for membranes and membrane processes. *J. Membr. Sci.* 120: 149-159.

Koros W.J., Hillock A., Wallace D., 2005. Next generation membranes for gas and vapor separations: research needs and opportunities. Presented at International Congress on Membranes and Membrane Processes, ICOM2005, Seoul, Korea, August 21-26.

Kotz J.C., Purcell K.F., 1991. Intermolecular forces, liquids, and solids. Chapter 13 in *Chemistry and Chemical Reactivity*, 2<sup>nd</sup> Ed., Saunders College Publishing, Holt, Rinehart and Winston, Inc., Orlando: 501-557.

Koyuncu I., Topacik D., Yuksel E., 2004. Reuse of reactive dyehouse wastewater by nanofiltration: process water quality and economical implications. *Sep. Purif. Technol.* 36(1): 77-85.



- Li W., Li J., Chen T., Zhao Z., Chen C., 2005. Study of nanofiltration for purifying fructo-oligosaccharides. II. Extended pore model. *J. Membr. Sci.* 258: 8-15.
- Lide D.R., 2000. *C.R.C. Handbook of Chemistry and Physics*, 81<sup>st</sup> Ed., CRC Press LLC.
- Lin K.M., Zhang X., Koseoglu S.S., 2004. Separation of tocopherol succinates from deodorizer distillate. *J. Food Lipids*, 11: 29-43.
- Livingston A., Peeva L., Han S., Nair D., Luthra S.S., Freitas dos Santos L.M., 2003. Membrane separation in green chemical processing – Solvent nanofiltration in liquid phase organic synthesis reactions. *Annals New York, Academy of Sciences*, 984: 123-141.
- Lodewijcks P., Van Rompaey H., Sleuwaert F., 2003. VOS-emissies naar de lucht bij de productie en het industrieel gebruik van coatings, inkt en lijm in Vlaanderen. Evaluatie van het reductiepotentieel en implementatie van de Europese Solventrichtlijn 1999/13/EG. AMINAL, pp. 356.
- Loeb S., Sourirajan S., 1962. *Adv. Chem. Ser.* 38: 117.
- Loncke P., Bobel H., Vanacker L., 1996. Milieugevaarlijke stoffen – Solventen. OVAM, Mechelen, pp. 95.
- Lonsdale H.K., Merten U., Riley R.L., 1965. Transport properties of cellulose acetate osmotic membranes, *J. Appl. Polym. Sci.* 9: 1341-1362.
- Luthra S.S., Yang X., Freitas dos Santos L.M., White L.S., Livingston A.G., 2001. Phase-transfer catalyst separation and re-use by solvent resistant nanofiltration membranes. *Chem. Comm.* 16: 1468-1469.
- Luthra S.S., Yang X., Freitas dos Santos L.M., White L.S., Livingston A.G., 2002. Homogeneous phase transfer catalyst recovery and re-use using solvent resistant membranes. *J. Membr. Sci.* 201: 65-75.
- Machado D.R., 1998. Solvent transport through nanofiltration membranes. PhD-Research Thesis, Technion – Israel Institute of Technology, February 1998.

Machado D.R., Hasson D., Semiat R., 1999. Effect of solvent properties on permeate flow through nanofiltration membranes. Part I: Investigation of parameters affecting solvent flux. *J. Membr. Sci.* 163: 93-102.

Machado D.R., Hasson D., Semiat R., 2000. Effect of solvent properties on permeate flow through nanofiltration membranes. Part II: Transport model. *J. Membr. Sci.* 166: 63-69.

Marcus Y., 1998. *Wiley Series in Solution Chemistry Volume 4: The properties of solvents.* John Wiley & Sons, Chichester, pp. 239.

Mason E.A., Lonsdale H.K., 1990. Statistical-mechanical theory of membrane transport. *J. Membr. Sci.* 51: 1-81.

Matsuura T., Sourirajan S., 1981. Reverse osmosis transport through capillary pores under the influence of surface forces. *Ind. Eng. Chem. Process Des. Dev.* 20 : 272-282.

McClellan A.L., 1989. *Tables of experimental dipole moments. Volume 3.* Rahara Enterprises, El Cerrito, pp. 1455.

Moe N. (GE), 2005. Personal communication.

Mulder M., 1996. *Basic principles of membrane technology, Second Edition,* Kluwer Academic Publishers, Dordrecht, pp. 564.

Musale D.A., Kumar A., 2000. Solvent and pH resistance of surface crosslinked chitosan/poly(acrylonitrile) composite nanofiltration membranes. *J. Appl. Pol. Sci.* 77(8): 1782-1793.

Nair D., Scarpello J.T., White L.S., Freitas dos Santos L.M., Vankelecom I.F.J., Livingston A.G., 2001. Semi-continuous NF-coupled Heck reactions as a new approach to improve productivity of homogeneous catalysts. *Tetrahedron Letters* 42: 8219-8222.

Nair C., Luthra S.S., Scarpello J.T., White L.S., Freitas dos Santos L.M., Livingston A.G., 2002. Homogeneous catalyst separation and re-use through nanofiltration of organic solvents. *Desalination* 147: 301-306.

Nakao S.I., Kimura S., 1982. Models of membrane transport phenomena and their applications for ultrafiltration data. *J. Chem. Eng. Jap.* 15(3): 200-205.

Nollet A., 1748. *Leçons de physique-experimentale*, Hippolyte-Louis Guerin, Paris.

Nozari A. (MET), 2005. Personal communication.

Nwuha V., 2000. Novel studies on membrane extraction of bioactive components of green tea in organic solvents: Part I. *J. Food Eng.* 44(4): 233-238.

Oikawa E., Katoh K., Aoki T., 1991. Characteristics of reverse osmosis membranes prepared from Schiff bases of polyallylamine in aprotic solvents and separation of inorganic and organic solutes through the membranes. *Sep. Sci. Technol.* 26(4): 569-584.

Owens D.K., Wendt R.C., 1969. Estimation of the surface free energy of polymers. *J. Appl. Pol. Sci.* 13: 1741-1747.

Paul D.R., 2004. Reformulation of the solution-diffusion theory of reverse osmosis. *J. Membr. Sci.* 241: 371-386.

Poiseuille J.L., 1841. *Comptes Rendus*, 11: 961, 1041.

Raman L.P., Cheryan M., Rajagopalan N., 1996. Solvent recovery and partial deacidification of vegetable oils by membrane technology. *Fett-Lipid* 98(1): 10-14.

Reddy K.K., Kawakatsu T., Snape J.B., Nakajima M., 1996. Membrane concentration and separation of L-aspartic acid and L-phenylalanine derivatives in organic solvents. *Sep. Sci. Technol.* 31(8) : 1161-1178.

Reichardt C., 2003. *Solvent and solvent effect in organic chemistry – Third, updated and enlarged edition*. Wiley-VCH Verlag GmbH & Co. KGaA, Weinheim, pp. 629.

Robinson J.P., Tarleton E.S., Millington C.R., Nijmeijer A., 2004. Solvent flux through dense polymeric nanofiltration membranes. *J. Membr. Sci.* 230: 29-37.

Roudman A.R., DiGiano F.A., 2000. Surface energy of experimental and commercial nanofiltration membranes: effects of wetting and natural organic matter fouling. *J. Membr. Sci.* 175: 61-73.

- Scarpello J.T., Nair D., Freitas dos Santos L.M., White L.S., Livingston A.G., 2002. The separation of homogeneous organometallic catalysts using solvent resistant nanofiltration. *J. Membr. Sci.* 203: 71-85.
- Schmidt M., Mirza S., Schubert R., Rodicker H., Kattanek S., Malisz J., 1999. Nanofiltration membranes for separation problems in organic solutions. *Chem. Eng. Techn.* 71(3): 199-206.
- Seader J.D., Henley E.J., 1998. *Separation Process Principles*. John Wiley & Sons, Inc. New York, pp. 886.
- Shukla R., Cheryan M., 2002. Performance of ultrafiltration membranes in ethanol-water solutions : effect of membrane conditioning. *J. Membr. Sci.* 198: 75-85.
- Silberberg M., Gold L.P., 1996. Intermolecular forces: Liquids, solids and changes of state. Chapter 11 in *Chemistry – The Molecular Nature of Matter and Change*. Mosby-Year Book, Inc., St-Louis: 412-462.
- Soltanieh M., Gill W.N., 1981. Review of reverse osmosis membranes and transport models. *Chem. Eng. Comm.* 12, 279-363.
- Spiegler K.S., Kedem O., 1966. Thermodynamics of hyperfiltration (RO): criteria for efficient membranes, *Desalination* 1: 311-326.
- Stafie N., Stamatialis D.F., Wessling M., 2003. Insight into the transport of hexane-solute systems through tailor-made composite membranes. *J. Membr. Sci.* 228: 103-116.
- Stemple K.T., Morris W.J., Paton G.I., 2003. Bioavailability of hydrophobic organic contaminants in soils: fundamental concepts and techniques for analysis. *Eur. J. Soil Sci.* 54: 809-818.
- Subramanian R., Nakajima M., Kawakatsu T., 1998. Processing of vegetable oils using polymeric composite membranes. *J. Food Eng.* 38(1): 41-56.
- Syracuse Research Corporation, 2003. Interactive LogKow (KowWin) Demo, [http://www.syrres.com/esc/est\\_kowdemo.htm](http://www.syrres.com/esc/est_kowdemo.htm).
- Theloke J., Obermeier A., Friedrich R., 2000. Ermittlung der Losemittelemissionen 1994 in Deutschland und Methoden zur Fortschreibung. *Umweltsbundesamt, Berlin*, pp. 312.

Tamura M., Kurata M., Odani H., 1955. *Bul. Chem. Soc. Jpn.* 28: 83.

Tsuru T., Sudou T., Kawahara S., Yoshioka T., Asaeda M., 2000. Permeation of liquids through inorganic membranes. *J. Coll. Int. Sci.* 228: 292-296.

Tsuru T., Sudoh T., Yoshioka T., Asaeda M., 2001. Nanofiltration in non-aqueous solutions by porous silica-zirconia membranes. *J. Membr. Sci.* 185: 253-261.

Tusel G.F., Brüscke H.E.A., 1985. Use of pervaporation systems in the chemical industry. *Desalination* 53(1-3): 327-338.

UNEP/IEO, 1989. Environmental aspects of the metal finishing industry: a technical guide. United Nations Publications, pp. 91.

Van Baelen D. (Indaver), 2005. Personal communication.

Van Braeckel D., Claeys B., 1999. Dossier Solventen. *Arbeid en Milieu, Berchem*, pp. 119.

Van der Bruggen B., Schaep J., Maes W., Wilms D., Vandecasteele C., 1998. Nanofiltration as a treatment method for the removal of pesticides from ground waters. *Desalination* 117(1-3): 139-147.

Van der Bruggen B., Schaep J., Wilms D., Vandecasteele C., 1999. Influence of molecular size, polarity, and charge on the retention of organic molecules by nanofiltration. *J. Membr. Sci.* 156: 29-41.

Van der Bruggen B., 2000. Removal of organic components from aqueous solution by nanofiltration. PhD thesis, Katholieke Universiteit Leuven, Belgium.

Van der Bruggen B., Schaep J., Wilms D., Vandecasteele C., 2000b. A comparison of models to describe the maximal retention of organic molecules in nanofiltration. *Sep. Sci. Tech.* 35(2): 169-182.

Van der Bruggen B., Devreese I., Vandecasteele C., 2001. Water reclamation in the textile industry: Nanofiltration of dye baths for wool dyeing. *Ind. Eng. Chem. Res.* 40(18): 3973-3978.

- Van der Bruggen B., Braeken L., Vandecasteele C., 2002. Evaluation of parameters describing flux decline in nanofiltration of aqueous solutions containing organic compounds. *Desalination* 147 (1-3): 281-288.
- Van Espen L., 2003. Evaluatie van het reductiepotentieel voor VOS-emissies naar het compartiment lucht: diverse sectoren. Deel II: Sectorbeschrijving en technische maatregelen. AMINAL, pp. 172.
- Van Gestel T., Vandecasteele C., Buekenhoudt A., Dotremont C., Luyten J., Leysen R., Van der Bruggen B., Maes G., 2002. Alumina and titania multilayer membranes for nanofiltration: preparation, characterization and chemical stability. *J. Membr. Sci.* 207: 73-89.
- Van Gestel T., Van der Bruggen B., Buekenhoudt A., Dotremont C., Luyten J., Vandecasteele C., Maes G., 2003. Surface modification of  $\gamma$ -Al<sub>2</sub>O<sub>3</sub>/TiO<sub>2</sub> multilayer membranes for applications in non-polar solvents. *J. Membr. Sci.* 224: 3-10.
- Van Hooste H. (OVAM), 2005. Personal communication.
- Vankelecom I.F.J., De Smet K., Gevers L.E.M., Livingston A., Nair D., Aerts S., Kuypers S., Jacobs P.A., 2004. Physico-chemical interpretation of the SRNF transport mechanism for solvents through dense silicone membranes. *J. Membr. Sci.* 231: 99-108.
- Van 't Hul J.P., Racz I.G. Reith, T., 1997. The application of membrane technology for reuse of process water and minimisation of waste water in a textile washing range. *J. Soc. Dyers and Colourists* 113(10): 287-294.
- Verniory A., Dubois R., Decoodt P., Gasse J.P., Lambert P.P., 1973. Measurement of permeability of biological membranes – Application to glomerular wall. *J. Gen. Physiol.* 62(4): 489-507.
- Watson B.M., Hornburg C.D., 1989. Low-energy membrane nanofiltration for removal of color, organics and hardness from drinking water supplies. *Desalination* 72(1-2): 11-22.
- Weast R.C., 1970. C.R.C. Handbook of chemistry and physics, 51<sup>st</sup> Ed., The Chemical Rubber Co., Cleveland.
- White L.S., Nitsch A.R., 2000. Solvent recovery from lube oil filtrates with a polyimide membrane. *J. Membr. Sci.* 179: 267-274.

White L.S., 2002. Transport properties of a polyimide solvent resistant nanofiltration membrane. *J. Membr. Sci.* 205: 191-202.

Whu J.A., Baltzis B.C., Sirkar K.K., 2000. Nanofiltration studies of larger organic microsolute in methanol solutions. *J. Membr. Sci.* 170: 159-172.

Wijmans J.G., Baker R.W., 1995. The solution-diffusion model: a review. *J. Membr. Sci.* 107: 1-21.

Wilke C.R., Chang P., 1955. *AIChE J.* 1: 264-270.

Willink S.H.D.T., 1993. *Chemiekaarten – Gegevens voor veilig werken met chemicaliën*. 9<sup>de</sup> editie. pp.1029.

Winterfeld P.H., Scriven L.E., Davis H.T., 1978. Approximation theory of interfacial tensions of multicomponent systems – applications to binary liquid-vapor tensions. *AIChE J.* 24: 1010-1014.

Yang X.J., Livingston A.G., Freitas dos Santos L., 2001. Experimental observations of nanofiltration with organic solvents. *J. Membr. Sci.* 190: 45-55.

Yilmaz H., 2002. Excess properties of alcohol – water systems at 298.15 K. *Turk. J. Phys.* 26: 243-246.

Young T., 1805. *Philos. Trans. R. Soc. London* 95: 65.

Zeman L., Wales M., 1981. Steric rejection of polymeric solutes by membranes with uniform pore size distribution. *Sep. Sci. Tech.* 16(3): 275-290.

Zsigmondy R., Bachmann W., 1918. *Z. Anorg. Chem.* 103: 119.

Zwijnenberg H.J., Krosse A., Ebert K., Peinemann K.V., Cuperus F.P., 1999. Acetone-stable nanofiltration membranes in deacidifying vegetable oil. *J. Am. Oil Chem. Soc.* 76(1): 83-87.





## Appendix A: Calculation of transport model for linear regression

Transport models consist of different algebraic structures. The models used in this work are recalculated into a mathematical form enabling linear regression, i.e.  $Y = mX + p$ . X and Y are variables of the regression and are functions of the respective model variables. m and p are the slope and intercept of the linear regression and are functions of the model constants a and/or b.

### A.1. Hagen-Poiseuille

$$J = \frac{\epsilon r^2}{8\eta} \Delta P$$

$$L = \frac{J}{\Delta P} = \frac{a}{\eta}$$

$$L = a \frac{1}{\eta}$$

### A.2. Jonsson-Boesen

$$J = \frac{\epsilon r^2}{8\eta} \frac{1}{1 + \frac{r^2 f_{sm} C}{8\eta M}} \frac{\Delta P}{\tau \Delta x}$$

$$J = \frac{a}{\eta} \frac{1}{1 + \frac{b}{\eta M}} \Delta P$$

$$L = \frac{J}{\Delta P} = \frac{aM}{\eta M + b}$$

$$\frac{1}{L} = \frac{\eta M + b}{aM}$$

$$\frac{M}{L} = \frac{1}{a}(\eta M) + \frac{b}{a}$$

**A.3. Machado *et al.***

$$J = \frac{\Delta P}{\phi'[(\gamma_c - \gamma_l) + f_1\eta] + f_2\eta}$$

$$L = \frac{J}{\Delta P} = \frac{1}{\phi'(\gamma_c - \gamma_l) + f_1\eta\phi' + f_2\eta}$$

$$\frac{1}{L} = \phi'(\gamma_c - \gamma_l) + f_1\eta\phi' + f_2\eta$$

$$\frac{1}{\eta L} = \phi' \frac{(\gamma_c - \gamma_l)}{\eta} + f_1\phi' + f_2$$

$$\frac{1}{\eta L} = a \frac{(\gamma_c - \gamma_l)}{\eta} + b$$

**A.4. This work**

$$J \propto \frac{V_m}{\eta \cdot \Delta\gamma}$$

$$J = a \frac{V_m}{\eta \cdot \Delta\gamma} \Delta P$$

$$L = \frac{J}{\Delta P} = a \frac{V_m}{\eta \cdot \Delta\gamma}$$

## Appendix B: Statistical analysis

Determination of statistical significance requires data sets of at least 20 couples, which were not available. Therefore statistical analysis was limited to the determination of the best fit. Fit error  $e$  and error variance  $s_e^2$  were used for descriptive statistical analysis.

Fit error  $e_i$  is the deviation between an experimental result  $y_i$  and a (theoretical) model value  $y_i'$ :

$$e_i = y_i - y_i' \quad (\text{B.1})$$

The total fit error  $e$  is the sum of all data couples' fit error:

$$e = \sum_i^n e_i \quad (\text{B.2})$$

The error variance for a series of data couples is calculated as the variance on the  $e_i$ -values:

$$s_e^2 = \sum_i^n \frac{e_i^2}{n} \quad (\text{B.3})$$

The data set providing the lowest value for the error variance corresponds to the best model fit.

### Appendix C: Ratio of effective solute diameters

According to the Stokes-Einstein equation [31], the effective solute diameter of component  $c$  in solvent  $s$  can be expressed as:

$$d_c^s = \frac{kT}{3\pi\eta D_{cs}} \quad (\text{C.1})$$

The diffusion coefficient  $D_{cs}$  is defined by the Wilke-Chang equation (Eq. 16), so that expression (A.1.) can be reformulated as:

$$d_c^s = \frac{kT}{3\pi\eta \left[ 7.4 \cdot 10^{-8} (\phi M_s)^{1/2} \frac{T}{\eta V_c^{0.6}} \right]} = \frac{kV_c^{0.6}}{2.22 \cdot 10^{-7} (\phi M_s)^{1/2}} \quad (\text{C.2})$$

The ratio of the effective diameters of a component  $c$  in two different solvent  $s_1$  and  $s_2$  is then calculated as:

$$\frac{d_c^{s_2}}{d_c^{s_1}} = \frac{\frac{kV_c^{0.6}}{2.22 \cdot 10^{-7} (\phi M_{s_2})^{1/2}}}{\frac{kV_c^{0.6}}{2.22 \cdot 10^{-7} (\phi M_{s_1})^{1/2}}} = \frac{(\phi M_{s_1})^{1/2}}{(\phi M_{s_2})^{1/2}} \quad (\text{C.3})$$

## List of publications

### In peer-reviewed international journals

Geens J., Demeyer K., Pauwelyn A.S., De Witte B., Vandecasteele C., Van der Bruggen B., 2005. Non-aqueous nanofiltration in the pharmaceutical industry: a case-study. In preparation.

Geens J., Boussu K., Vandecasteele C., Van der Bruggen B., 2005. Modelling of solute transport in non-aqueous nanofiltration. Submitted for publication in *Journal of Membrane Science*.

Van Gerven T., Block C., Geens J., Cornelis G., Vandecasteele C., 2005. Environmental response indicators for the industrial and energy sector in Flanders. Submitted for publication in *Cleaner Production*.

Geens J., Van der Bruggen B., Vandecasteele C., 2005. Transport model for solvent permeation through nanofiltration membranes, *Separation and Purification Technology*. In press.

Geens J., Hillen A., Bettens B., Van der Bruggen B., Vandecasteele C., 2005. Solute transport in non-aqueous nanofiltration: effect of membrane material, *Journal of Chemical Technology and Biotechnology*, 80(12): 1371-1377.

Geens J., Peeters K., Van der Bruggen B., Vandecasteele C., 2005. Polymeric nanofiltration of binary water-alcohol mixtures: Influence of feed composition and membrane properties on permeability and solute rejection, *Journal of Membrane Science*, 255: 255-264.

Van der Bruggen B., Jansen J.C., Figoli A., Geens J., Van Baelen D., Drioli E., Vandecasteele C., 2004. Determination of parameters affecting transport in polymeric membranes: Parallels between pervaporation and nanofiltration. *Journal of Physical Chemistry B* 108(35): 13273-13279.

Van der Bruggen B., Kim J.H., DiGiano F.A., Geens J., Vandecasteele C., 2004. Influence of MF pretreatment on NF performance for aqueous solutions containing particles and an organic foulant *Separation and Purification Technology* 36(3): 203-213.

Geens J., Van der Bruggen B., Vandecasteele C., 2004. Characterisation of the solvent stability of polymeric nanofiltration membranes by measurement of contact angles and swelling, *Chemical Engineering Science* 59: 1161-1164.

Van der Bruggen B., Geens J., Vandecasteele C., 2002. Fluxes and rejections for nanofiltration with solvent stable polymeric membranes in water, ethanol and n-hexane, *Chemical Engineering Science* 57: 2511-2518.

Van der Bruggen B., Geens J., Vandecasteele C., 2002. Influence of organic solvents on the performance of polymeric nanofiltration membranes, *Separation Science and Technology* 37(4): 783-797.

### **Conference proceedings**

Geens J., 2006. Modelling of solute transport in non-aqueous NF. International Workshop Membranes in Solvent Filtration, Leuven, Belgium, March 23-24.

Geens J., Van der Bruggen B., Verrecht B., Buekenhoudt A., Dotremont C., Vandecasteele C., 2005. Nanofiltration in organic solvents: comparison between polymeric and ceramic membranes. Proceedings of Conference on Porous Ceramic Materials 2005 (PCM), Brugge, Belgium, October 20-21. In press.

Van der Bruggen B., Geens J., Vandecasteele C., 2001. Characterisation of the solvent stability of polymeric nanofiltration membranes. Proceedings of AIChE 2001 Annual Meeting, Reno, Nevada, USA, November 4-9 2001, vol. 2, 1012-1019.

### **Contribution to international conference (unpublished, abstract or poster)**

Geens J., Van der Bruggen B., Vandecasteele C., 2005. Nanofiltration of organic solvents: a comparison between polymeric and ceramic membranes. 11de NMG Posterdag Membraantechnologie, Ede, The Netherlands, October 27.

Braeken L., Geens J., Van der Bruggen B., Vandecasteele C., 2005. Modeling of flux decline during nanofiltration of organic compounds in aqueous solution. International Congress on Membranes and Membrane Processes (ICOM2005), Seoul, Korea, August 21-26.

Geens J., Van der Bruggen B., Vandecasteele C., 2005. Nanofiltration of organic solvents: a comparison between polymeric and ceramic membranes. International Congress on Membranes and Membrane Processes (ICOM2005), Seoul, Korea, August 21-26.

Geens J., Van der Bruggen B., Vandecasteele C., 2004. Fluxes of binary mixtures of water, methanol and ethanol: evaluation of a new transport model for organic solvents. Annual Meeting AIChE, Austin, Texas, USA, November 8-12.

Geens J., Van der Bruggen B., Vandecasteele C., 2004. A new transport model for solvent permeation through nanofiltration membranes. Advanced Membrane Technology II, ECI Conference, May 24-28.

Van der Bruggen B., Geens J., Peeters K., Vandecasteele C., 2004. Experimental observations of nanofiltration with binary mixtures of water, methanol and ethanol. Advanced Membrane Technology II, ECI Conference, May 24-28.

Geens J., 2003. Nanofiltration of organic solvents using polymeric and ceramic membranes. Network Young Membranes (NYM5), Barcelona, Spain, October 2-3, 128-129.

#### **Book chapter**

Van der Bruggen B., Geens J., 2005. Nanofiltration. Chapter in 'Advanced Membrane Science and Technology' (Eds. Sirkar K., Ho W., Matsuura T., Fane A.G.). In press.

#### **Other publications**

Geens J., Cornelis G., Vandecasteele C., De Grootte W., Sanders A., Van Hooste H., 2004. Milieu- en natuurrapport Vlaanderen, MIRA-T 2004, 1.3 Industrie, Lannoo Campus, Leuven, 71-82.

Geens J., Van Baelen D., Vandecasteele C., De Grootte W., Umans L., Van Hooste H., 2003. Milieu- en natuurrapport Vlaanderen, MIRA-T 2003, 1.2 Industrie, Lannoo Campus, Leuven, 53-65.

#### **Award**

European Membrane Society (EMS) Award 2003 for the paper 'Van der Bruggen B., Geens J., Vandecasteele C., 2002. Fluxes and rejections for nanofiltration with solvent stable polymeric membranes in water, ethanol and n-hexane. Chem. Eng. Sci. 57(13): 2511-2518.'





## Curriculum vitae

Family name: Geens  
First name: Jeroen  
Date of birth: March 19, 1978  
Place of birth: Lier  
Nationality: Belgian

1991 – 1996 High School Sint-Jan Berchmanscollege, Westmalle  
Latin & Mathematics

1996 – 2001 Bachelor/Master in Chemical Engineering  
Katholieke Universiteit Leuven  
Cum laude

2001 – 2005 Research assistant, PhD student  
Department of Chemical Engineering  
Katholieke Universiteit Leuven

2005 – ... Engineer Chemical Process Technology  
Chemical Production Engineering  
Janssen Pharmaceutica, Geel

February 15, 2006 PhD-thesis